ECT*

Advances in predicting nuclear matter at finite temperature

Arianna Carbone (ECT*-Trento, Italy)

International Workshop “Infinite and finite nuclear matter” (INFINUM)

JINR, Dubna - 20 March 2019

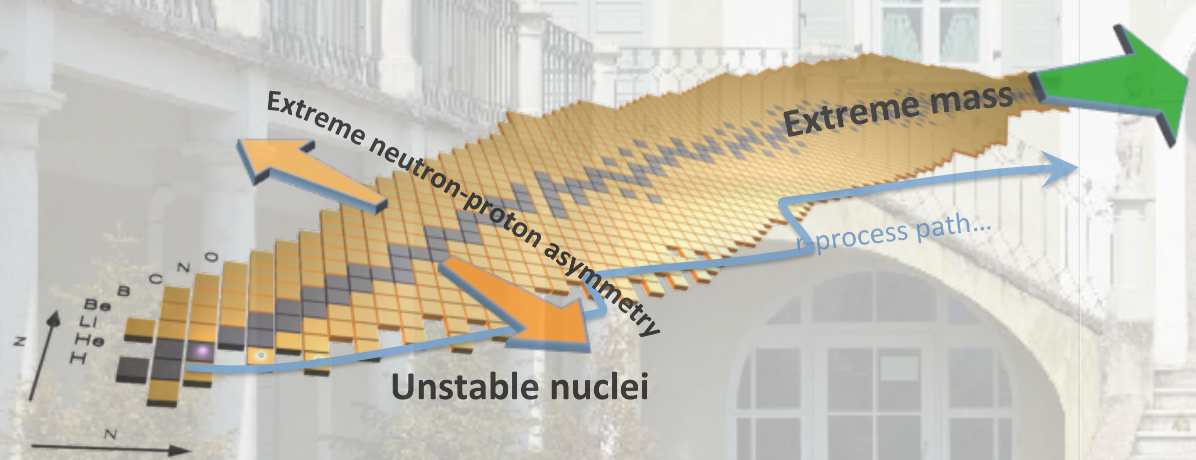

FONDAZIONE BRUNO KESSLER

Ab initio low-energy nuclear theory

Solve the nuclear many-body problem from first principles

Employing reliable methods with predictive power

Ab initio low-energy nuclear theory

Solve the nuclear many-body problem from <u>first principles</u>

<u>Employing reliable methods with predictive power</u>

- Structure and reactions of nuclei

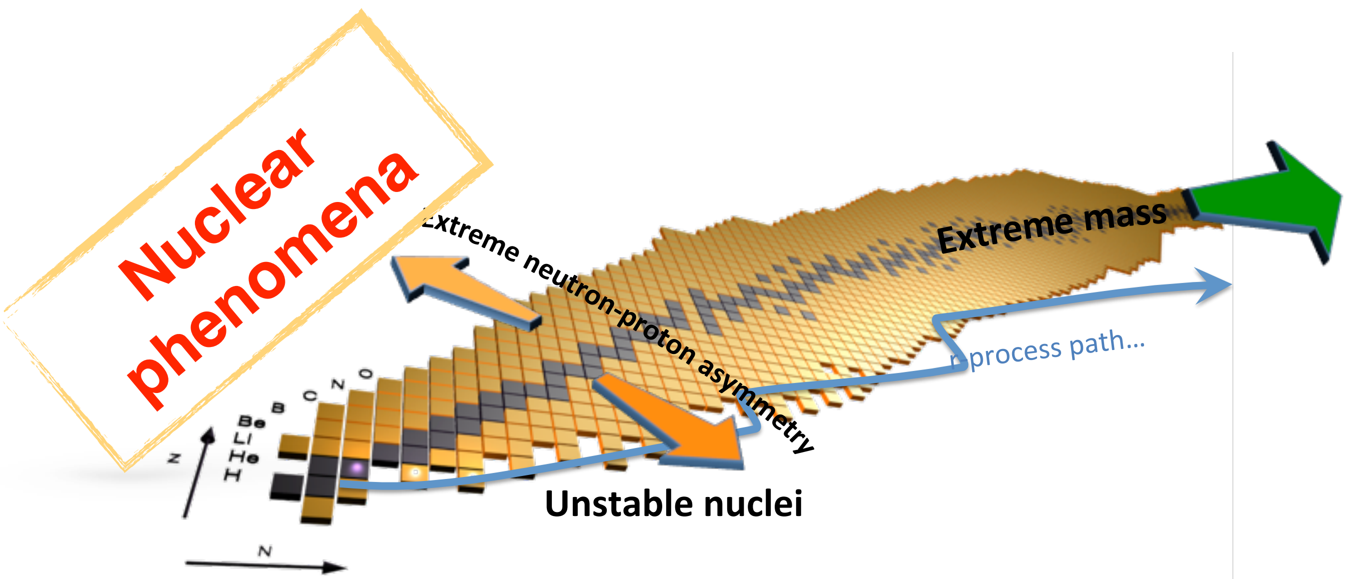

Ab initio low-energy nuclear theory

Solve the nuclear many-body problem from first principles

Employing reliable methods with predictive power

- Structure and reactions of nuclei
- Structure and dynamics of neutron stars

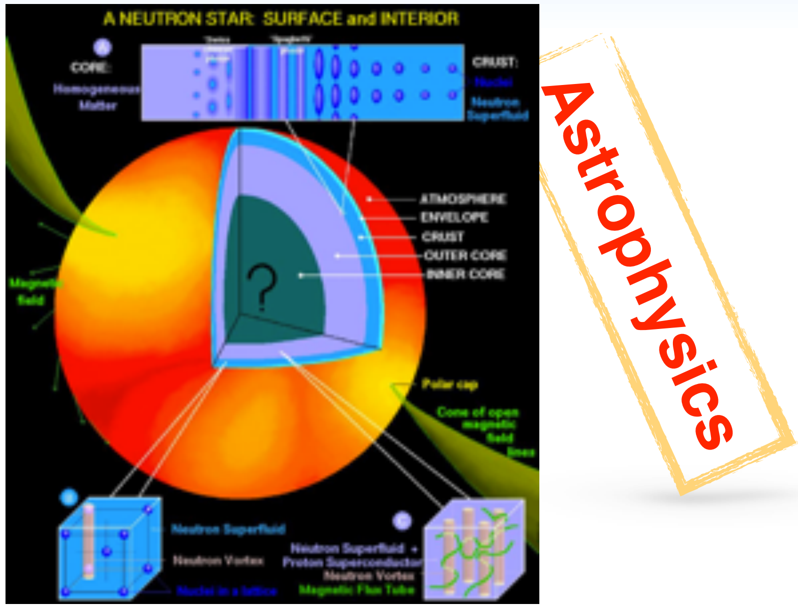

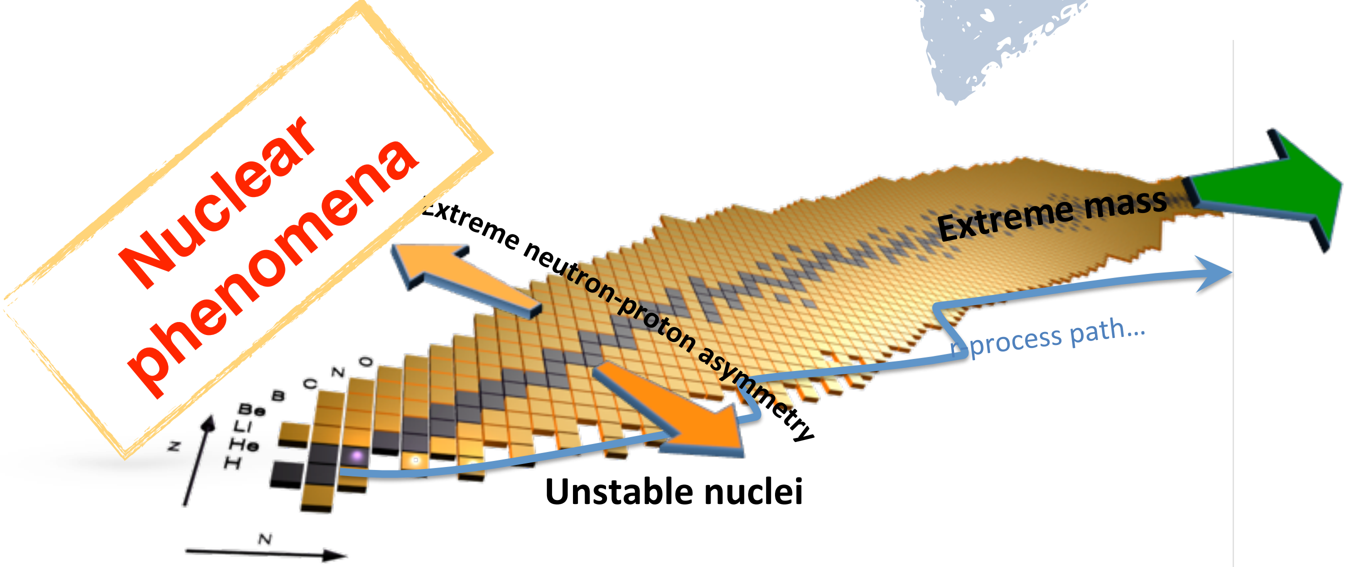

Ab initio low-energy nuclear theory

Solve the nuclear many-body problem from first principles

Employing reliable methods with predictive power

- Structure and reactions of nuclei
- Structure and dynamics of neutron stars

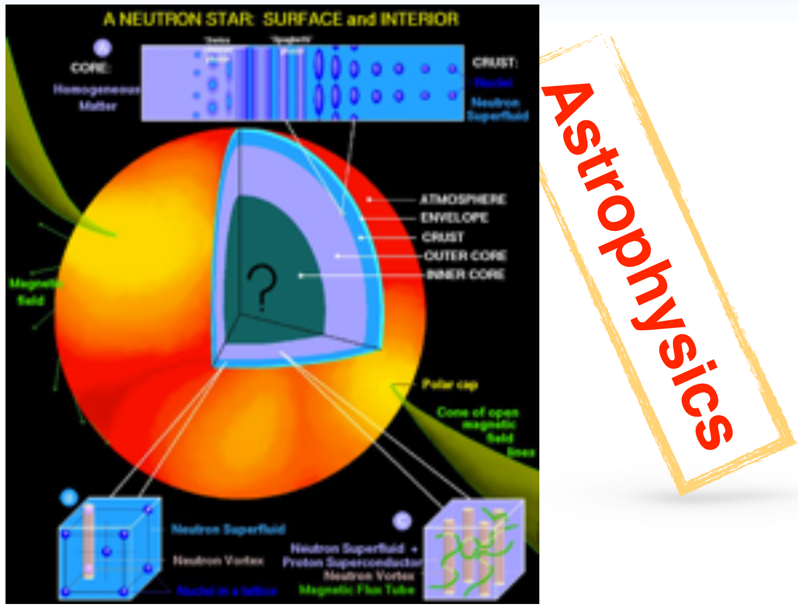

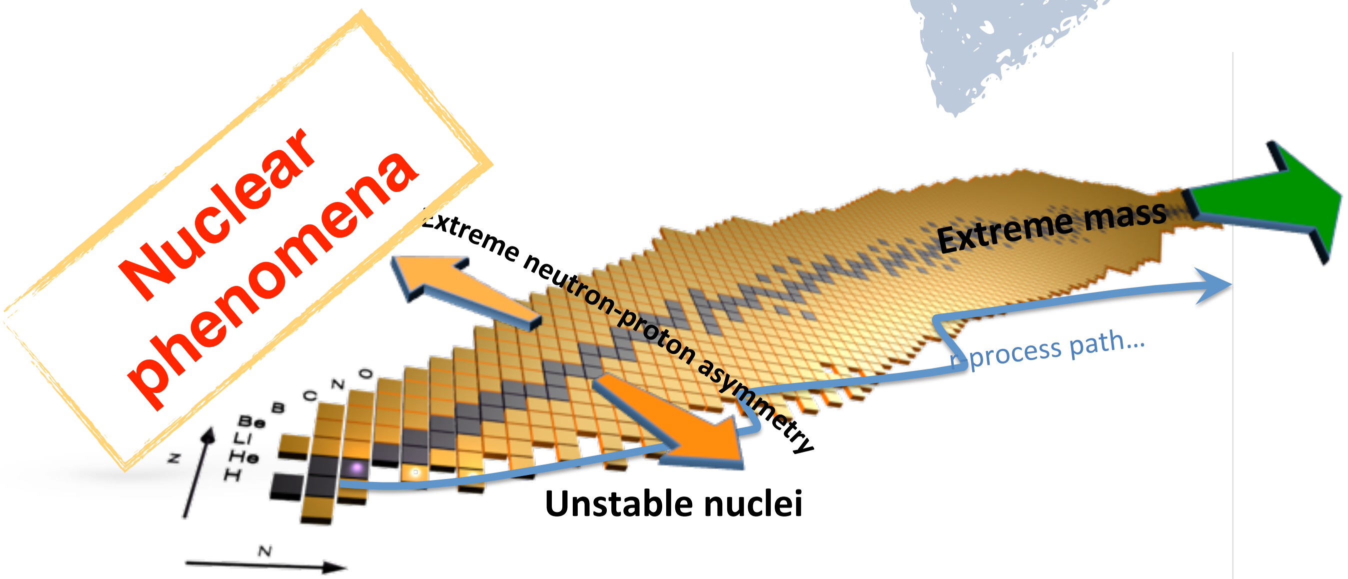

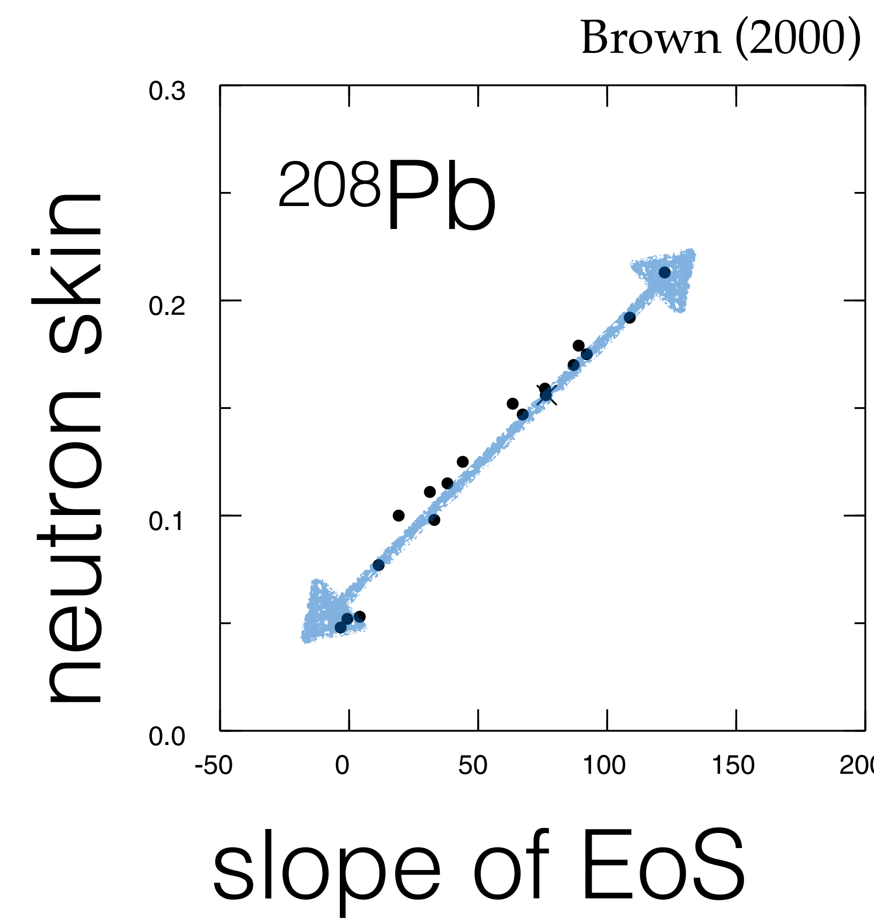

neutron-rich nuclei and neutron matter: a strong correlation

Ab initio low-energy nuclear theory

Solve the nuclear many-body problem from first principles

Employing reliable methods with predictive power

- Structure and reactions of nuclei
- Structure and dynamics of neutron stars

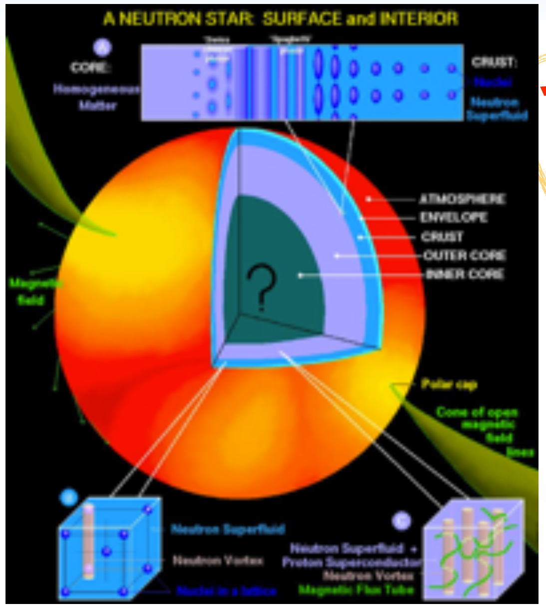

Astrophysics

Nuclear phenomena

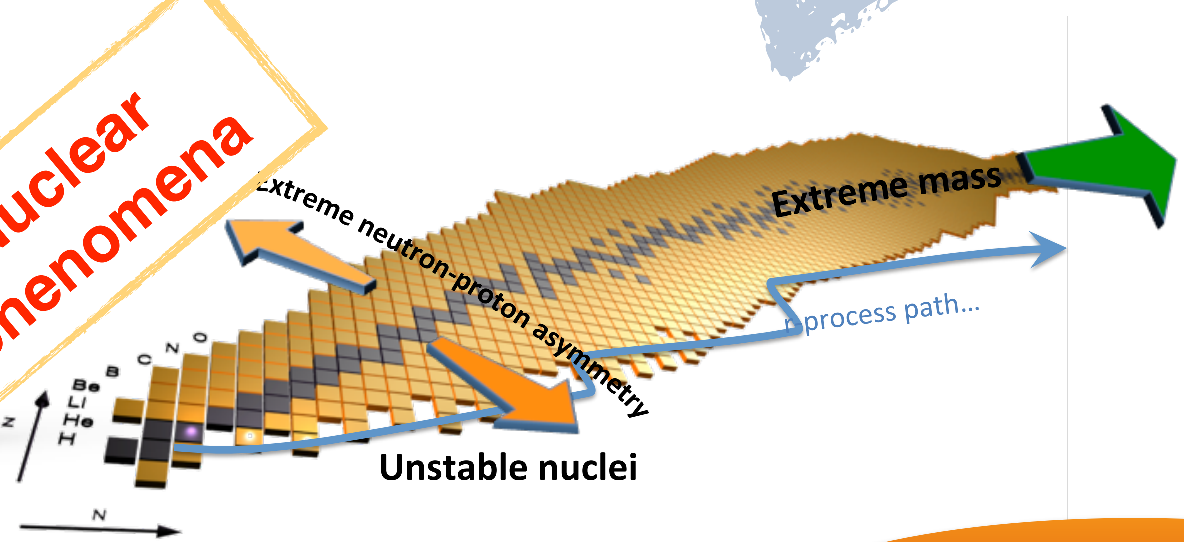

Predict infinite matter

Brown (2000)

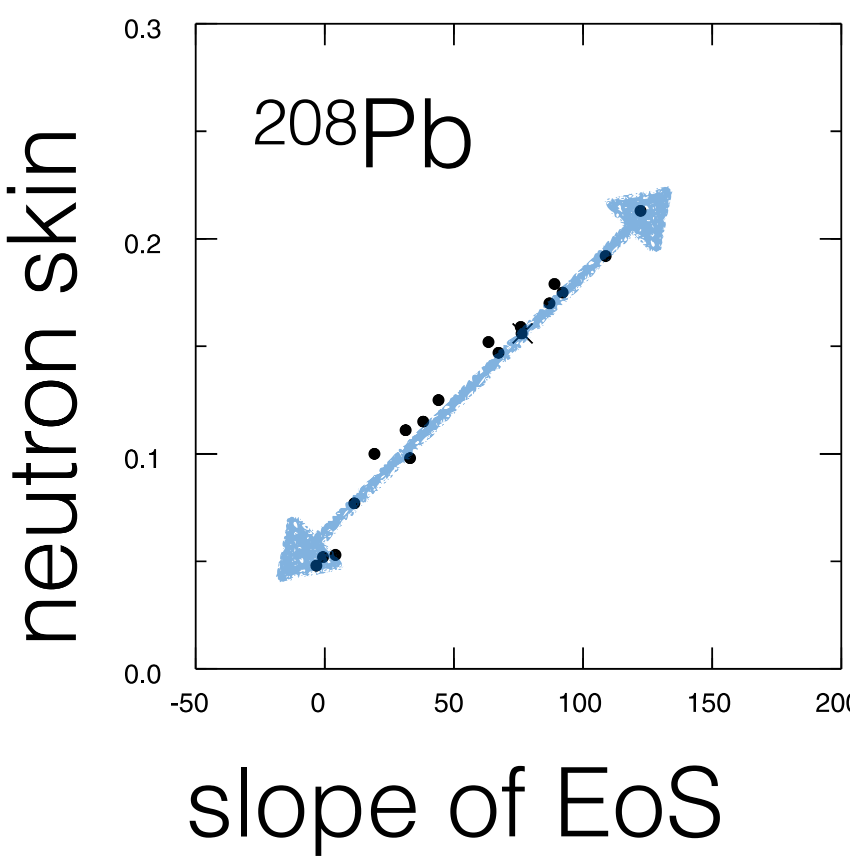

neutron-rich nuclei and neutron matter: a strong correlation

How do we proceed in this endeavour?

How do we proceed in this endeavour?

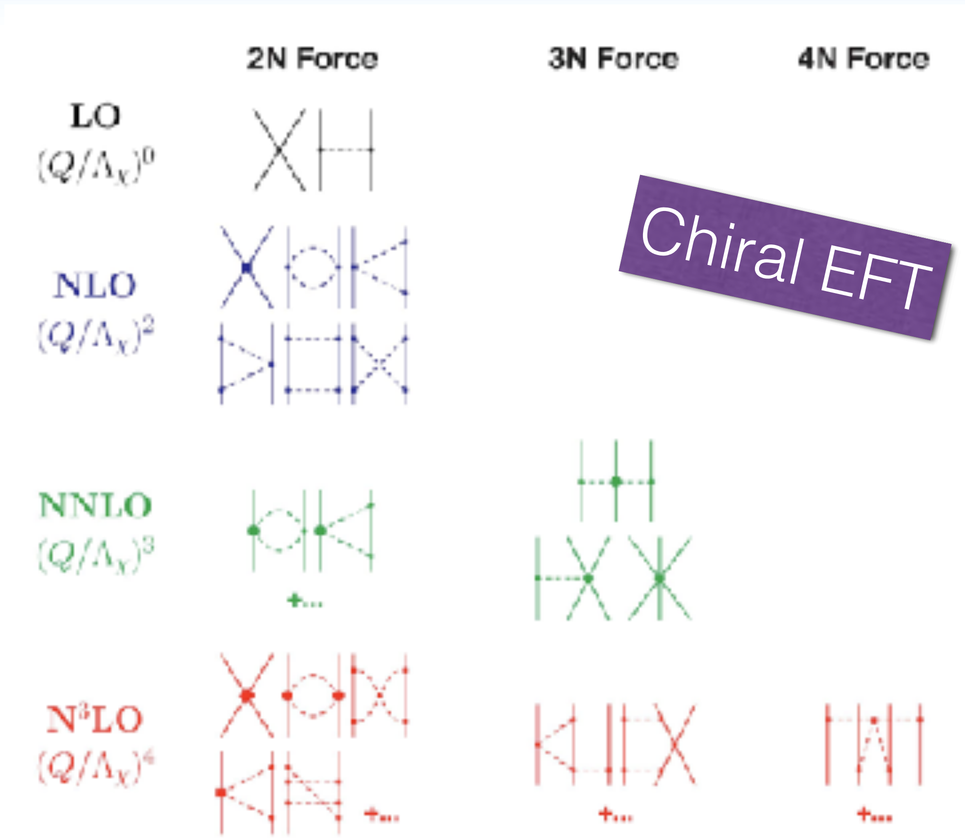

We start from defining the Hamiltonian

degrees of freedom and interactions

How do we proceed in this endeavour?

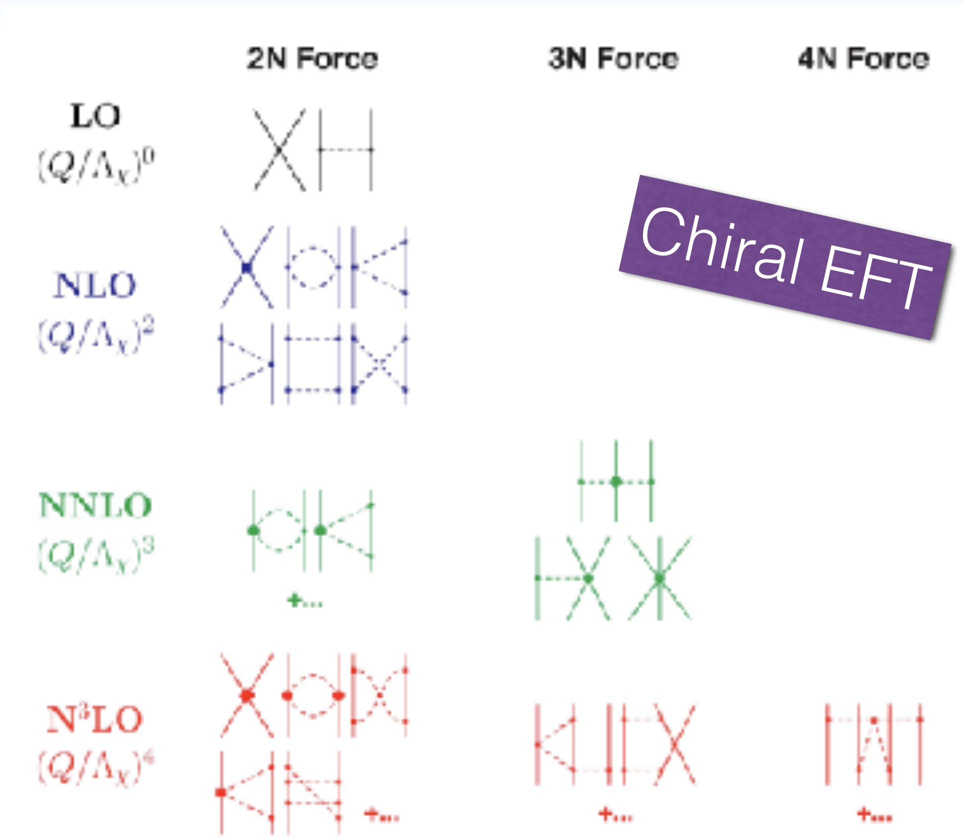

We start from defining the Hamiltonian

<u>degrees of freedom and interactions</u>

Then we solve the Schrödinger equation

<u>many-body approach</u>

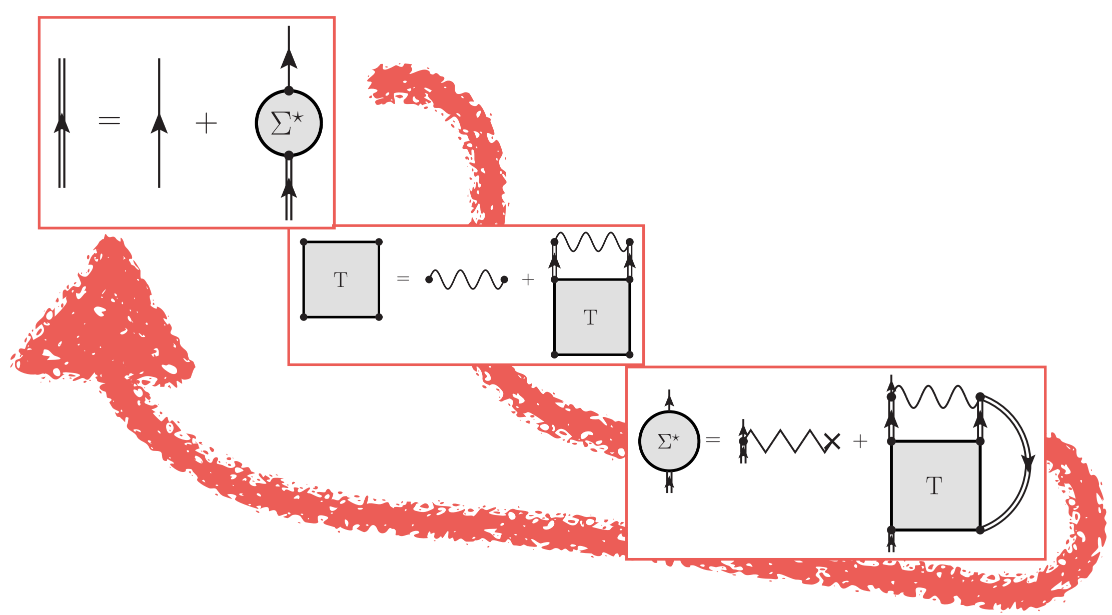

Self-consistent Green's function method

Dickhoff & Barbieri, PPNP **52**, 377 (2004)

Self-consistent Green's functions

- Green's function: a tool to solve the nuclear many-body problem

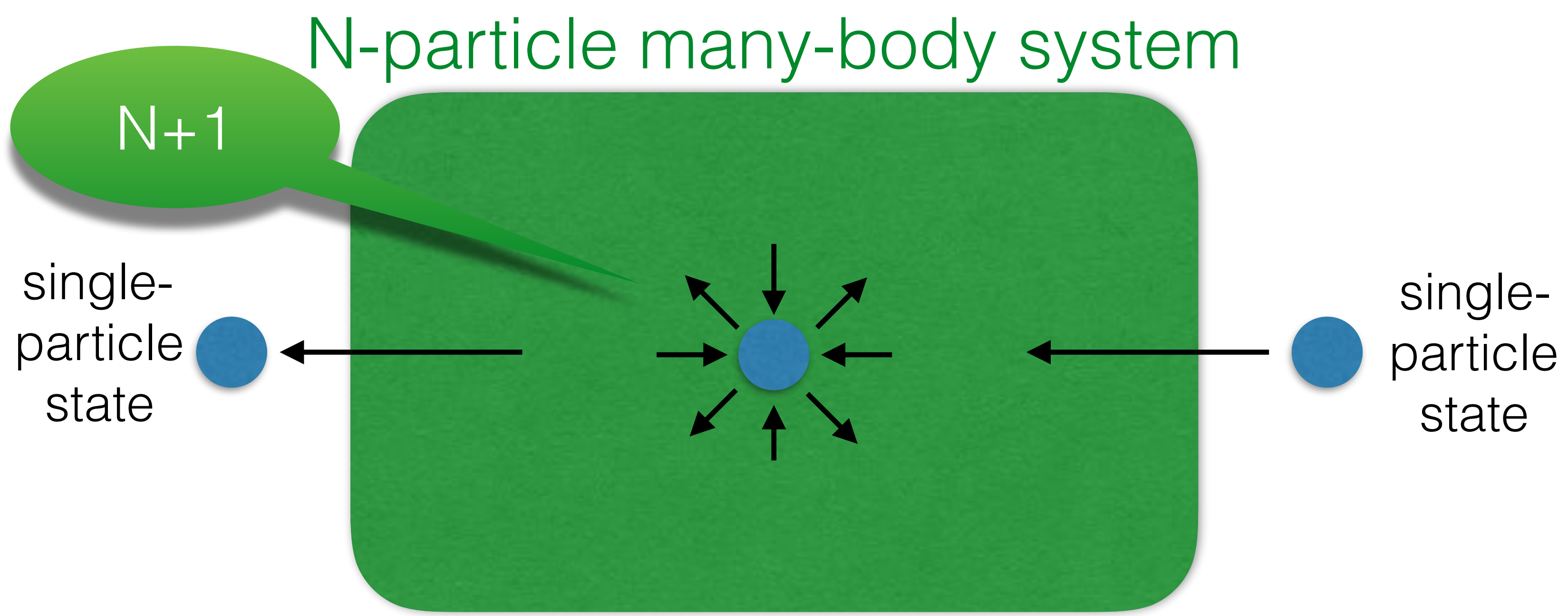

Self-consistent Green's functions

- Green's function: a tool to solve the nuclear many-body problem

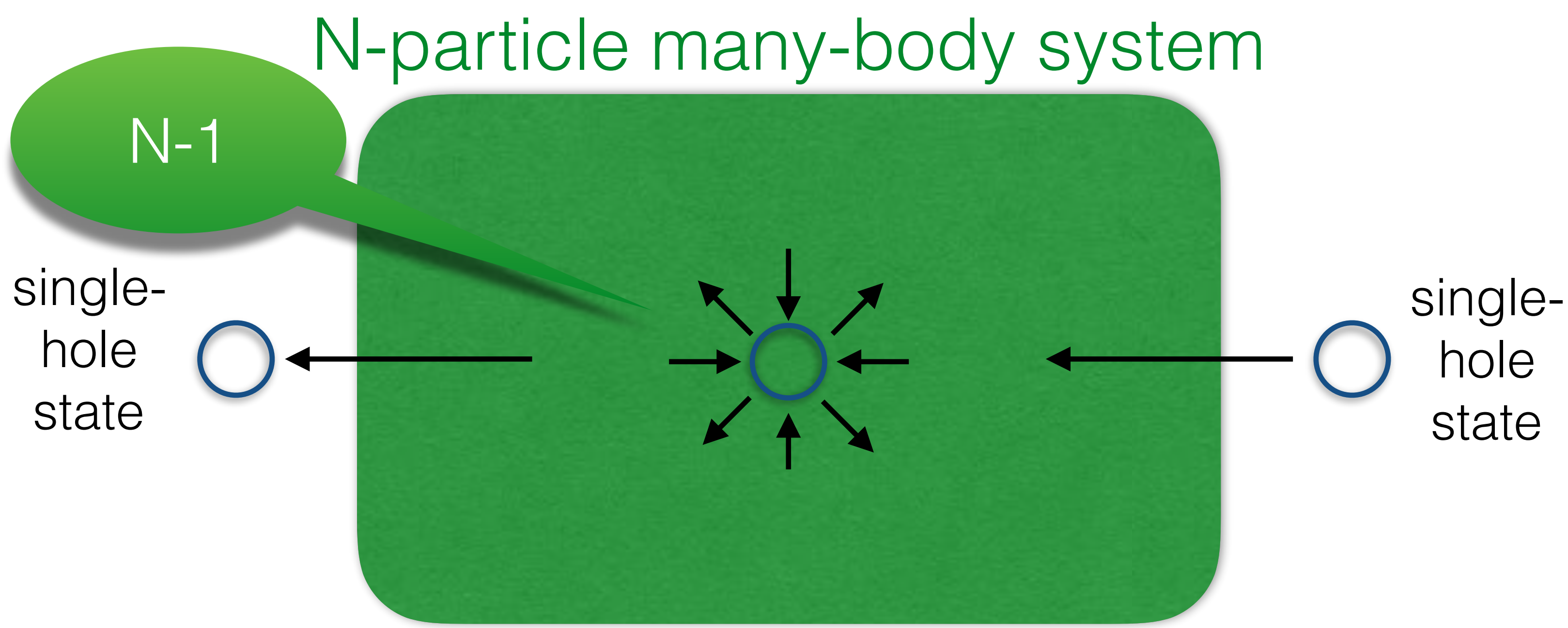

Self-consistent Green's functions

- Green's function: a tool to solve the nuclear many-body problem

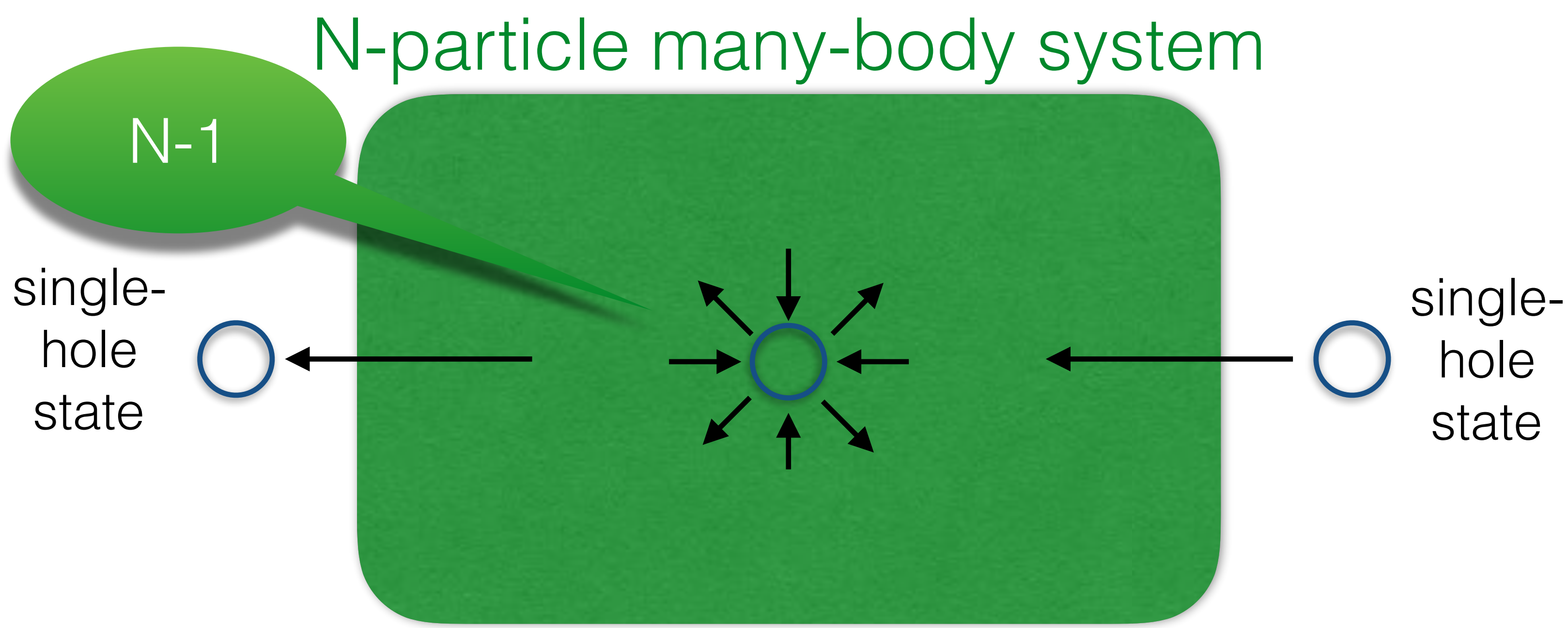

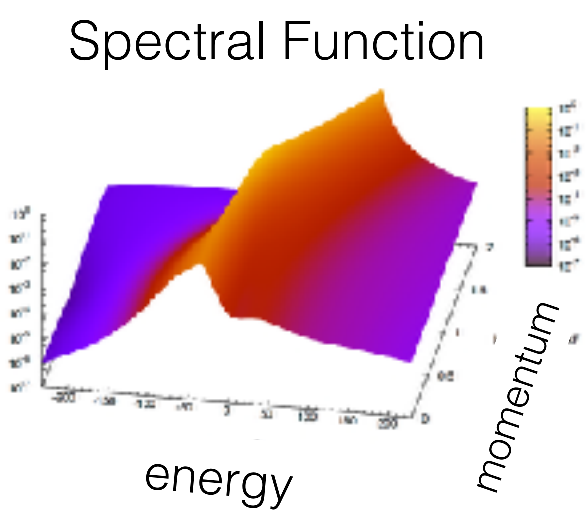

Self-consistent Green's functions

- Green's function: a tool to solve the nuclear many-body problem

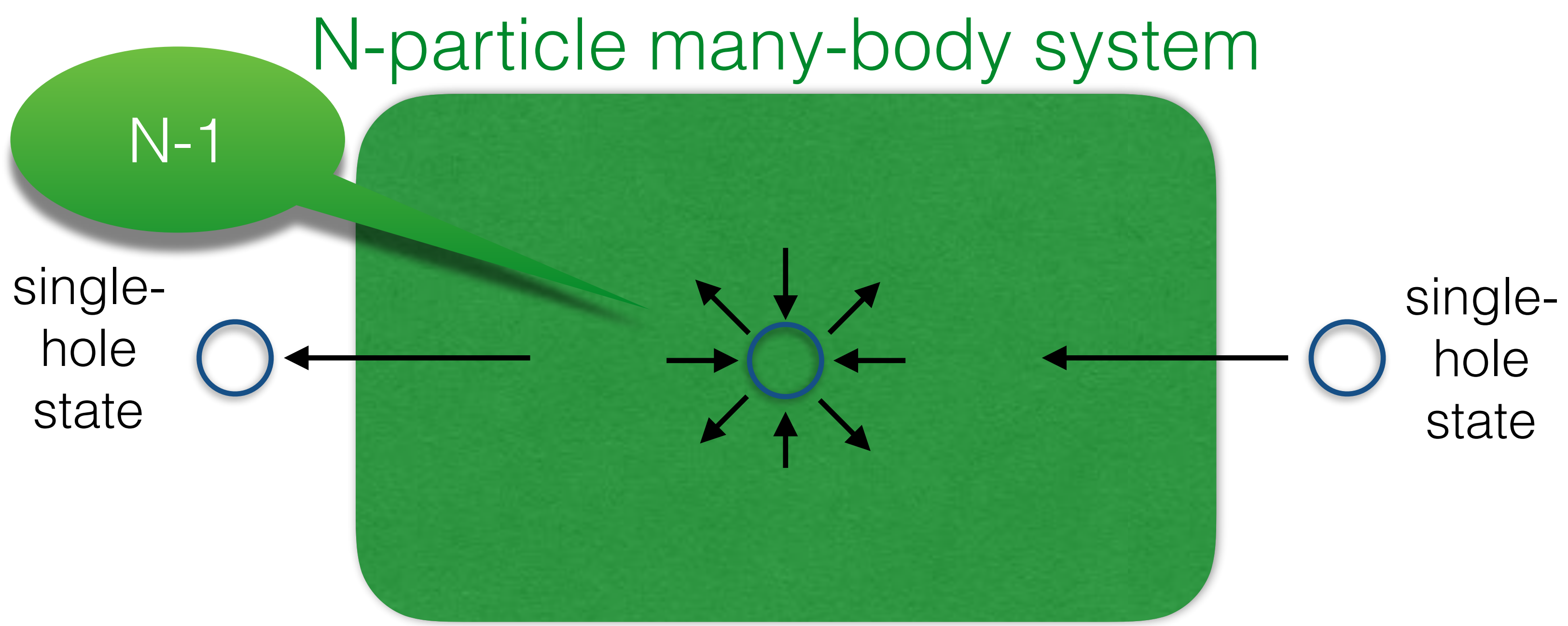

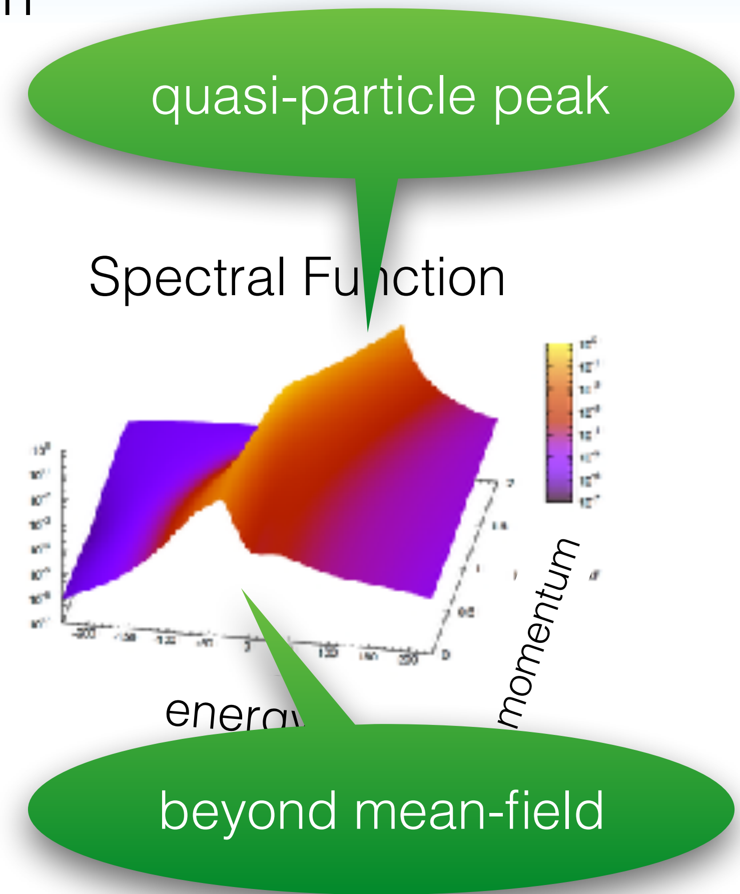

Self-consistent Green's functions

- Green's function: a tool to solve the nuclear many-body problem

N-particle many-body system

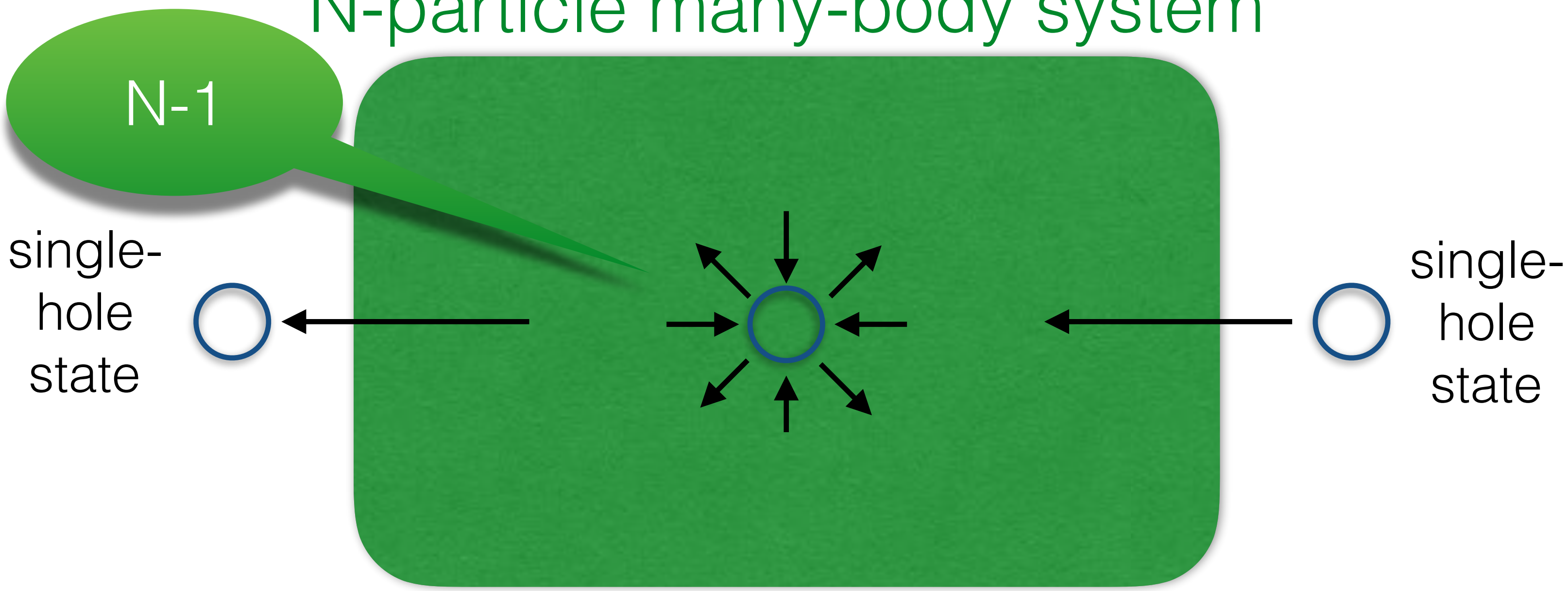

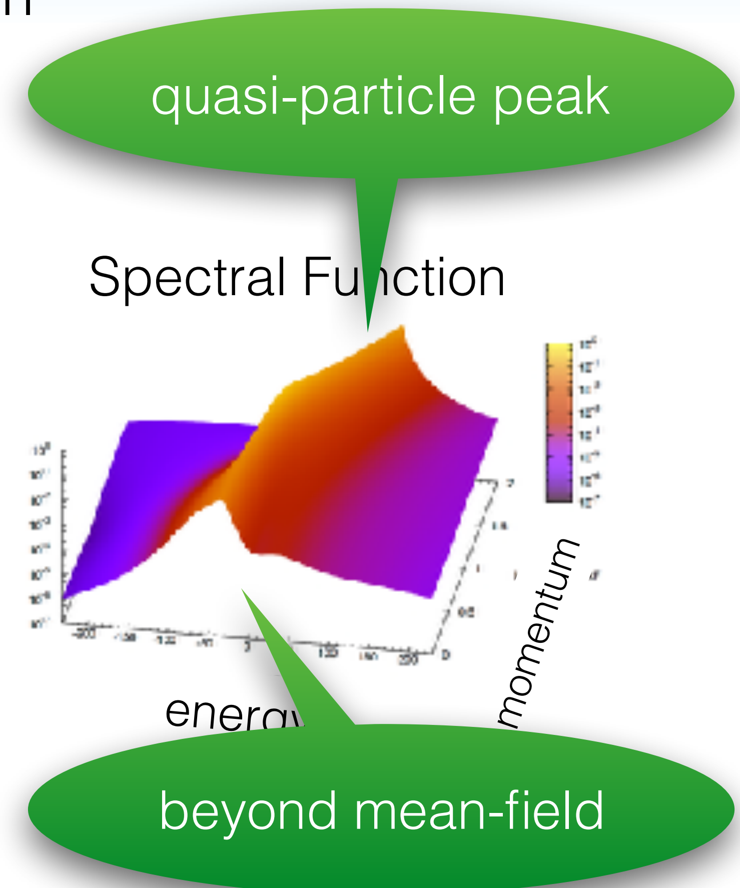

- Self-consistent nonperturbative method:

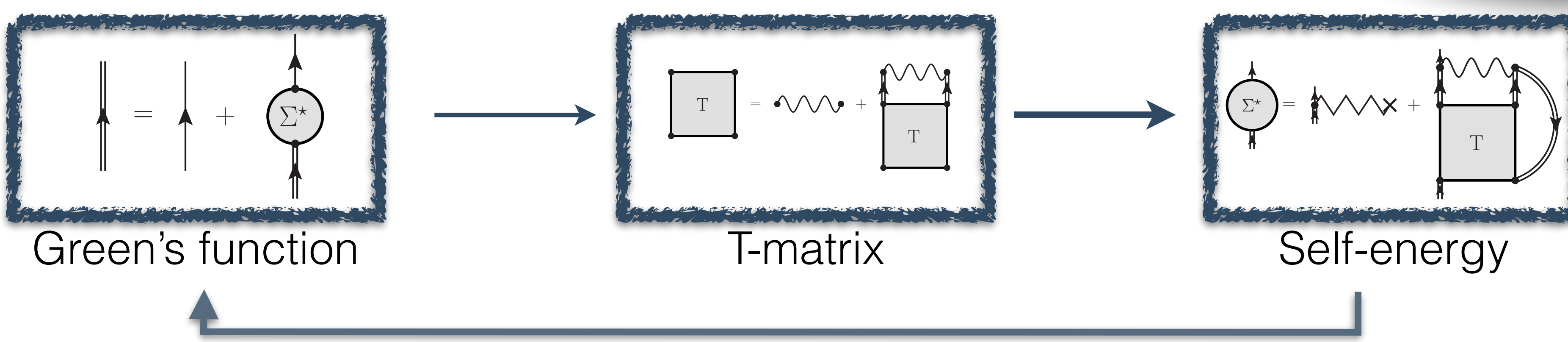

Dyson equation

Self-consistent Green's functions

- Green's function: a tool to solve the nuclear many-body problem

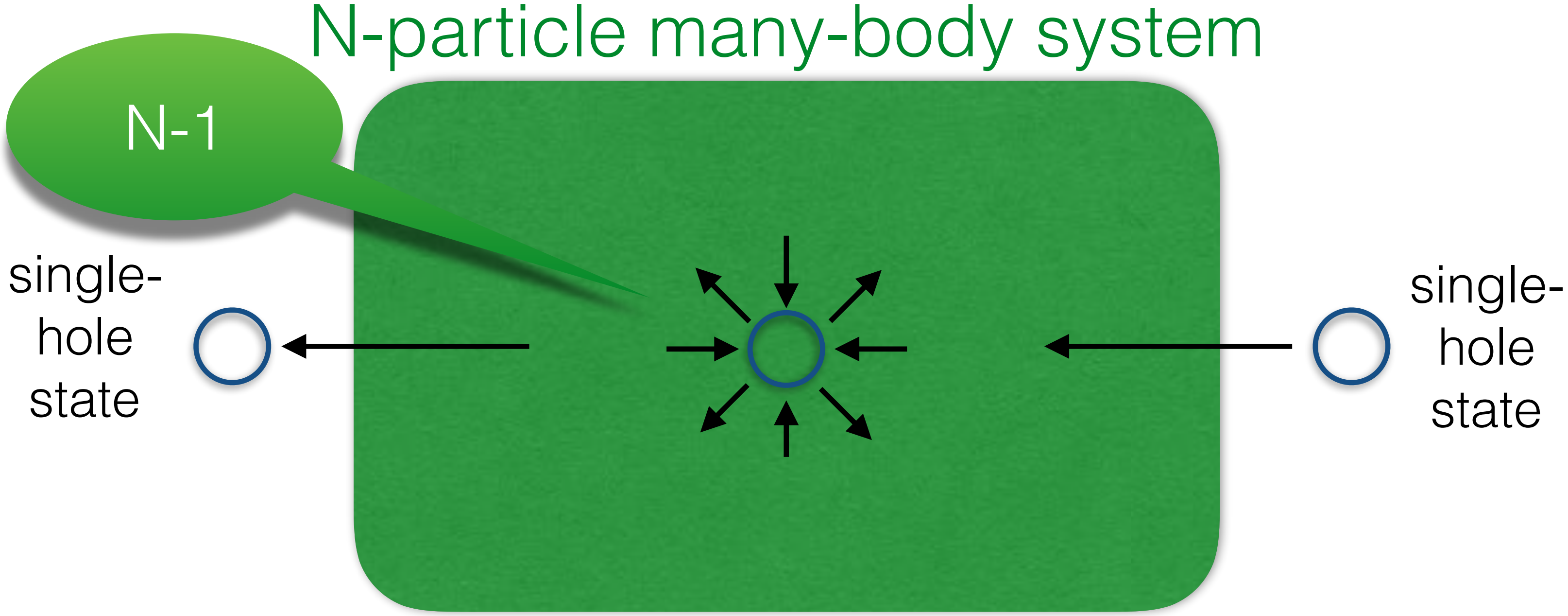

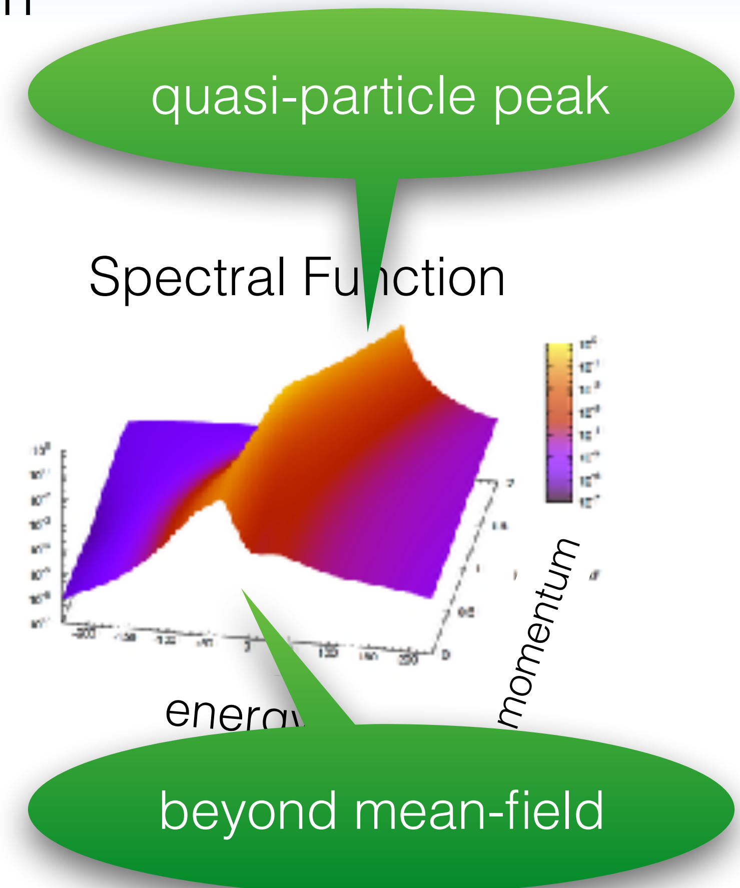

- Self-consistent nonperturbative method:

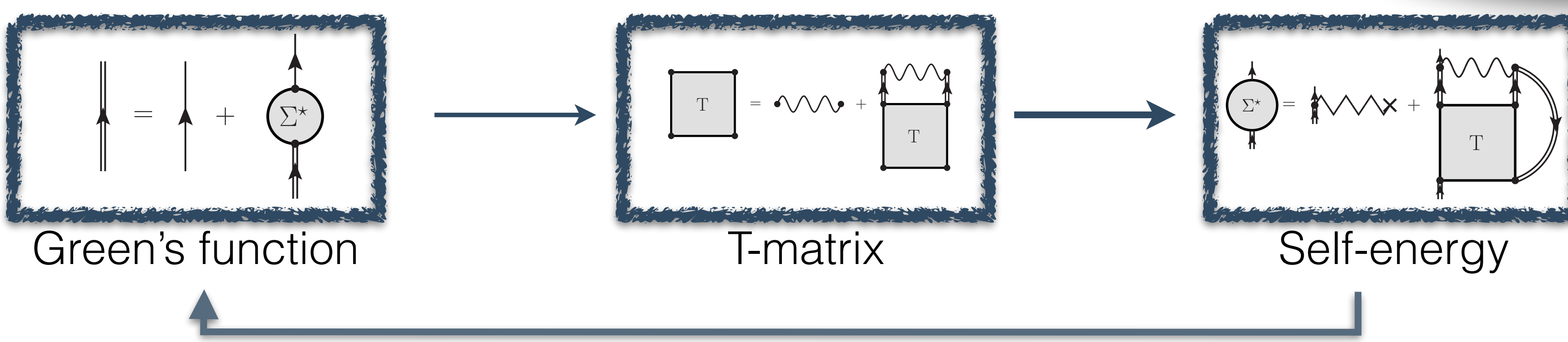

Dyson equation

- Breakthrough: full formal extension to consistently include 3BFs

Carbone, Cipollone, Barbieri, Rios, Polls, PRC **88**, 054326 (2013)

The need for 3-body nuclear forces

Koltun sumrule

$$\frac{E}{A} = \frac{\nu}{\rho}\int\frac{\mathrm{d}^3p}{(2\pi)^3}\int\frac{\mathrm{d}\omega}{2\pi}\frac{1}{2}\left\{\frac{p^2}{2m}+\omega\right\}\boxed{\mathcal{A}(p,\omega)}f(\omega) - \frac{1}{2}\boxed{\langle\Psi^N|\hat{W}|\Psi^N\rangle}$$

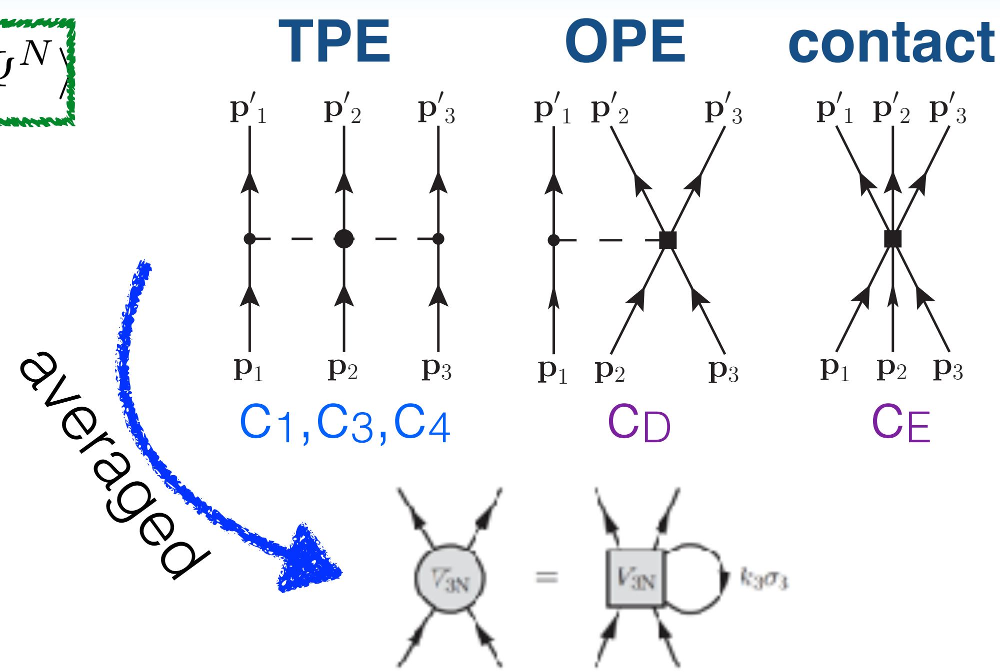

The need for 3-body nuclear forces

Koltun sumrule

$$\frac{E}{A} = \frac{\nu}{\rho} \int \frac{d^3p}{(2\pi)^3} \int \frac{d\omega}{2\pi} \frac{1}{2} \left\{ \frac{p^2}{2m} + \omega \right\} \boxed{\mathcal{A}(p,\omega)} f(\omega) - \frac{1}{2} \boxed{\langle \Psi^N | \hat{W} | \Psi^N \rangle}$$

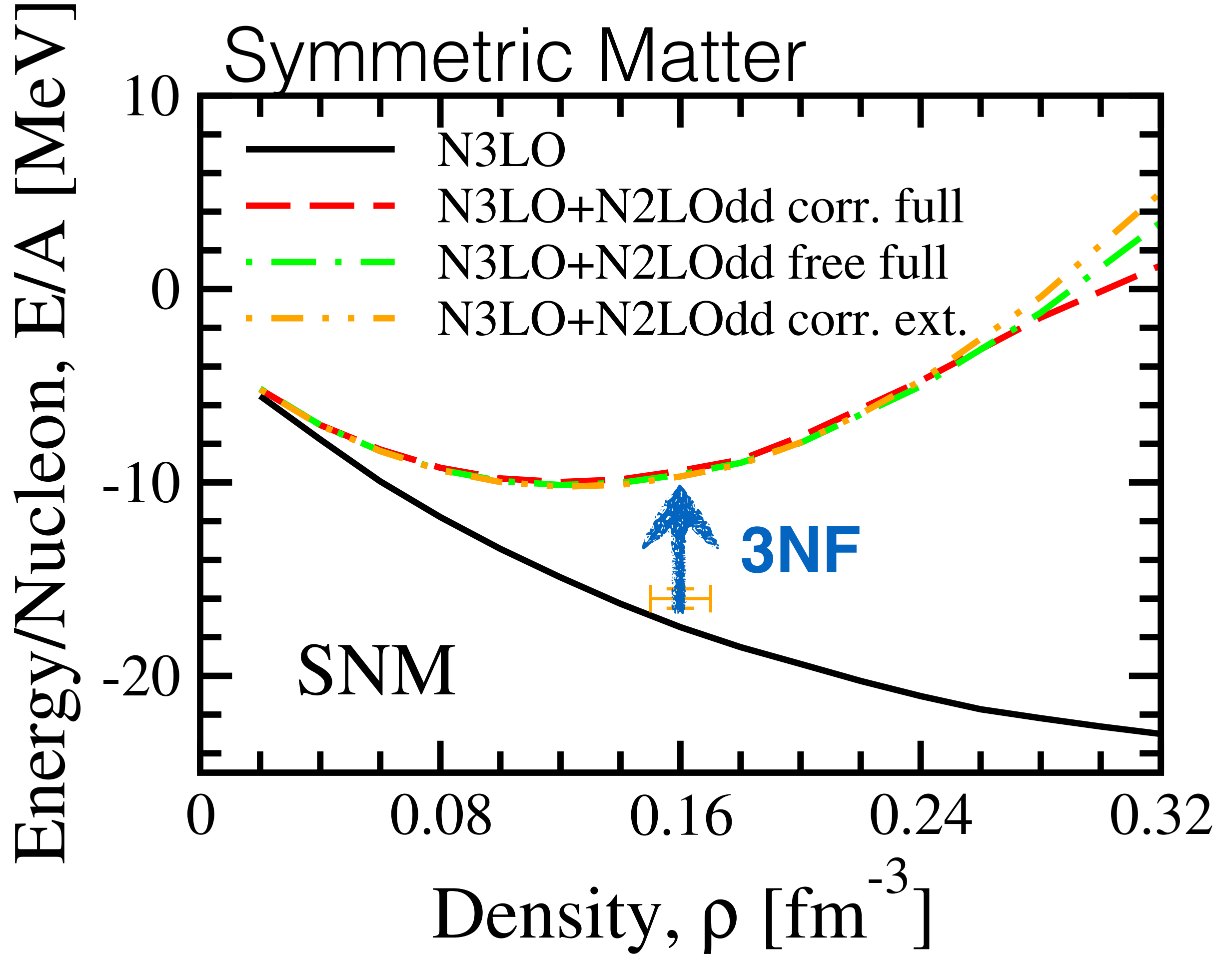

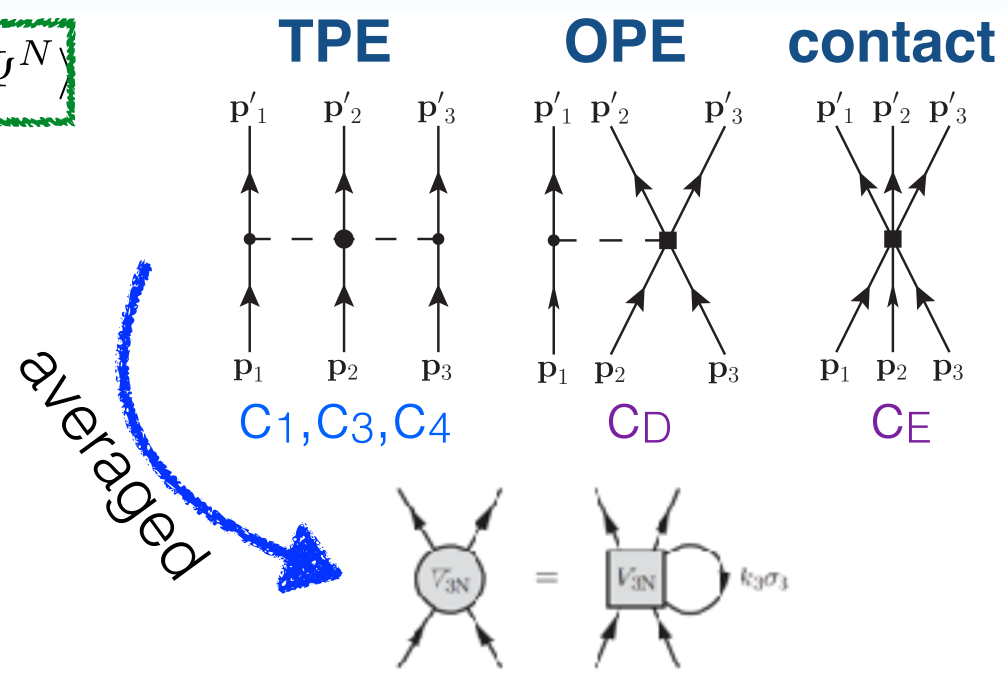

- Improved prediction of saturation density

Carbone, Rios, Polls, PRC 88, 044302 (2013)
Carbone, Rios, Polls, PRC 90, 054322 (2014)

The need for 3-body nuclear forces

Koltun sumrule

$$\frac{E}{A} = \frac{\nu}{\rho} \int \frac{d^3p}{(2\pi)^3} \int \frac{d\omega}{2\pi} \frac{1}{2} \left\{ \frac{p^2}{2m} + \omega \right\} \boxed{\mathcal{A}(p,\omega)} f(\omega) - \frac{1}{2} \boxed{\langle \Psi^N | \hat{W} | \Psi^N \rangle}$$

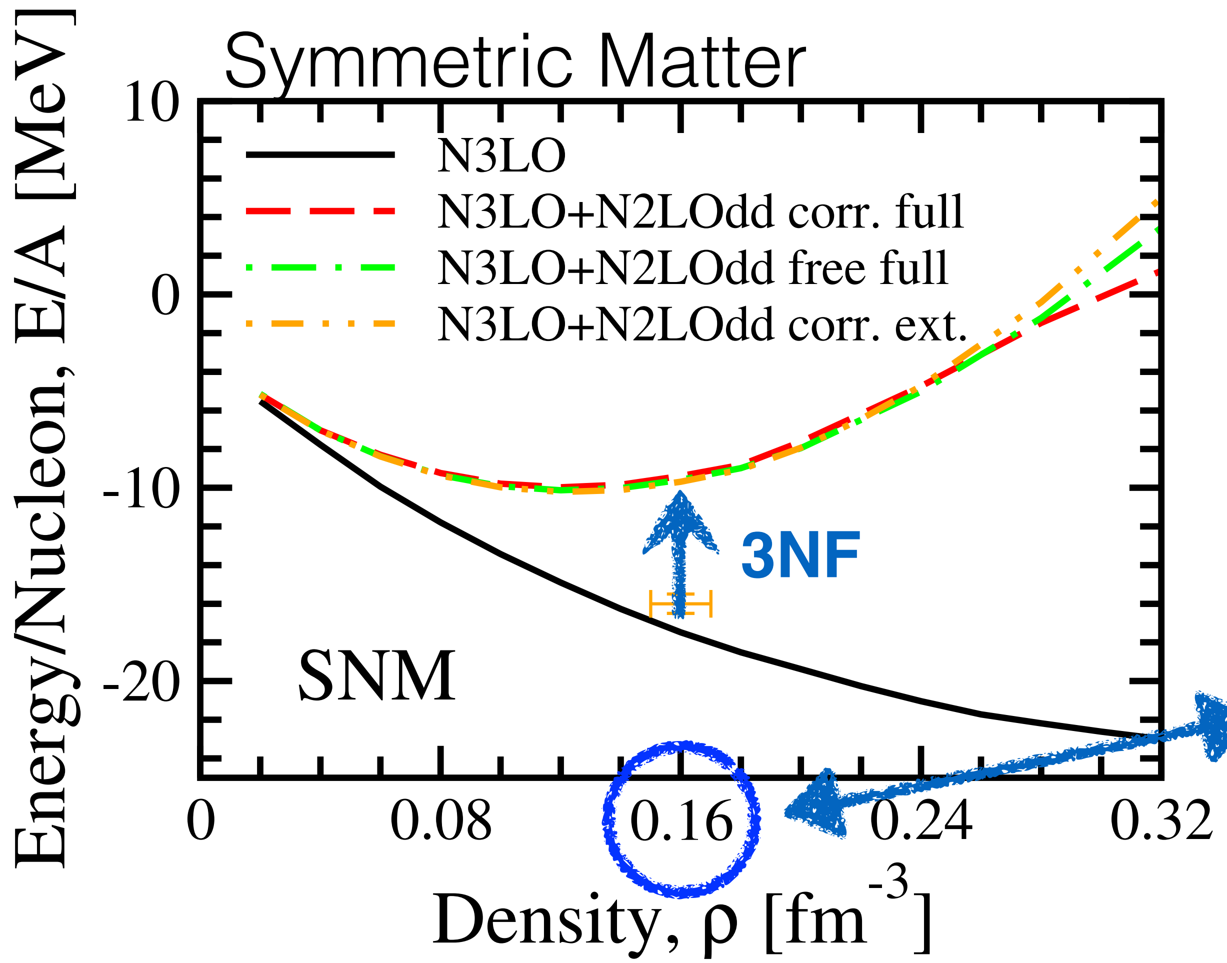

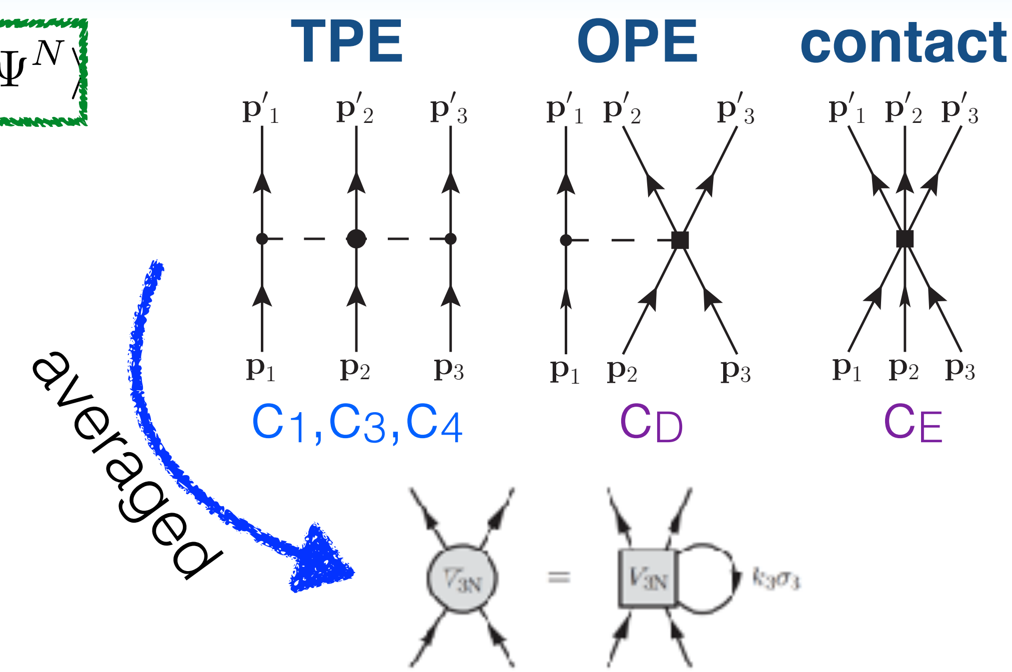

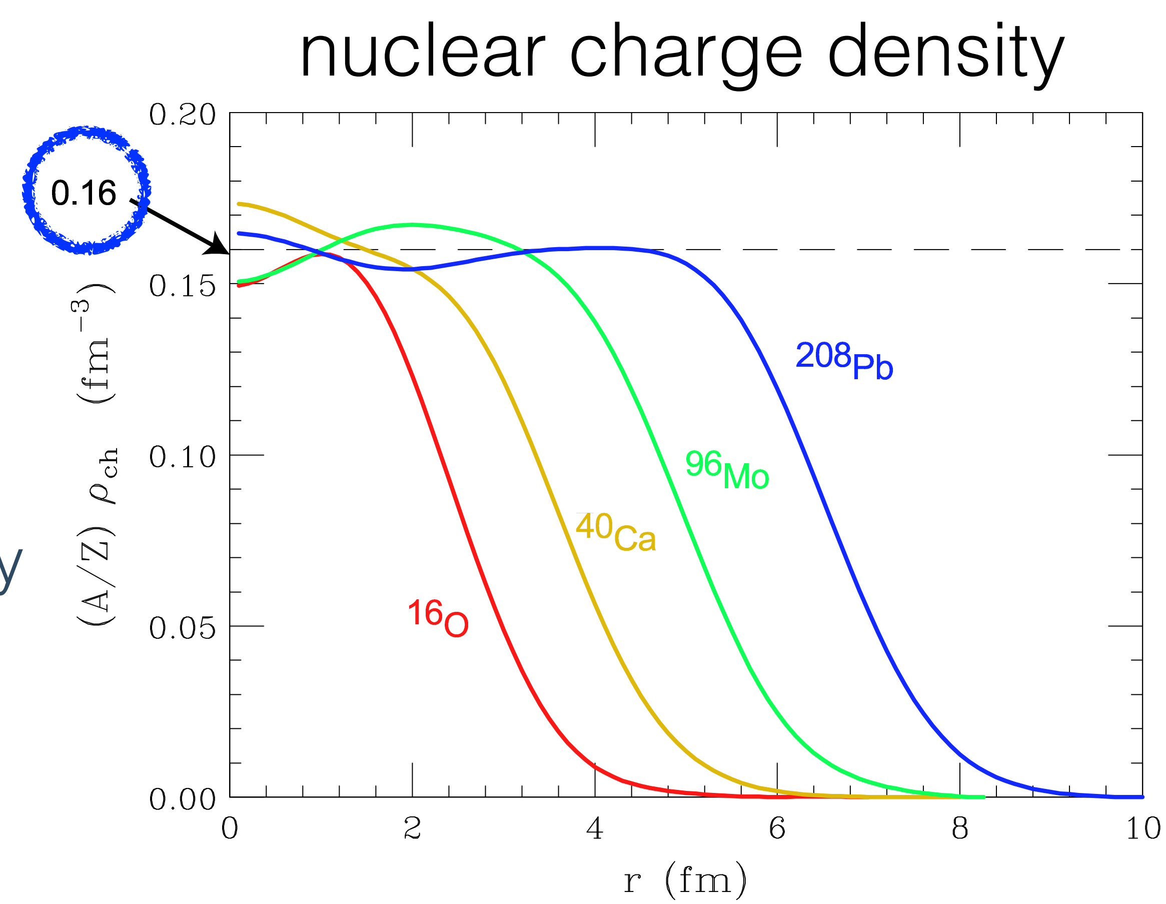

Courtesy of O. Benhar

- Improved prediction of saturation density

Carbone, Rios, Polls, PRC 88, 044302 (2013)
Carbone, Rios, Polls, PRC 90, 054322 (2014)

The need for 3-body nuclear forces

Koltun sumrule

$$\frac{E}{A} = \frac{\nu}{\rho} \int \frac{d^3p}{(2\pi)^3} \int \frac{d\omega}{2\pi} \frac{1}{2} \left\{ \frac{p^2}{2m} + \omega \right\} \mathcal{A}(p,\omega) f(\omega) - \frac{1}{2} \langle \Psi^N | \hat{W} | \Psi^N \rangle$$

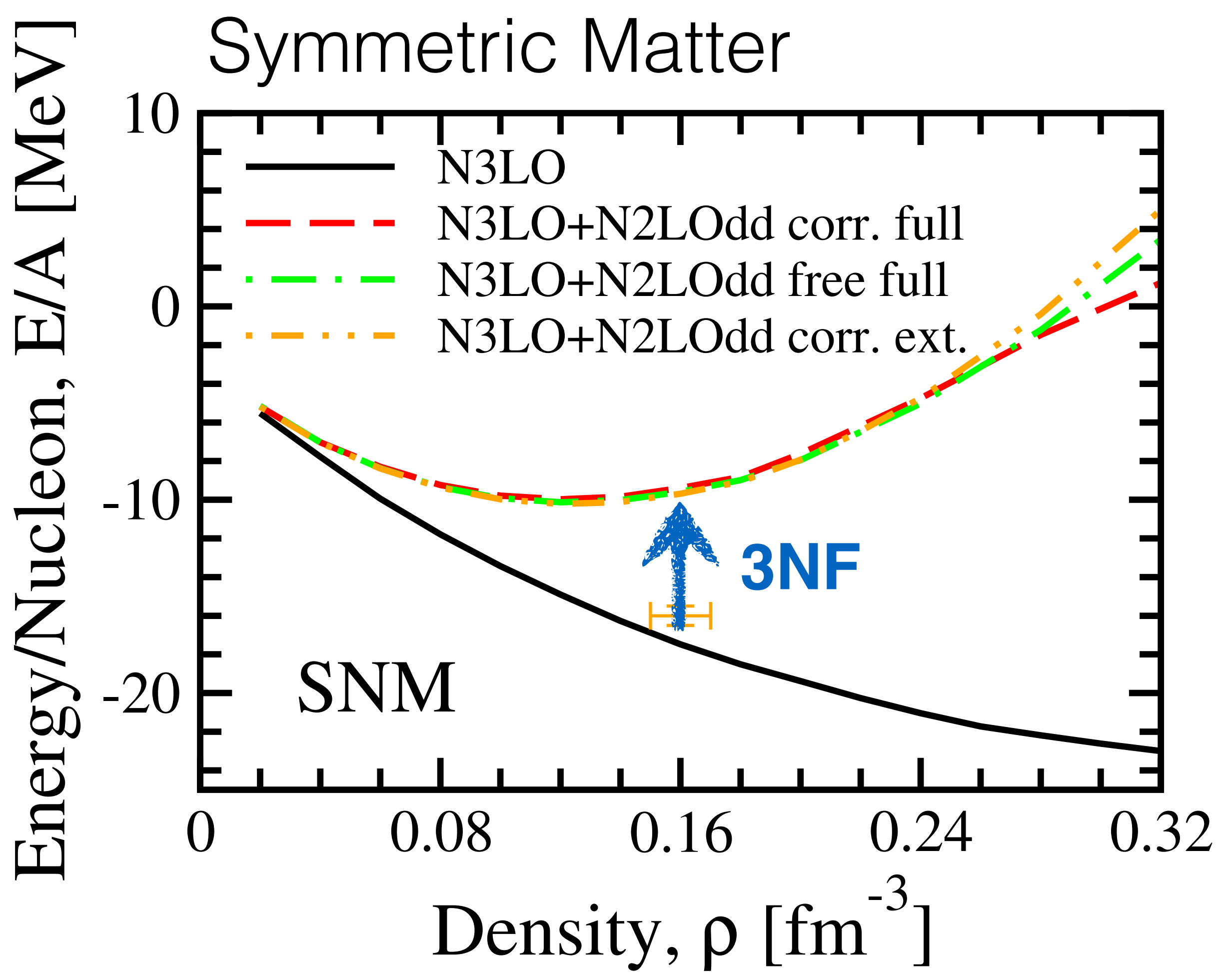

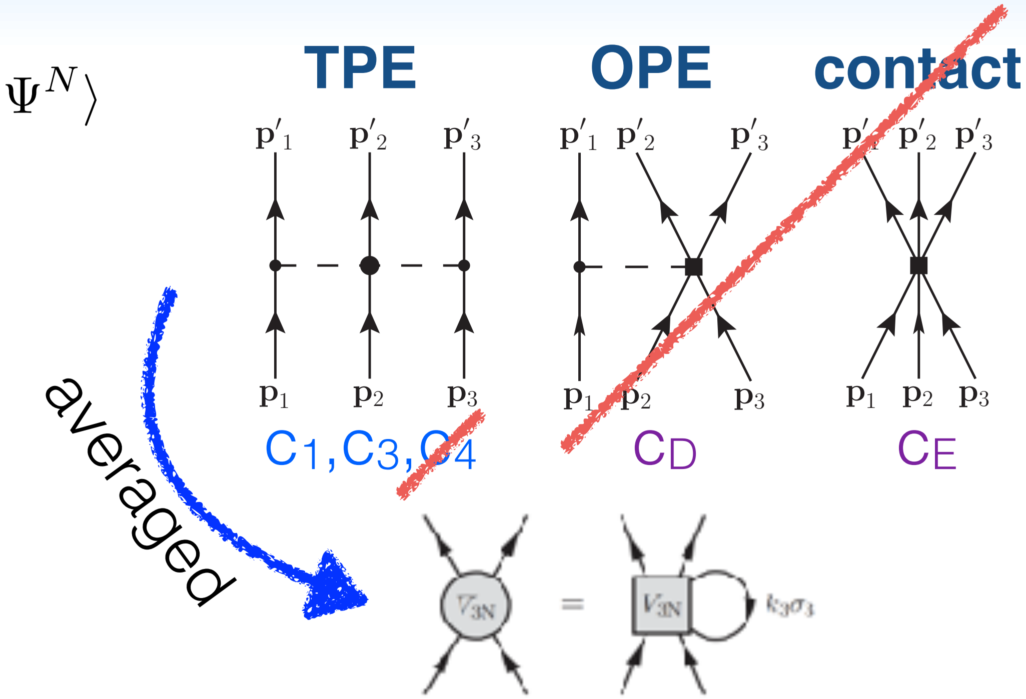

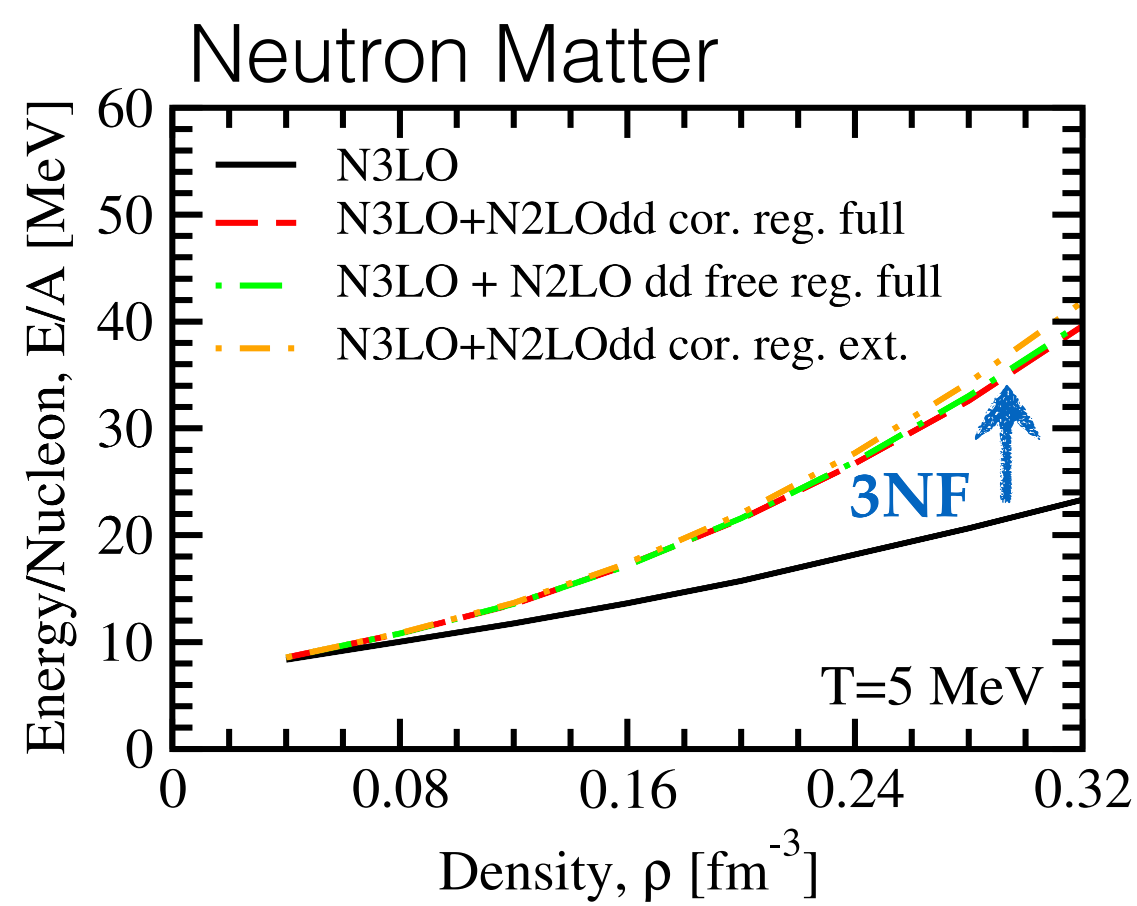

- Improved prediction of saturation density
- Neutron matter energy stiffens

Carbone, Rios, Polls, PRC 88, 044302 (2013)
Carbone, Rios, Polls, PRC 90, 054322 (2014)

Saturation point according to different Hamiltonians

Carbone *(in preparation)*

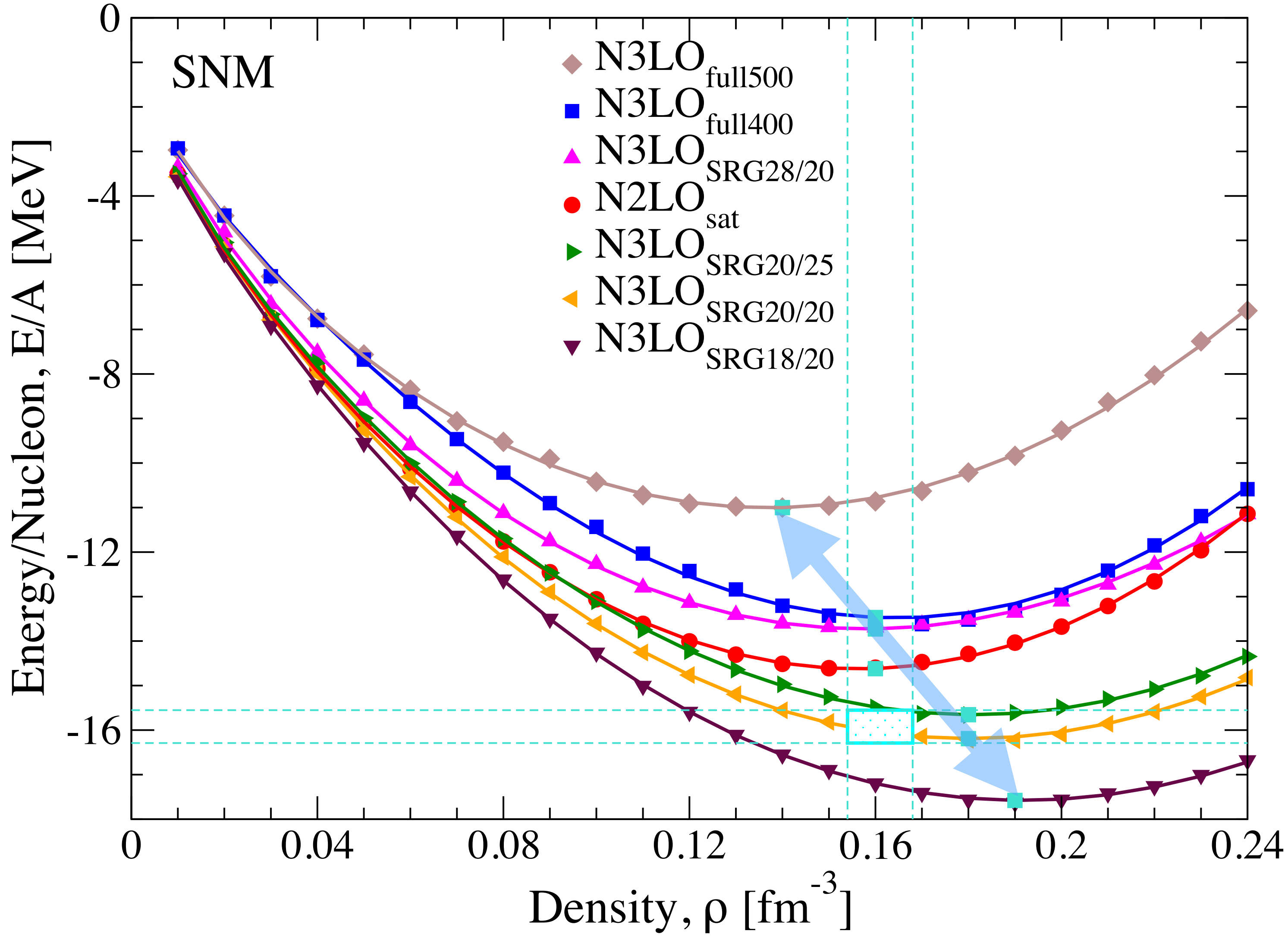

Chiral hamiltonians

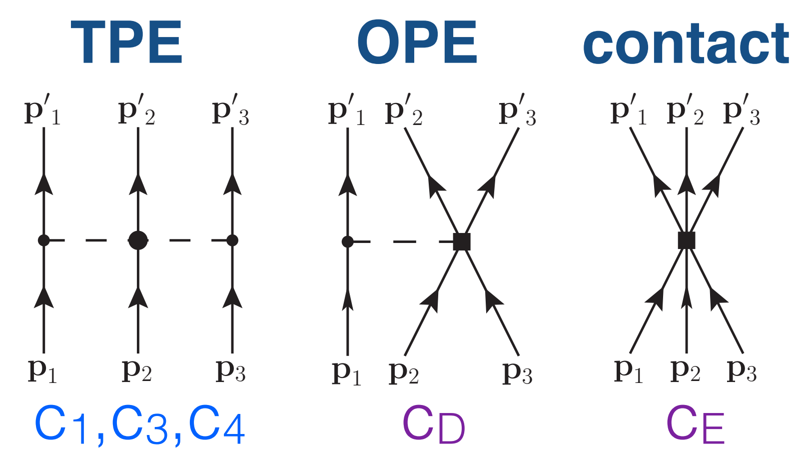

Some low-energy constants are fit to few-body properties

Theoretical uncertainty band

based on the nuclear hamiltonian

Saturation point according to different Hamiltonians

Carbone *(in preparation)*

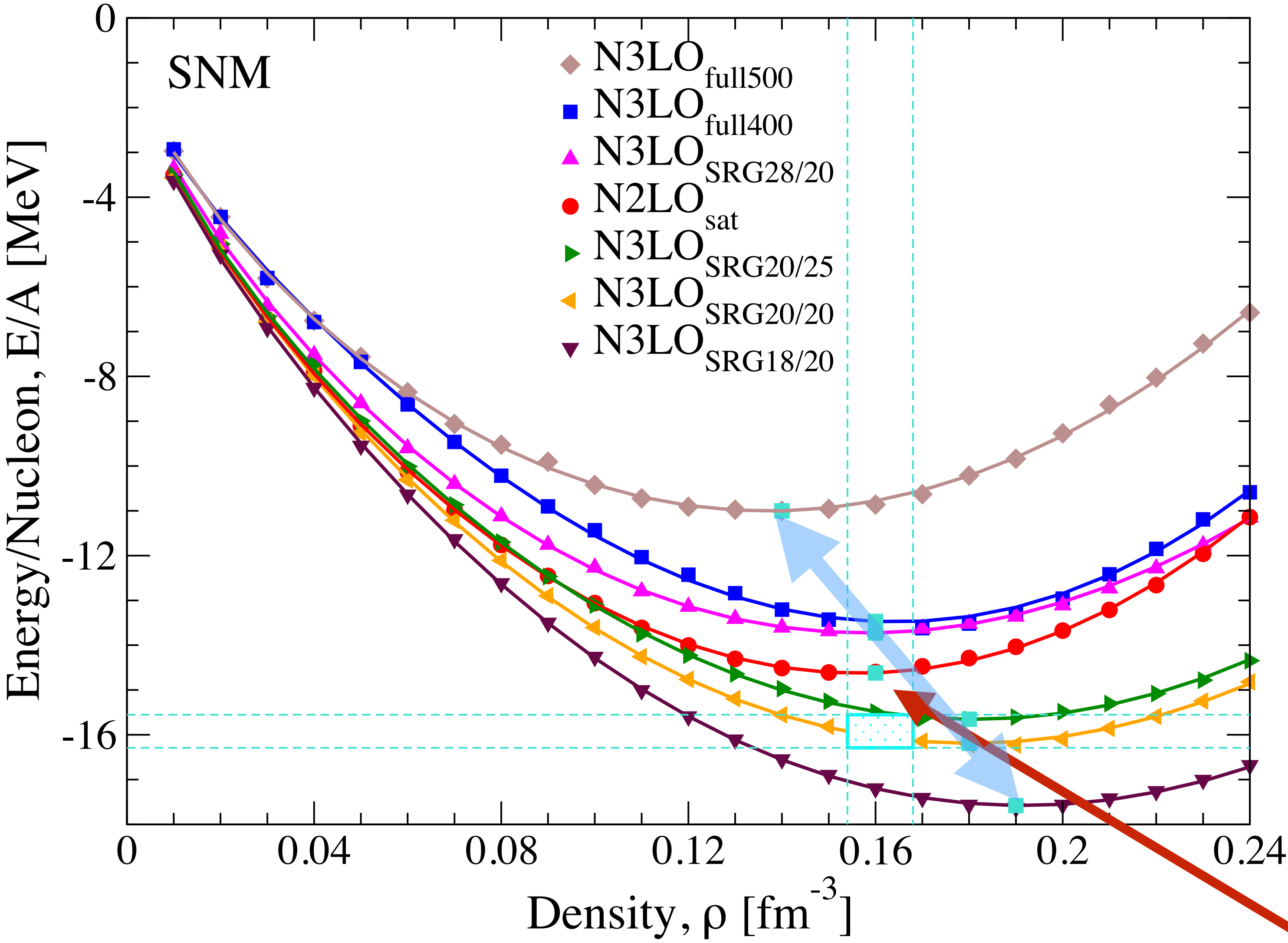

Chiral hamiltonians

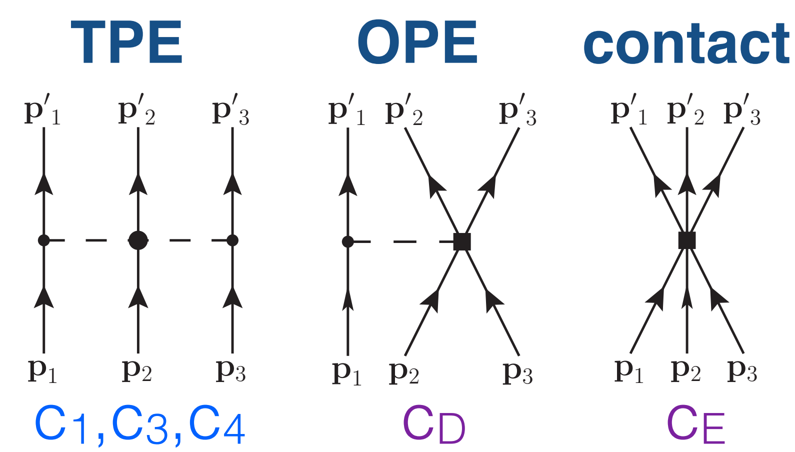

Some low-energy constants are fit to few-body properties

Theoretical uncertainty band

based on the nuclear hamiltonian

N2LOsat (2N+3N):
predicts saturation density
fit to mid-mass nuclei too

Saturation point according to different Hamiltonians

Carbone *(in preparation)*

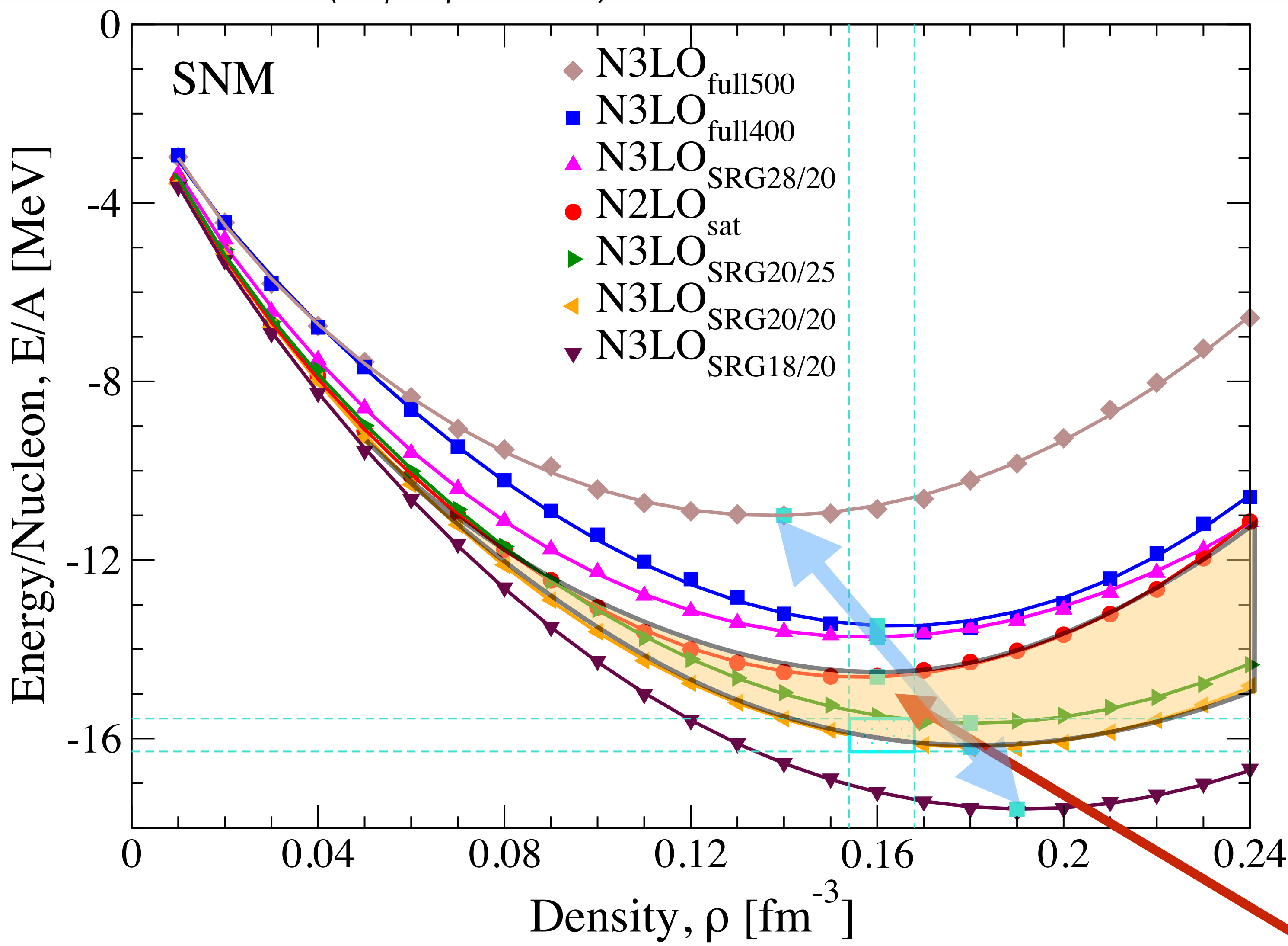

Chiral hamiltonians

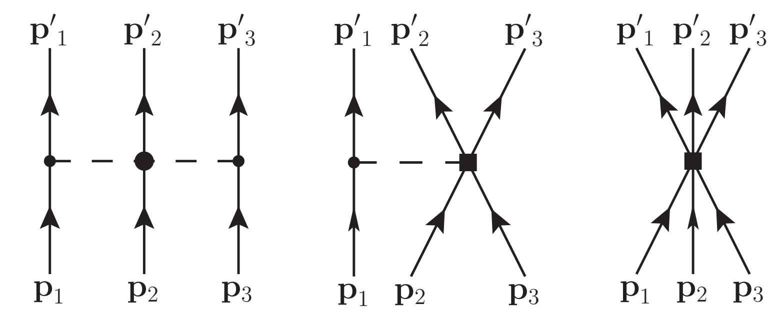

C_1, C_3, C_4 C_D C_E

Some low-energy constants are fit to few-body properties

Theoretical uncertainty band

based on the nuclear hamiltonian

N2LOsat (2N+3N): predicts saturation density fit to mid-mass nuclei too

2N $N2LO_{sat}$+3N N2LO

2N $N3LO_{SRG-1}$+3N N2LO

2N $N3LO_{SRG-2}$+3N N2LO

Predictions for the Symmetry Energy and slope L

Energy of asymmetric matter

$$\frac{E}{A}(\rho,\beta) \simeq \frac{E_{\mathrm{SNM}}}{A}(\rho) + \frac{S}{A}(\rho)\beta^2$$

$\beta = 1$

$$\frac{S}{A}(\rho) \simeq \frac{E_{\mathrm{PNM}}}{A}(\rho) - \frac{E_{\mathrm{SNM}}}{A}(\rho)$$

Symmetry energy

	SRG1	SRG2	SAT
Sv (MeV)	31.6	30.6	25.8
L (MeV)	49.3	48.7	37.4
K (MeV)	290	270	213

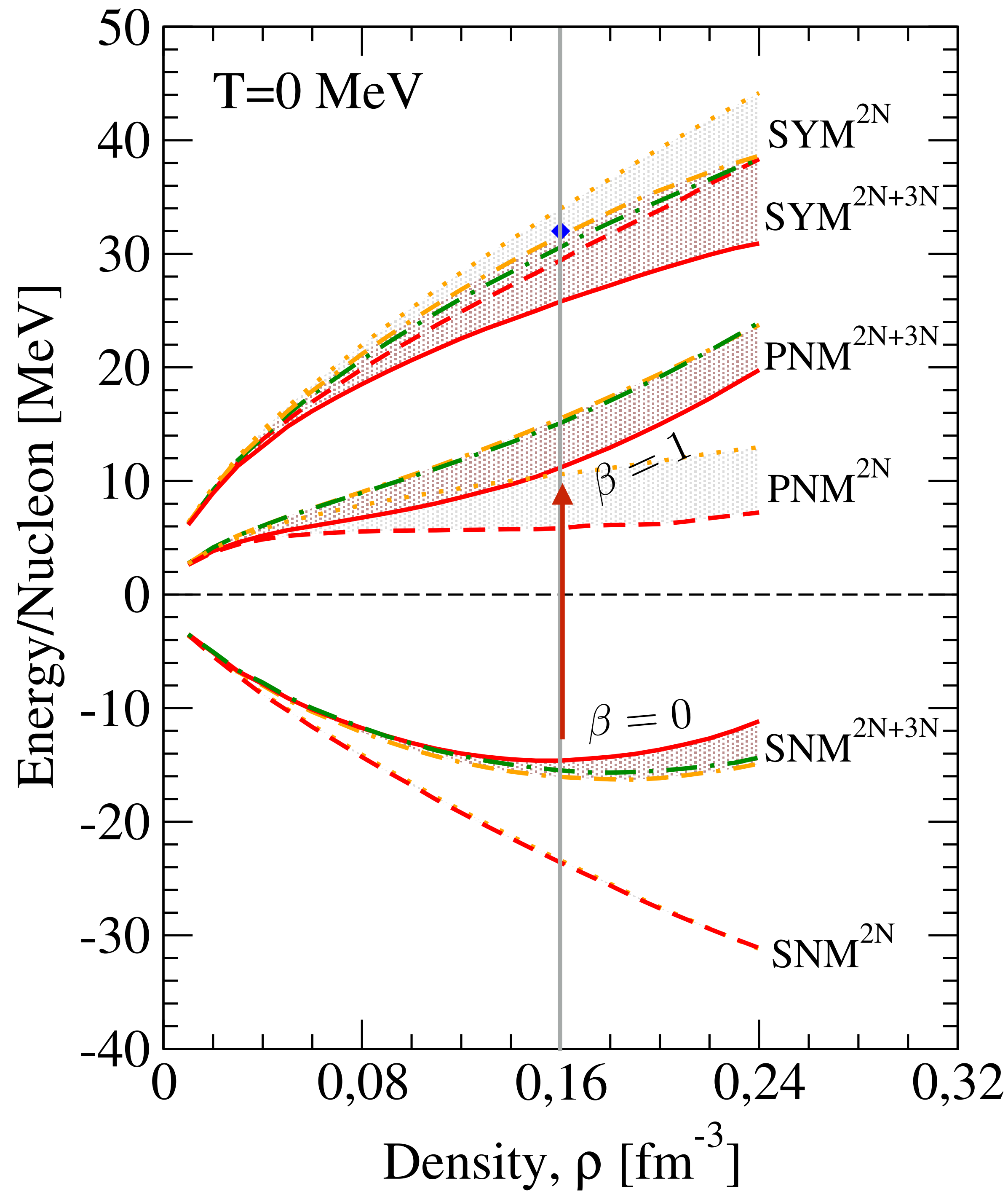

Predictions for the Symmetry Energy and slope L

Energy of asymmetric matter

$$\frac{E}{A}(\rho,\beta) \simeq \frac{E_{\rm SNM}}{A}(\rho) + \frac{S}{A}(\rho)\beta^2$$

$\beta = 1$

$$\frac{S}{A}(\rho) \simeq \frac{E_{\rm PNM}}{A}(\rho) - \frac{E_{\rm SNM}}{A}(\rho)$$

Symmetry energy

	SRG1	SRG2	SAT
Sv (MeV)	31.6	30.6	25.8
L (MeV)	49.3	48.7	37.4
K (MeV)	290	270	213

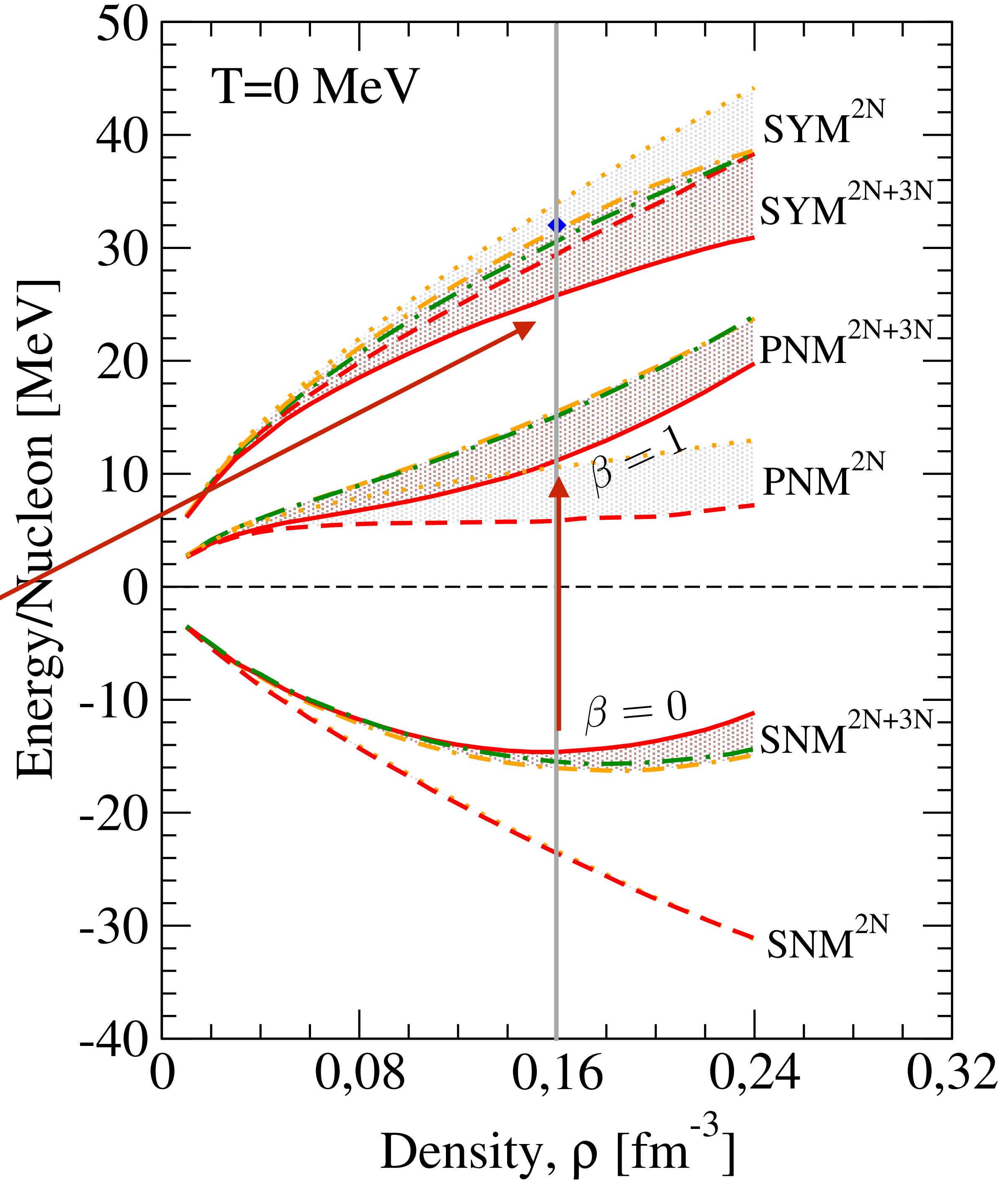

Predictions for the Symmetry Energy and slope L

Energy of asymmetric matter

$$\frac{E}{A}(\rho,\beta) \simeq \frac{E_{\mathrm{SNM}}}{A}(\rho) + \frac{S}{A}(\rho)\beta^2$$

$\beta = 1$

$$\frac{S}{A}(\rho) \simeq \frac{E_{\mathrm{PNM}}}{A}(\rho) - \frac{E_{\mathrm{SNM}}}{A}(\rho)$$

Symmetry energy

	SRG1	SRG2	SAT
Sv (MeV)	31.6	30.6	25.8
L (MeV)	49.3	48.7	37.4
K (MeV)	290	270	213

Similar saturating points but different symmetry energy predictions

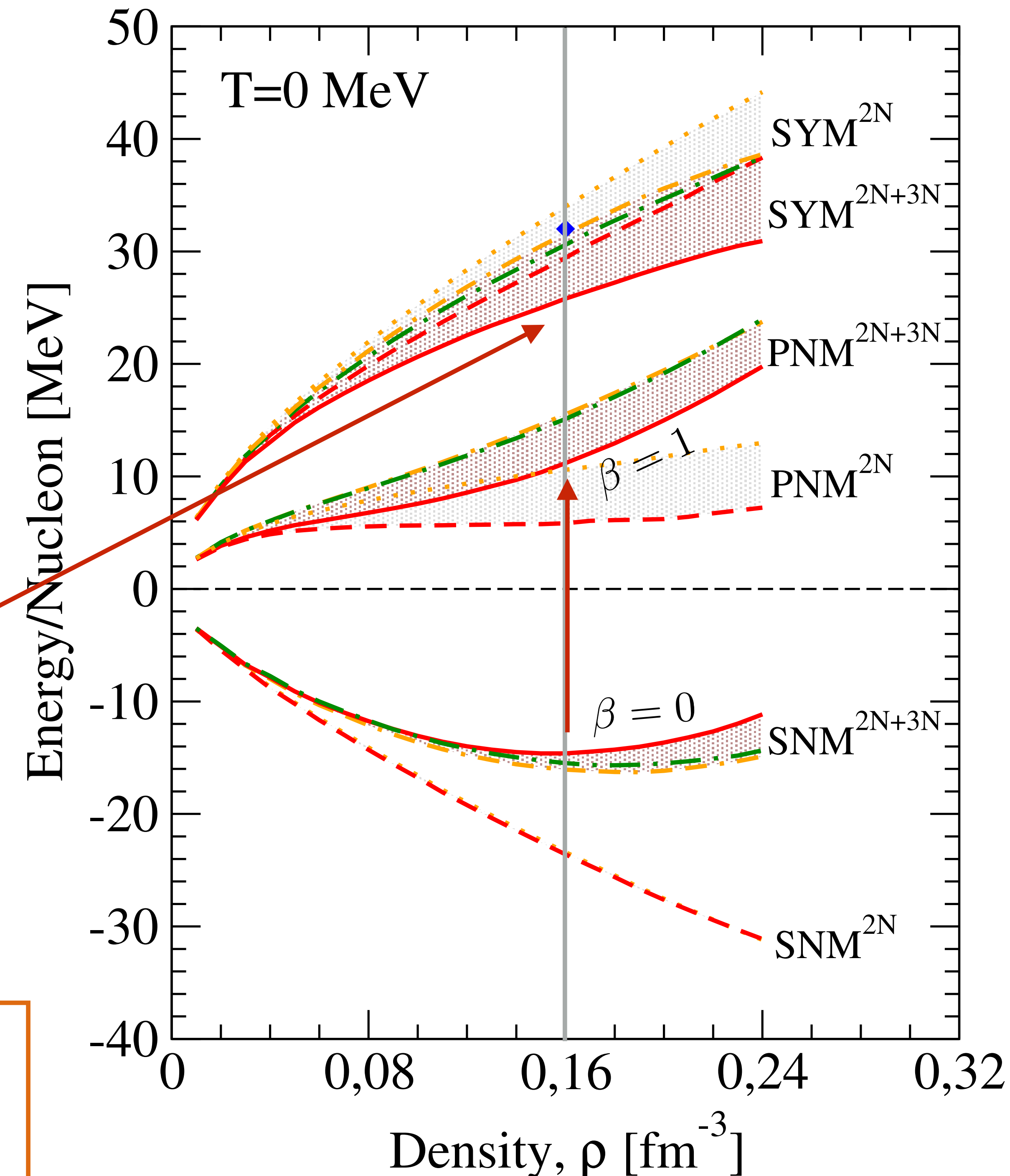

Constraining stellar equations of state from ab initio results

Drischler, Carbone, Hebeler, Schwenk PRC94, 054307 (2016)

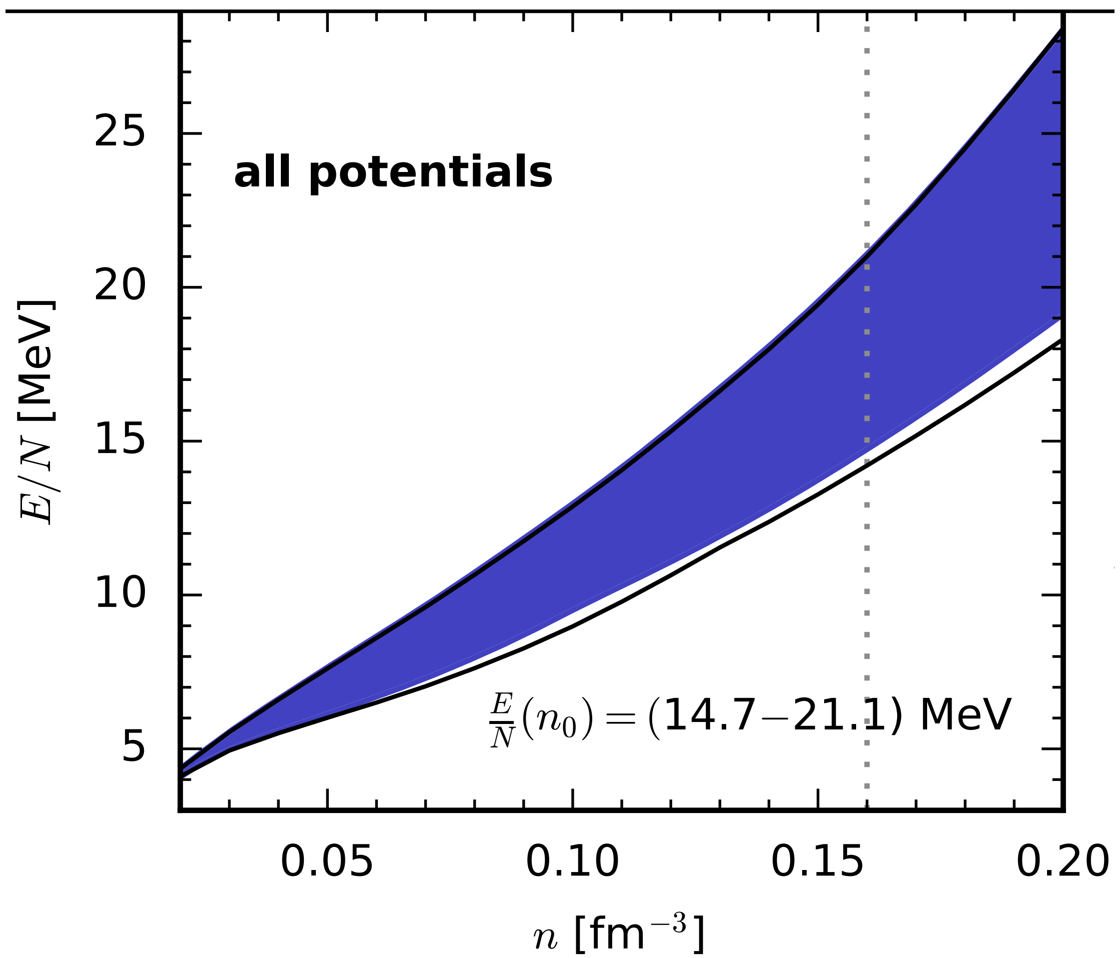

1. Pure neutron matter with chiral forces

Constraining stellar equations of state from ab initio results

Drischler, Carbone, Hebeler, Schwenk PRC94, 054307 (2016)

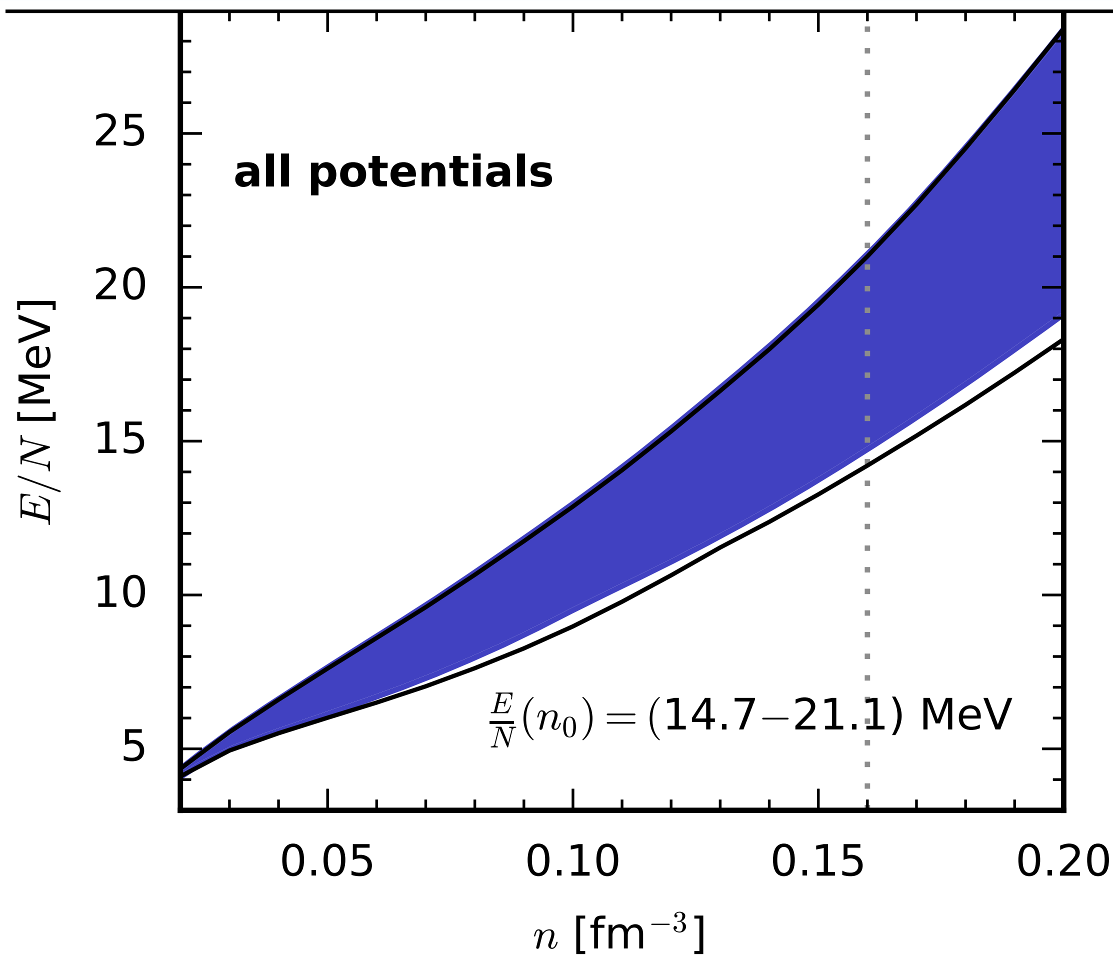

1.
Pure neutron matter with chiral forces

2.
Ab initio uncertainty around saturation pins down probability distribution of neutron star radius

$$12.00 < R_{1.4} < 13.45$$

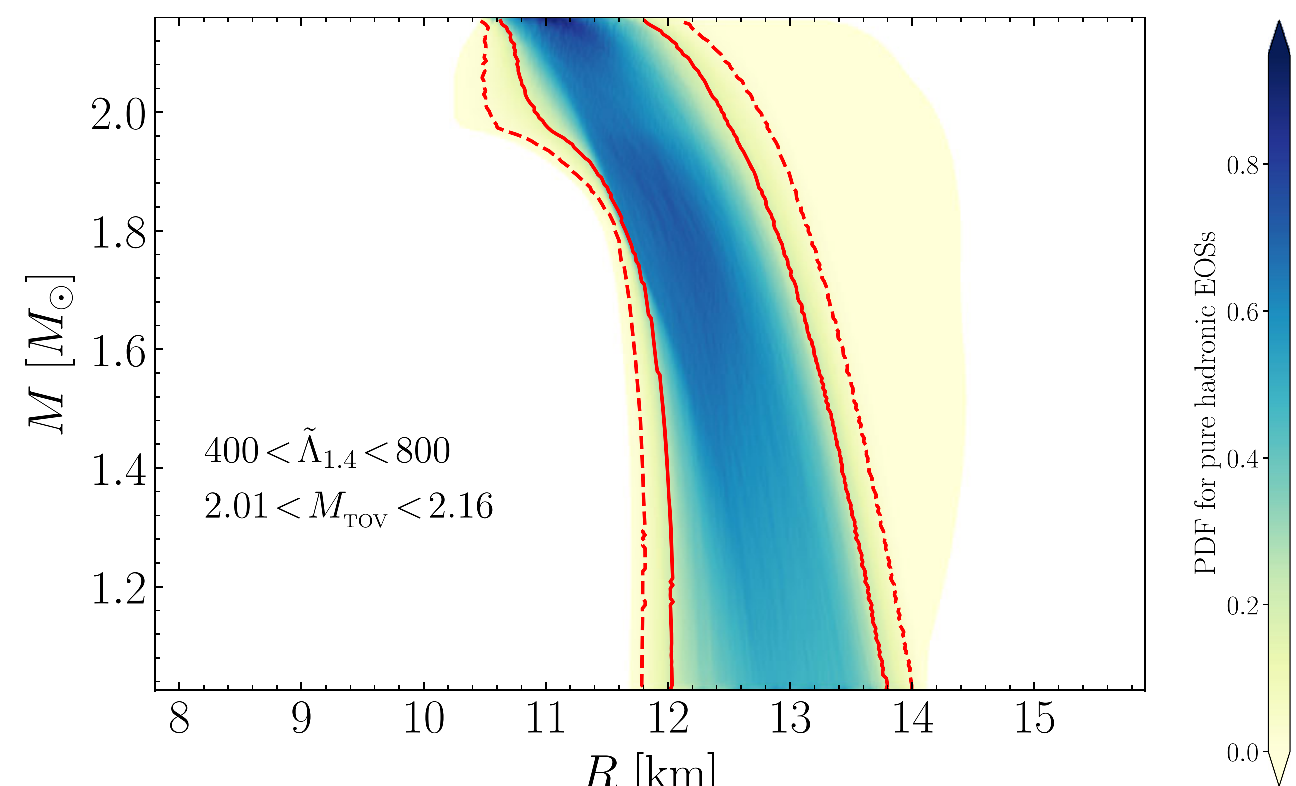

Most, Weih, Rezzolla & Schaffner-Bielich, PRL120, 261103 (2018)

Free energy and pressure at varying temperature

Symmetric nuclear matter

Free-energy	Pressure
$F = E - TS$	$P = \rho(\mu - F)$

increasing temperature

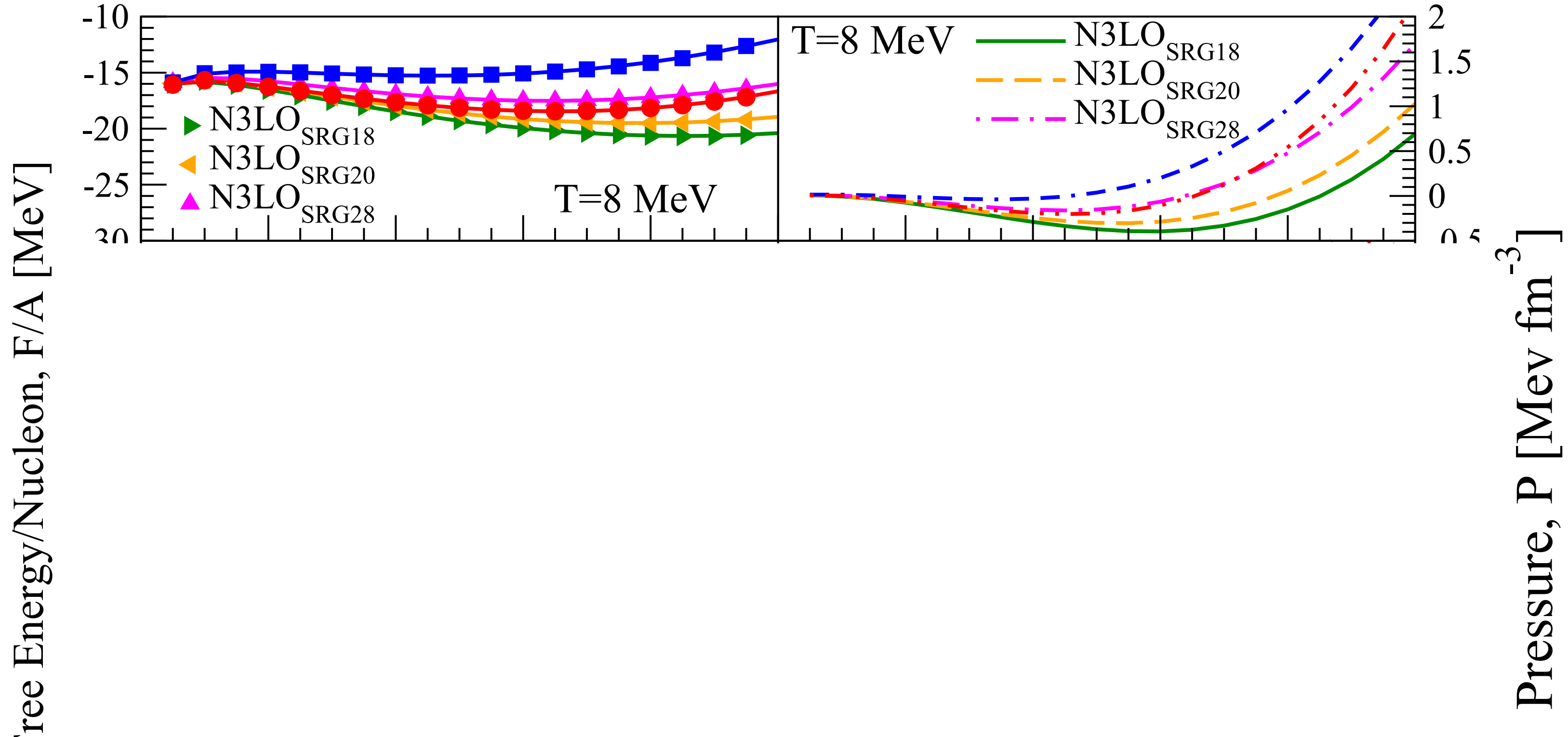

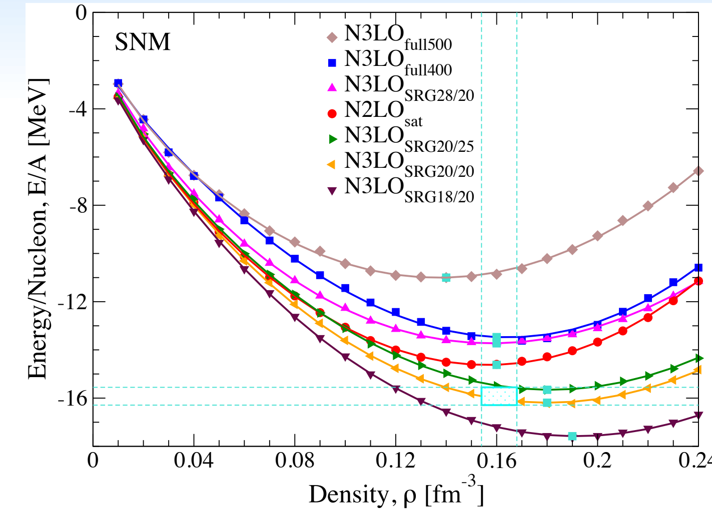

- similar behaviour to zero T energy
- Concave pressure behavior: liquid-gas phase transition

2N N3LO EM500 (SRG L=1.8fm^{-1})+ 3N N2LO (L=2.0fm^{-1})
2N N3LO EM500 (SRG L=2.0fm^{-1})+ 3N N2LO (L=2.0m^{-1})
2N N3LO EM500 (SRG L=2.8fm^{-1})+ 3N N2LO (L=2.0fm^{-1})
N2LOsat 2N + 3N
2N N3LO EM500 + 3N N2LO

Carbone, Polls, Rios PRC 98 025804 (2018)

Free energy and pressure at varying temperature

Free-energy	Pressure
$F = E - TS$	$P = \rho(\mu - F)$

increasing temperature

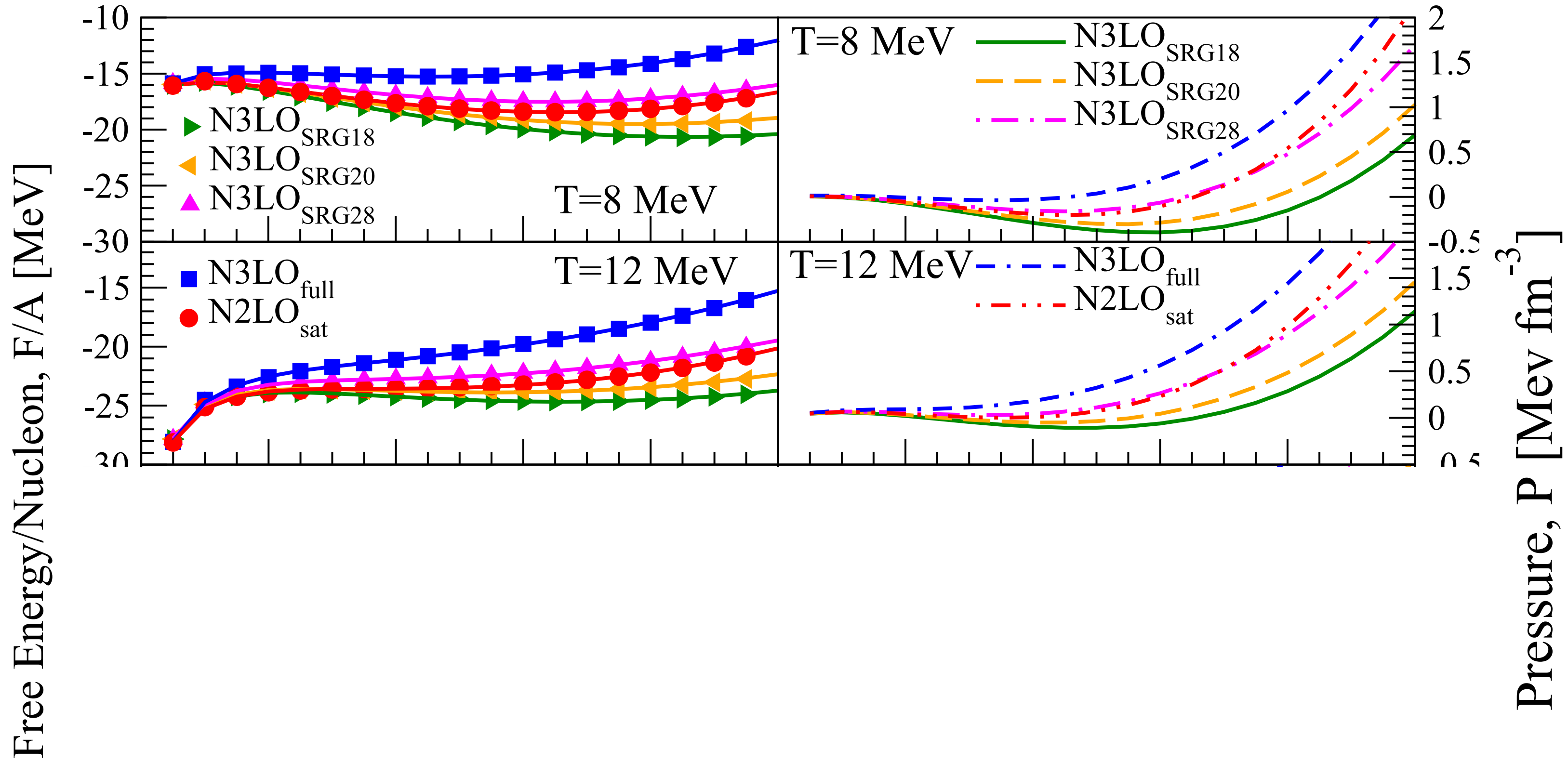

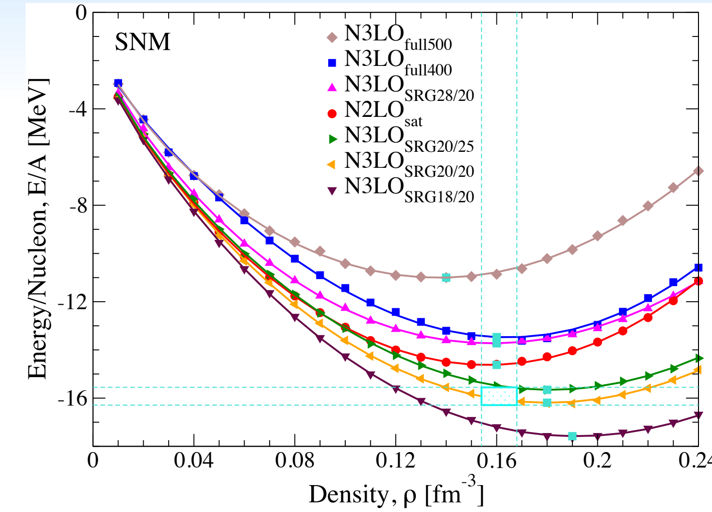

- similar behaviour to zero T energy
- Concave pressure behavior: liquid-gas phase transition

2N N3LO EM500 (SRG L=1.8fm^{-1})+ 3N N2LO (L=2.0fm^{-1})
2N N3LO EM500 (SRG L=2.0fm^{-1})+ 3N N2LO (L=2.0m^{-1})
2N N3LO EM500 (SRG L=2.8fm^{-1})+ 3N N2LO (L=2.0fm^{-1})
N2LOsat 2N + 3N
2N N3LO EM500 + 3N N2LO

Carbone, Polls, Rios PRC 98 025804 (2018)

Free energy and pressure at varying temperature

Symmetric nuclear matter

Free-energy

$$F = E - TS$$

Pressure

$$P = \rho(\mu - F)$$

increasing temperature

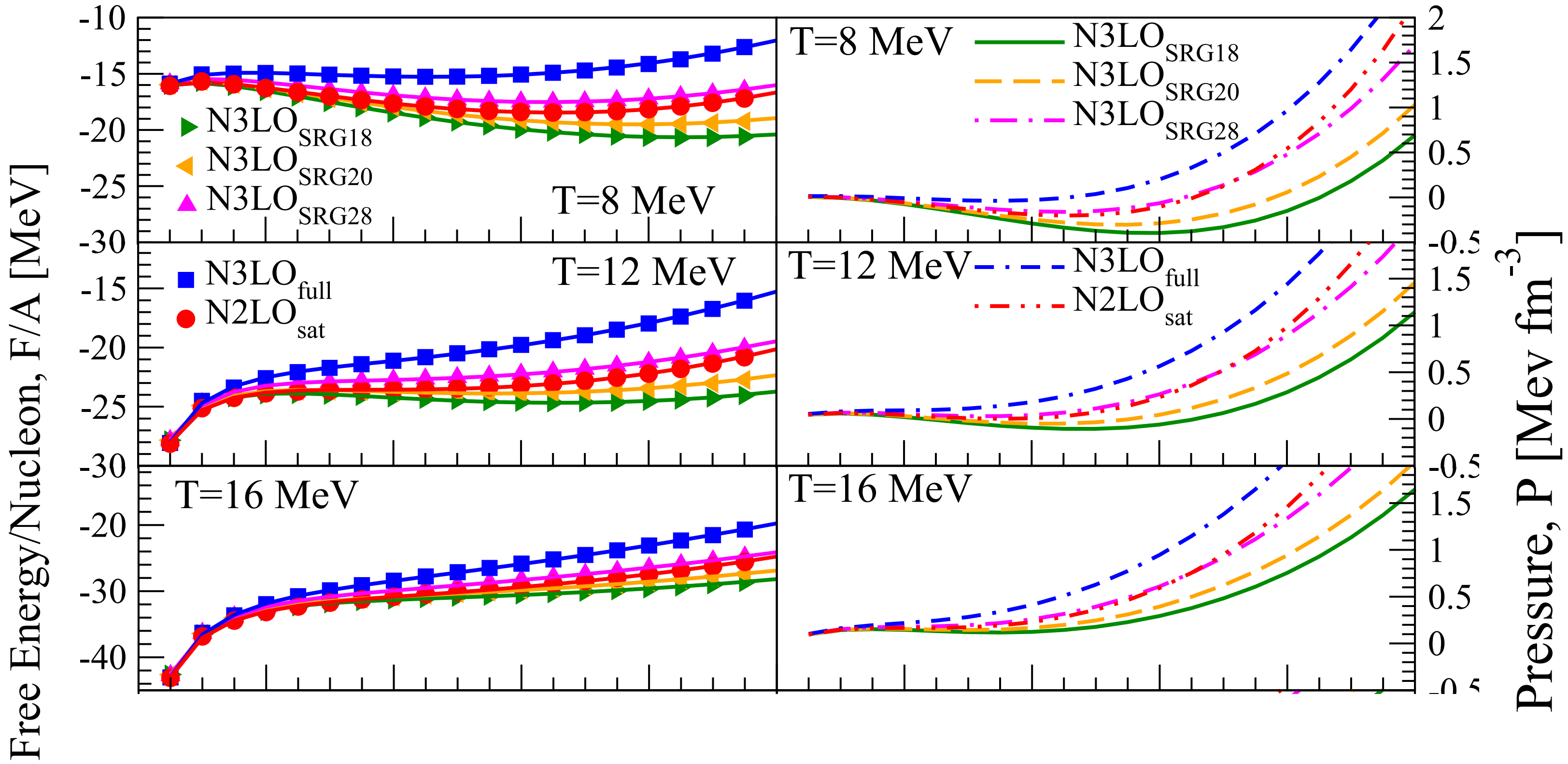

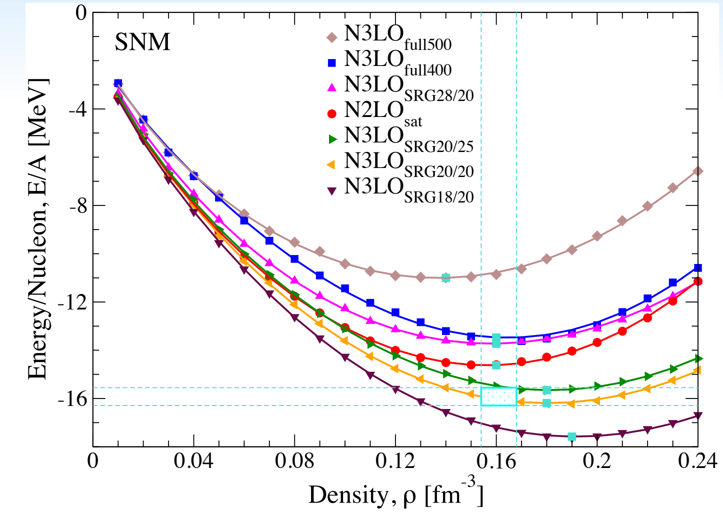

- similar behaviour to zero T energy
- Concave pressure behavior: liquid-gas phase transition

2N N3LO EM500 (SRG L=1.8fm^{-1})+ 3N N2LO (L=2.0fm^{-1})

2N N3LO EM500 (SRG L=2.0fm^{-1})+ 3N N2LO (L=2.0m^{-1})

2N N3LO EM500 (SRG L=2.8fm^{-1})+ 3N N2LO (L=2.0fm^{-1})

N2LOsat 2N + 3N

2N N3LO EM500 + 3N N2LO

Carbone, Polls, Rios PRC 98 025804 (2018)

Symmetric nuclear matter

Free energy and pressure at varying temperature

Free-energy $F = E - TS$

Pressure $P = \rho(\mu - F)$

increasing temperature

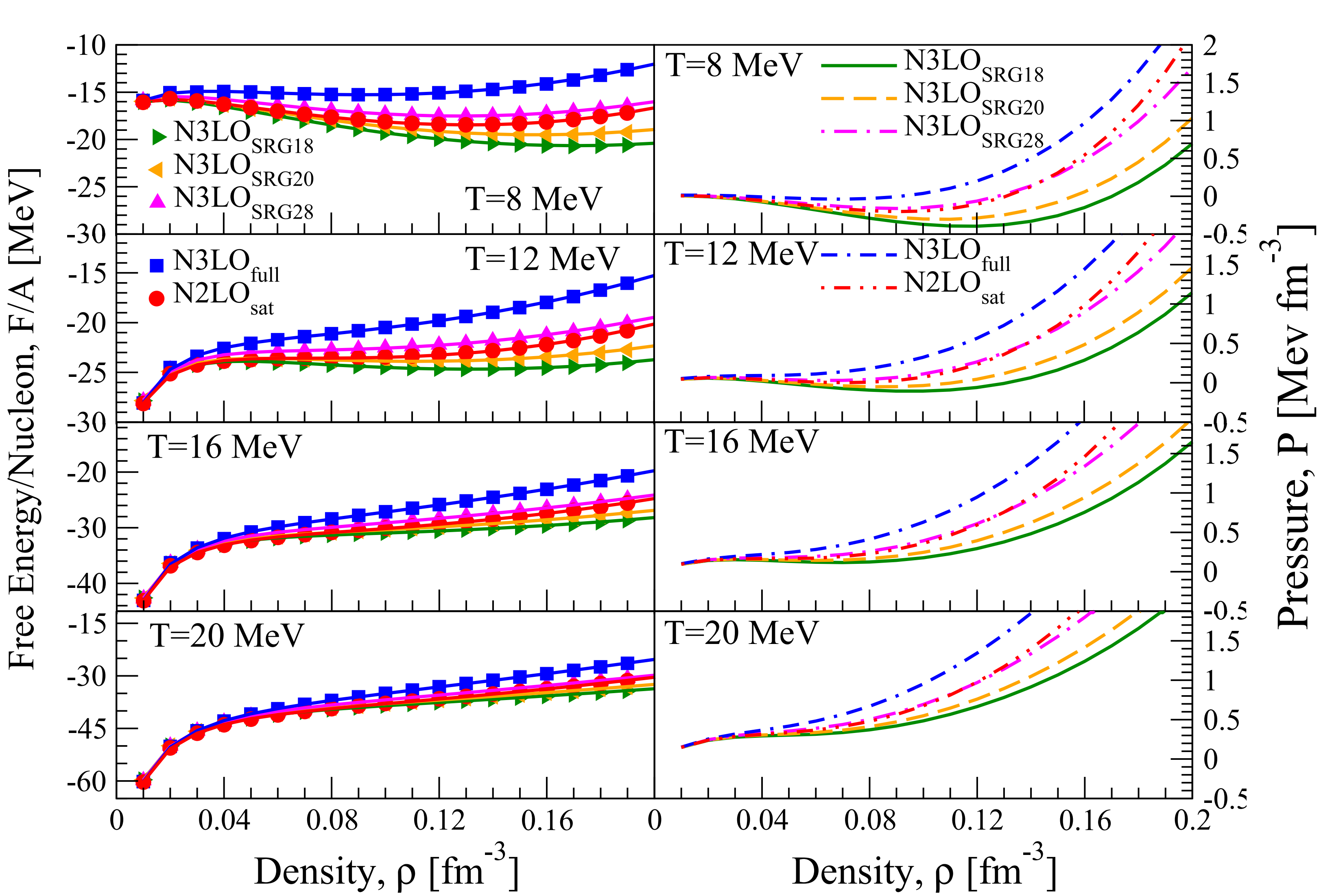

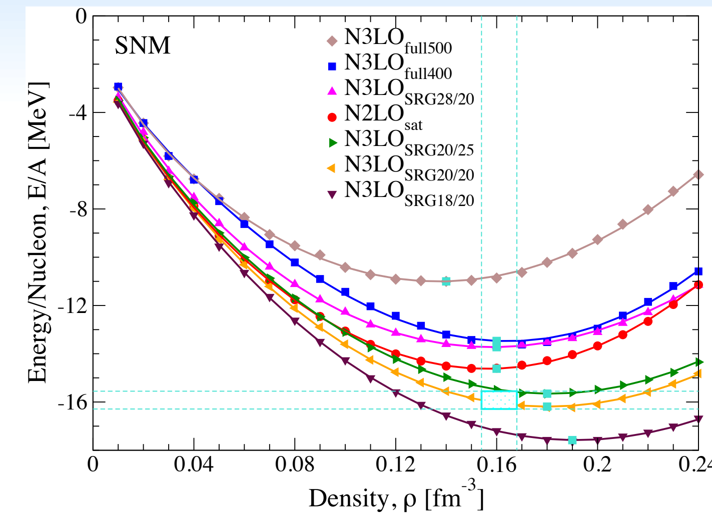

- similar behaviour to zero T energy
- Concave pressure behavior: liquid-gas phase transition

2N N3LO EM500 (SRG L=1.8fm^{-1})+ 3N N2LO (L=2.0fm^{-1})
2N N3LO EM500 (SRG L=2.0fm^{-1})+ 3N N2LO (L=2.0m^{-1})
2N N3LO EM500 (SRG L=2.8fm^{-1})+ 3N N2LO (L=2.0fm^{-1})
N2LOsat 2N + 3N
2N N3LO EM500 + 3N N2LO

Carbone, Polls, Rios PRC 98 025804 (2018)

Many-body uncertainty for finite-T properties

Symmetric nuclear matter

Free-energy

$$F = E - TS$$

Pressure

$$P = \rho(\mu - F)$$

evolved potentials to unevolved

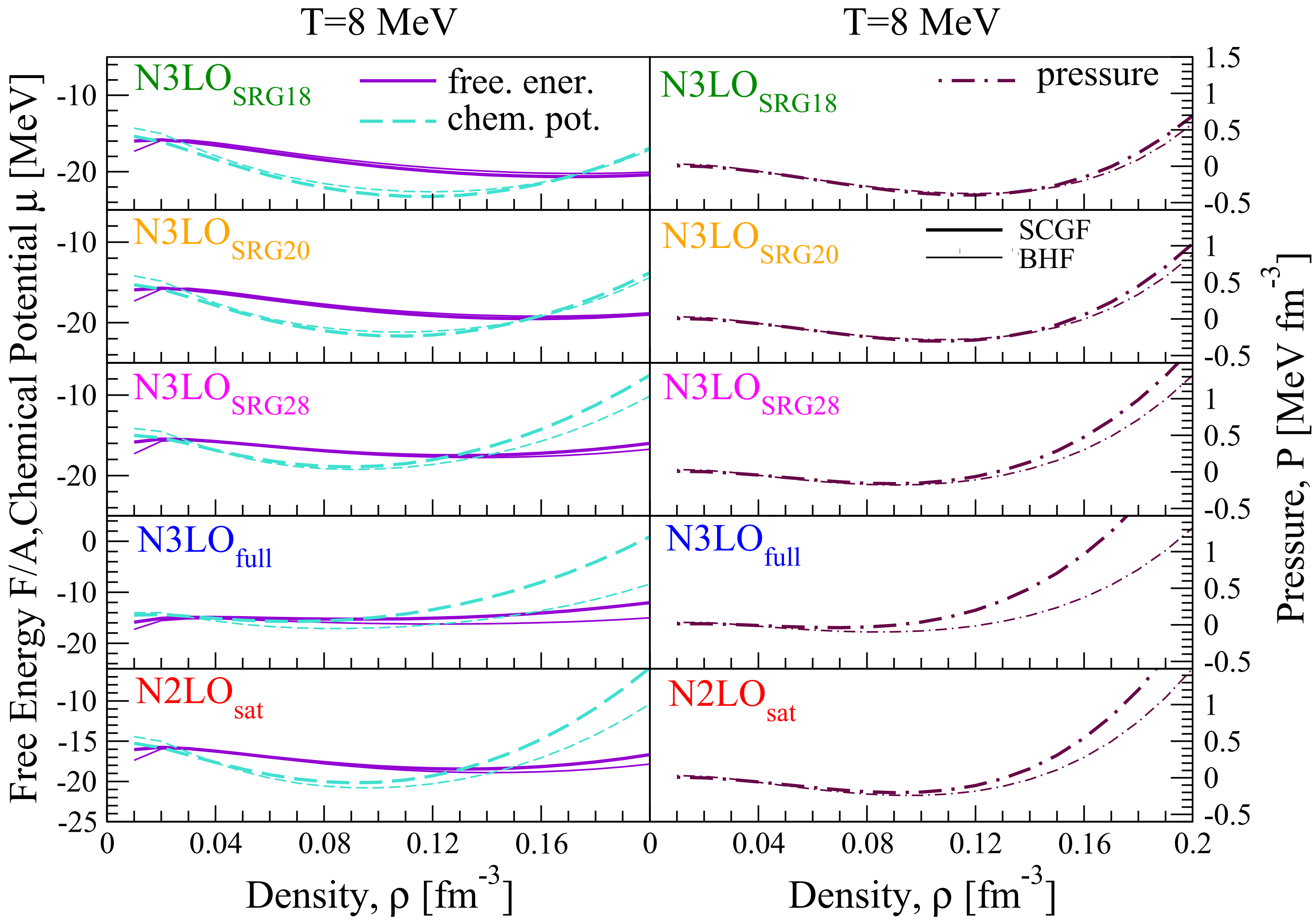

2N N3LO EM500 (SRG L=1.8fm^{-1})+ 3N N2LO (L=2.0fm^{-1})
2N N3LO EM500 (SRG L=2.0fm^{-1})+ 3N N2LO (L=2.0m^{-1})
2N N3LO EM500 (SRG L=2.8fm^{-1})+ 3N N2LO (L=2.0fm^{-1})
N2LOsat 2N + 3N
2N N3LO EM500 + 3N N2LO

Carbone, Polls, Rios PRC 98 025804 (2018)

Many-body uncertainty for finite-T properties

Free-energy

$$F = E - TS$$

Pressure

$$P = \rho(\mu - F)$$

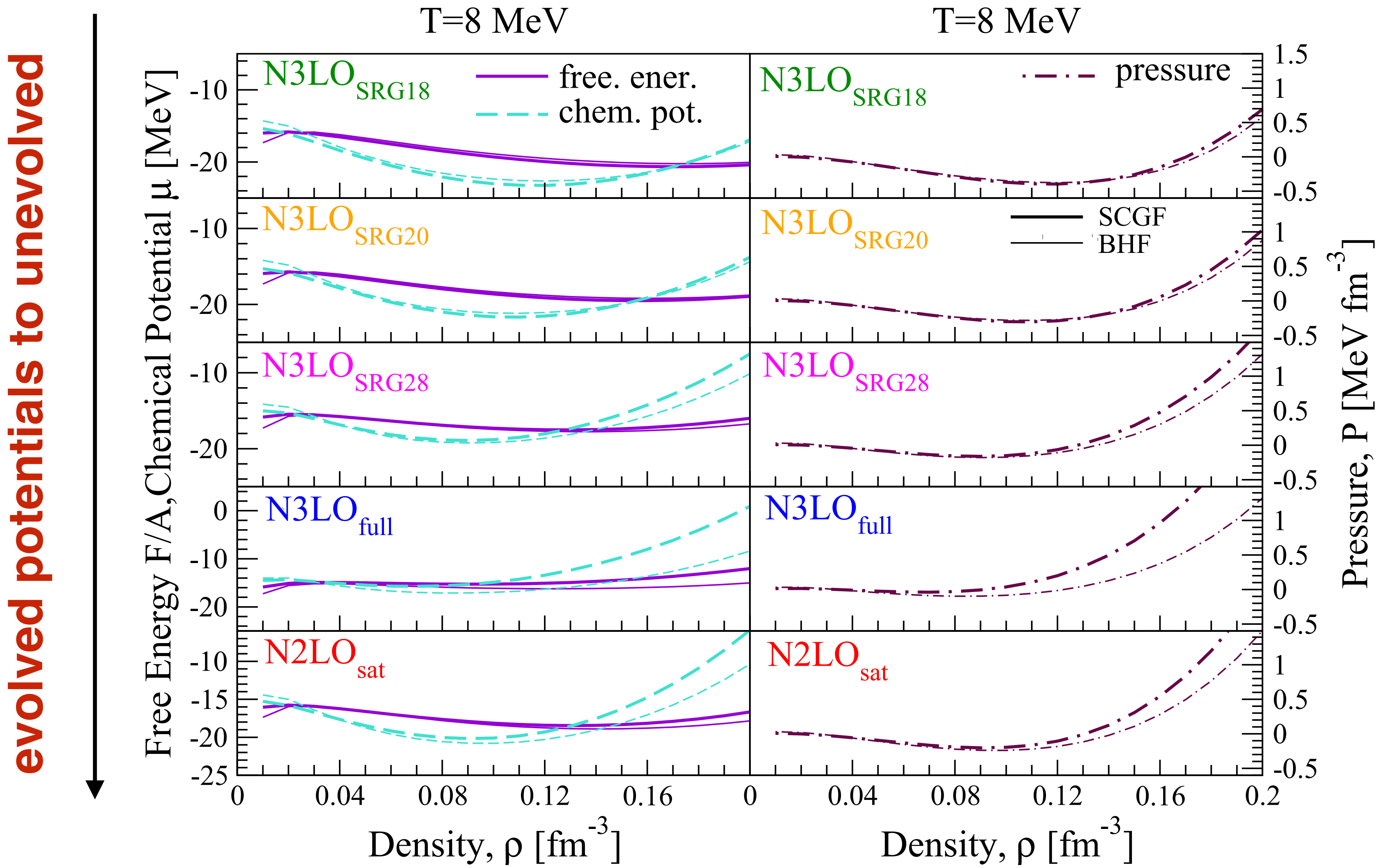

- Free-energy and chemical potential cross at P=0

2N N3LO EM500 (SRG L=1.8fm^{-1})+ 3N N2LO (L=2.0fm^{-1})

2N N3LO EM500 (SRG L=2.0fm^{-1})+ 3N N2LO (L=2.0m^{-1})

2N N3LO EM500 (SRG L=2.8fm^{-1})+ 3N N2LO (L=2.0fm^{-1})

N2LOsat 2N + 3N

2N N3LO EM500 + 3N N2LO

Carbone, Polls, Rios PRC 98 025804 (2018)

Many-body uncertainty for finite-T properties

Free-energy

$$F = E - TS$$

Pressure

$$P = \rho(\mu - F)$$

evolved potentials to unevolved

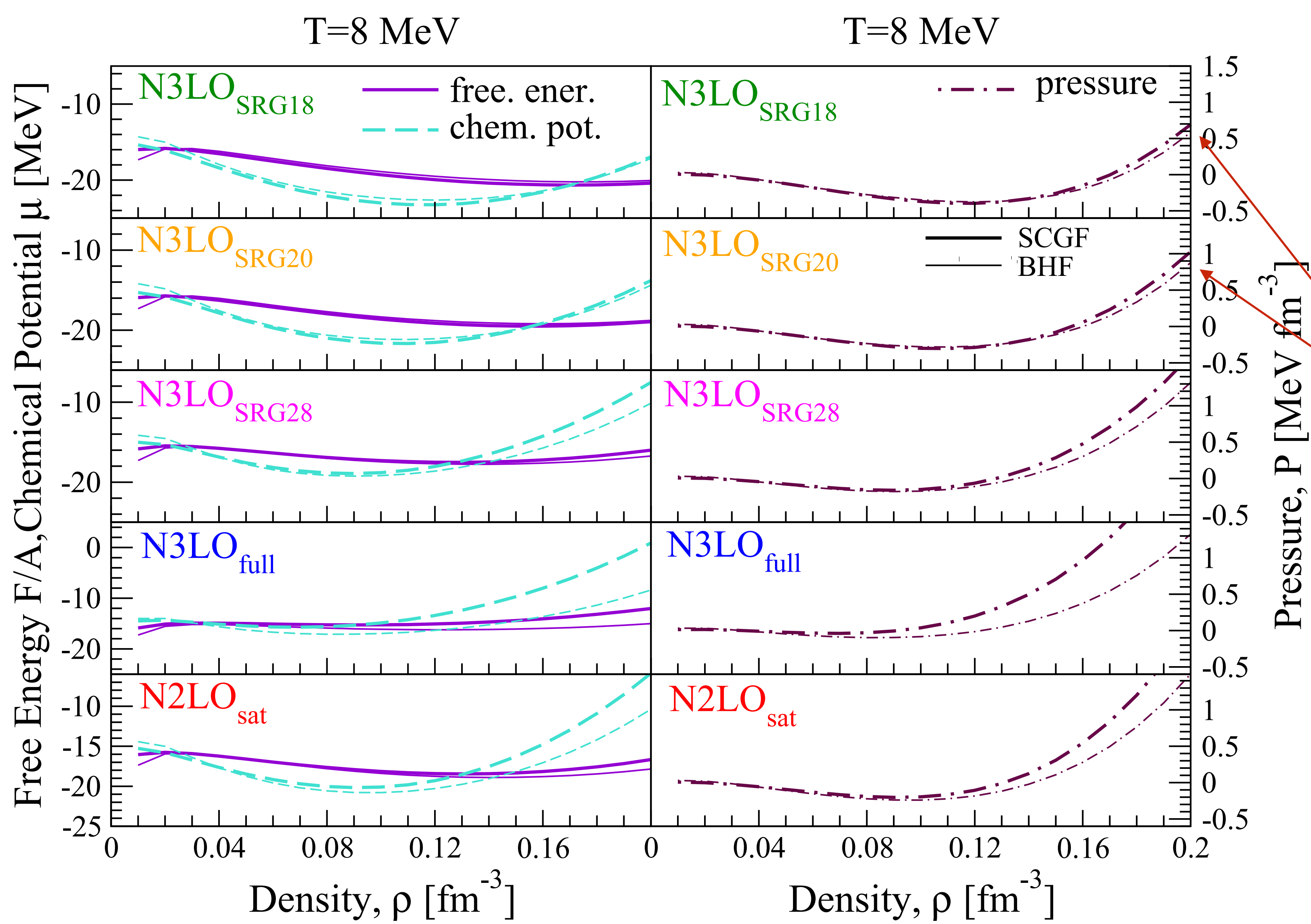

- Free-energy and chemical potential cross at P=0
- smaller many-body error band for evolved potentials: hole-hole states less important

2N N3LO EM500 (SRG L=1.8fm^{-1})+ 3N N2LO (L=2.0fm^{-1})
2N N3LO EM500 (SRG L=2.0fm^{-1})+ 3N N2LO (L=2.0m^{-1})
2N N3LO EM500 (SRG L=2.8fm^{-1})+ 3N N2LO (L=2.0fm^{-1})
N2LOsat 2N + 3N
2N N3LO EM500 + 3N N2LO

Carbone, Polls, Rios PRC 98 025804 (2018)

Symmetric nuclear matter

Many-body uncertainty for finite-T properties

Free-energy

$$F = E - TS$$

Pressure

$$P = \rho(\mu - F)$$

evolved potentials to unevolved

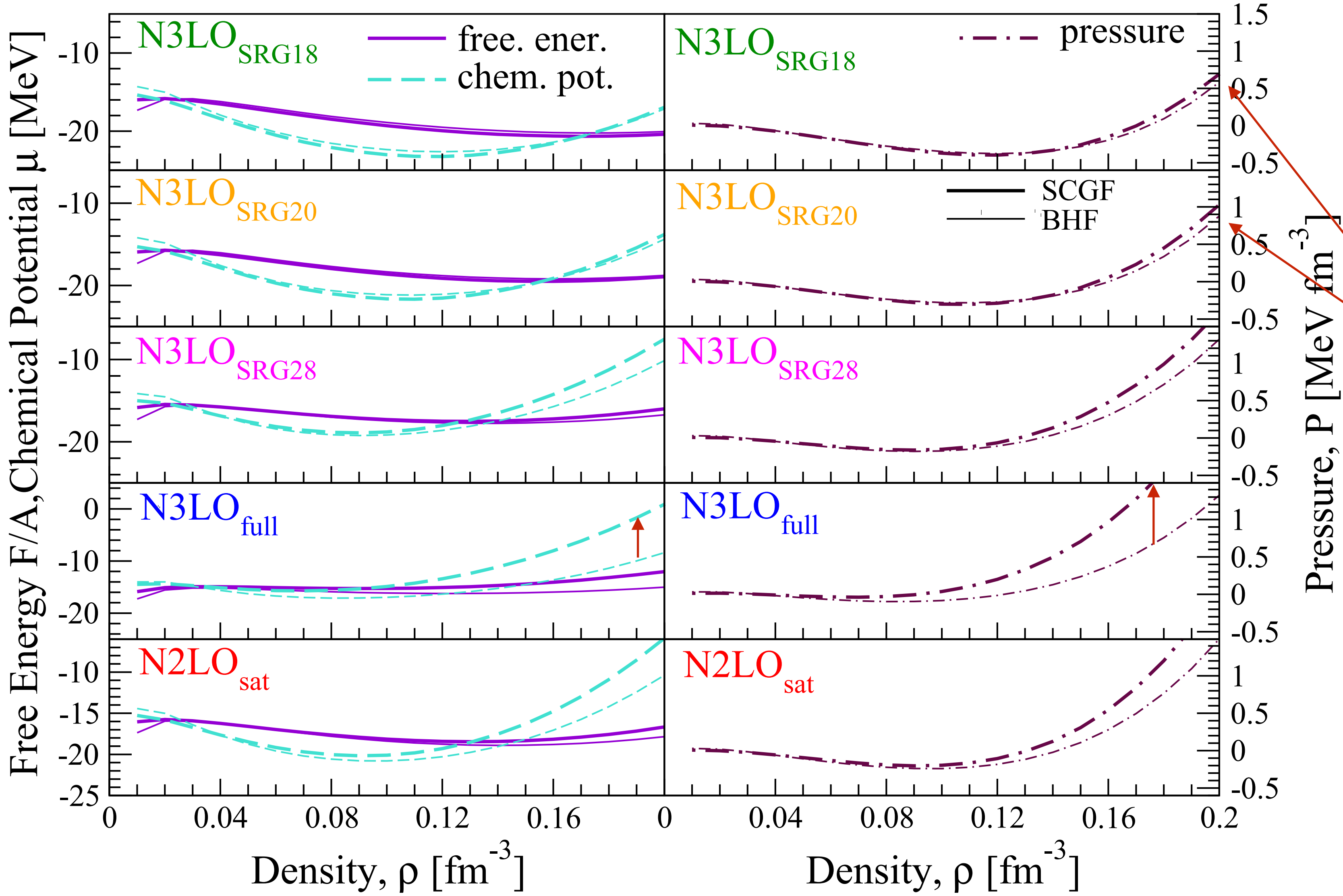

- Free-energy and chemical potential cross at P=0
- smaller many-body error band for evolved potentials: hole-hole states less important
- uncertainty band increases with density: hole-hole states add repulsion

2N N3LO EM500 (SRG L=1.8fm^{-1})+ 3N N2LO (L=2.0fm^{-1})
2N N3LO EM500 (SRG L=2.0fm^{-1})+ 3N N2LO (L=2.0m^{-1})
2N N3LO EM500 (SRG L=2.8fm^{-1})+ 3N N2LO (L=2.0fm^{-1})
N2LOsat 2N + 3N
2N N3LO EM500 + 3N N2LO

Carbone, Polls, Rios PRC 98 025804 (2018)

The liquid-gas phase transition and critical point

Carbone, Polls, Rios PRC 98 025804 (2018)

N2LOsat (2N+3N)

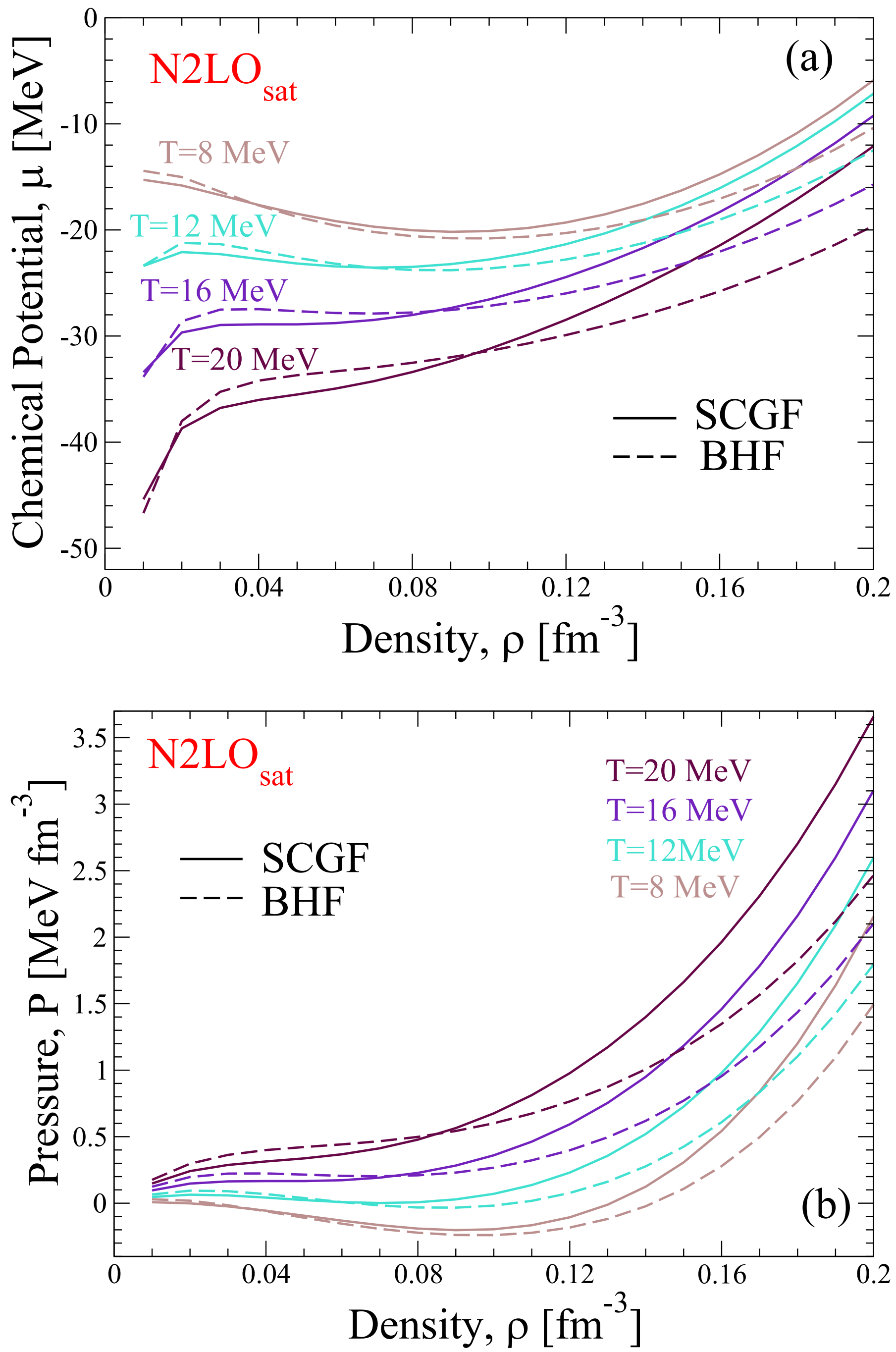

Spinodal

$$\frac{\partial \mu}{\partial \rho_g} = \frac{\partial \mu}{\partial \rho_l} = 0$$

$$\frac{\partial P}{\partial \rho_g} = \frac{\partial P}{\partial \rho_l} = 0$$

Coexistence

$$\mu(\rho_g) = \mu(\rho_l)$$

$$P(\rho_g) = P(\rho_l)$$

The liquid-gas phase transition and critical point

Carbone, Polls, Rios PRC 98 025804 (2018)

N2LOsat (2N+3N)

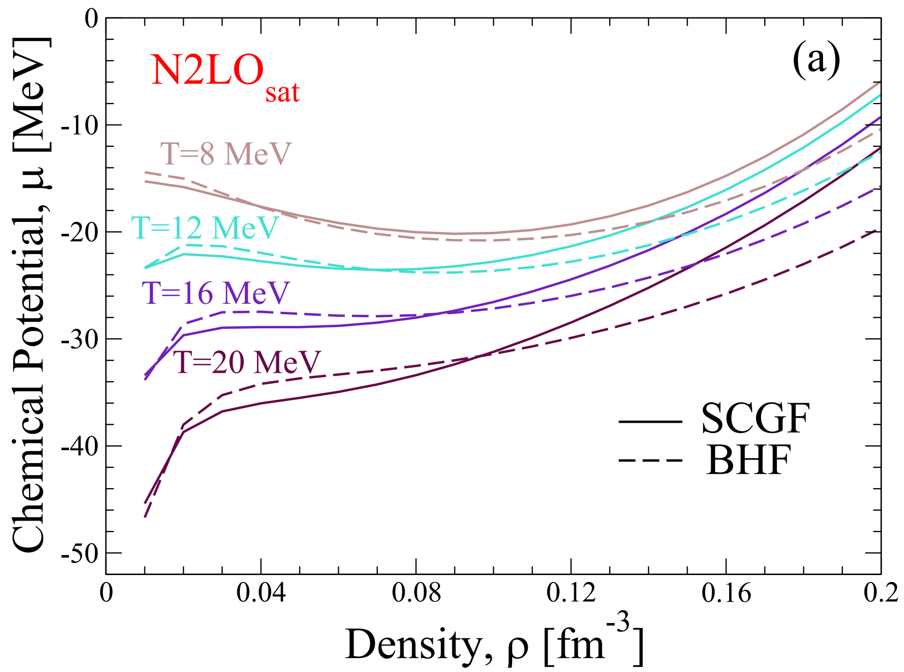

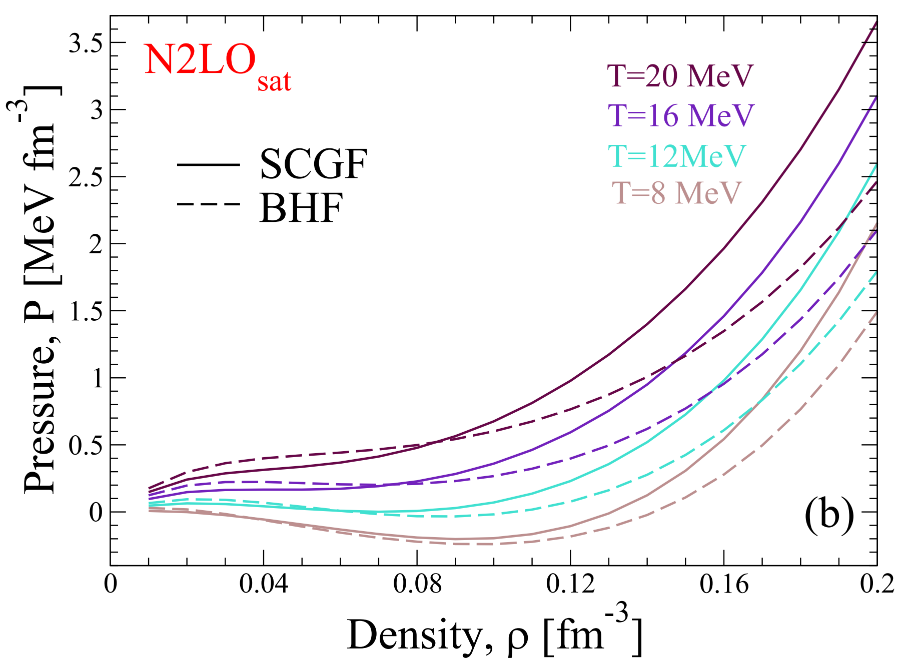

Spinodal

$$\frac{\partial \mu}{\partial \rho_g} = \frac{\partial \mu}{\partial \rho_l} = 0$$

$$\frac{\partial P}{\partial \rho_g} = \frac{\partial P}{\partial \rho_l} = 0$$

Coexistence

$$\mu(\rho_g) = \mu(\rho_l)$$

$$P(\rho_g) = P(\rho_l)$$

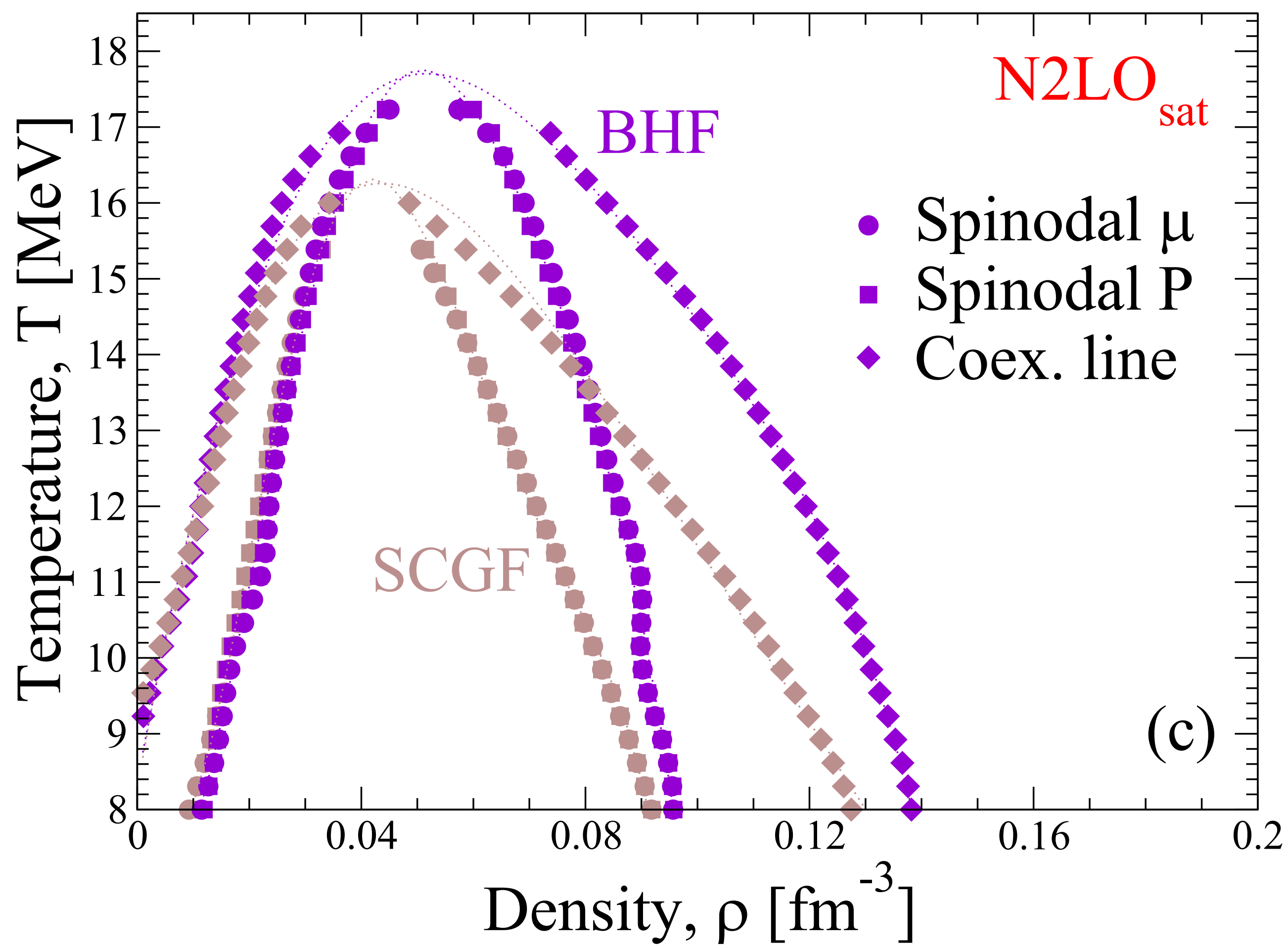

- Many-body difference increase with density
- Higher critical temperature for BHF results

The liquid-gas phase transition and critical point

Carbone, Polls, Rios PRC 98 025804 (2018)

SCGF	ρ_c (fm^{-3})	T_c (MeV)
N3LO$_{SRG18}$	0.048	18.6
N3LO$_{SRG20}$	0.047	17.4
N3LO$_{SRG28}$	0.043	15.3
N2LO$_{sat}$	0.043	16.3
N3LO$_{full}$	0.038	11.5

$\mu(\rho_g) = \mu(\rho_l)$ $P(\rho_g) = P(\rho_l)$

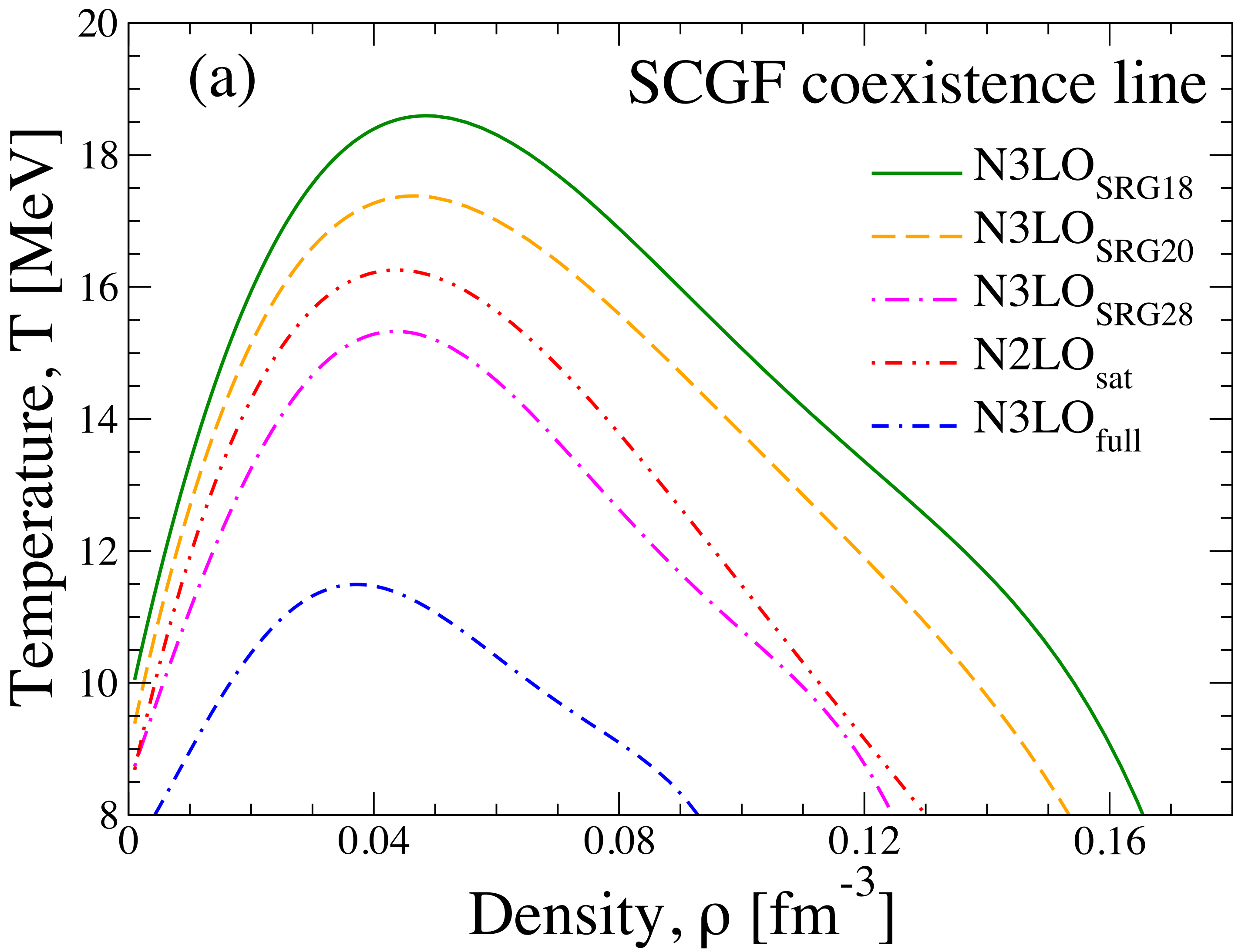

- Predicted critical temperature ~ T=~[15-19] MeV
- Experimental outcomes: T= ~[15-20] MeV)

The saturation energy vs the critical temperature

Carbone, Polls, Rios PRC 98 025804 (2018)

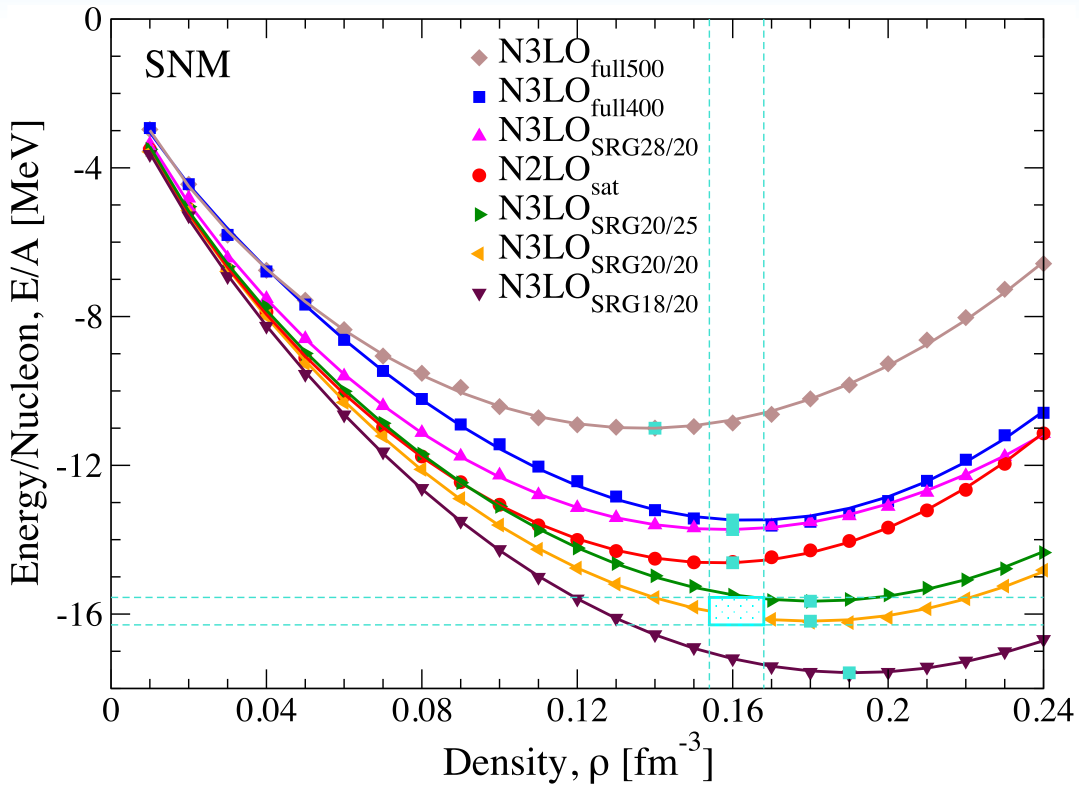

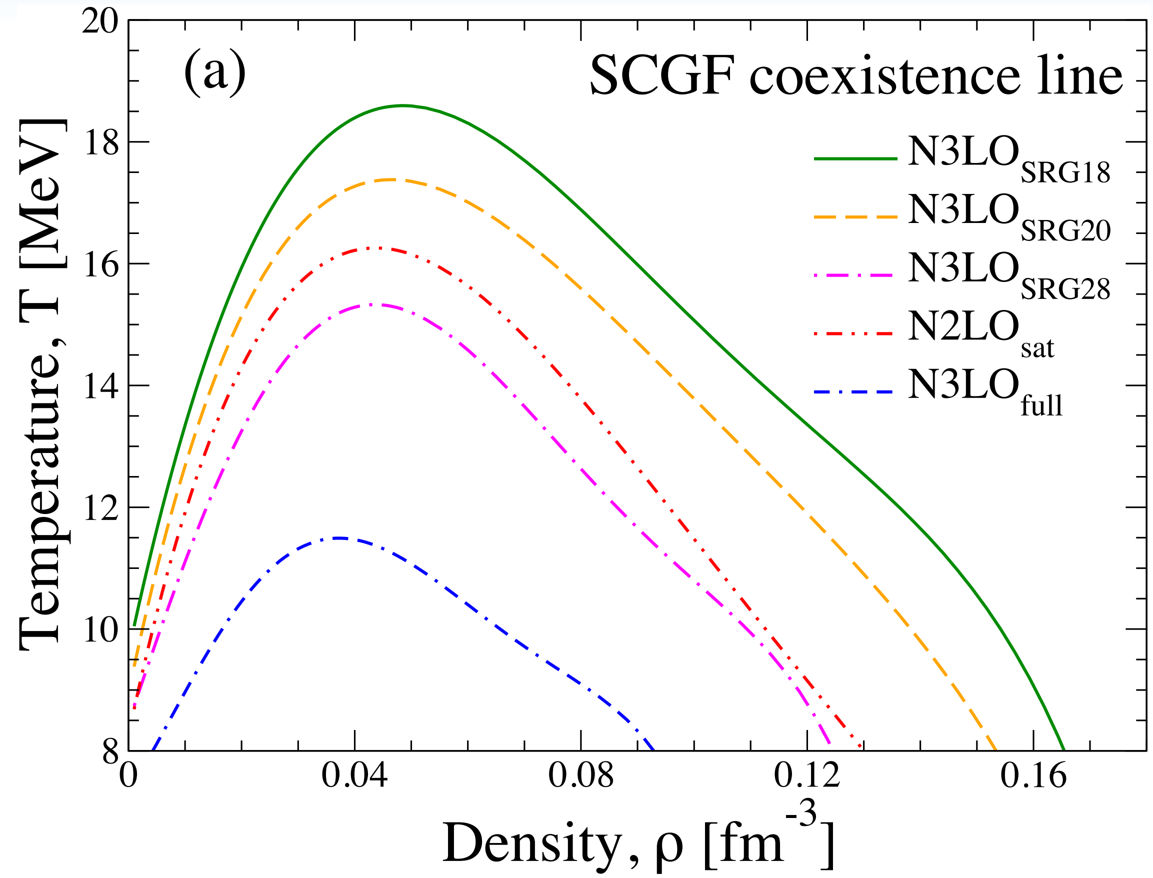

The saturation energy vs the critical temperature

Carbone, Polls, Rios PRC 98 025804 (2018)

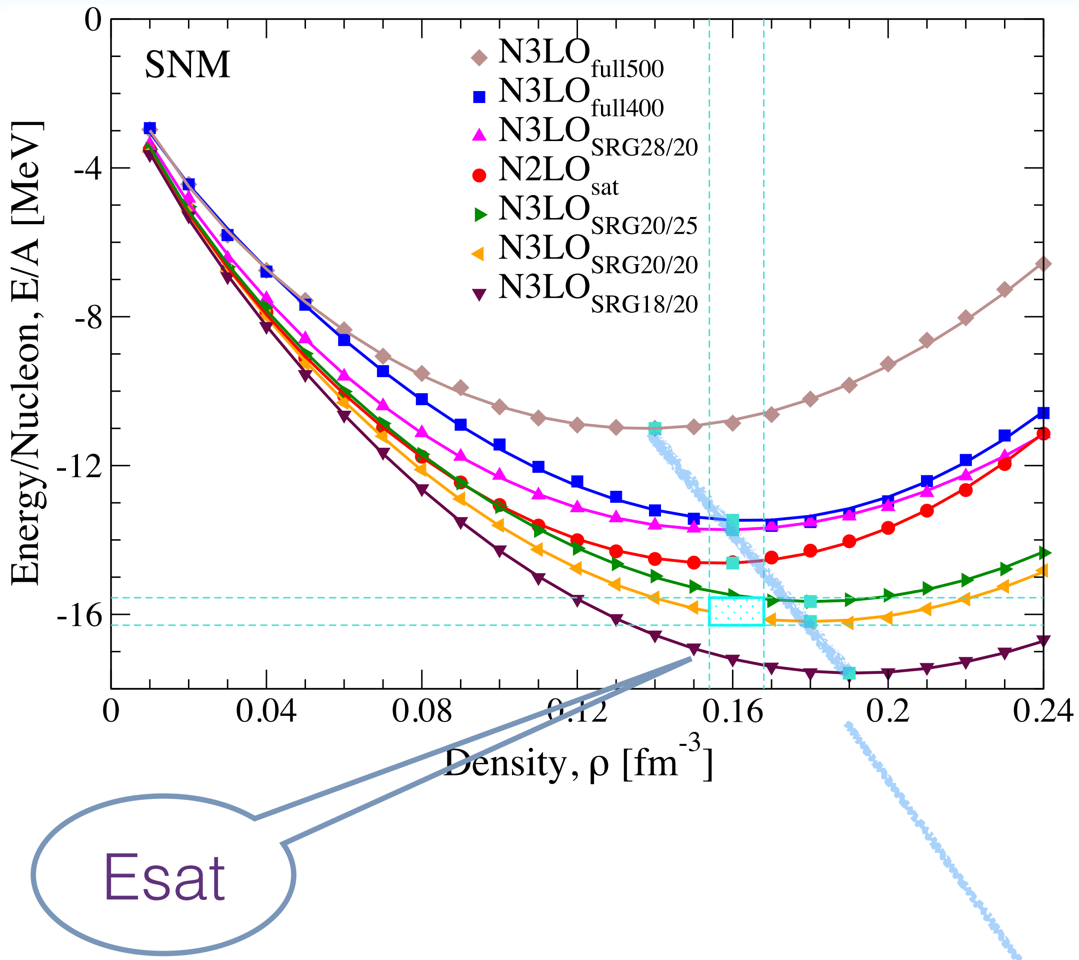

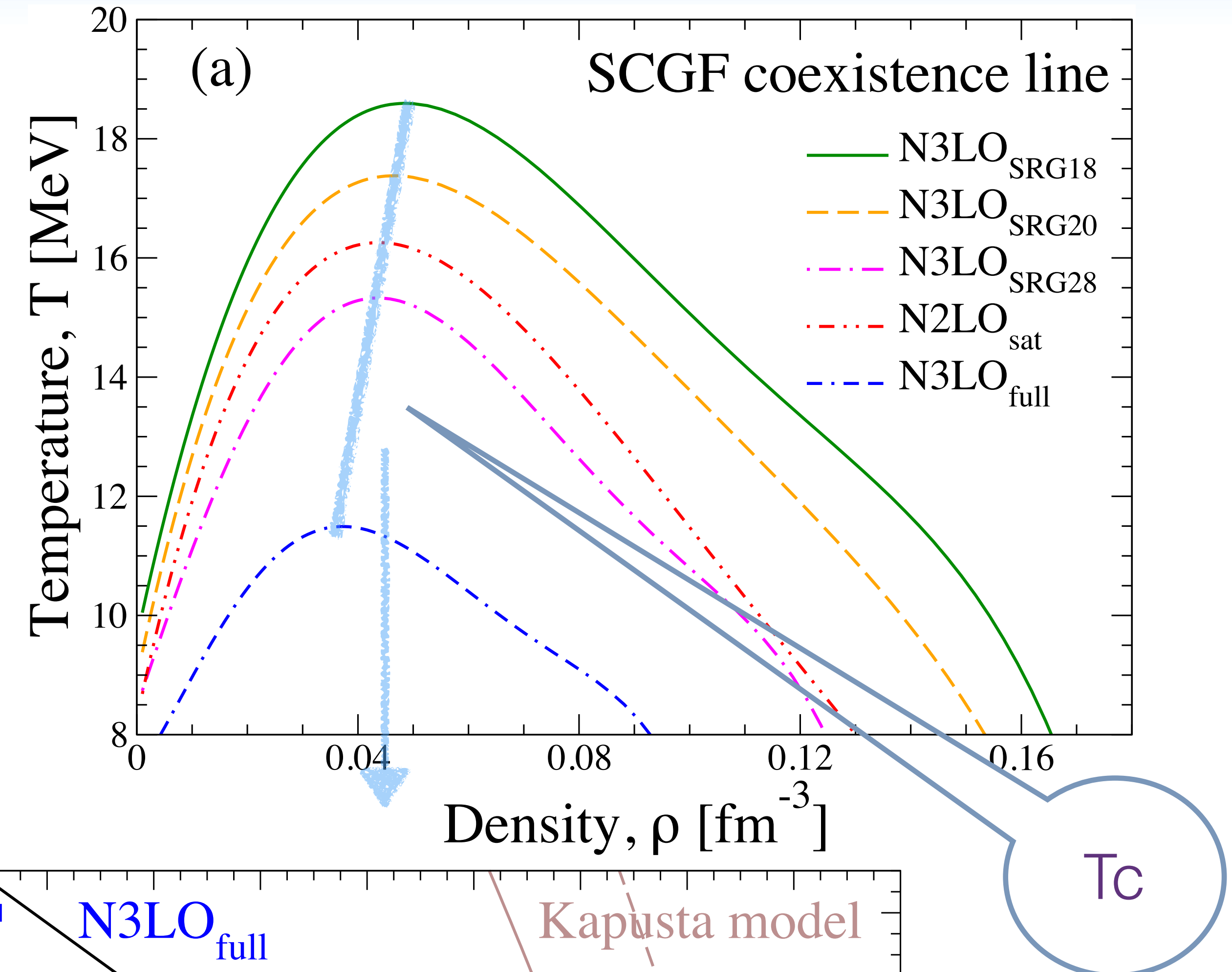

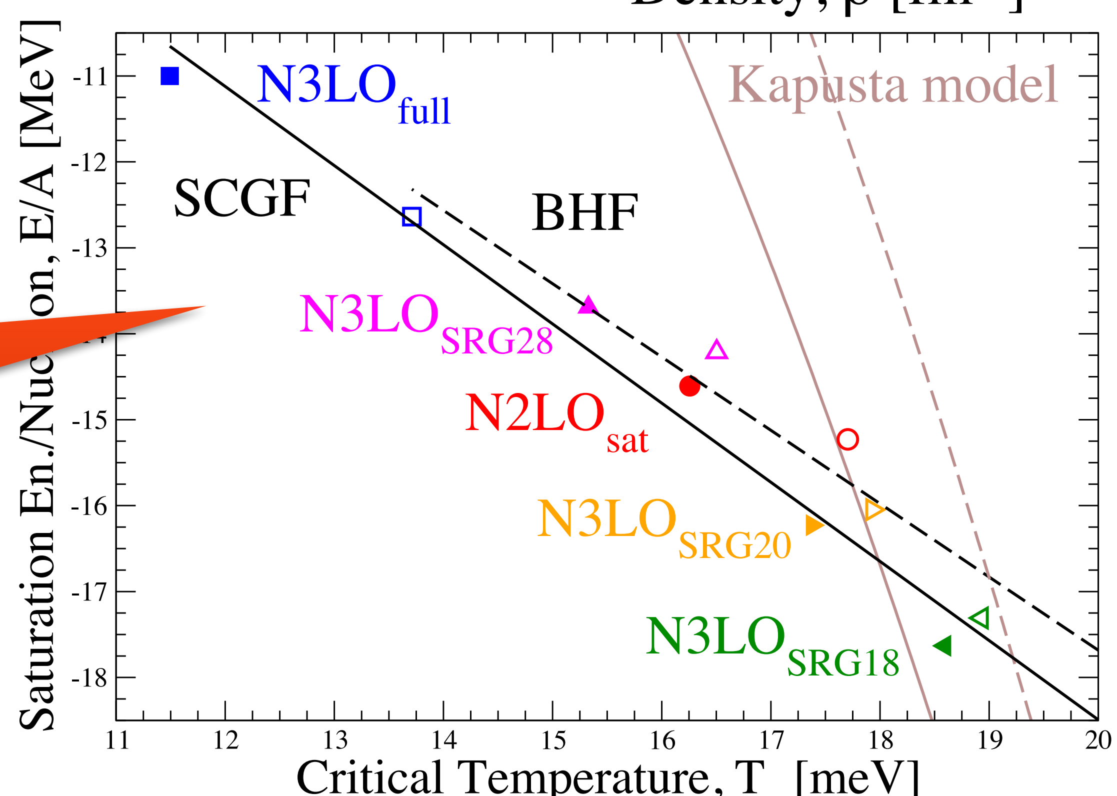

theoretical uncertainty bands correlate: helpful in pinning down the critical temperature

Thermal effects in EoS for astrophysical simulations

$$P_{\mathrm{cold}} + P_{\mathrm{thermal}} \longrightarrow P_{\mathrm{th}} = (\underline{\Gamma_{\mathrm{th}}} - 1)\rho E_{\mathrm{th}}$$

Constant value

Astrophysical EoS

$$\Gamma_{\mathrm{th}} = 1 + \frac{P_{\mathrm{th}}}{\rho E_{\mathrm{th}}}$$

Carbone & Schwenk *(in preparation)*

Thermal effects in EoS for astrophysical simulations

$$P_{\text{cold}} + P_{\text{thermal}} \longrightarrow P_{\text{th}} = (\Gamma_{\text{th}} - 1)\rho E_{\text{th}}$$

Astrophysical EoS

Constant value

$$\Gamma_{\text{th}} = 1 + \frac{P_{\text{th}}}{\rho E_{\text{th}}}$$

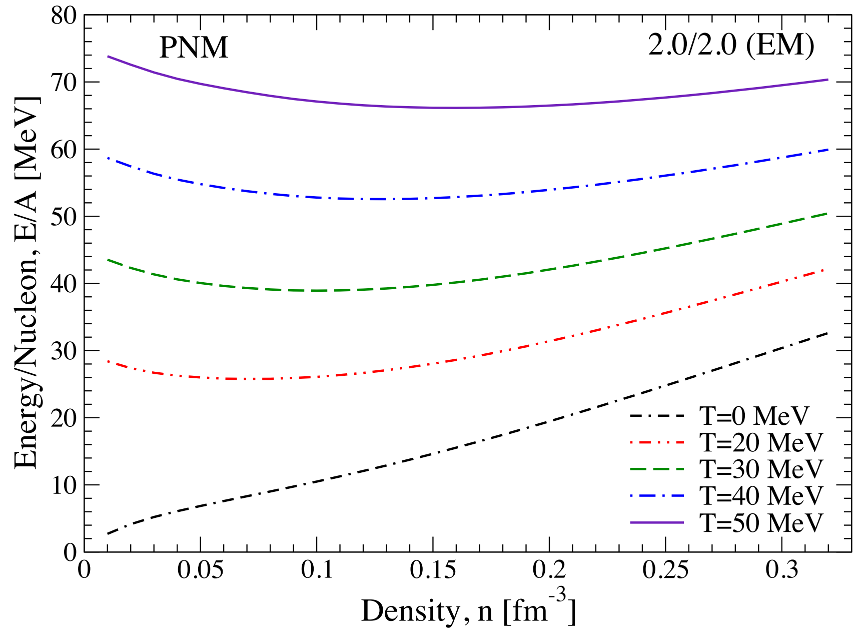

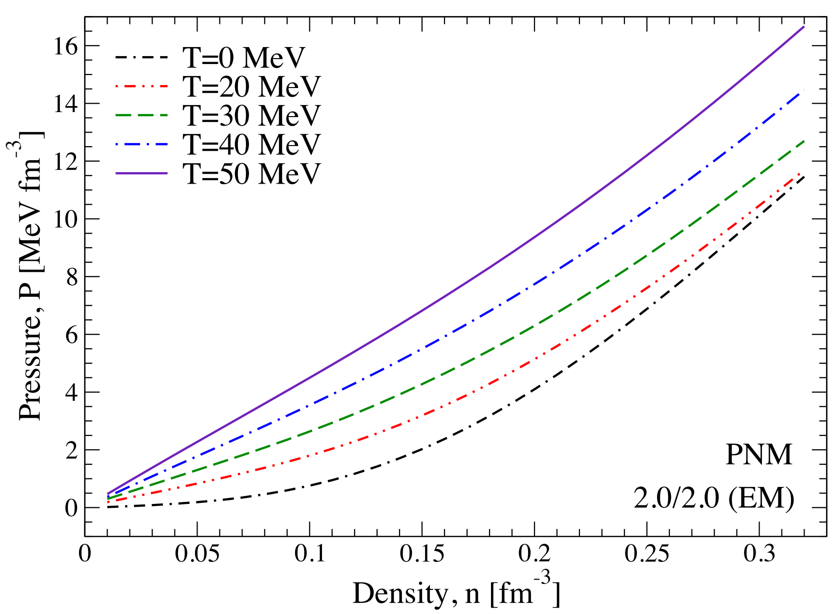

Carbone & Schwenk *(in preparation)*

Thermal effects in EoS for astrophysical simulations

$$P_{\text{cold}} + P_{\text{thermal}} \longrightarrow P_{\text{th}} = \underline{(\Gamma_{\text{th}} - 1)}\rho E_{\text{th}}$$

Constant value

Astrophysical EoS

$$\Gamma_{\text{th}} = 1 + \frac{P_{\text{th}}}{\rho E_{\text{th}}}$$

$$E_{\text{th}} = E(T) - E_0$$

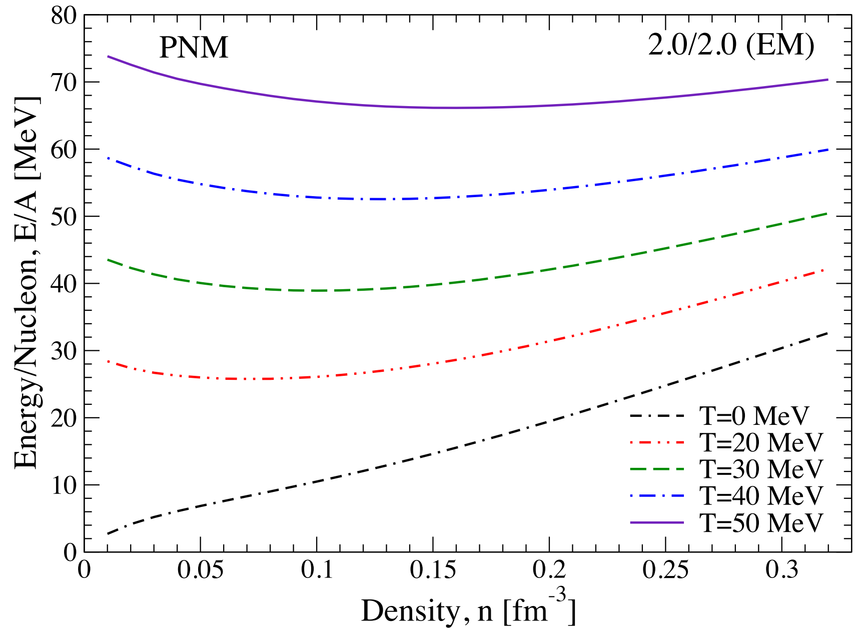

increasing temperature

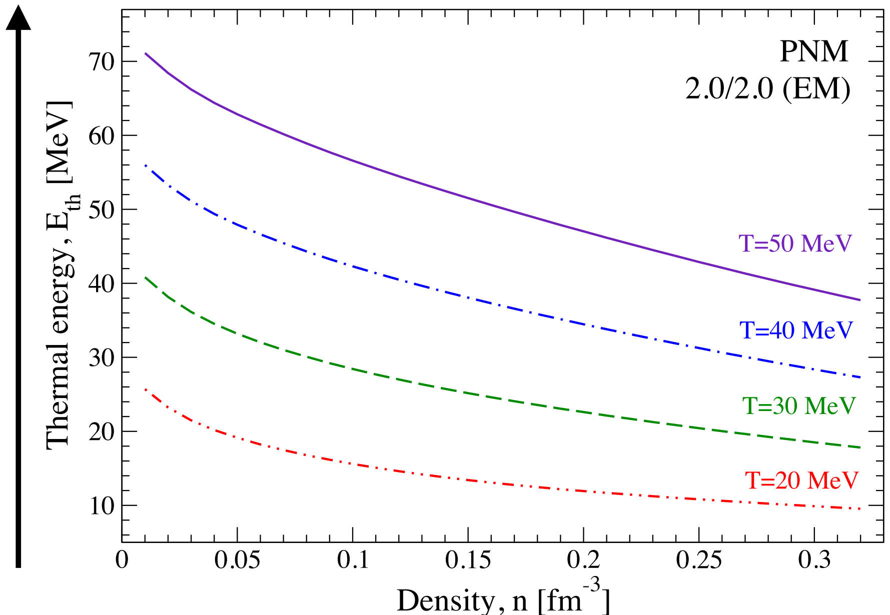

$$P_{\text{th}} = P(T) - P_0$$

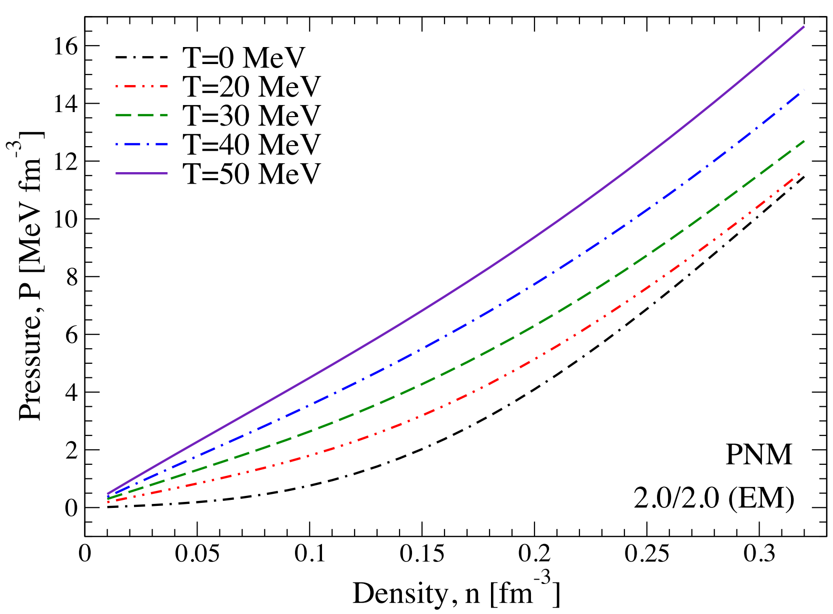

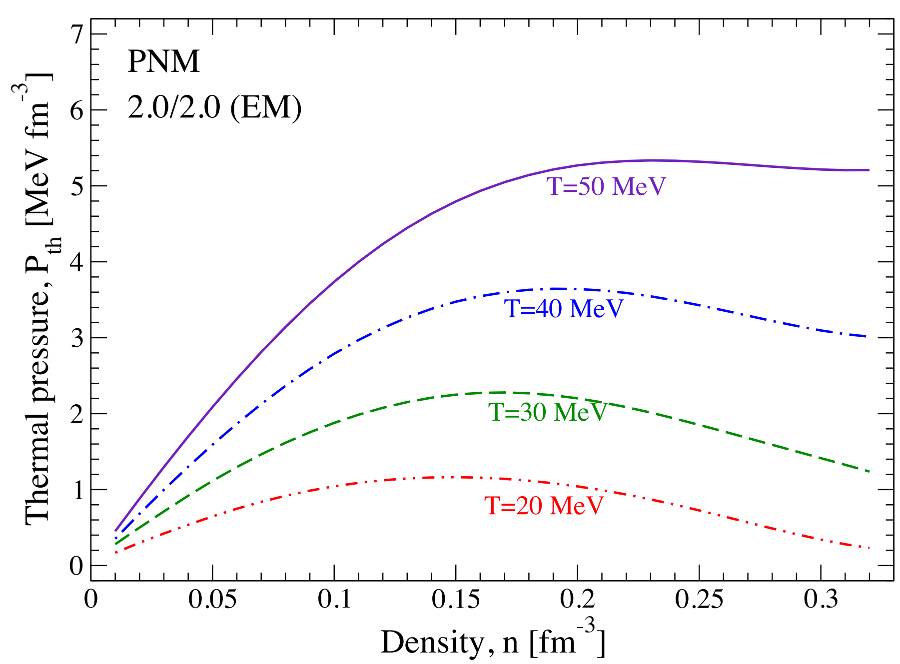

increasing temperature

Carbone & Schwenk *(in preparation)*

Thermal effects in EoS for astrophysical simulations

$$P_{\rm cold} + P_{\rm thermal} \longrightarrow P_{\rm th} = \underline{(\Gamma_{\rm th}} - 1)\rho E_{\rm th}$$

Constant value

Astrophysical EoS

$$\Gamma_{\rm th} = 1 + \frac{P_{\rm th}}{\rho E_{\rm th}}$$

ideal gas

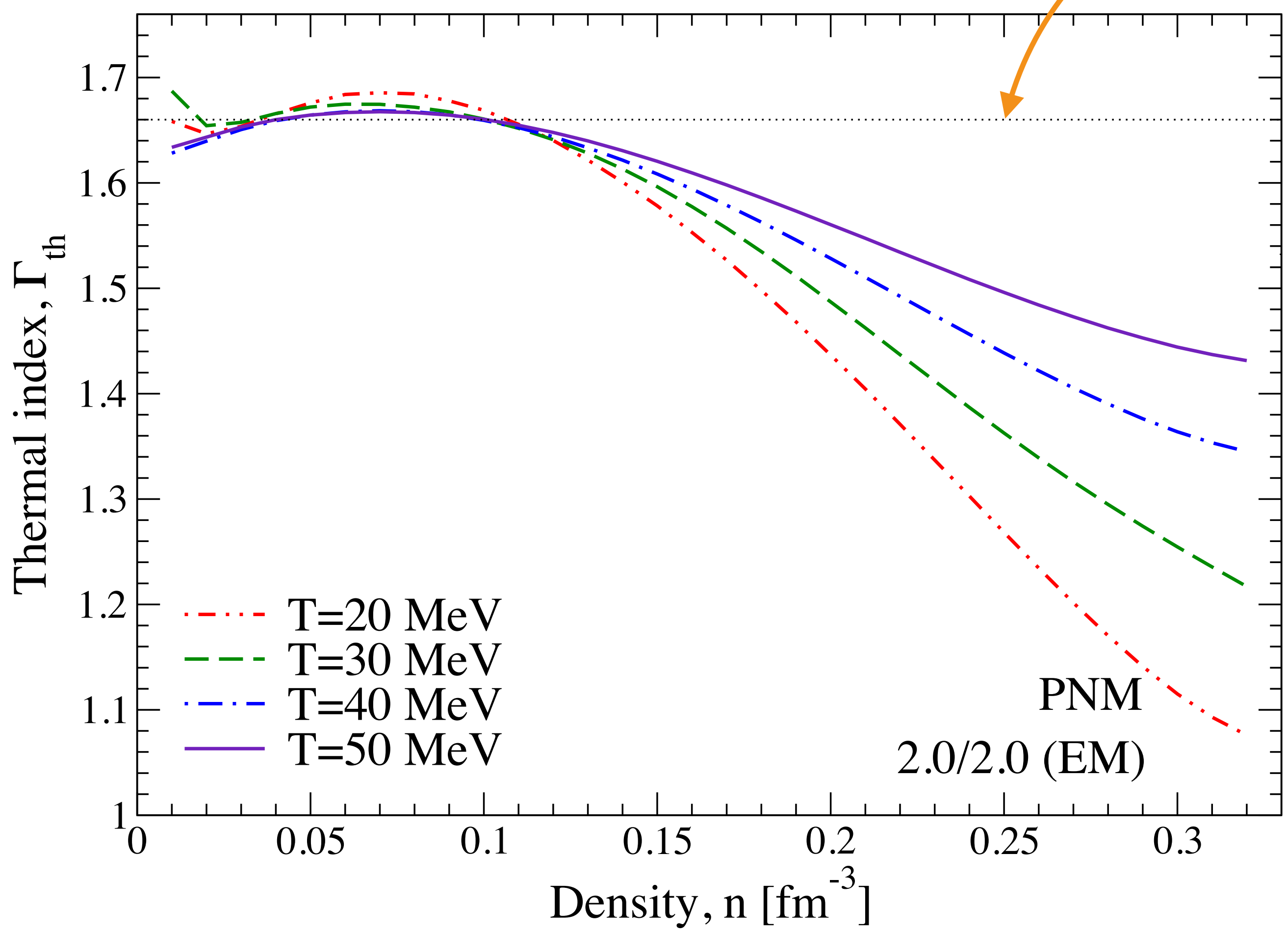

Carbone & Schwenk *(in preparation)*

Thermal effects in EoS for astrophysical simulations

$$P_{\rm cold} + P_{\rm thermal} \longrightarrow P_{\rm th} = (\Gamma_{\rm th} - 1)\rho E_{\rm th}$$

Constant value

Astrophysical EoS

$$\Gamma_{\rm th} = 1 + \frac{P_{\rm th}}{\rho E_{\rm th}}$$

ideal gas

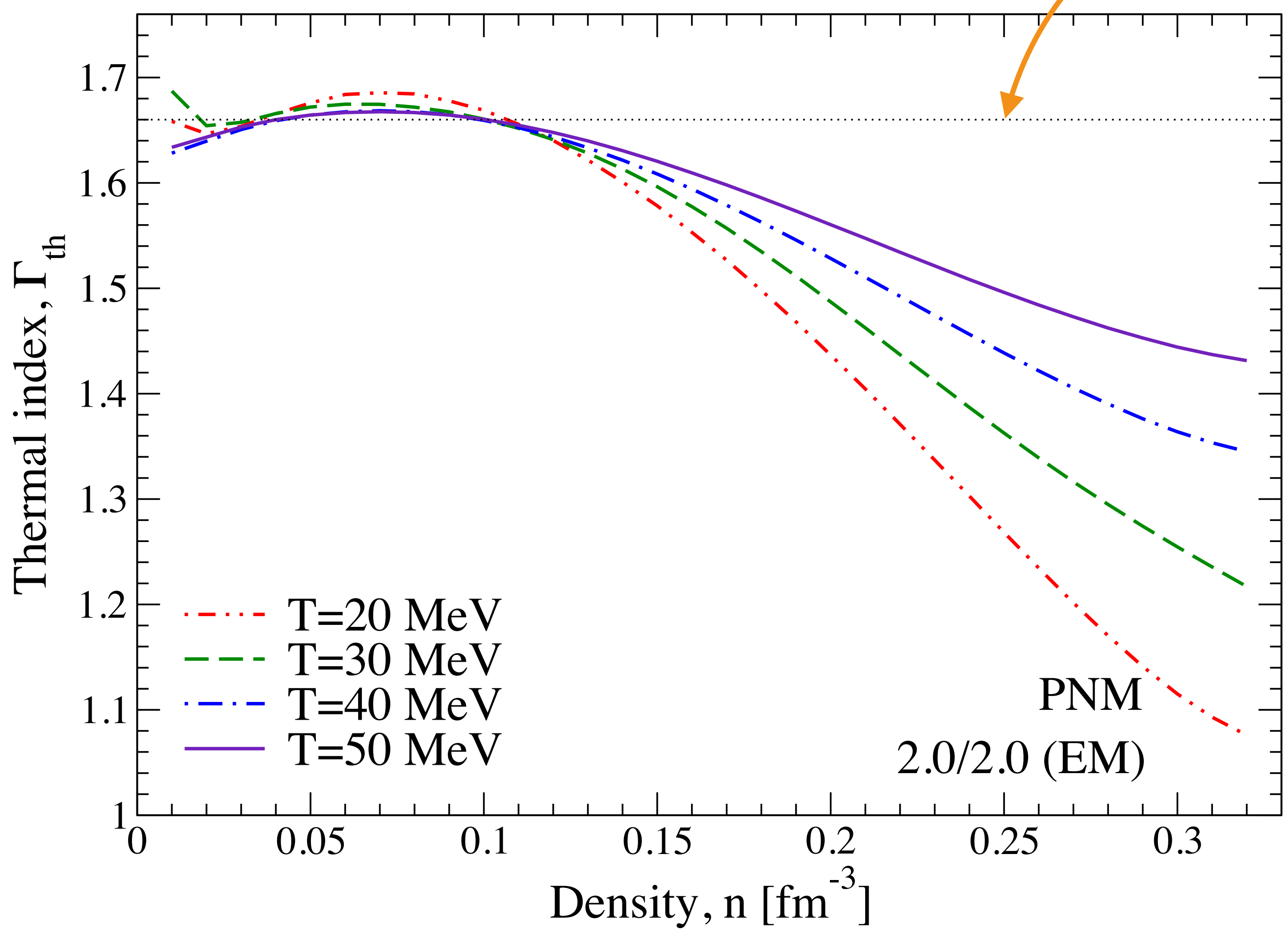

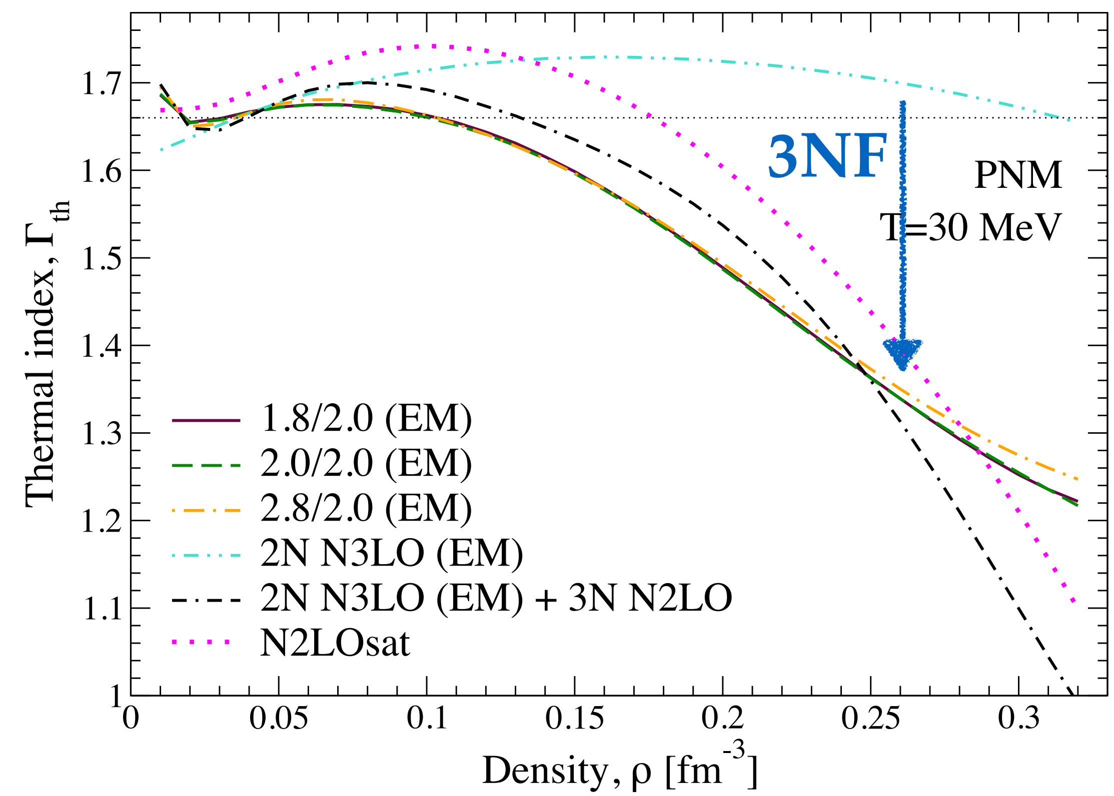

suppression due to 3-body forces

Carbone & Schwenk *(in preparation)*

Thermal effects in EoS for astrophysical simulations

$$P_{\rm cold} + P_{\rm thermal} \longrightarrow P_{\rm th} = \underline{(\Gamma_{\rm th}} - 1)\rho E_{\rm th}$$

Constant value

Astrophysical EoS

$$\Gamma_{\rm th} = 1 + \frac{P_{\rm th}}{\rho E_{\rm th}}$$

$$E_{\rm th} = E(T) - E_0$$

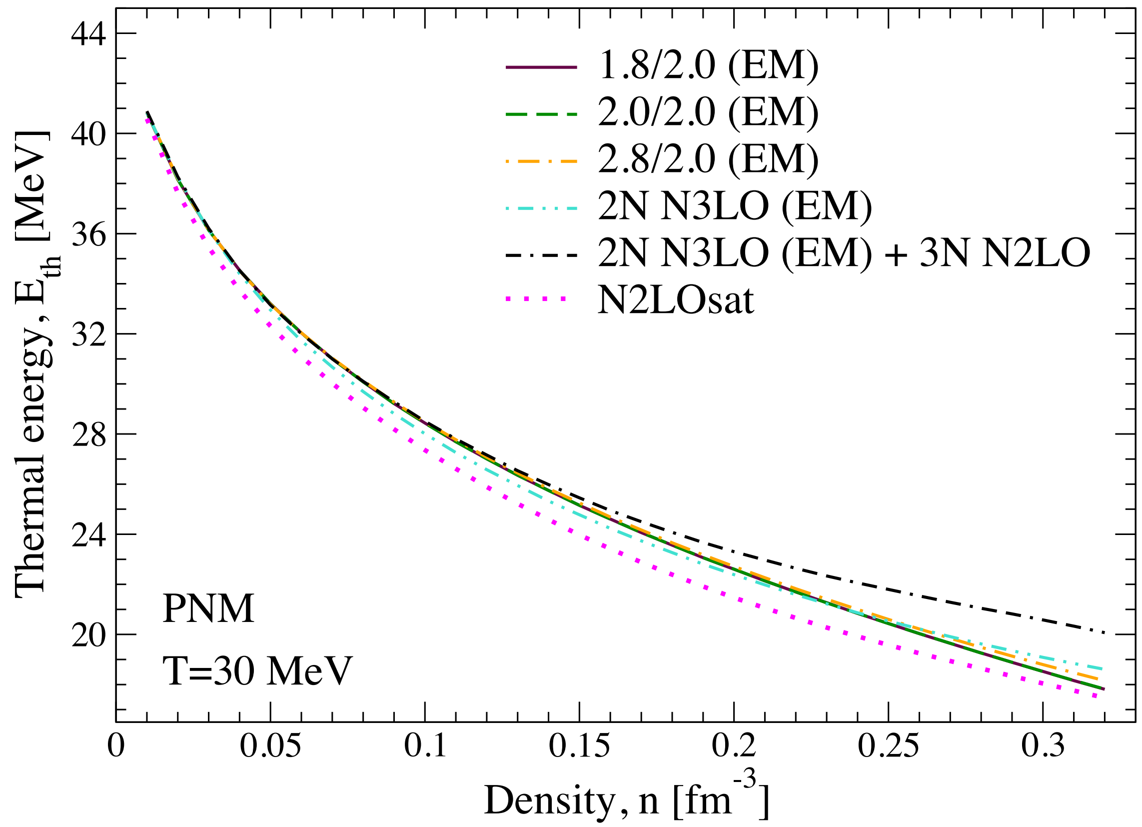

$$P_{\rm th} = P(T) - P_0$$

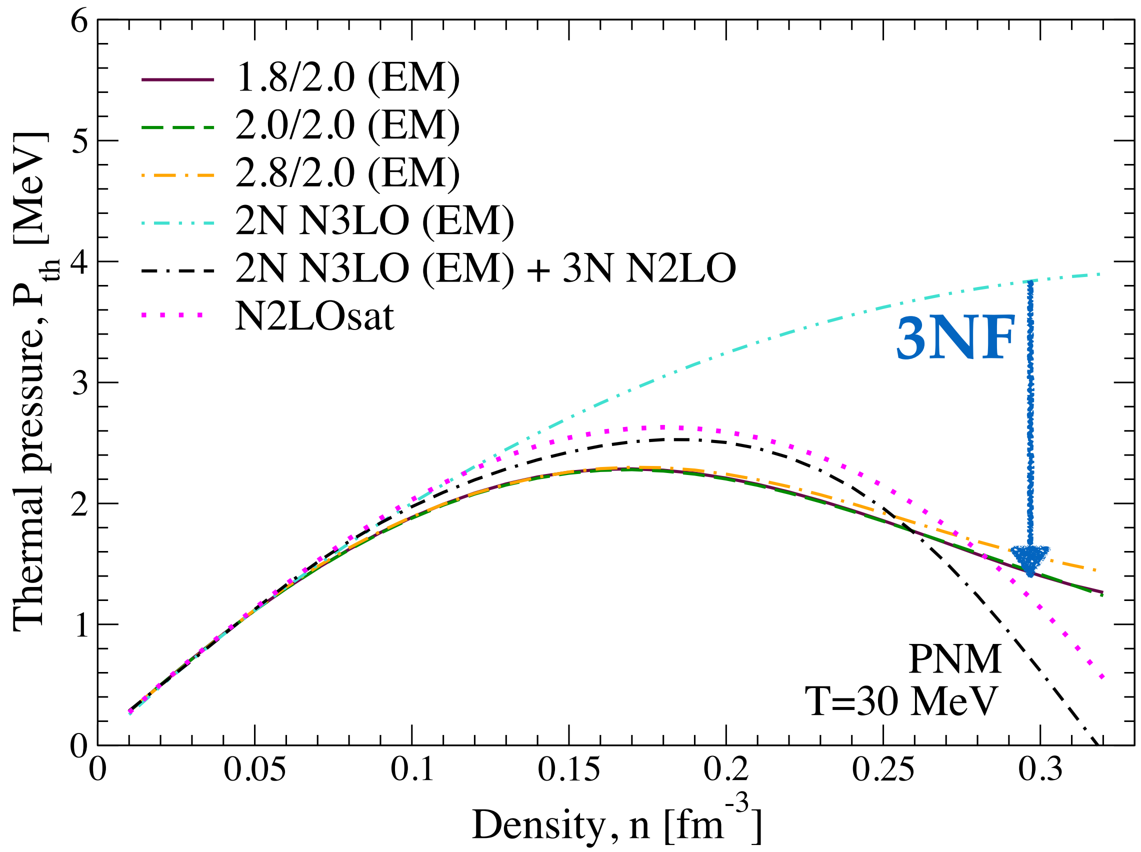

suppression due to 3-body forces

Carbone & Schwenk *(in preparation)*

Thermal effects in EoS for astrophysical simulations

$$P_{\rm cold} + P_{\rm thermal} \longrightarrow P_{\rm th} = (\Gamma_{\rm th} - 1)\rho E_{\rm th}$$

Constant value

Astrophysical EoS

$$\Gamma_{\rm th} = 1 + \frac{P_{\rm th}}{\rho E_{\rm th}}$$

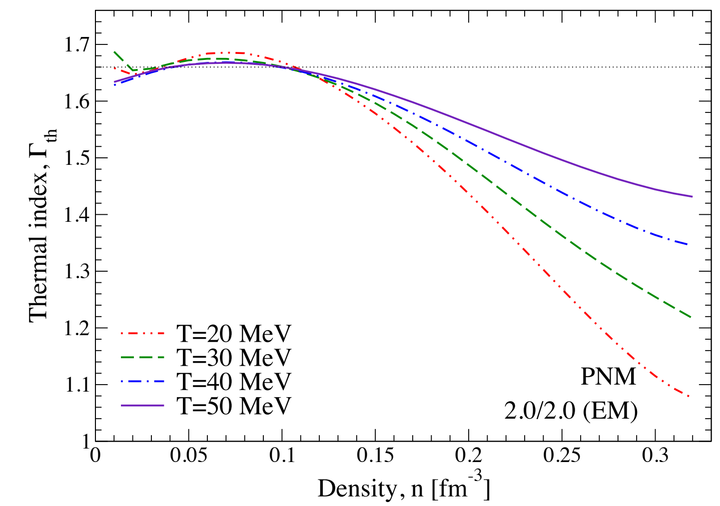

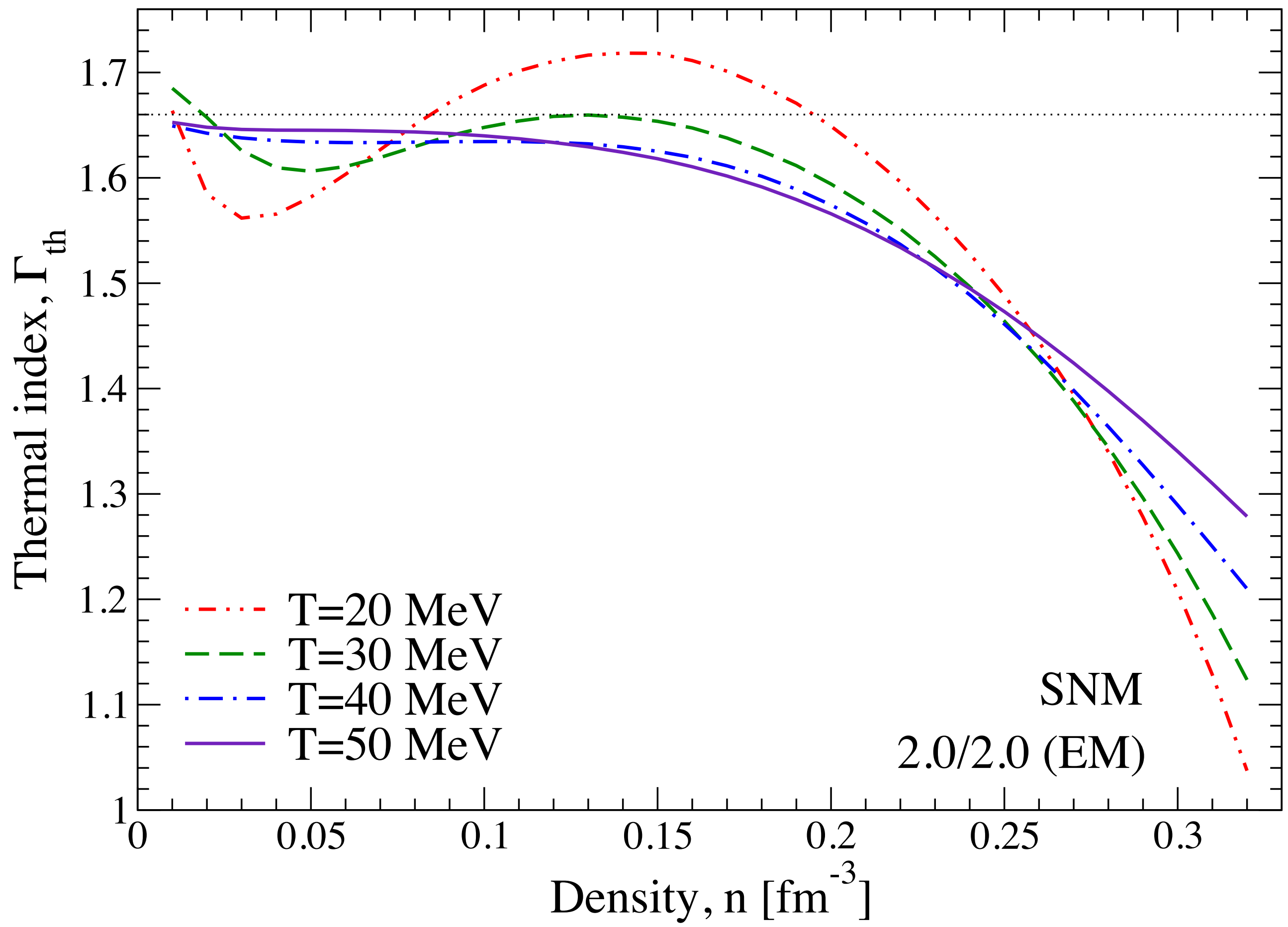

- strength of thermal effects
- stiffness of pressure at T=0

Carbone & Schwenk *(in preparation)*

Thermal effects in EoS for astrophysical simulations

$$P_{\rm cold} + P_{\rm thermal} \longrightarrow P_{\rm th} = (\underline{\Gamma_{\rm th}} - 1)\rho E_{\rm th}$$

Constant value

Astrophysical EoS

$$\Gamma_{\rm th} = 1 + \frac{P_{\rm th}}{\rho E_{\rm th}}$$

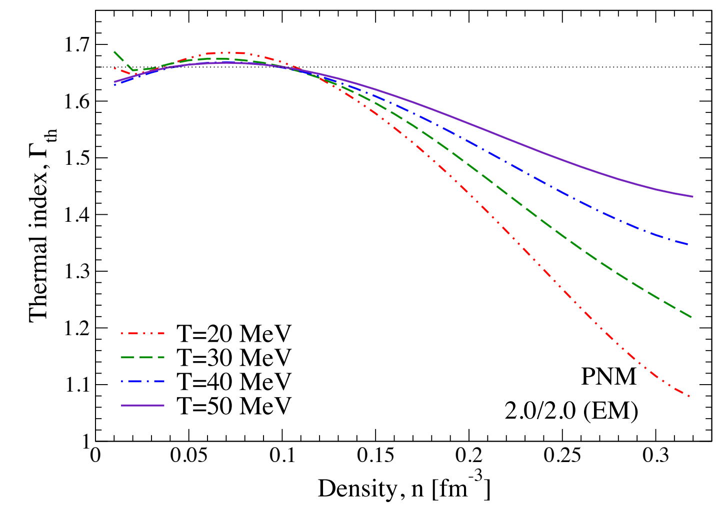

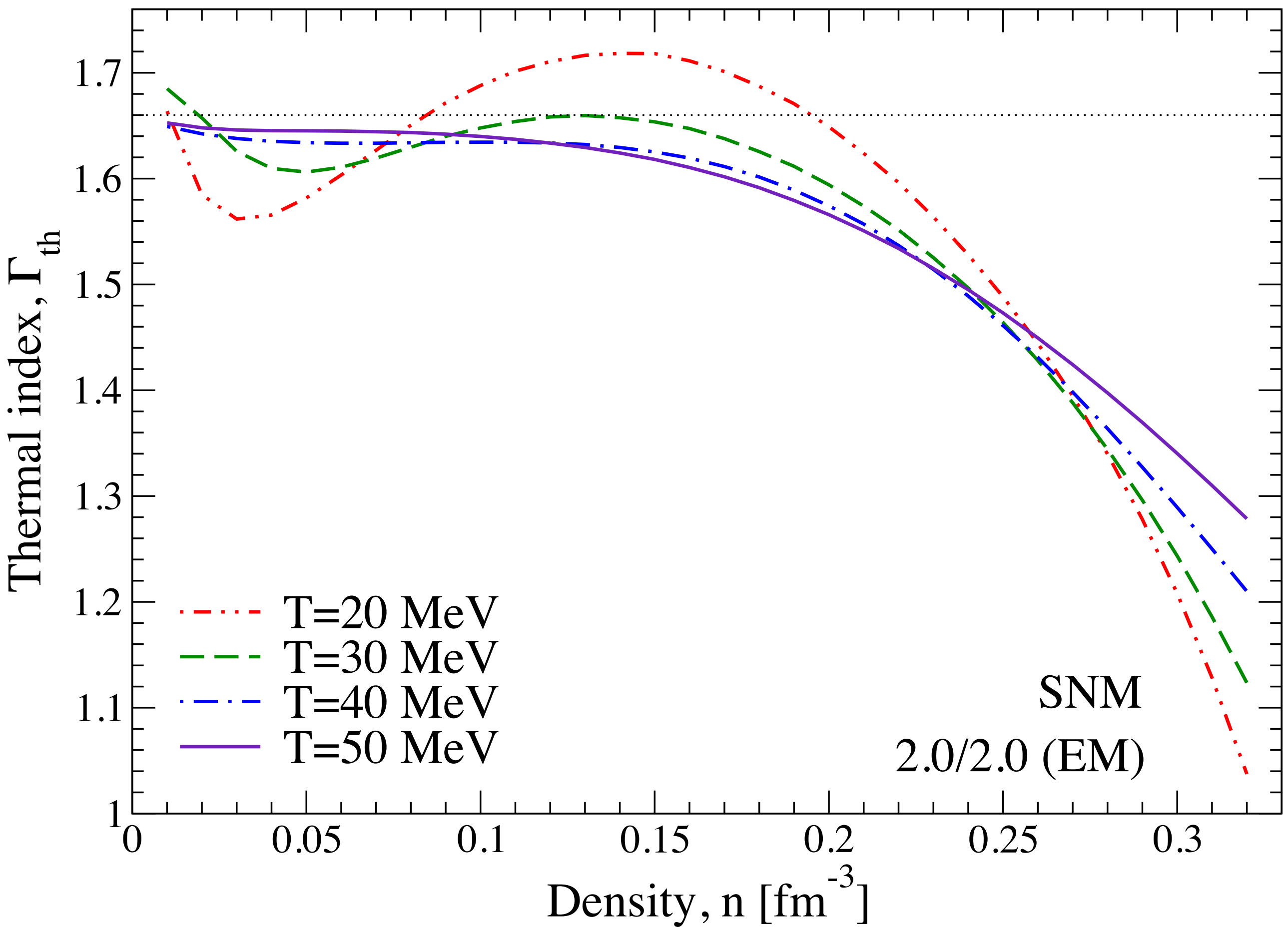

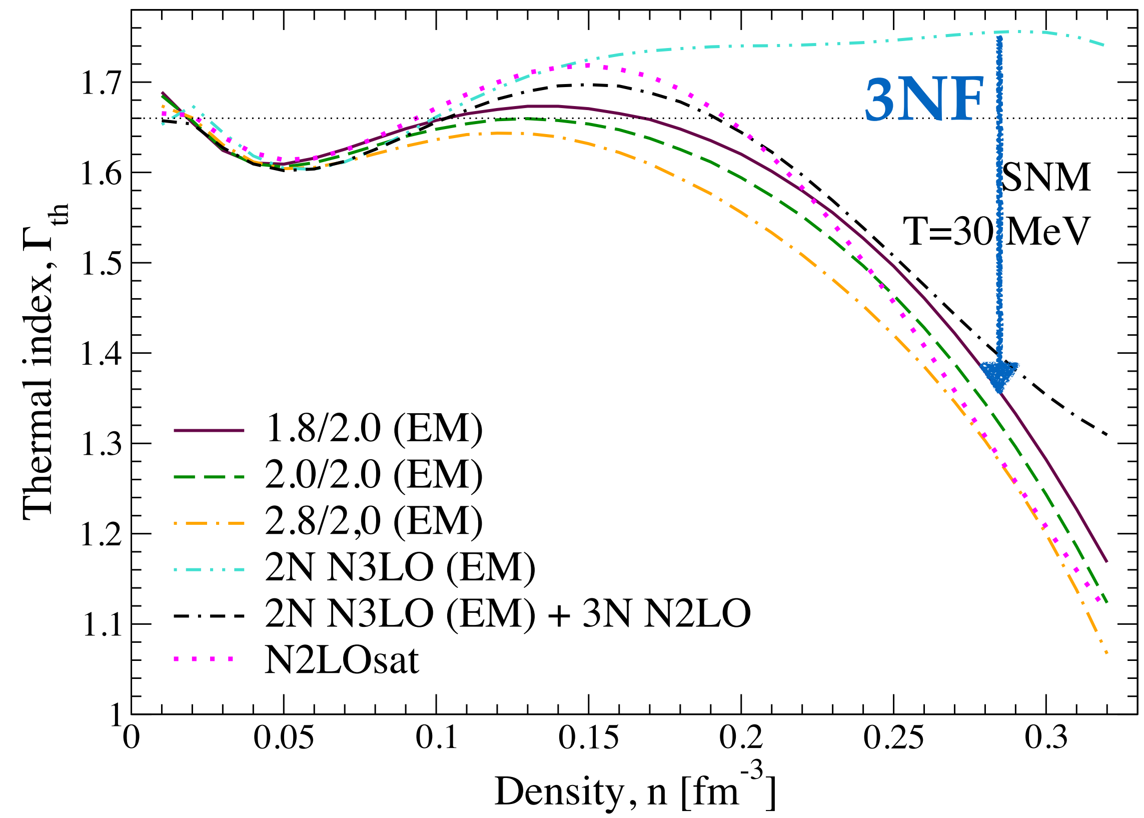

- strength of thermal effects
- stiffness of pressure at T=0

Carbone & Schwenk *(in preparation)*

Thermal index parametrized via effective mass

$$\Gamma_{\rm th} = 1 + \frac{P_{\rm th}}{\rho E_{\rm th}} \longrightarrow \boxed{\Gamma_{\rm th} = \frac{5}{3} - \frac{\rho}{m^\star}\frac{dm^\star}{d\rho}}$$

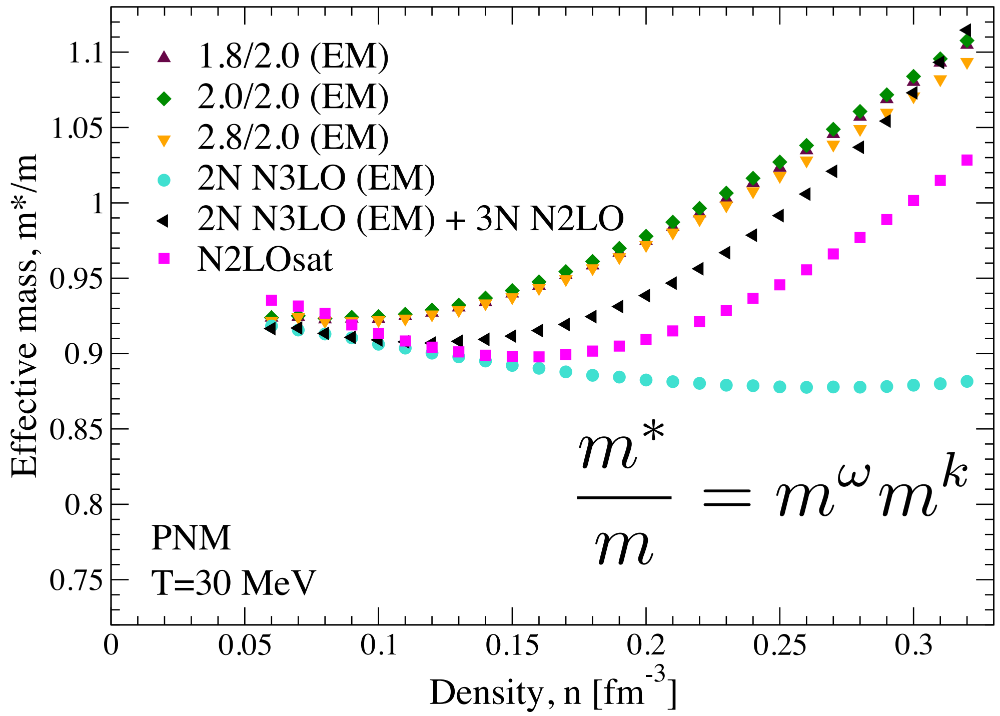

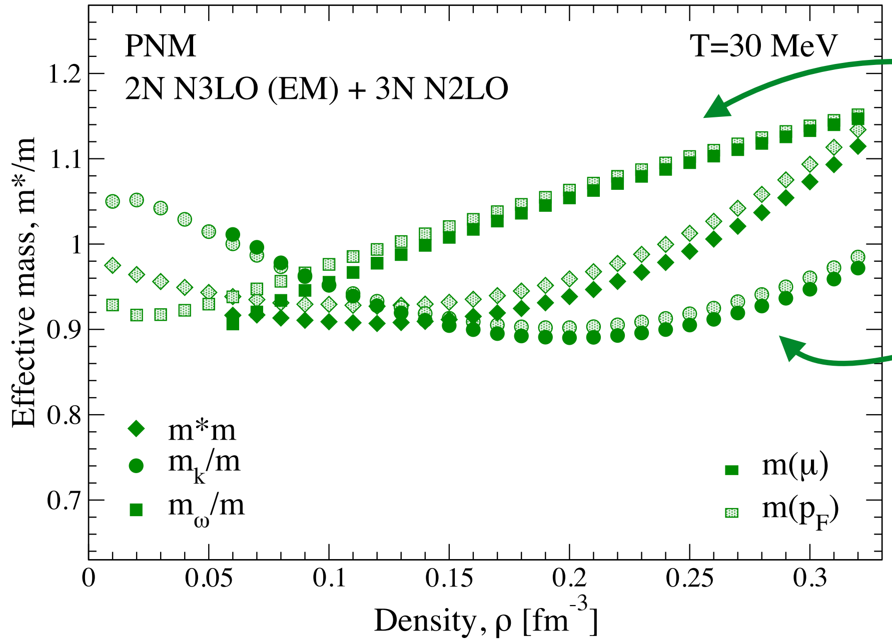

$$m^\omega = 1 - \frac{\partial \mathrm{Re}\Sigma(p,\omega)}{\partial \omega}$$

$$m^k = \left(1 + \frac{m}{p}\frac{\partial \mathrm{Re}\Sigma(p,\omega)}{\partial p}\right)^{-1}$$

Carbone & Schwenk *(in preparation)*

Thermal index parametrized via effective mass

$$\Gamma_{\rm th} = 1 + \frac{P_{\rm th}}{\rho E_{\rm th}} \longrightarrow \boxed{\Gamma_{\rm th} = \frac{5}{3} - \frac{\rho}{m^\star}\frac{dm^\star}{d\rho}}$$

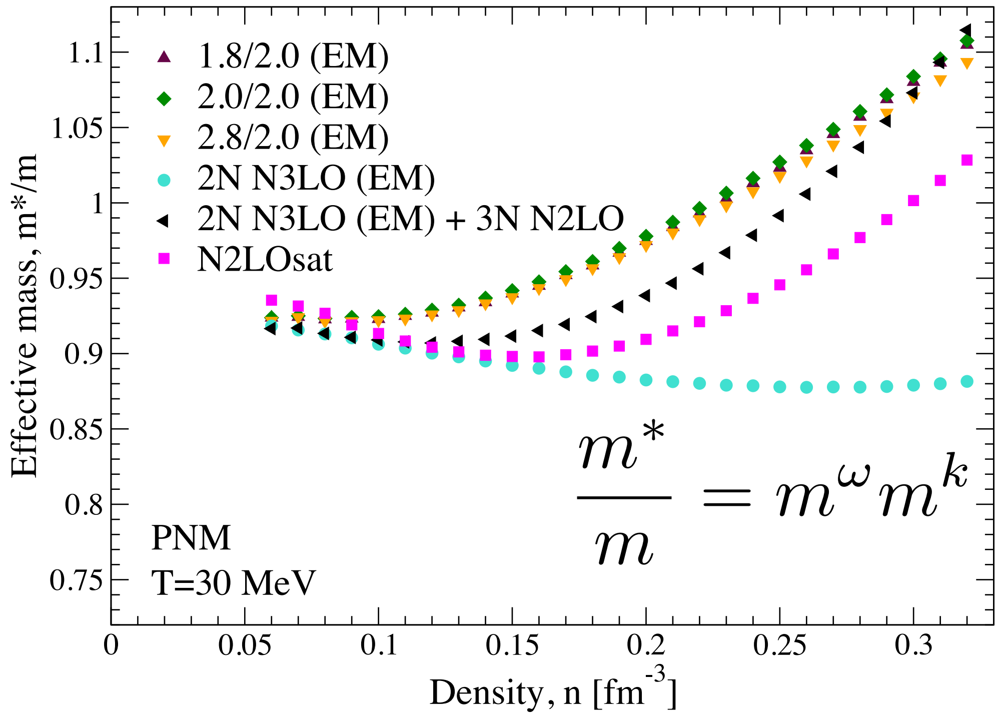

$$\frac{m^*}{m} = m^\omega m^k$$

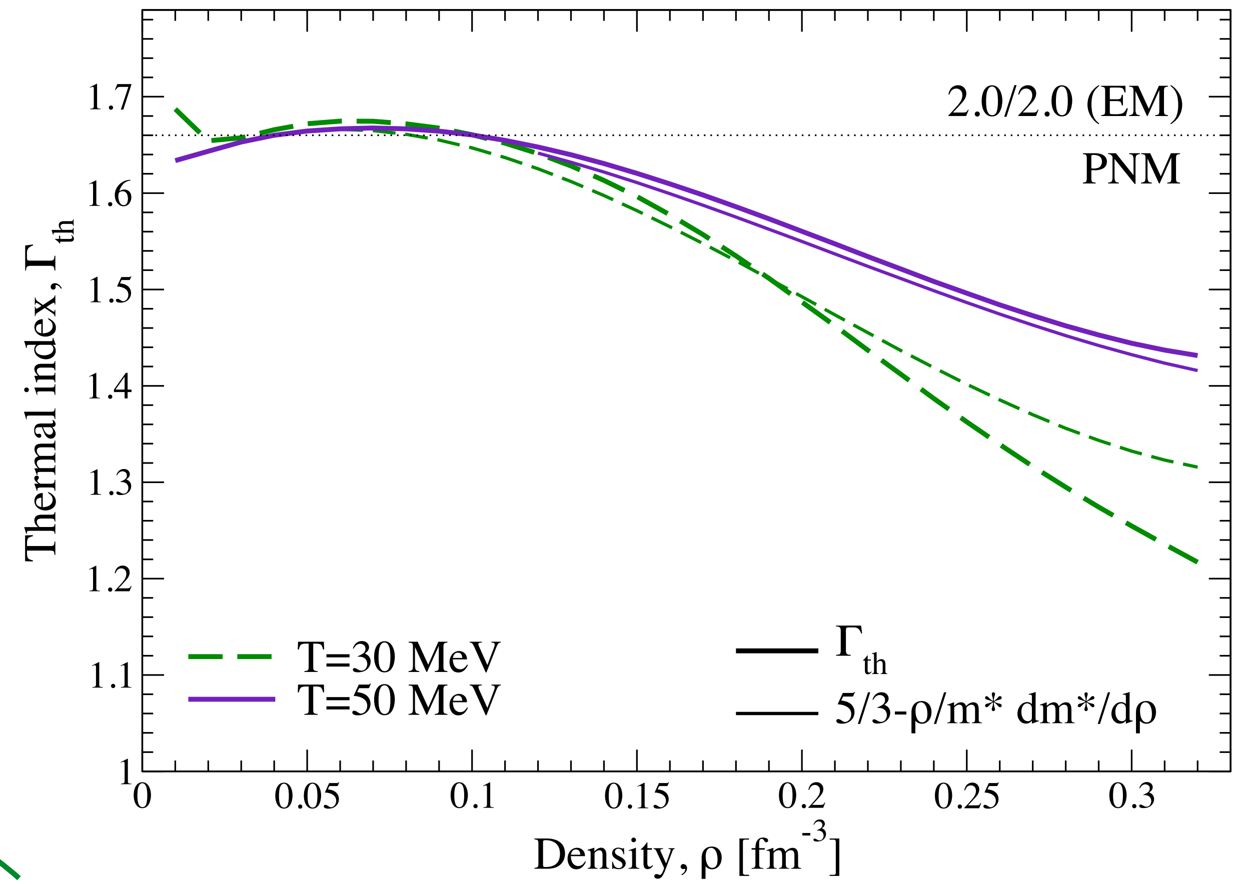

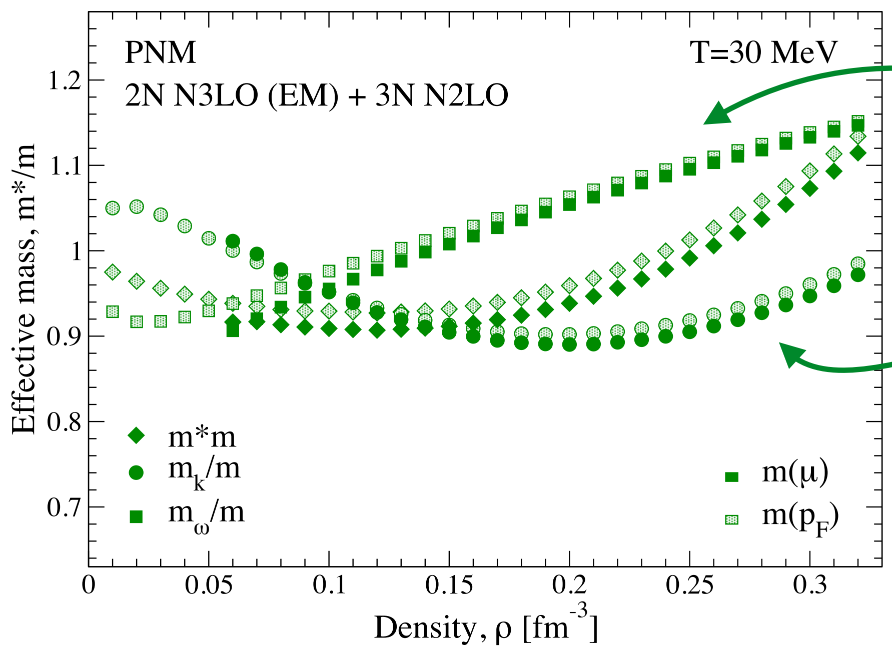

$$m^\omega = 1 - \frac{\partial \mathrm{Re}\Sigma(p,\omega)}{\partial \omega}$$

$$m^k = \left(1 + \frac{m}{p}\frac{\partial \mathrm{Re}\Sigma(p,\omega)}{\partial p}\right)^{-1}$$

Carbone & Schwenk *(in preparation)*

Take home messages

Take home messages

- ⋆ Convenient approach to tackle down properties of nuclear systems

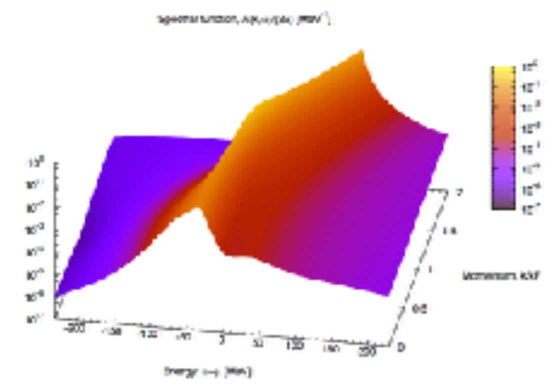

Take home messages

- ★ Convenient approach to tackle down properties of nuclear systems
- ★ Pinning saturation point is not enough for reasonable predictions of symmetry energy

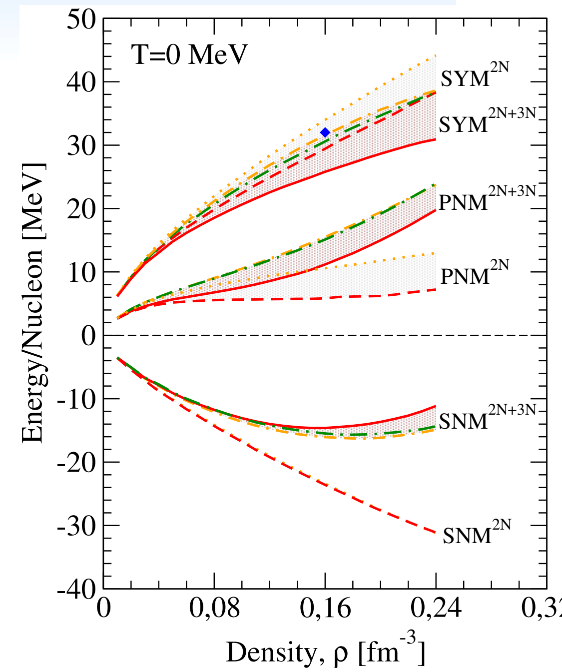

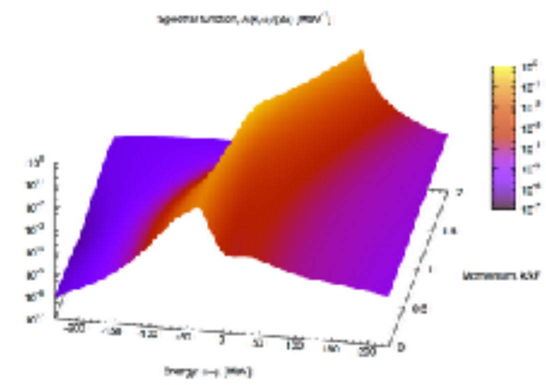

Take home messages

- ★ Convenient approach to tackle down properties of nuclear systems
- ★ Pinning saturation point is not enough for reasonable predictions of symmetry energy
- ★ Ab initio PNM can constrain NS radius

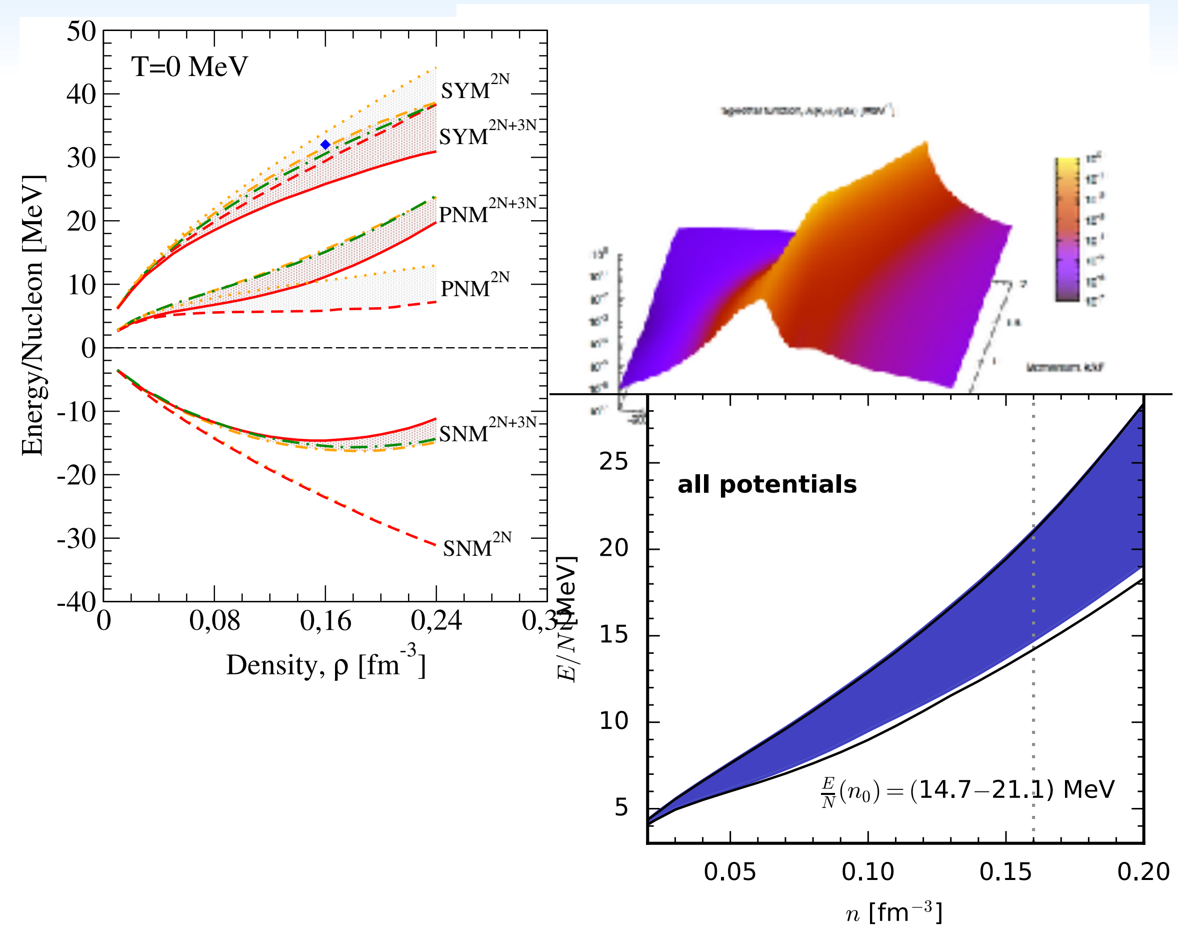

Take home messages

- ★ Convenient approach to tackle down properties of nuclear systems
- ★ Pinning saturation point is not enough for reasonable predictions of symmetry energy
- ★ Ab initio PNM can constrain NS radius
- ★ Acceptable results for the liquid-gas critical temperature

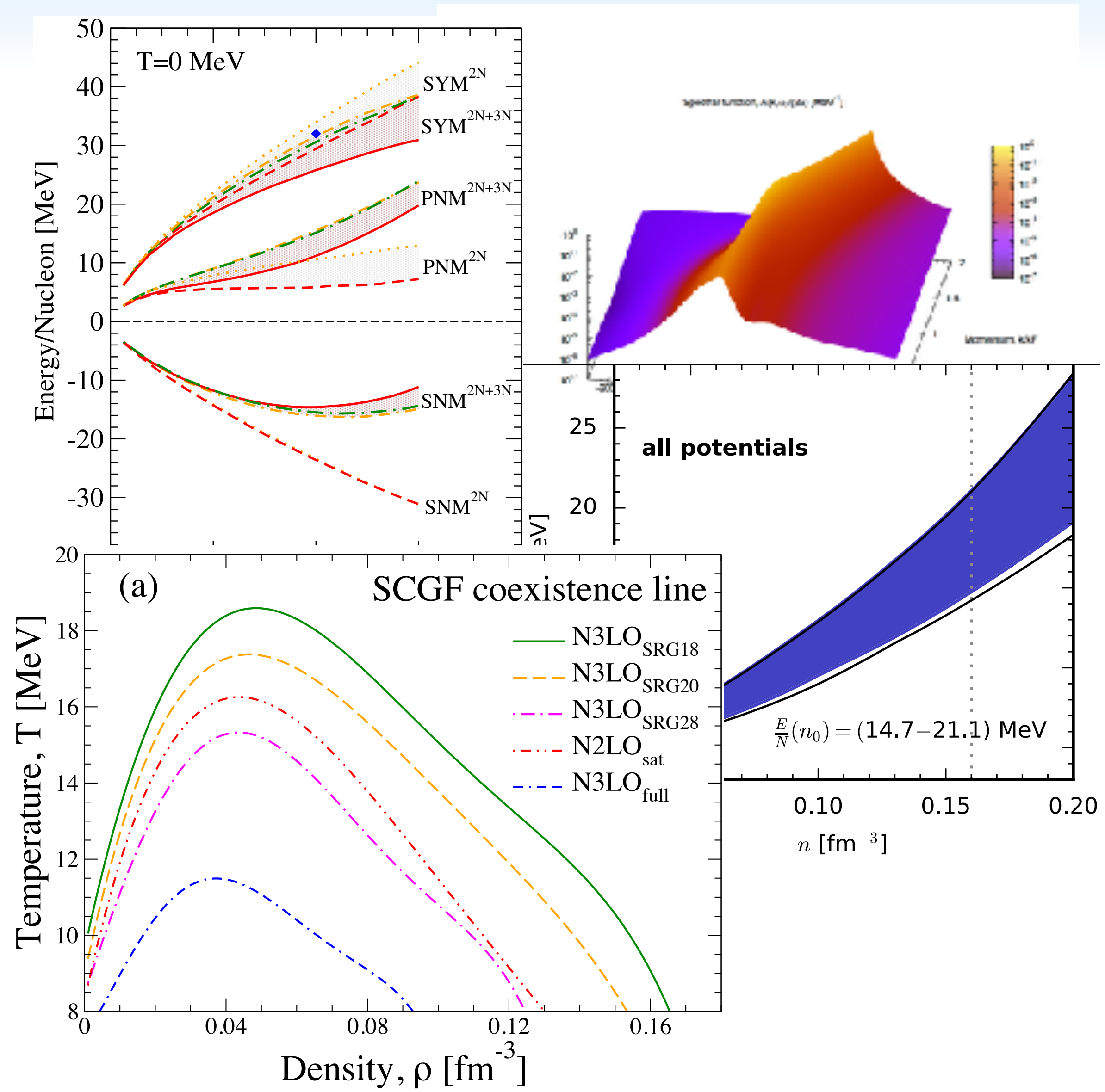

Take home messages

- ★ Convenient approach to tackle down properties of nuclear systems
- ★ Pinning saturation point is not enough for reasonable predictions of symmetry energy
- ★ Ab initio PNM can constrain NS radius
- ★ Acceptable results for the liquid-gas critical temperature
- ★ Correlations between Esat and Tc

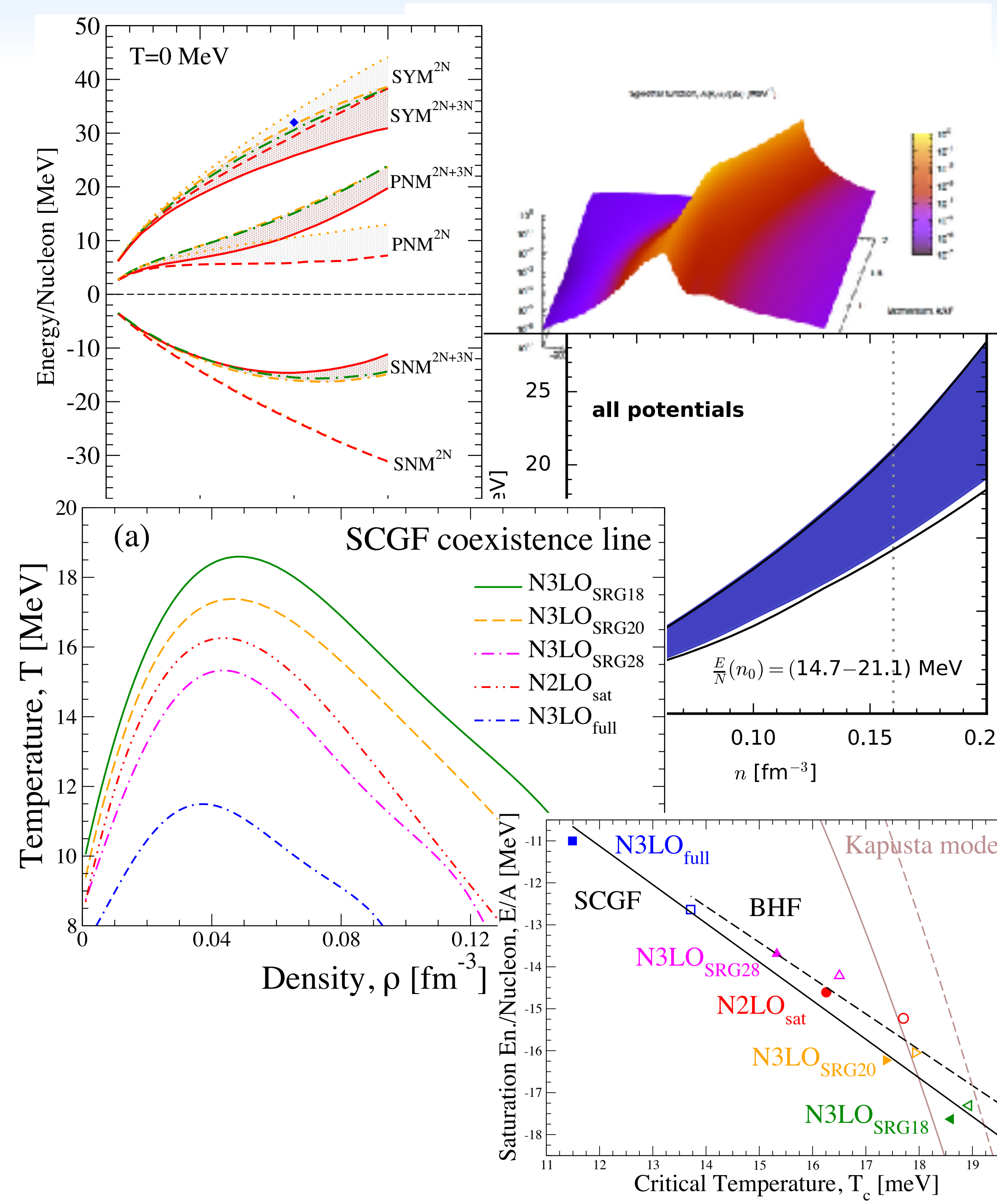

Take home messages

★ Convenient approach to tackle down properties of nuclear systems

★ Pinning saturation point is not enough for reasonable predictions of symmetry energy

★ Ab initio PNM can constrain NS radius

★ Acceptable results for the liquid-gas critical temperature

★ Correlations between Esat and Tc

★ Thermal effects are important for astrophysical applications

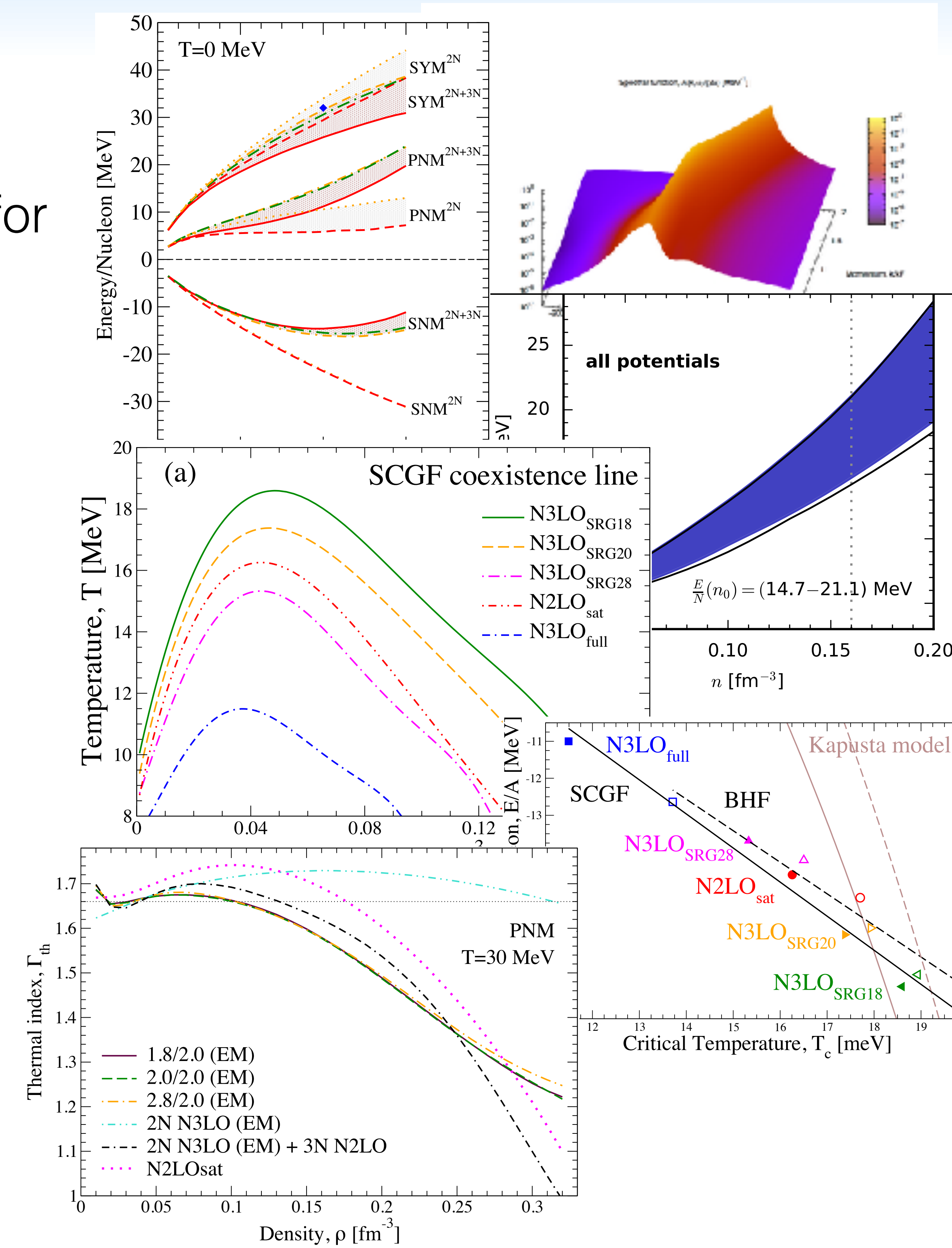

Take home messages

- ★ Convenient approach to tackle down properties of nuclear systems
- ★ Pinning saturation point is not enough for reasonable predictions of symmetry energy
- ★ Ab initio PNM can constrain NS radius
- ★ Acceptable results for the liquid-gas critical temperature
- ★ Correlations between Esat and Tc
- ★ Therm... astro...

Thank you for your attention!

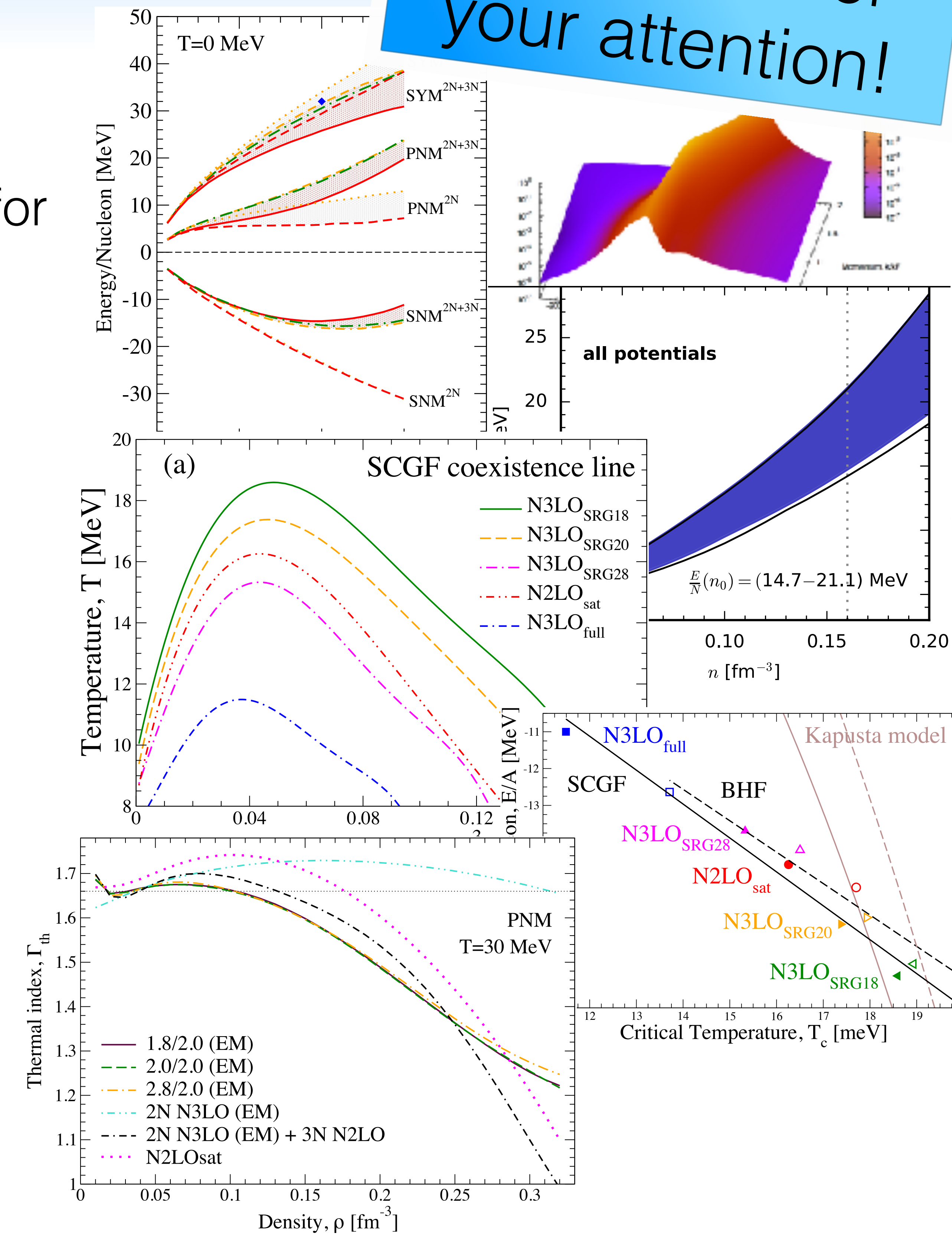

Universitat de Barcelona — A. Polls

University of Surrey — A. Rios, C. Barbieri

Technische Universität Darmstadt — C. Drischler, P. Klos, K. Hebeler, A. Schwenk

Backup

Extended SCGF approach

Carbone, Cipollone, Barbieri, Rios, Polls, PRC **88**, 054326 (2013)

2B

2B + 3B

1. define **effective interactions**:

Interaction

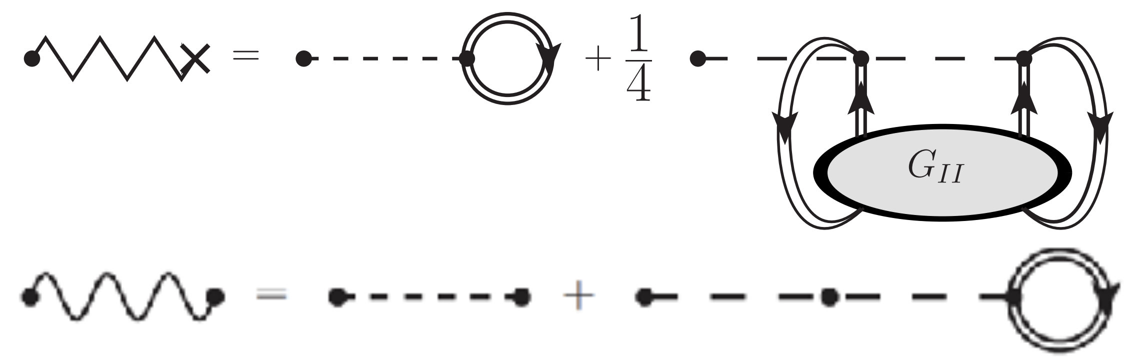

2. modify **ladder approximation**:

T-matrix

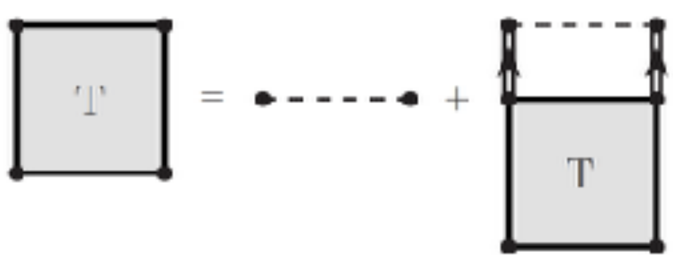

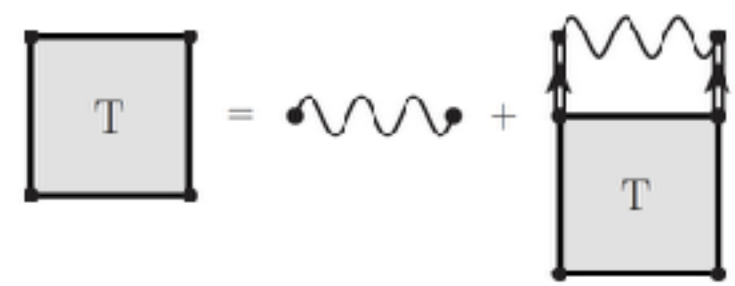

3. correct **diagrams counting**:

Self-energy

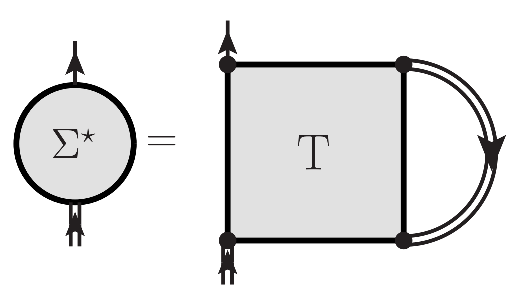

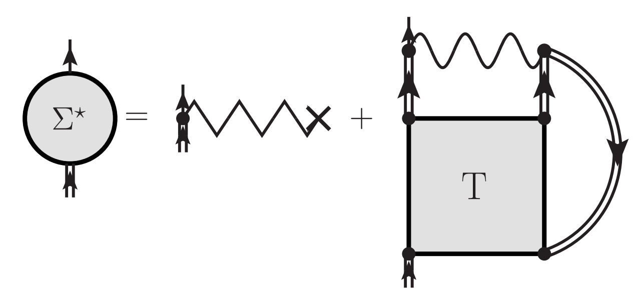

Extended SCGF approach

Carbone, Cipollone, Barbieri, Rios, Polls, PRC **88**, 054326 (2013)

2B → **2B + 3B**

1. define **effective interactions**:

Interaction

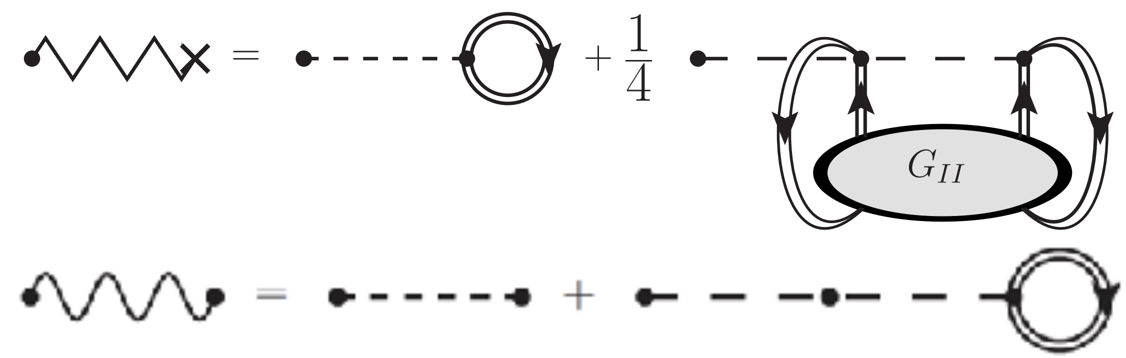

2. modify **ladder approximation**:

T-matrix

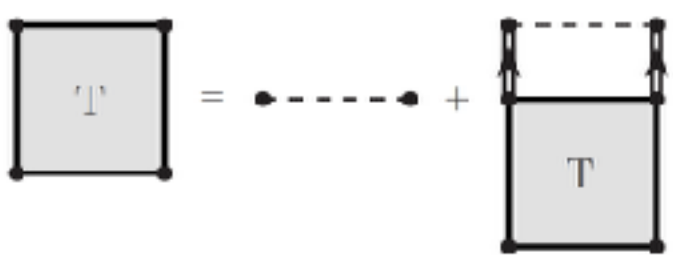

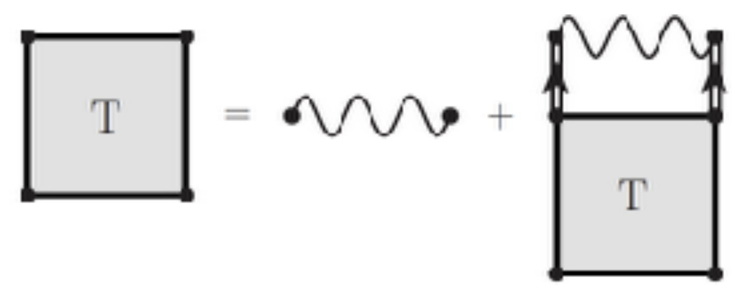

3. correct **diagrams counting**:

Self-energy

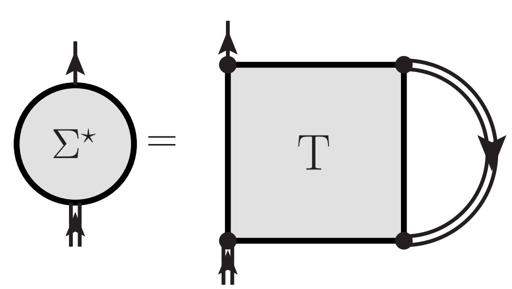

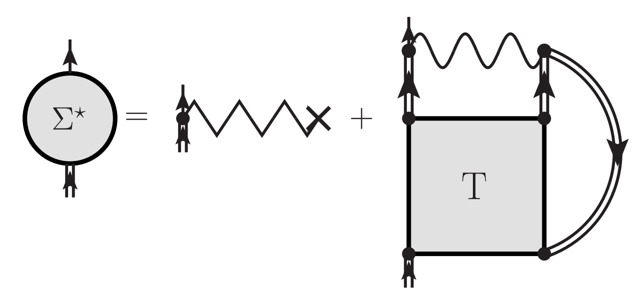

Extended SCGF approach

Carbone, Cipollone, Barbieri, Rios, Polls, PRC **88**, 054326 (2013)

2B → **2B + 3B**

1. define **effective interactions**:

Interaction

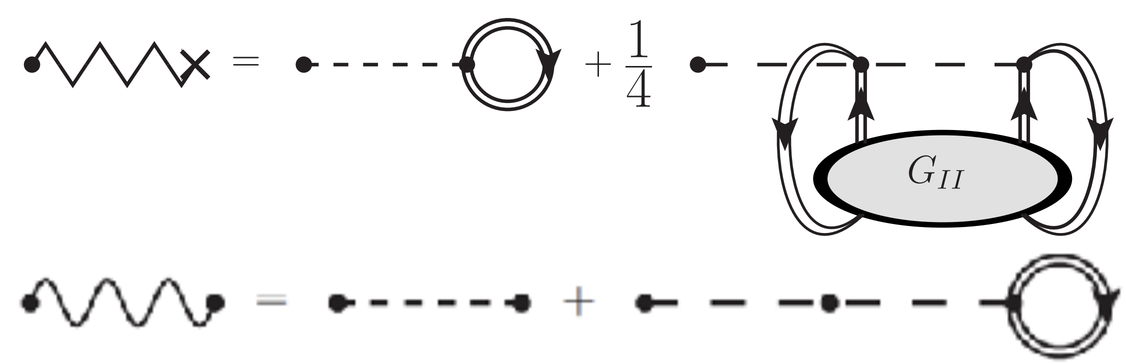

2. modify **ladder approximation**:

T-matrix

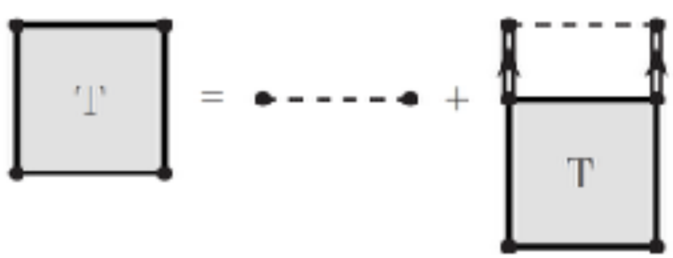

3. correct **diagrams counting**:

Self-energy

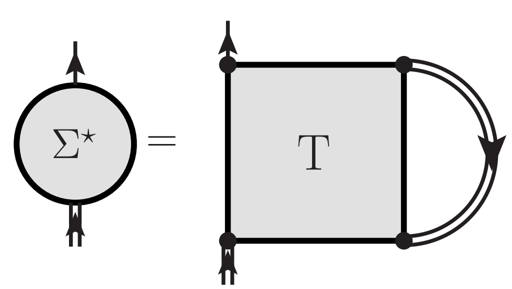

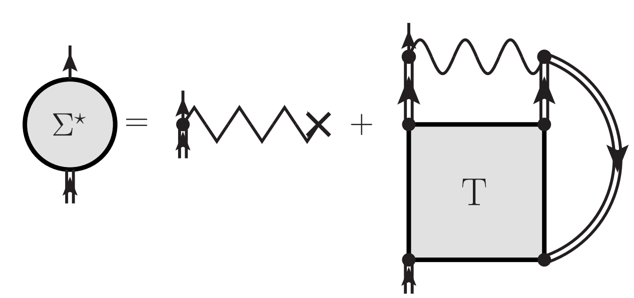

Extended SCGF approach

Carbone, Cipollone, Barbieri, Rios, Polls, PRC **88**, 054326 (2013)

2B → **2B + 3B**

1. define **effective interactions**:

Interaction

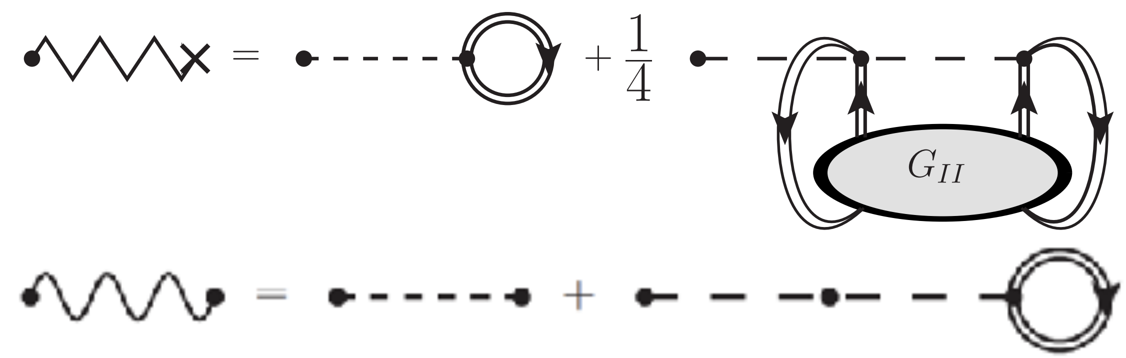

2. modify **ladder approximation**:

T-matrix

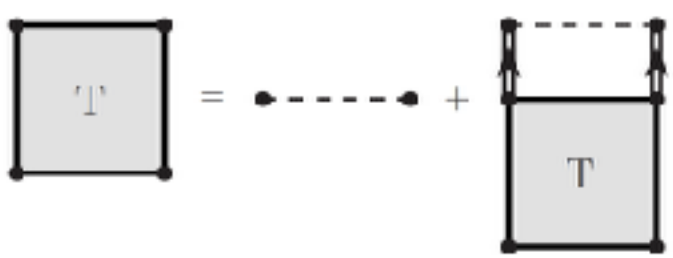

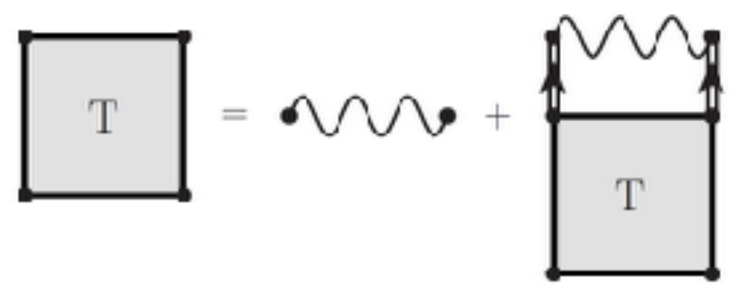

3. correct **diagrams counting**:

Self-energy

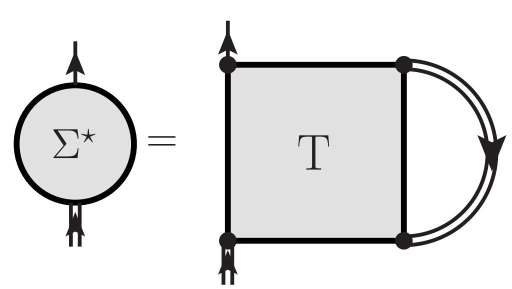

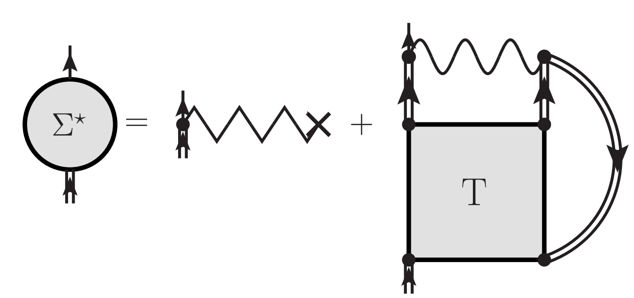

Extended SCGF approach

Carbone, Cipollone, Barbieri, Rios, Polls, PRC **88**, 054326 (2013)

2B → **2B + 3B**

1. define **effective interactions**:

Interaction

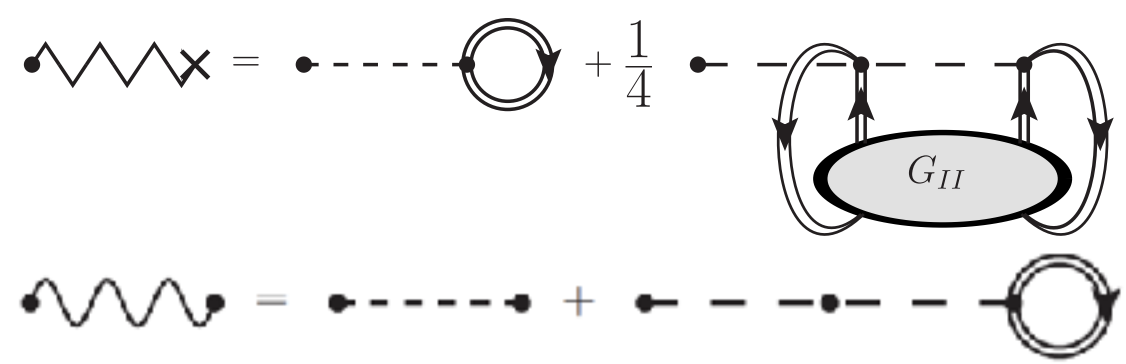

2. modify **ladder approximation**:

T-matrix

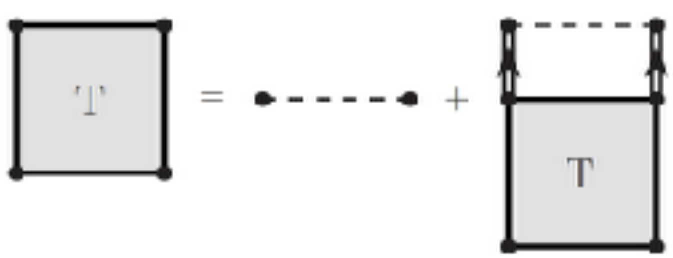

3. correct **diagrams counting**:

Self-energy

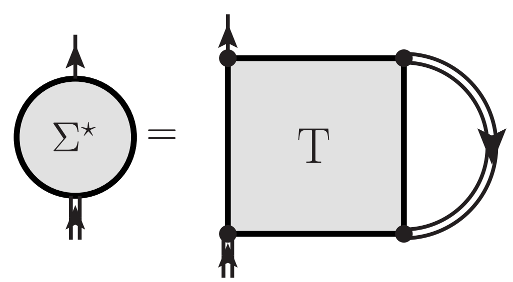

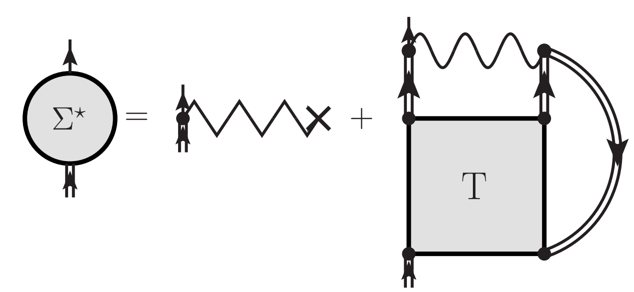

Extended SCGF approach

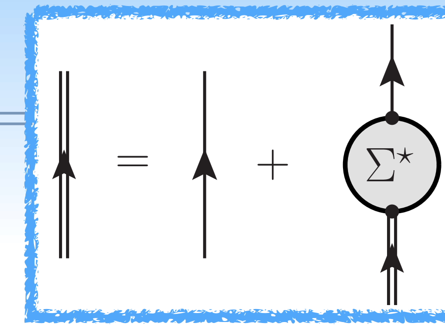

Carbone, Cipollone, Barbieri, Rios, Polls, PRC **88**, 054326 (2013)

2B → **2B + 3B**

1. define **effective interactions**:

Interaction

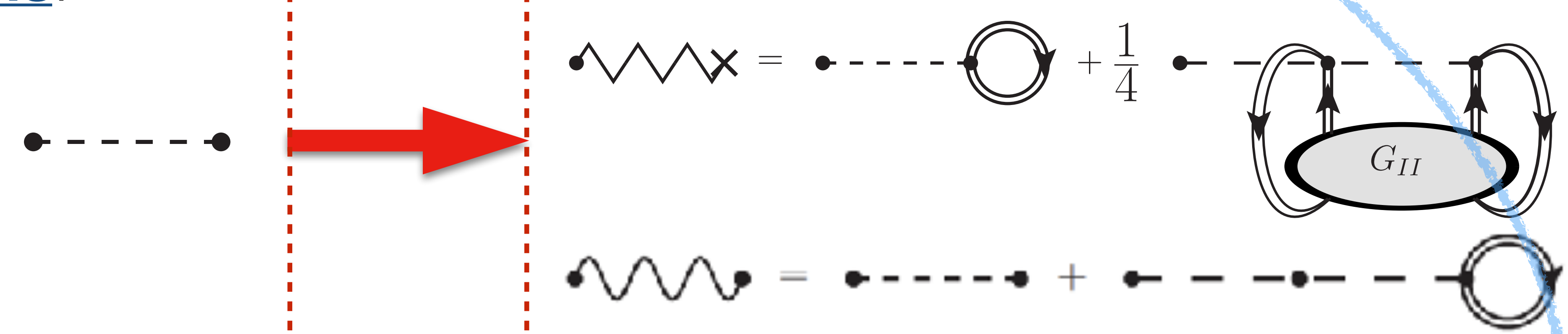

2. modify **ladder approximation**:

T-matrix

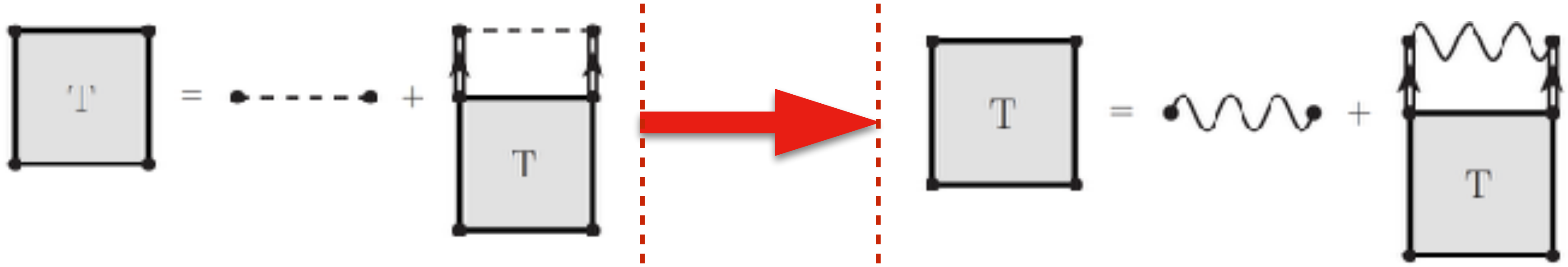

3. correct **diagrams counting**:

Self-energy

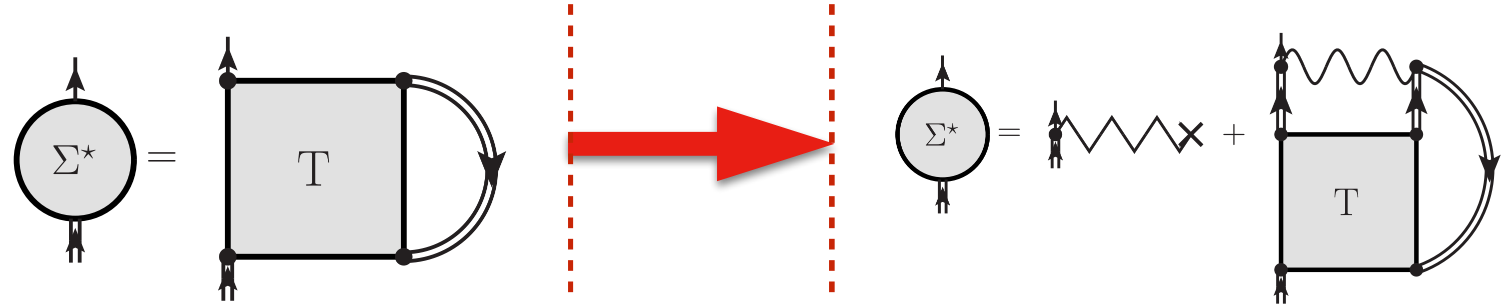

The 4-pt vertex function

Carbone, Cipollone, Barbieri, Rios, Polls, PRC **88**, 054326 (2013)

Obtain the interacting vertex function including 3body forces:

The 4-pt vertex function:

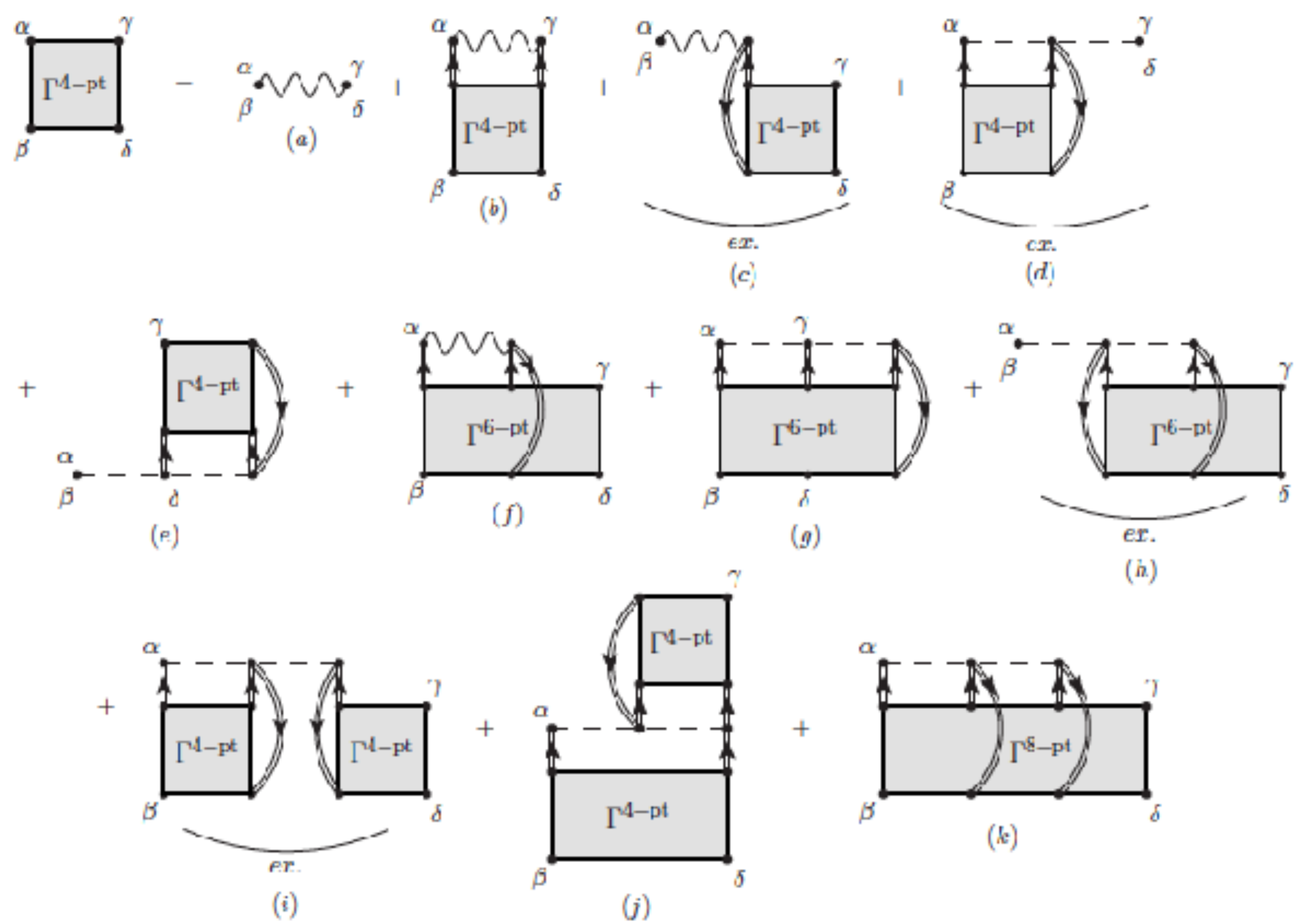

It's an equation including the 4-pt, 6-pt and 8-pt interacting vertex functions!

The 4-pt vertex function

Carbone, Cipollone, Barbieri, Rios, Polls, PRC **88**, 054326 (2013)

Obtain the interacting vertex function including 3body forces:

The 4-pt vertex function:

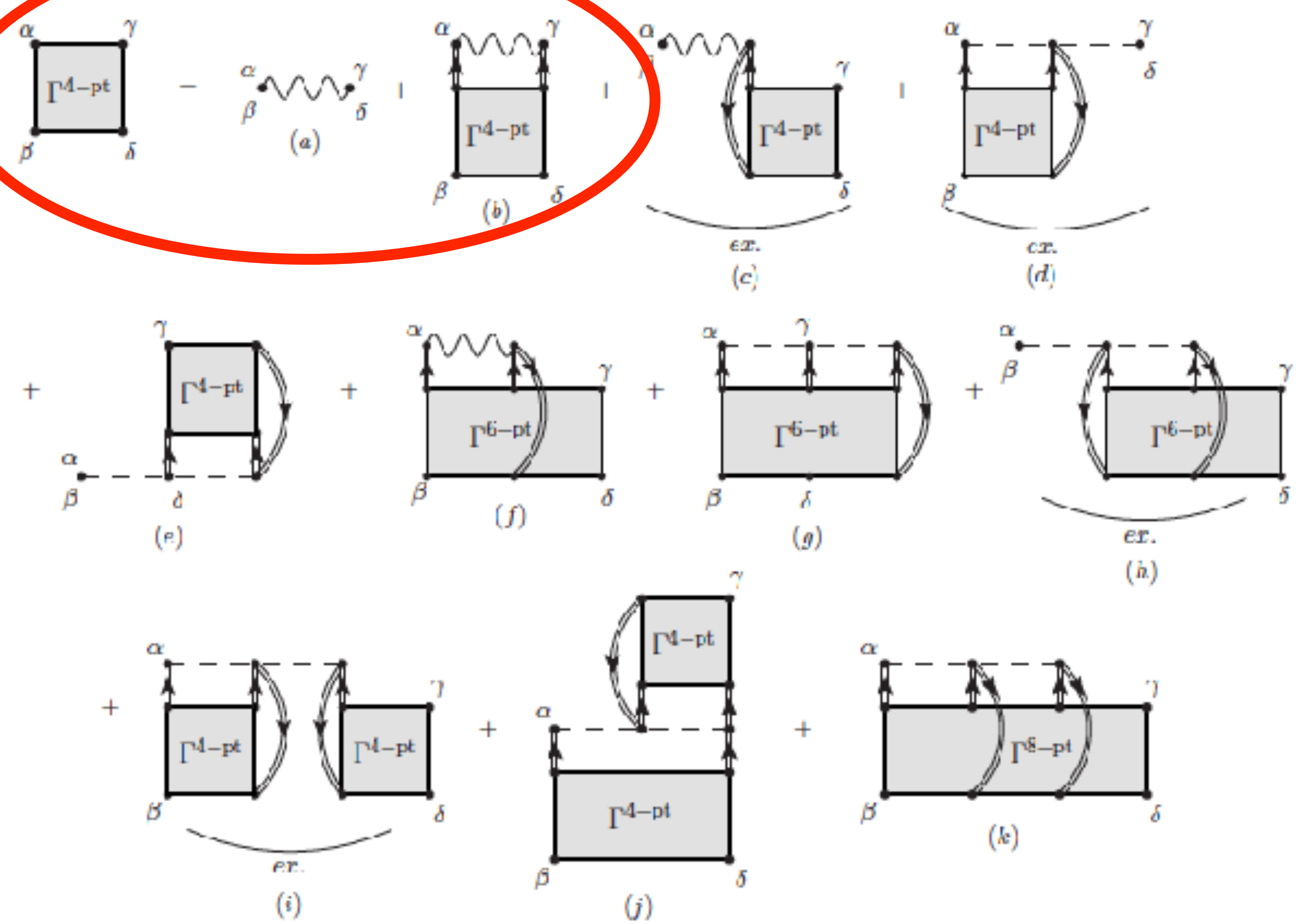

It's an equation including the 4-pt, 6-pt and 8-pt interacting vertex functions!

The single-particle self-energy

Carbone, Cipollone, Barbieri, Rios, Polls, PRC **88**, 054326 (2013)

Calculate self-energy paying attention to the effective terms

Self-energy:

2B

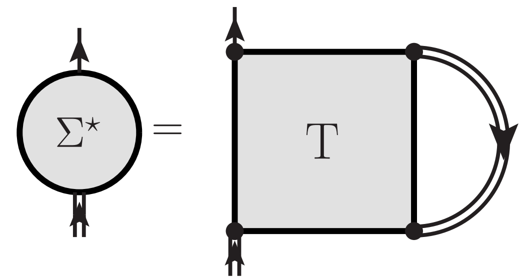

2B + 3B

Residual 3NF

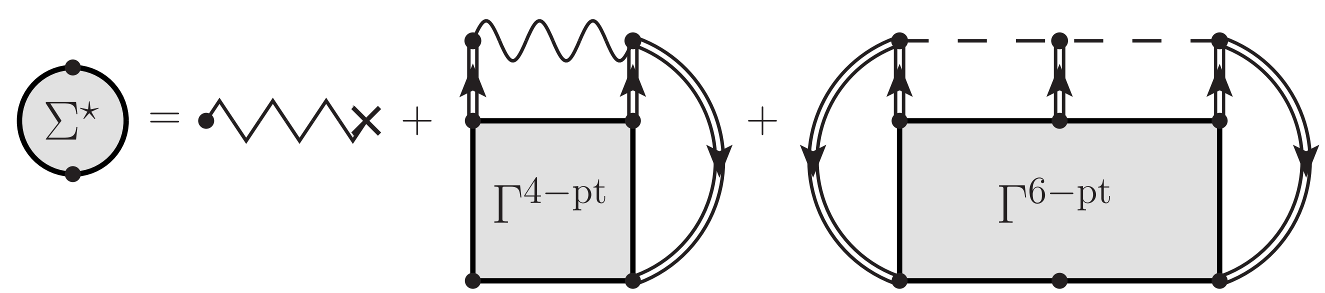

The single-particle self-energy

Carbone, Cipollone, Barbieri, Rios, Polls, PRC **88**, 054326 (2013)

Calculate self-energy paying attention to the effective terms

Self-energy:

2B

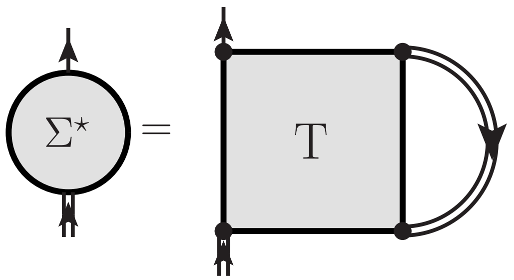

2B + 3B

Residual 3NF

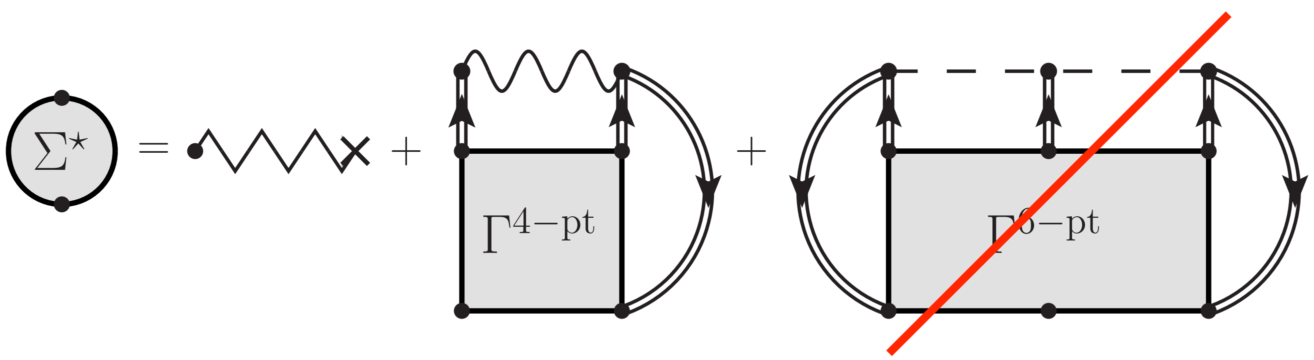

The single-particle self-energy

Carbone, Cipollone, Barbieri, Rios, Polls, PRC **88**, 054326 (2013)

Calculate self-energy paying attention to the effective terms

Self-energy:

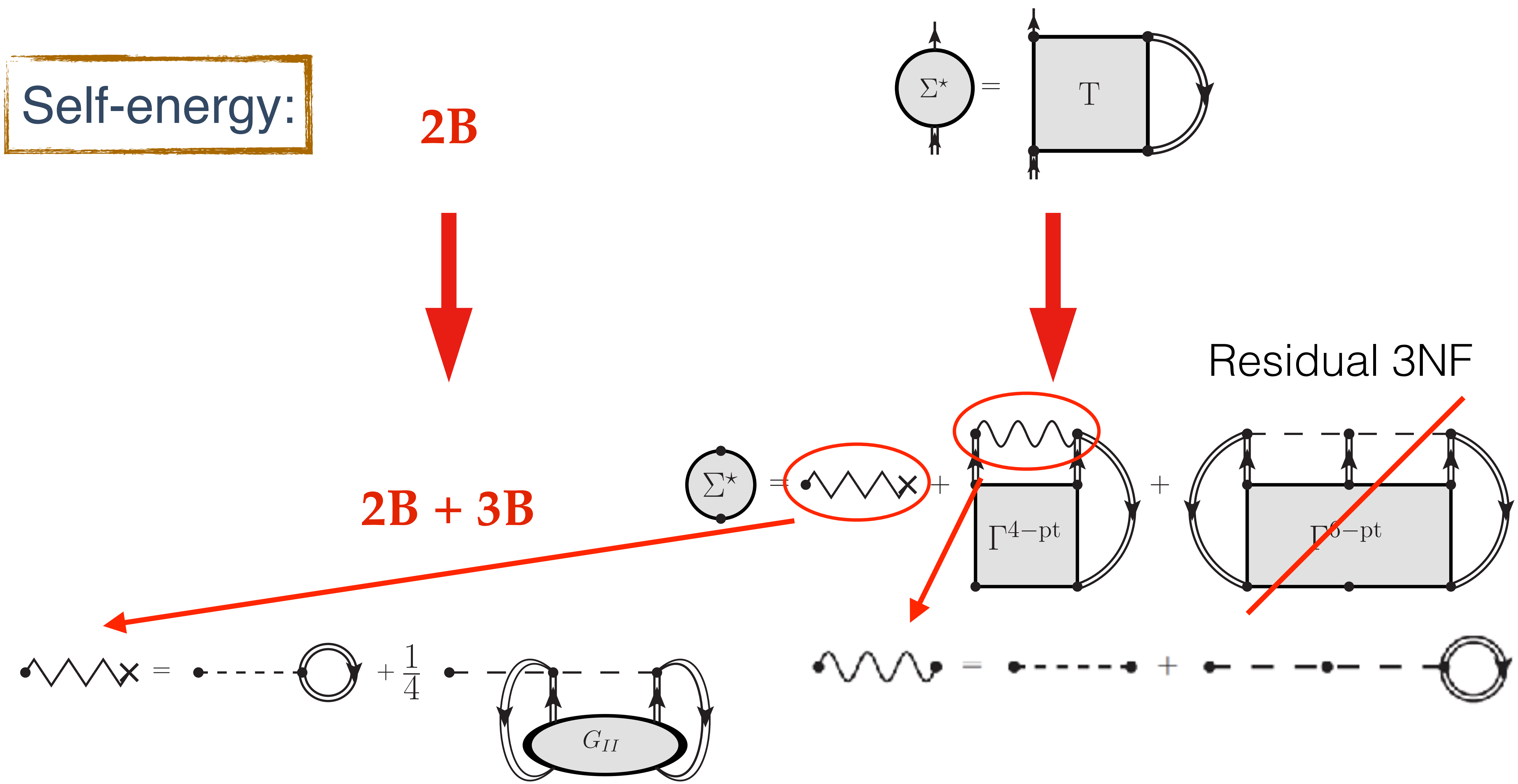

The single-particle self-energy

Carbone, Cipollone, Barbieri, Rios, Polls, PRC **88**, 054326 (2013)

Calculate self-energy paying attention to the effective terms

Self-energy:

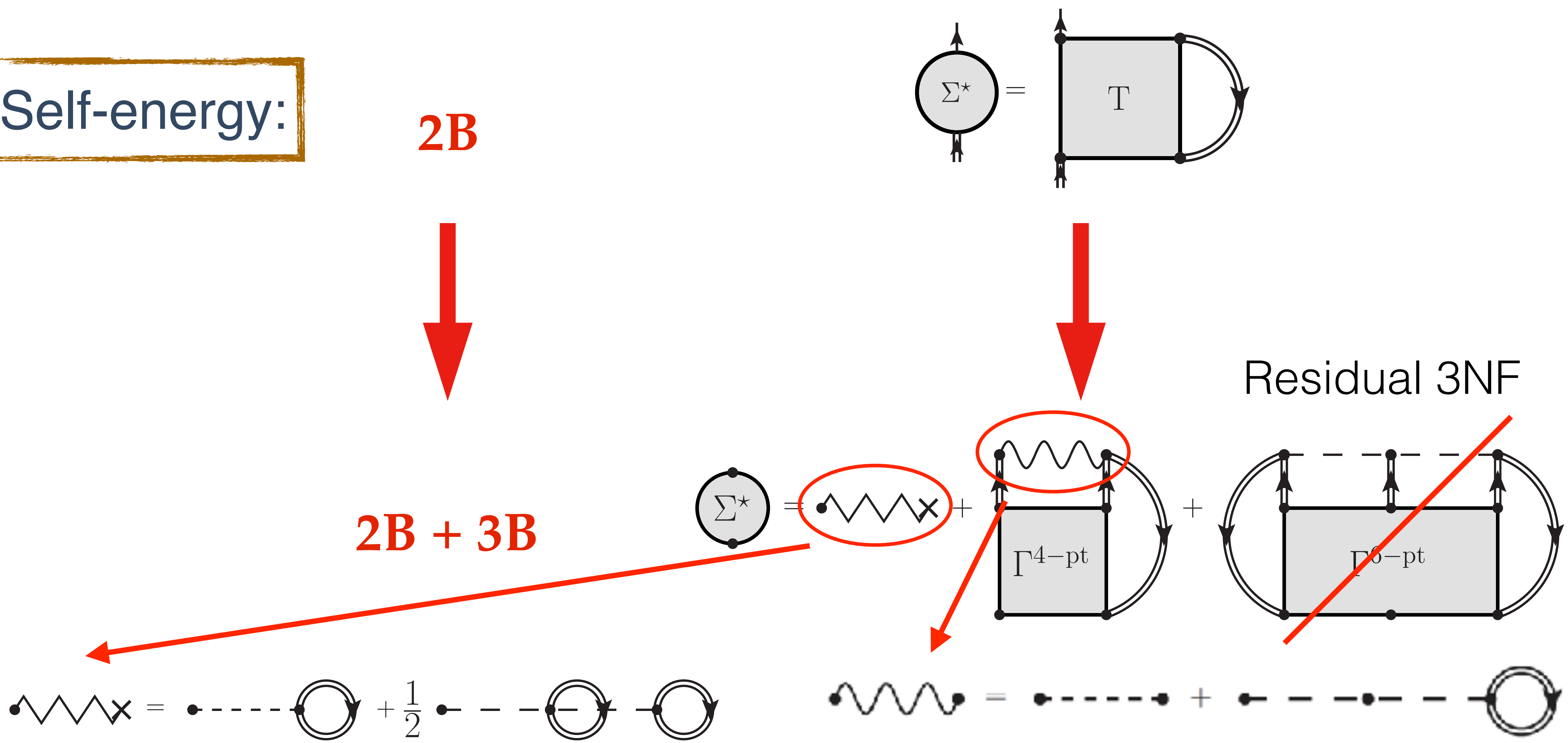

Define a new sum rule

Carbone, Cipollone, Barbieri, Rios, Polls, PRC **88**, 054326 (2013)

$$E^N = \langle \Psi^N | \hat{H} | \Psi^N \rangle = \langle \Psi^N | \hat{T} | \Psi^N \rangle + \langle \Psi^N | \hat{V} | \Psi^N \rangle + \langle \Psi^N | \hat{W} | \Psi^N \rangle$$

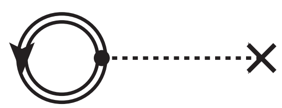

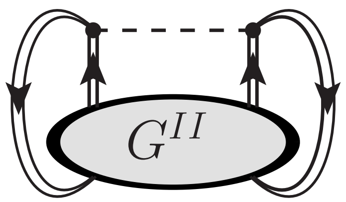

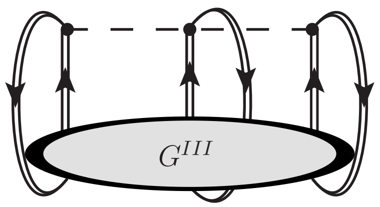

- Galitskii-Migdal-Koltun sumrule modified:

$$\sum_\alpha \int_{-\infty}^{E^N - E^{N-1}} \mathrm{d}\omega\, \omega \frac{1}{\pi} \mathrm{Im}\, G_{\alpha\alpha}(\omega) = \langle \Psi^N | \hat{T} | \Psi^N \rangle + 2 \langle \Psi^N | \hat{V} | \Psi^N \rangle + 3 \langle \Psi^N | \hat{W} | \Psi^N \rangle$$

$$\boxed{\frac{E}{A} = \frac{\nu}{\rho} \int \frac{\mathrm{d}^3 p}{(2\pi)^3} \int \frac{\mathrm{d}\omega}{2\pi} \frac{1}{2} \left\{ \frac{p^2}{2m} + \omega \right\} \mathcal{A}(p,\omega) f(\omega) - \frac{1}{2} \langle \Psi^N | \hat{W} | \Psi^N \rangle}$$

Define a new sum rule

Carbone, Cipollone, Barbieri, Rios, Polls, PRC **88**, 054326 (2013)

$$E^N = \langle \Psi^N | \hat{H} | \Psi^N \rangle = \langle \Psi^N | \hat{T} | \Psi^N \rangle + \langle \Psi^N | \hat{V} | \Psi^N \rangle + \langle \Psi^N | \hat{W} | \Psi^N \rangle$$

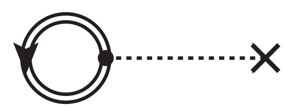

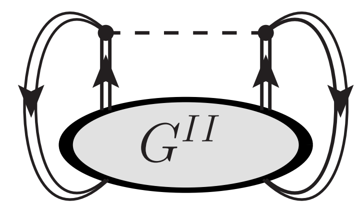

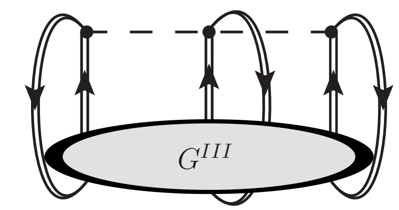

- Galitskii-Migdal-Koltun sumrule modified:

$$\sum_\alpha \int_{-\infty}^{E^N - E^{N-1}} \mathrm{d}\omega \, \omega \frac{1}{\pi} \mathrm{Im}\, G_{\alpha\alpha}(\omega) = \langle \Psi^N | \hat{T} | \Psi^N \rangle + 2 \langle \Psi^N | \hat{V} | \Psi^N \rangle + 3 \langle \Psi^N | \hat{W} | \Psi^N \rangle$$

$$\boxed{\frac{E}{A} = \frac{\nu}{\rho} \int \frac{\mathrm{d}^3 p}{(2\pi)^3} \int \frac{\mathrm{d}\omega}{2\pi} \frac{1}{2} \left\{ \frac{p^2}{2m} + \omega \right\} \mathcal{A}(p,\omega) f(\omega) - \frac{1}{2} \langle \Psi^N | \hat{W} | \Psi^N \rangle}$$

Modified Koltun sum rule

Carbone, Cipollone, Barbieri, Rios, Polls, PRC **88**, 054326 (2013)

$$\frac{E}{A} = \frac{\nu}{\rho}\int \frac{\mathrm{d}^3 p}{(2\pi)^3}\int \frac{\mathrm{d}\omega}{2\pi}\frac{1}{2}\left\{\frac{p^2}{2m}+\omega\right\}\mathcal{A}(p,\omega)f(\omega) - \frac{1}{2}\langle\Psi^N|\hat{W}|\Psi^N\rangle$$

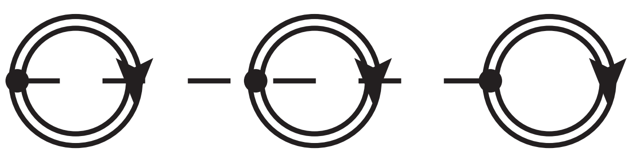

1st order fully dressed

$$\frac{E}{A} = \frac{\nu}{\rho}\int \frac{\mathrm{d}^3 p}{(2\pi)^3}\int \frac{\mathrm{d}\omega}{2\pi}\frac{1}{2}\left\{\frac{p^2}{2m}+\omega - \frac{1}{3}\Sigma_{HF}^{3NF}(p)\right\}\mathcal{A}(p,\omega)f(\omega)$$

Why nuclear matter from chiral EFT?

Epelbaum *et al.*, Rev. Mod. Phys. 81, 1773(2009)
Machleidt *et al.*, Phys. Rep. 503, 1 (2011)

Power counting

- Effective theory of QCD
- Nucleons & pions as d.o.f.
- Power counting expansion
- Hierarchy of many-body forces
- Theoretical uncertainties

Over 20 years of ongoing improvement

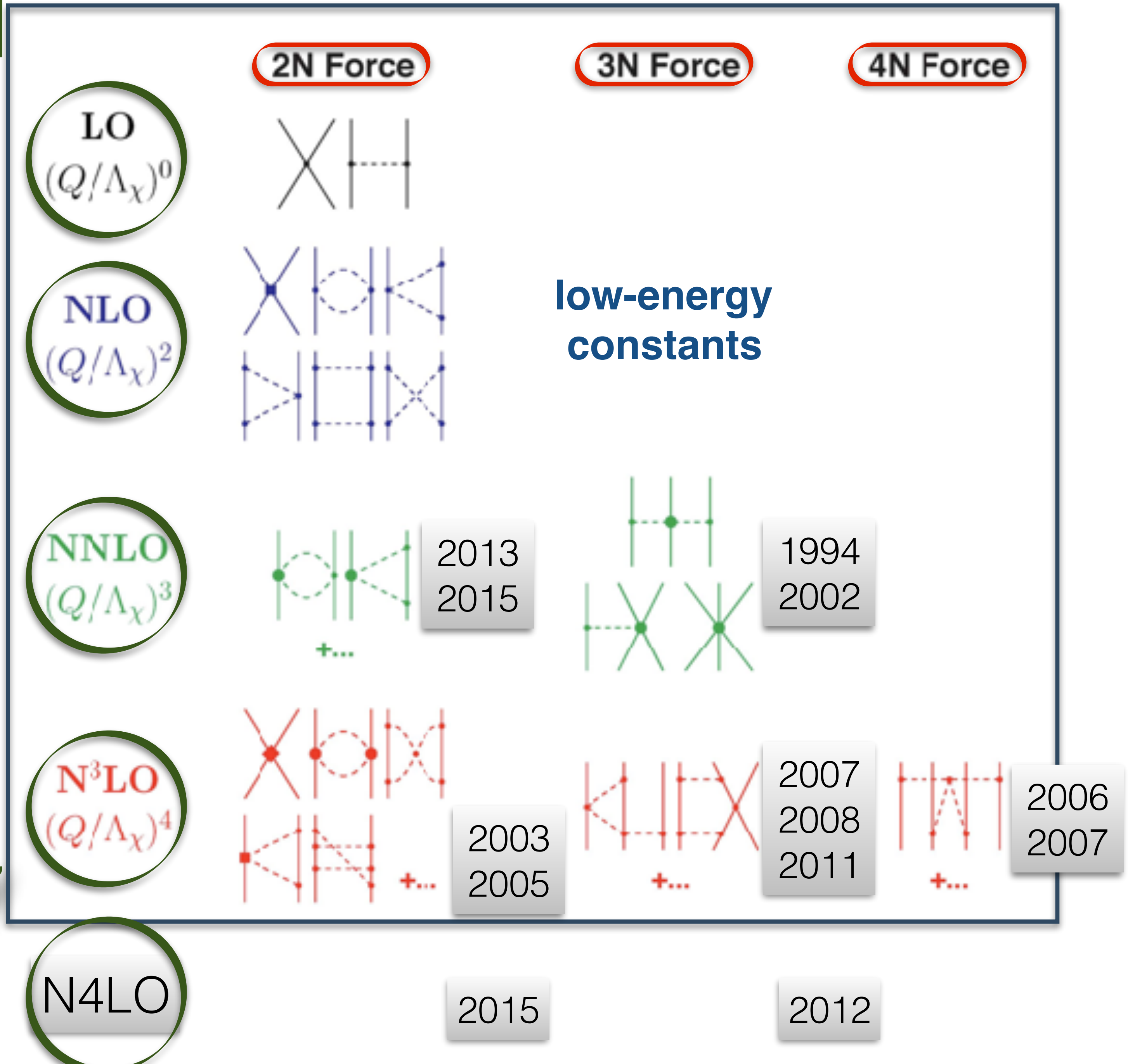

Temperature dependence

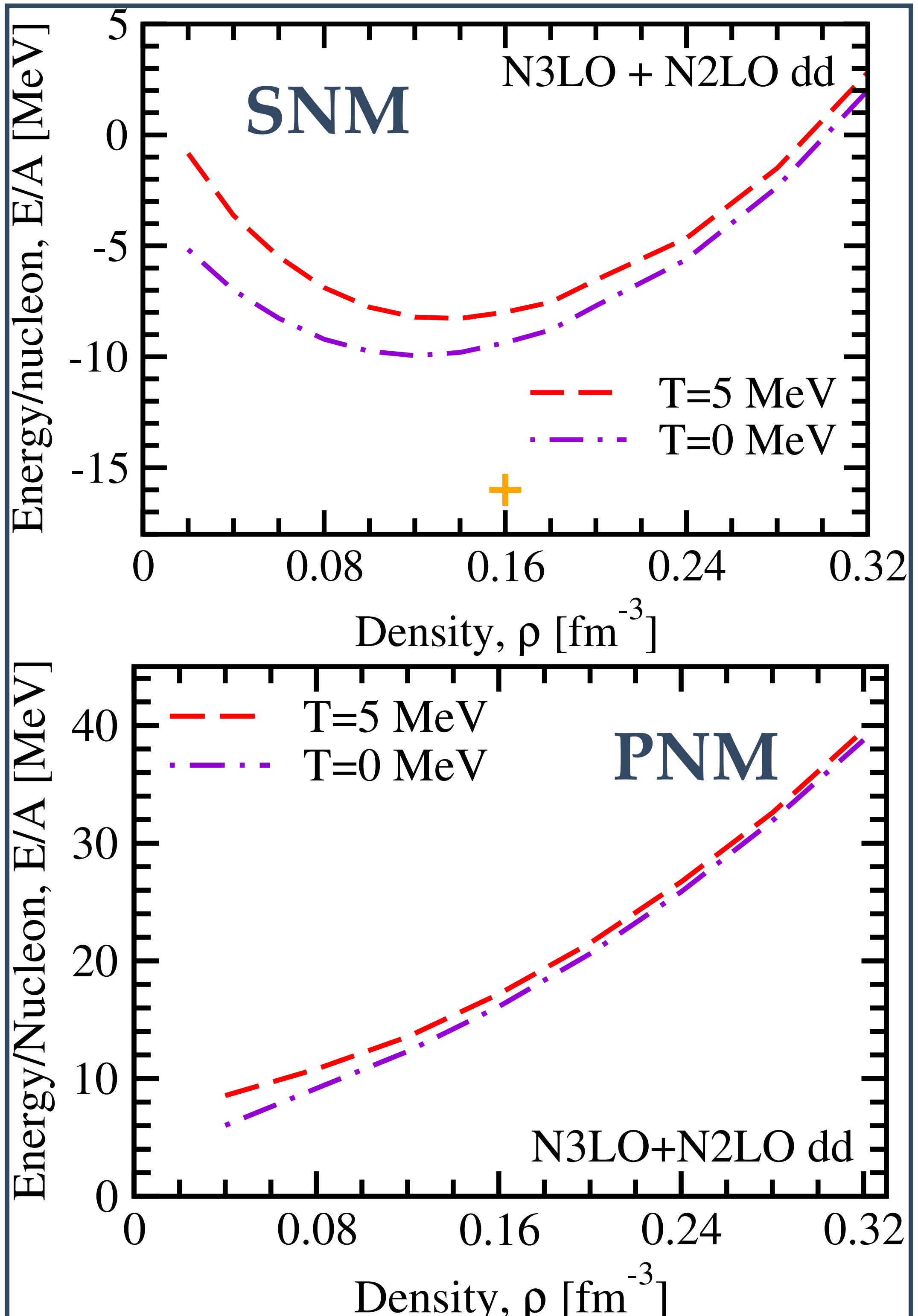

- overcome pairing instability at zero-T
- exploit the Sommerfeld expansion for low temperatures
  - energy: $e \sim e_0 + a\,T^2$
  - free-energy: $f \sim f_0 - a\,T^2$
- semi-sum is an estimate of zero-T results

$\Delta E_{SNM}(\rho_0)$~1.4 MeV, $\Delta E_{PNM}(\rho_0)$~1 MeV

Spectral vision of the nuclear interaction

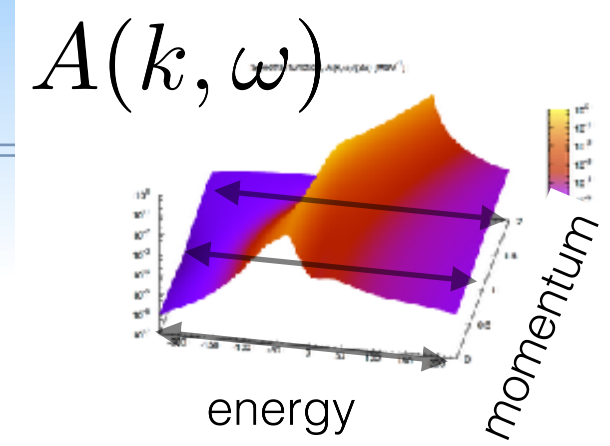

Rios, Carbone, Polls, PRC 96, 014003 (2017)

Hard-core

Soft-core

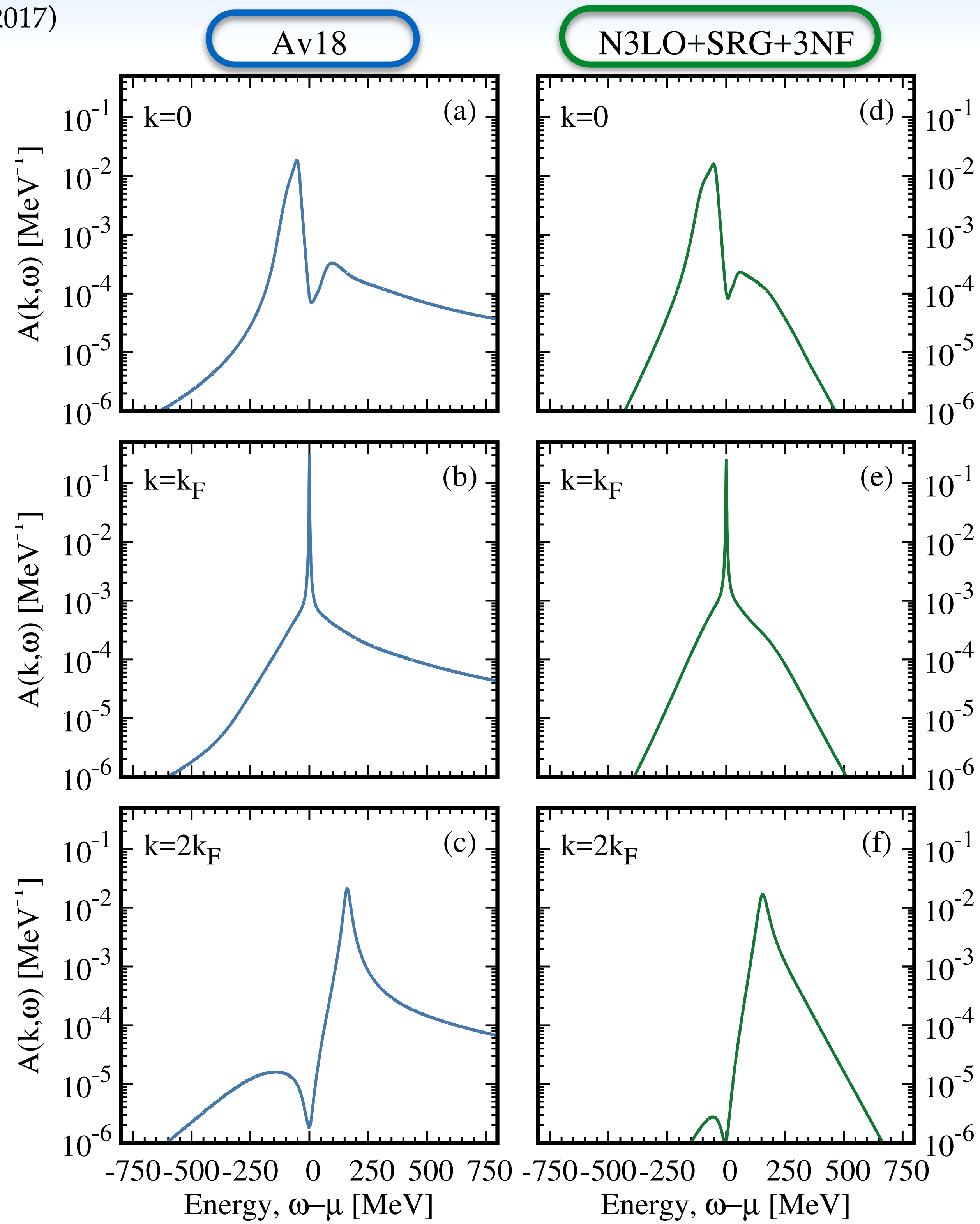

$\rho = 0.20\mathrm{fm}^{-3}$

$k_{\mathrm{F}} = 283\,\mathrm{MeV}$

SNM

Spectral vision of the nuclear interaction

Rios, Carbone, Polls, PRC 96, 014003 (2017)

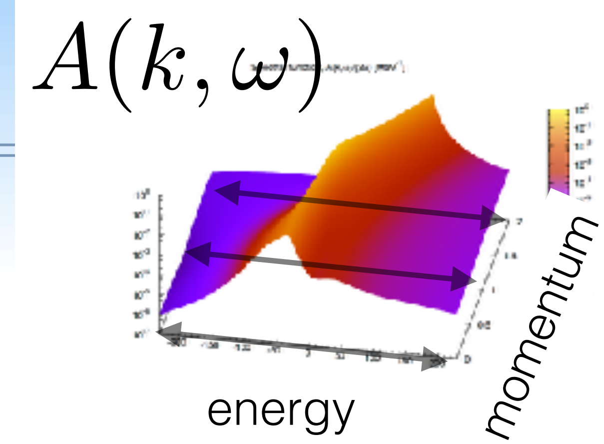

Hard-core

Soft-core

high-energy tails populated

high-energy tails suppressed

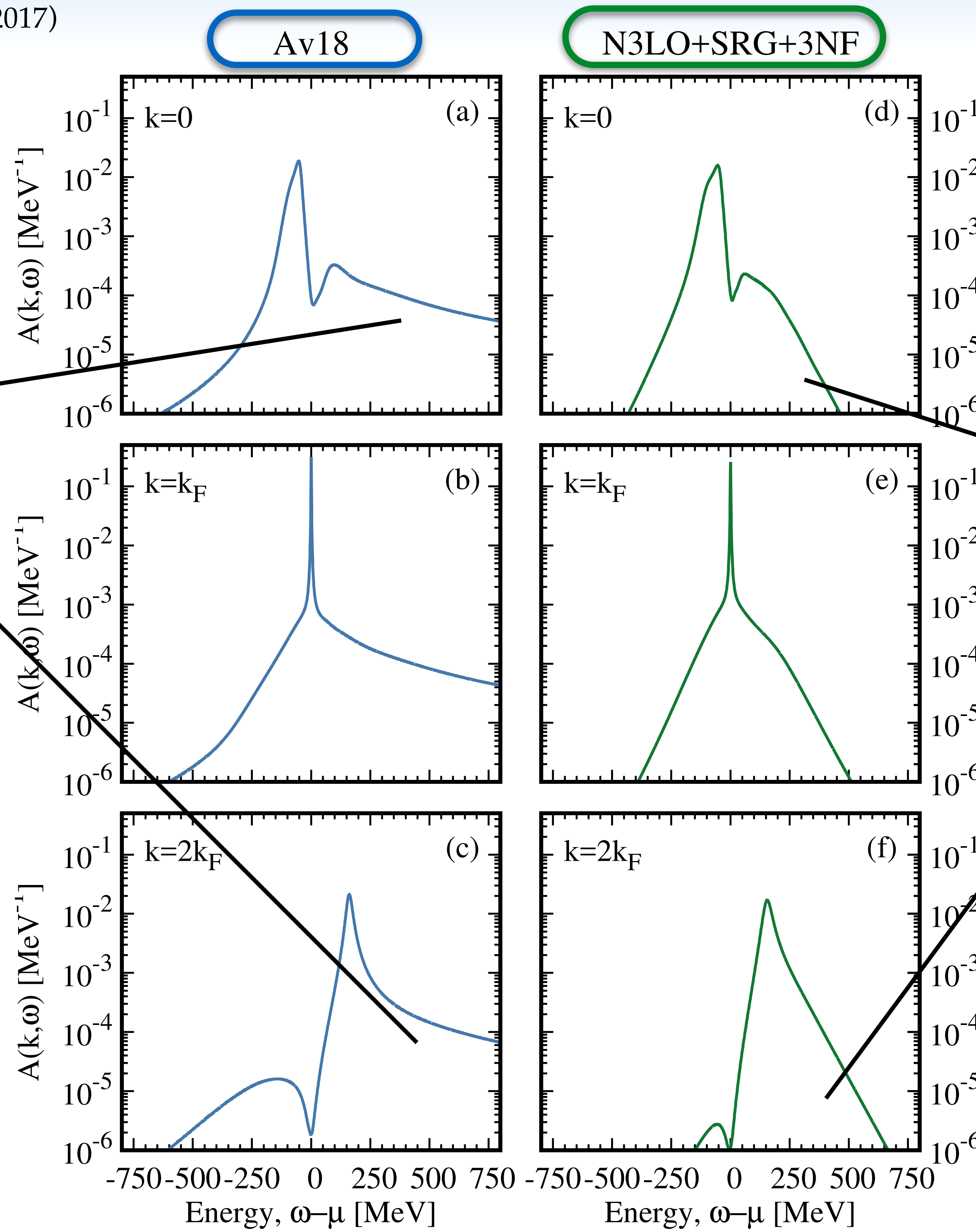

$$\rho = 0.20\mathrm{fm}^{-3}$$

$$k_\mathrm{F} = 283\,\mathrm{MeV}$$

SNM

Spectral vision of the nuclear interaction

Rios, Carbone, Polls, PRC 96, 014003 (2017)

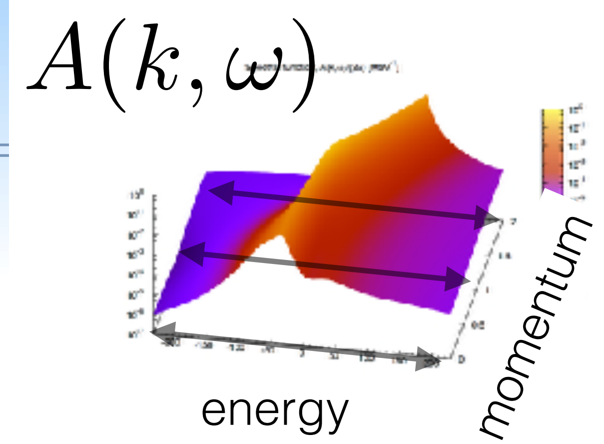

Hard-core

Soft-core

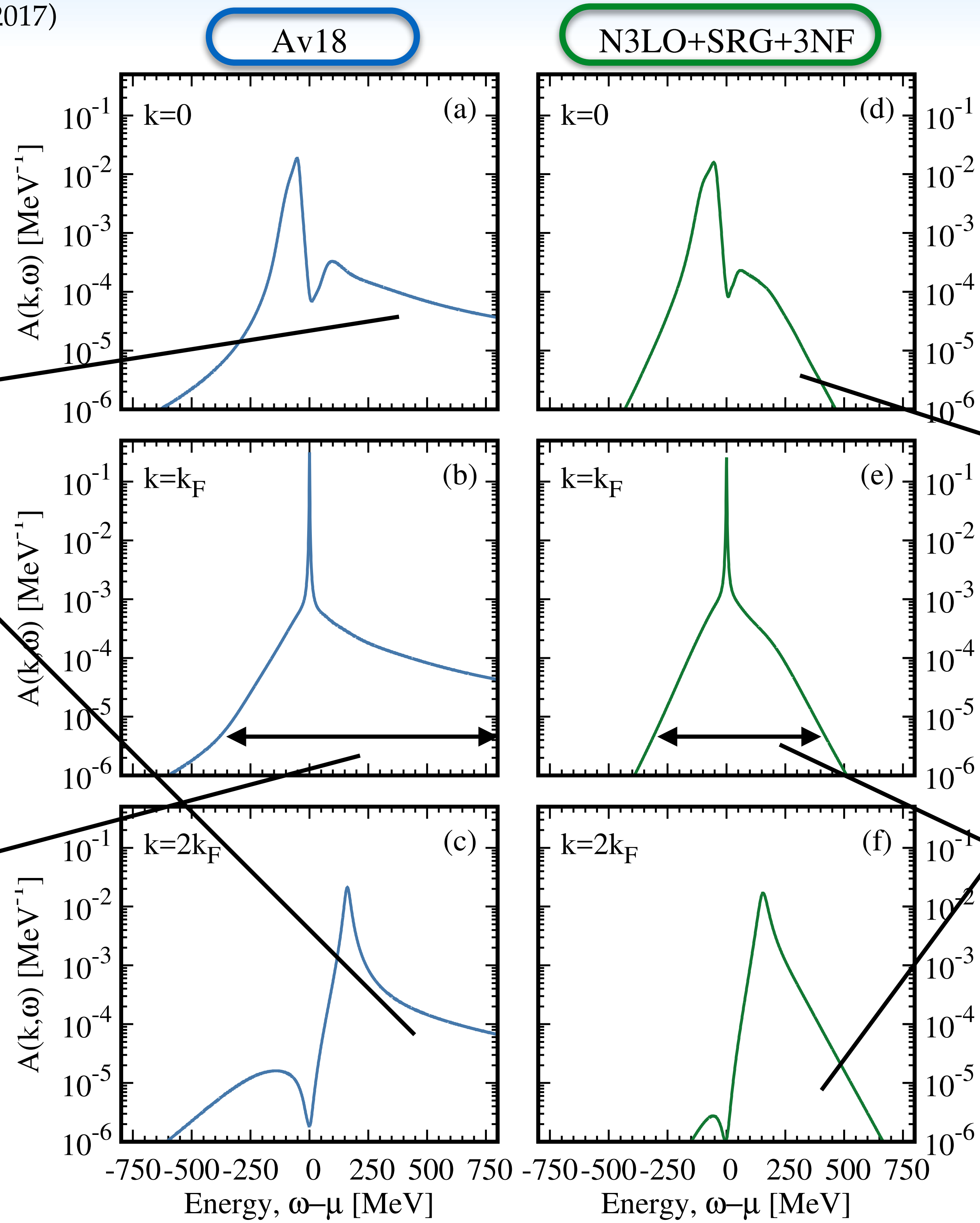

high-energy tails populated

high-energy tails suppressed

bigger fragmentation

smaller fragmentation

$\rho = 0.20\text{fm}^{-3}$

$k_{\text{F}} = 283\,\text{MeV}$

SNM

Spectral vision of the nuclear interaction

Rios, Carbone, Polls, PRC 96, 014003 (2017)

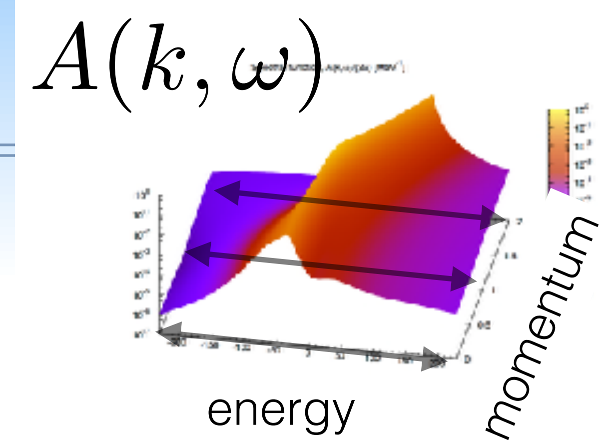

Hard-core

high-energy tails populated

bigger fragmentation

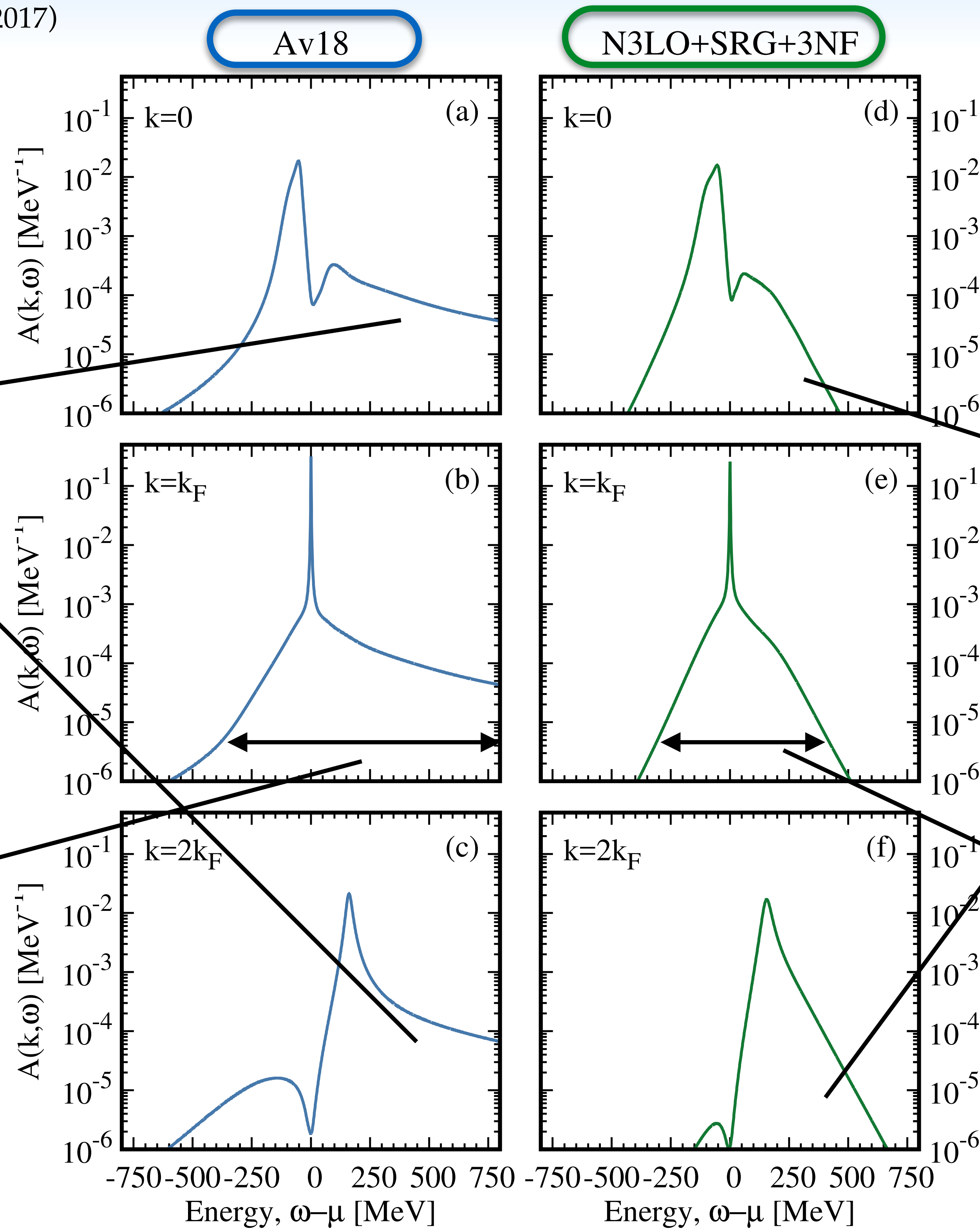

Soft-core

high-energy tails suppressed

smaller fragmentation

$$\rho = 0.20\text{fm}^{-3}$$

$$k_\text{F} = 283\,\text{MeV}$$

SNM

$$m_k^{(n)} = \int_{-\infty}^{\infty} \frac{d\omega}{2\pi} \omega^n A_k(\omega)$$

Understand fragmentation of nuclear states from sum rules

Understanding nuclear states fragmentation

$$m_k^{(1)} = \int_{-\infty}^{\infty} \frac{d\omega}{2\pi} \omega \mathcal{A}_k(\omega)$$

mean distribution

$$\boxed{m_k^{(1)} = \frac{\hbar^2 k^2}{2m} + \Sigma_k^{\infty}}$$

Hartree-Fock like energy: increasing with k

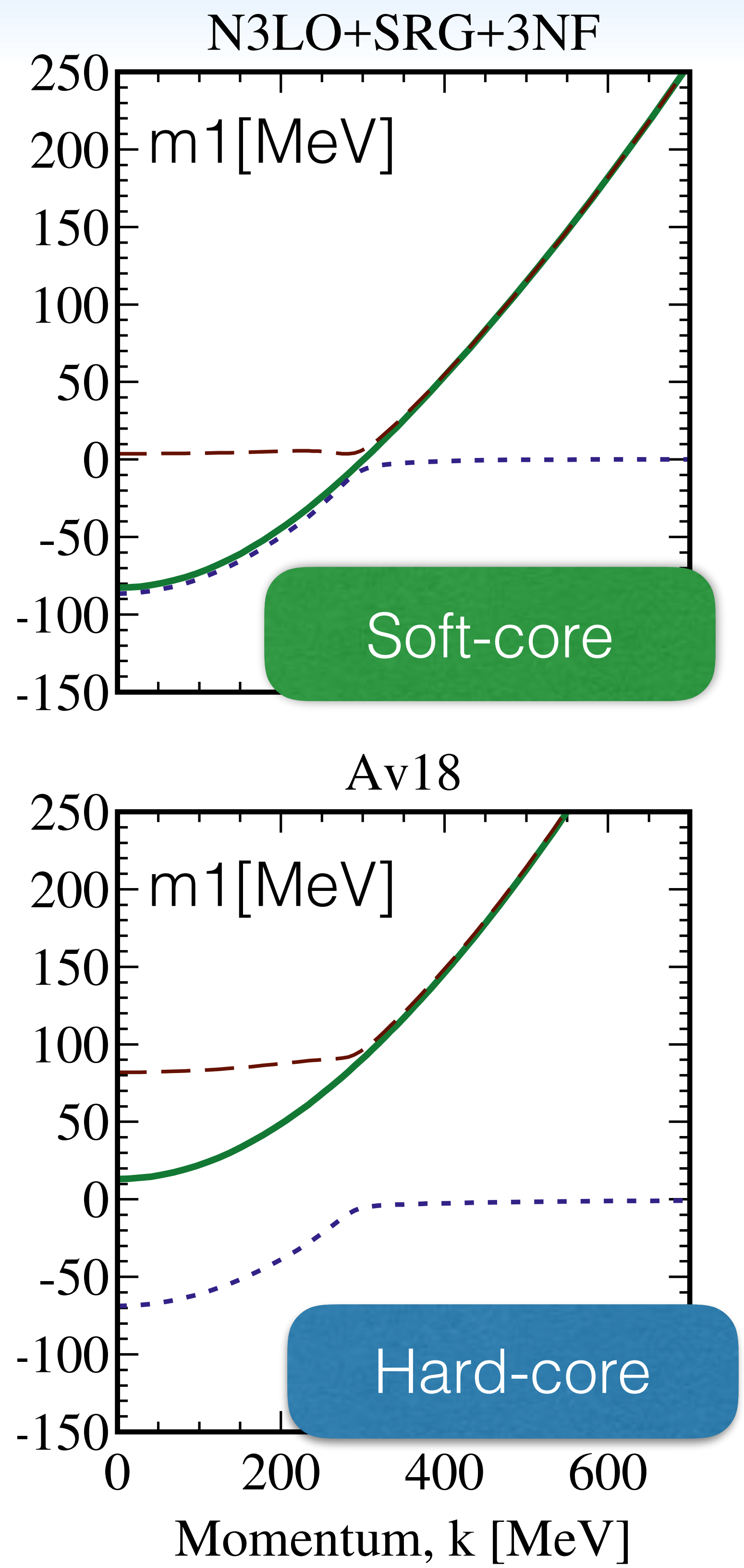

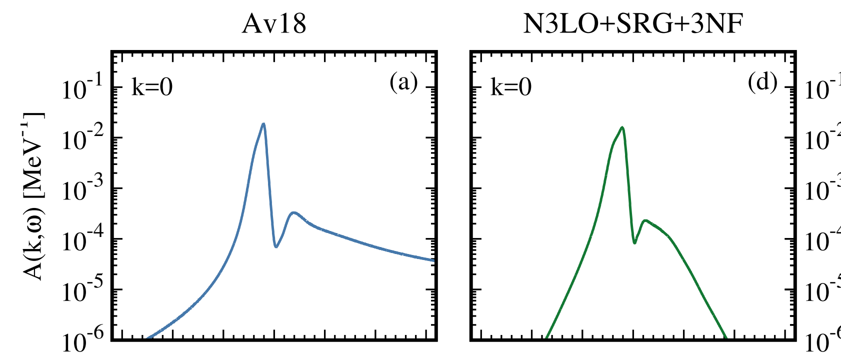

$$\rho = 0.20\mathrm{fm}^{-3}$$

$$k_{\mathrm{F}} = 283\,\mathrm{MeV}$$

SNM

Rios, Carbone, Polls, PRC 96, 014003 (2017)

Understanding nuclear states fragmentation

$$m_k^{(1)} = \int_{-\infty}^{\infty} \frac{d\omega}{2\pi} \omega \mathcal{A}_k(\omega)$$

mean distribution

$$\boxed{m_k^{(1)} = \frac{\hbar^2 k^2}{2m} + \Sigma_k^{\infty}}$$

Hartree-Fock like energy: increasing with k

1.
- strength of integrated peak below kF
- strongly suppressed above kF

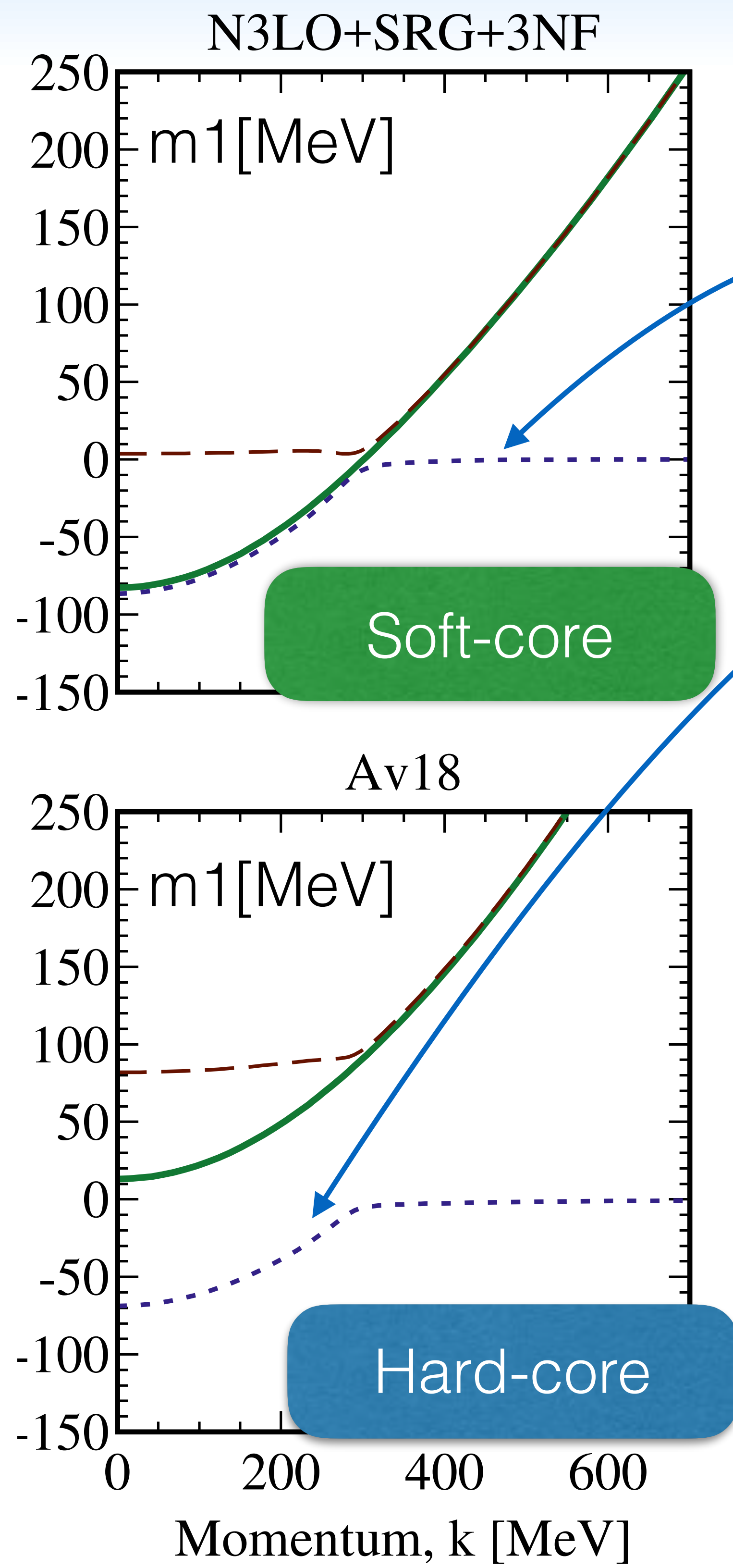

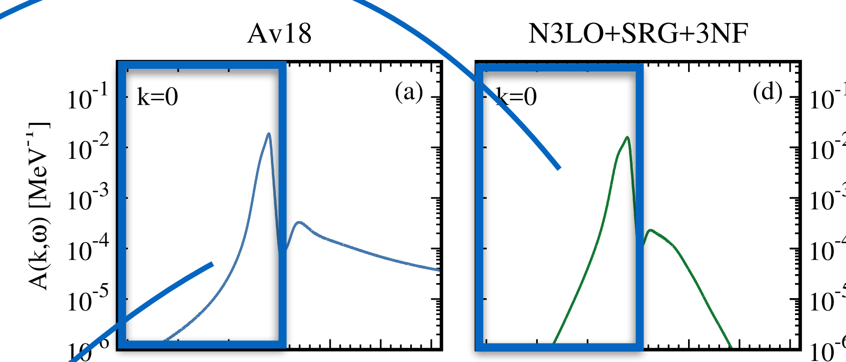

$$\rho = 0.20 \mathrm{fm}^{-3}$$

$$k_F = 283\,\mathrm{MeV}$$

SNM

Rios, Carbone, Polls, PRC 96, 014003 (2017)

Understanding nuclear states fragmentation

$$m_k^{(1)} = \int_{-\infty}^{\infty} \frac{d\omega}{2\pi} \omega \mathcal{A}_k(\omega)$$

mean distribution

$$\boxed{m_k^{(1)} = \frac{\hbar^2 k^2}{2m} + \Sigma_k^{\infty}}$$

Hartree-Fock like energy: increasing with k

1.
- strength of integrated peak below kF
- strongly suppressed above kF

2.
- weight of high-energy tails below kF
- steep increase above kF, peak integrated

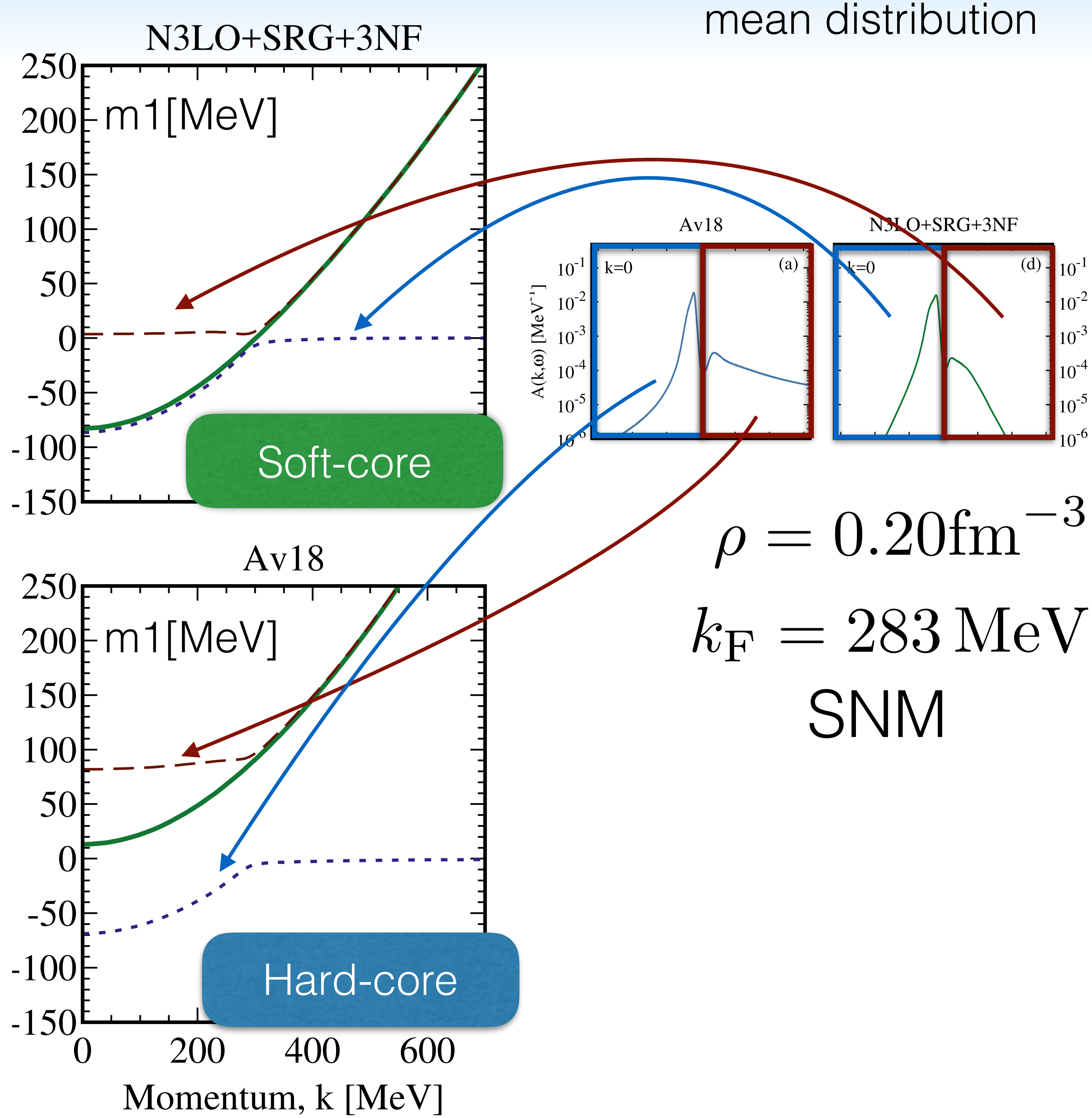

$\rho = 0.20\mathrm{fm}^{-3}$

$k_F = 283\,\mathrm{MeV}$

SNM

Rios, Carbone, Polls, PRC 96, 014003 (2017)

Understanding nuclear states fragmentation

$$m_k^{(1)} = \int_{-\infty}^{\infty} \frac{d\omega}{2\pi} \omega \mathcal{A}_k(\omega)$$

mean distribution

$$\boxed{m_k^{(1)} = \frac{\hbar^2 k^2}{2m} + \Sigma_k^{\infty}}$$

Hartree-Fock like energy: increasing with k

1.
- strength of integrated peak below kF
- strongly suppressed above kF

2.
- weight of high-energy tails below kF
- steep increase above kF, peak integrated

Rios, Carbone, Polls, PRC 96, 014003 (2017)

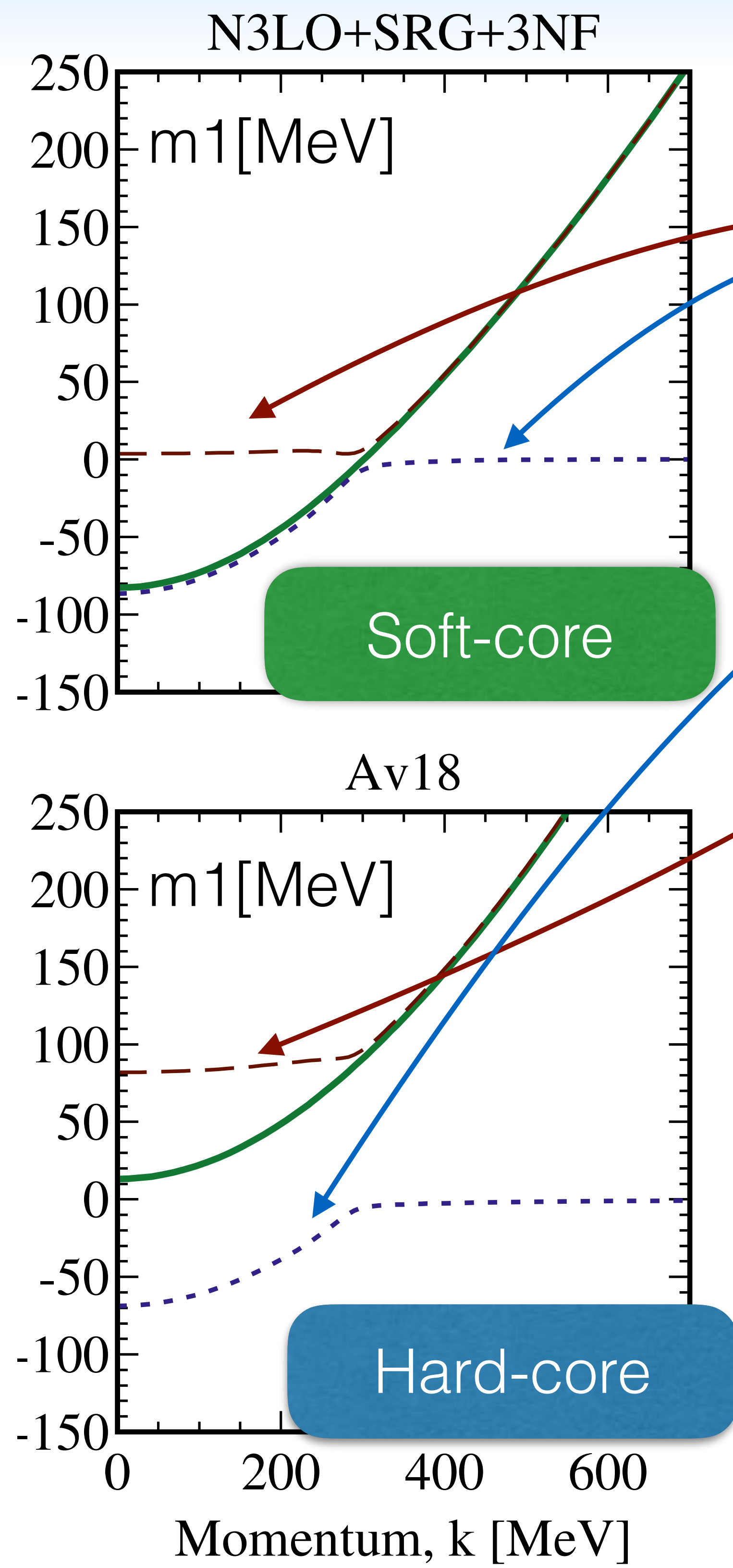

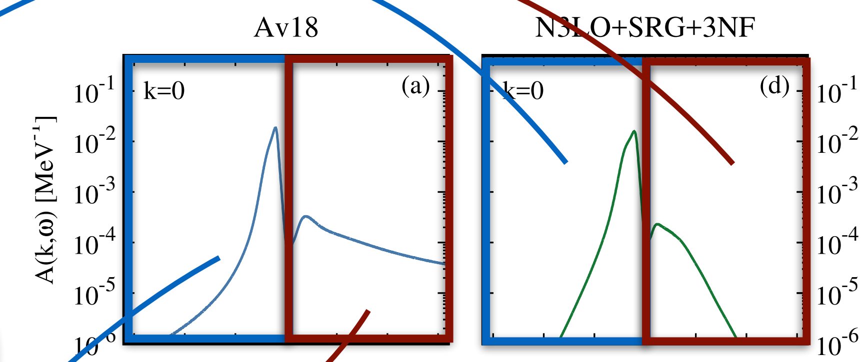

$$\rho = 0.20 \mathrm{fm}^{-3}$$

$$k_{\mathrm{F}} = 283\,\mathrm{MeV}$$

SNM

First sum rule always positive for hard-core potentials

Understanding nuclear forces from sum rules

$$m_k^{(2)} = \int_{-\infty}^{\infty} \frac{d\omega}{2\pi} \omega^2 \mathcal{A}_k(\omega)$$

Rios, Carbone, Polls, PRC 96, 014003 (2017)

$$m_k^{(2)} = [m_k^{(1)}]^2 + \sigma_k^2$$

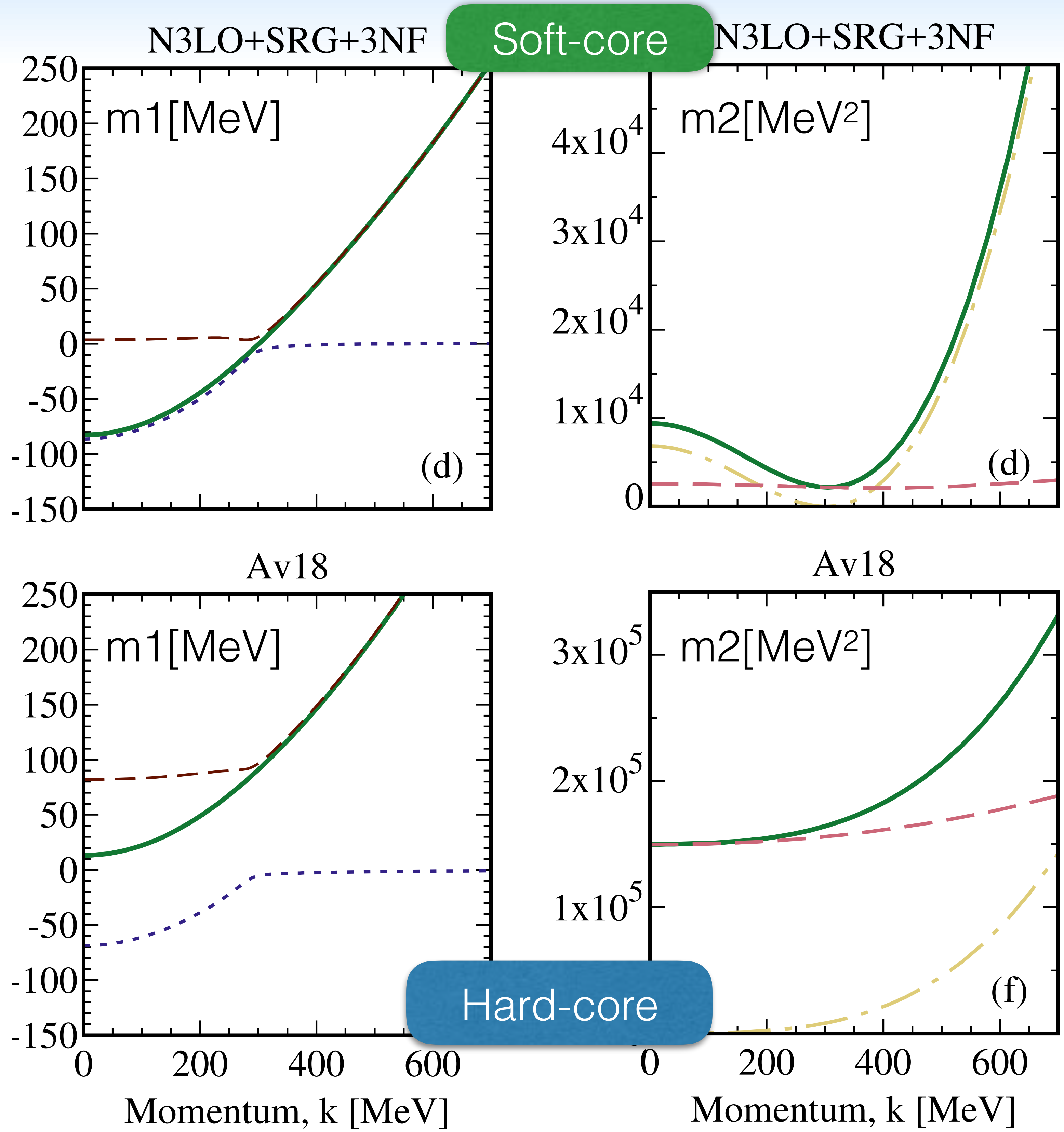

Understanding nuclear forces from sum rules

$$m_k^{(2)} = \int_{-\infty}^{\infty} \frac{d\omega}{2\pi} \omega^2 \mathcal{A}_k(\omega)$$

Rios, Carbone, Polls, PRC 96, 014003 (2017)

$$m_k^{(2)} = \boxed{[m_k^{(1)}]^2} + \sigma_k^2$$

Quadratic first sum rule always increasing for hard-core potentials

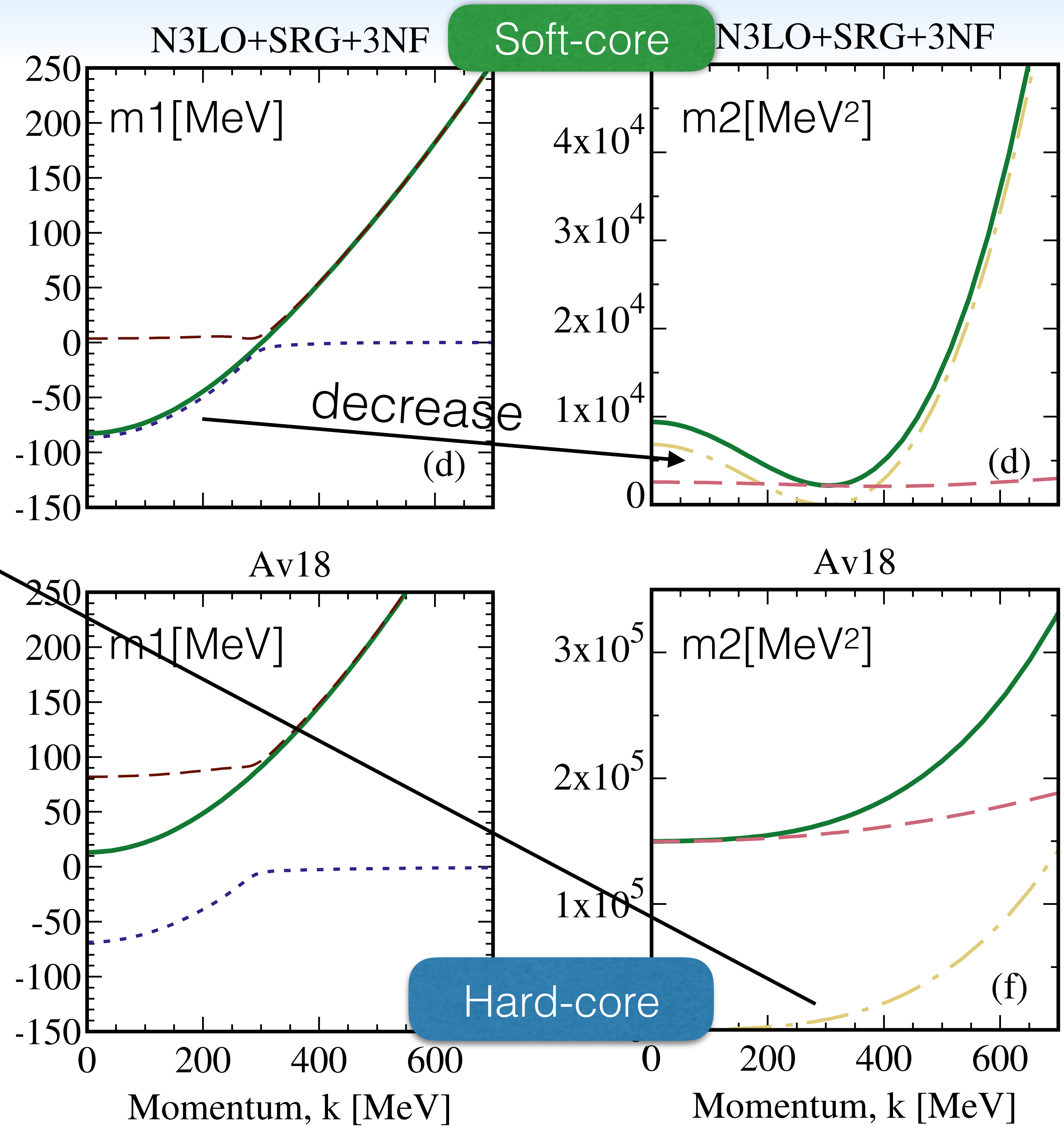

Understanding nuclear forces from sum rules

$$m_k^{(2)} = \int_{-\infty}^{\infty} \frac{d\omega}{2\pi} \omega^2 \mathcal{A}_k(\omega)$$

Rios, Carbone, Polls, PRC 96, 014003 (2017)

$$m_k^{(2)} = \boxed{[m_k^{(1)}]^2} + \boxed{\sigma_k^2}$$

Quadratic first sum rule always increasing for hard-core potentials

variance of the spectral function

negligible for soft forces increasing for hard ones

$$\sigma_k^2 = -\int_{-\infty}^{+\infty} \frac{d\omega}{\pi} \mathrm{Im}\Sigma_k(\omega)$$

beyond mean-field effects

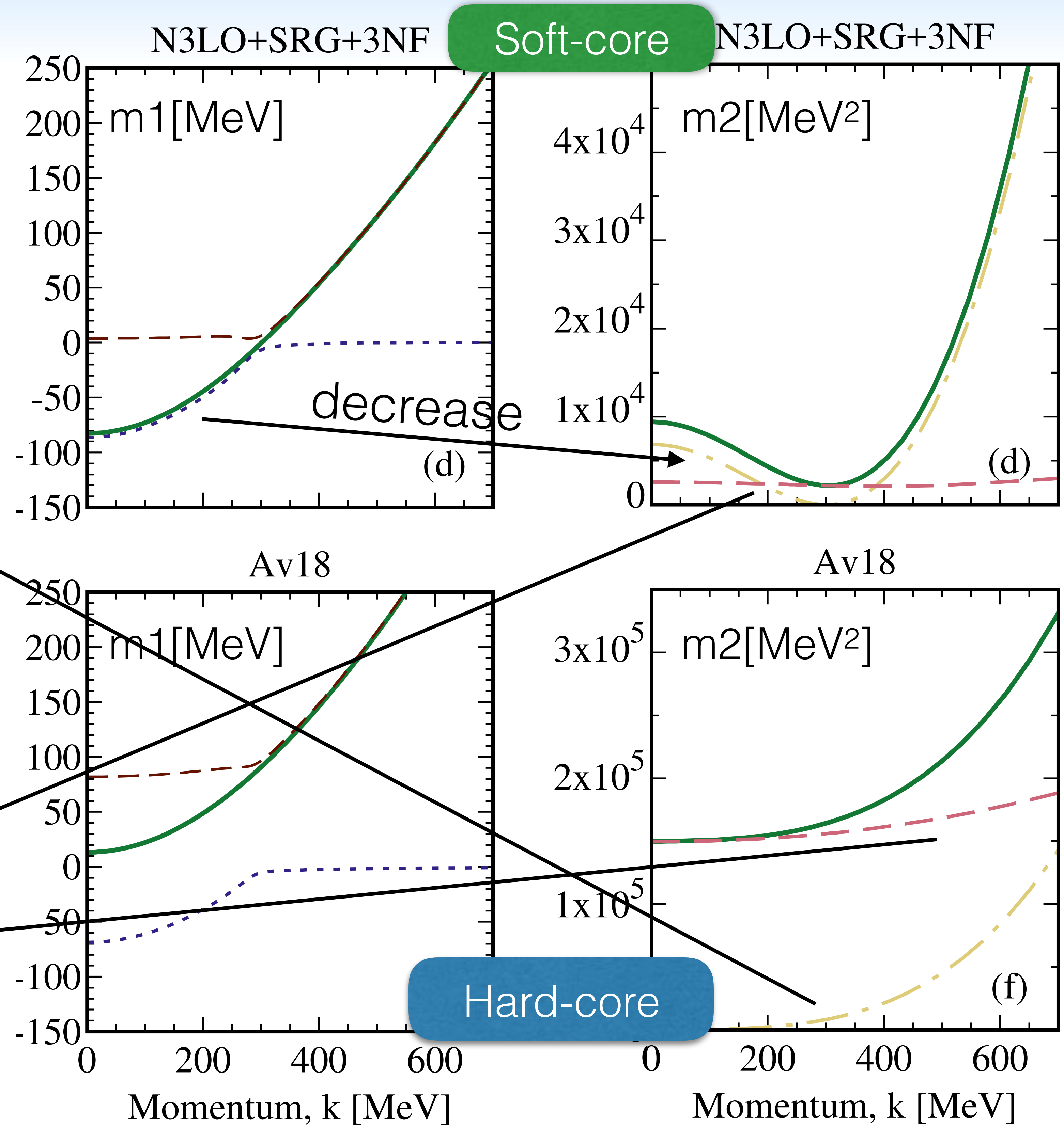

The variance as a proxy of softness

$\rho = 0.20\mathrm{fm}^{-3}$

$k_\mathrm{F} = 283\,\mathrm{MeV}$

SNM

Rios, Carbone, Polls, PRC 96, 014003 (2017)

$$\sigma_k^2 = -\int_{-\infty}^{+\infty} \frac{d\omega}{\pi} \mathrm{Im}\Sigma_\mathrm{k}(\omega)$$

- beyond-mean field effects
- strongly suppressed in soft forces
- less fragmentation of states
- narrower quasi-particle peaks
- variance varies with RG scale

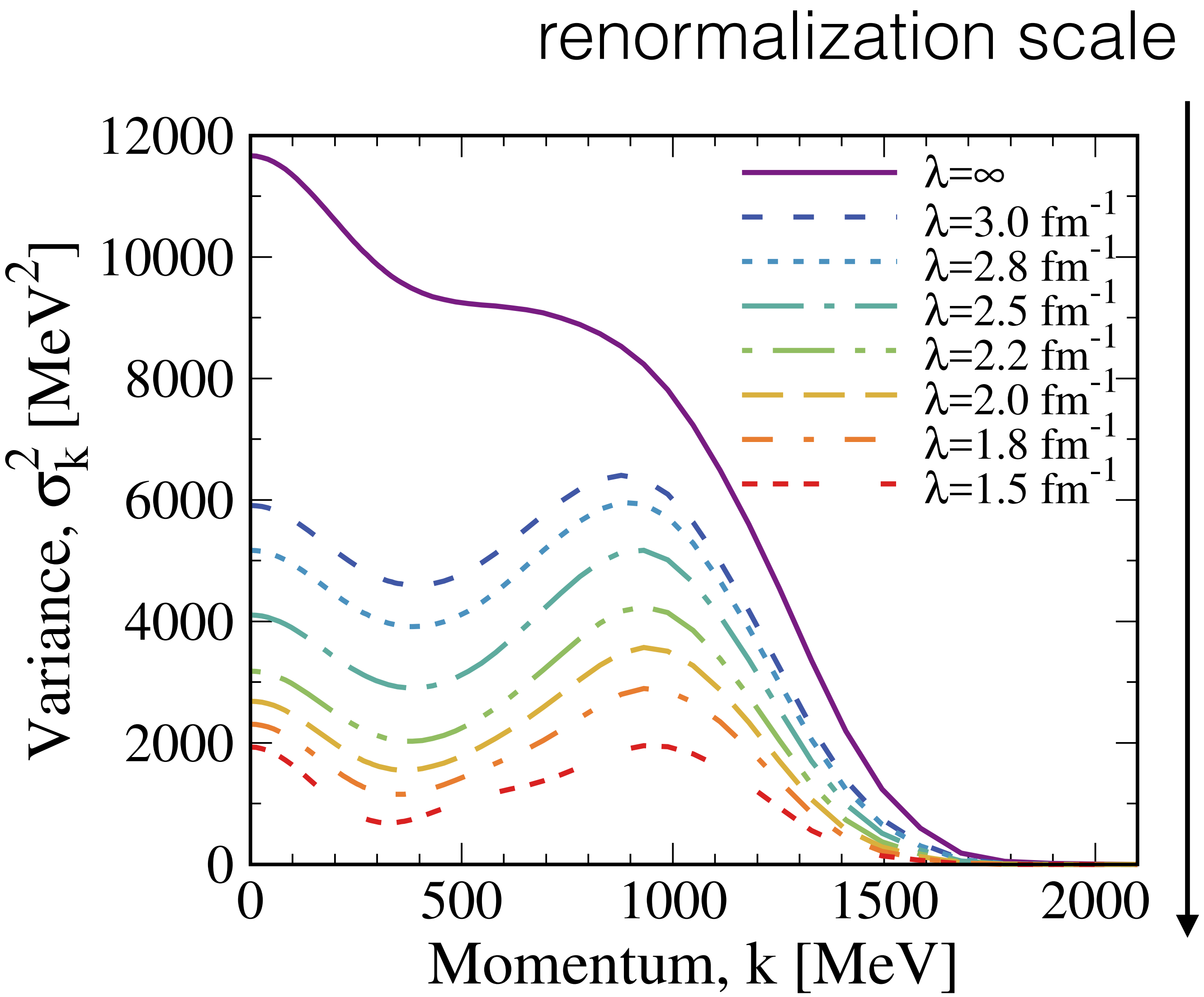

The variance as a proxy of softness

$\rho = 0.20\text{fm}^{-3}$

$k_F = 283\,\text{MeV}$

SNM

Rios, Carbone, Polls, PRC 96, 014003 (2017)

$$\sigma_k^2 = -\int_{-\infty}^{+\infty} \frac{d\omega}{\pi} \text{Im}\Sigma_k(\omega)$$

- beyond-mean field effects
- strongly suppressed in soft forces
- less fragmentation of states
- narrower quasi-particle peaks
- variance varies with RG scale

renormalization scale

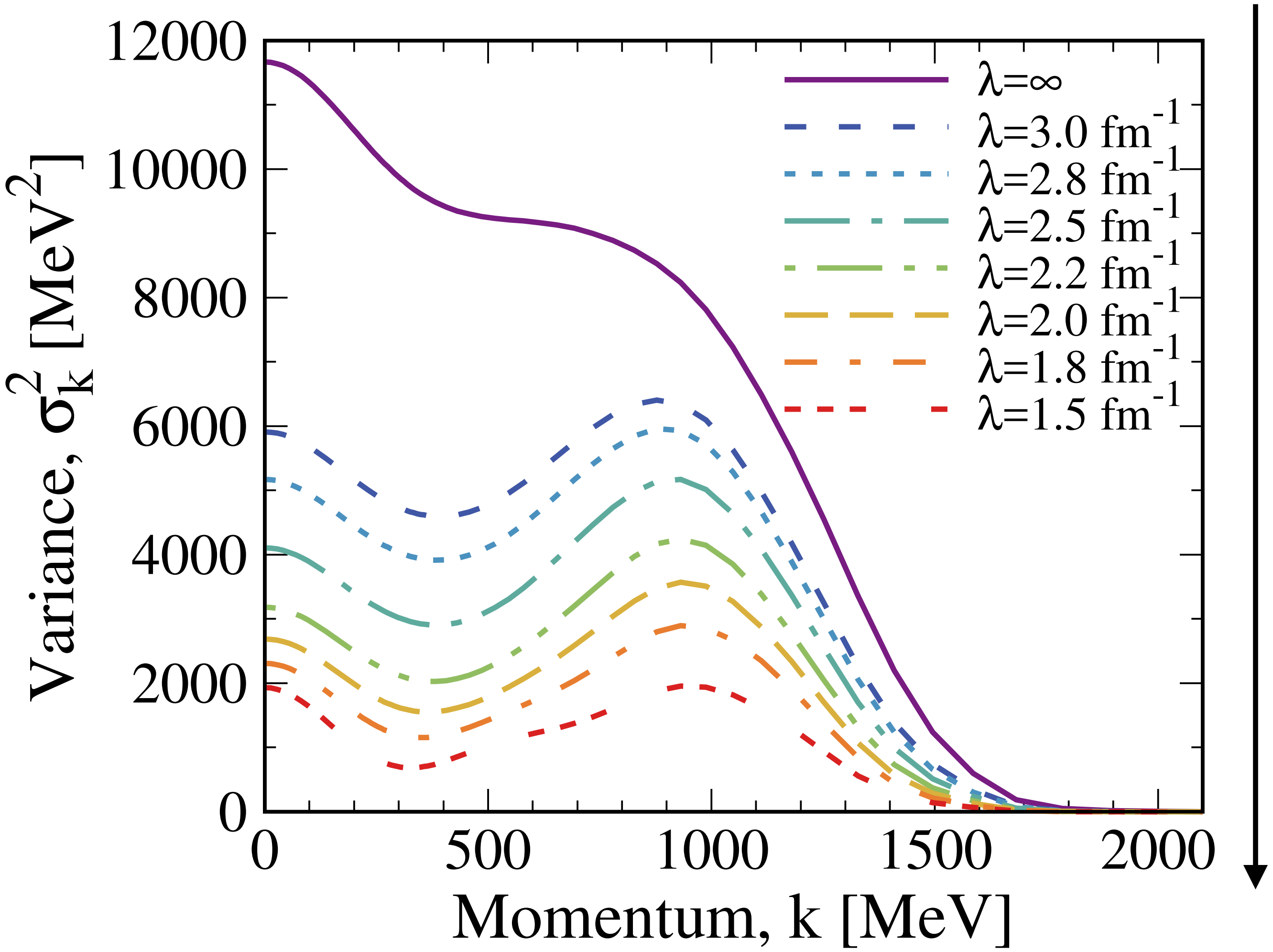

Sum rules provide a measurement of hardness (or softness) of nuclear potential

Relation to effective single-particle energies in finite nuclei

Momentum distribution according to different Hamiltonians

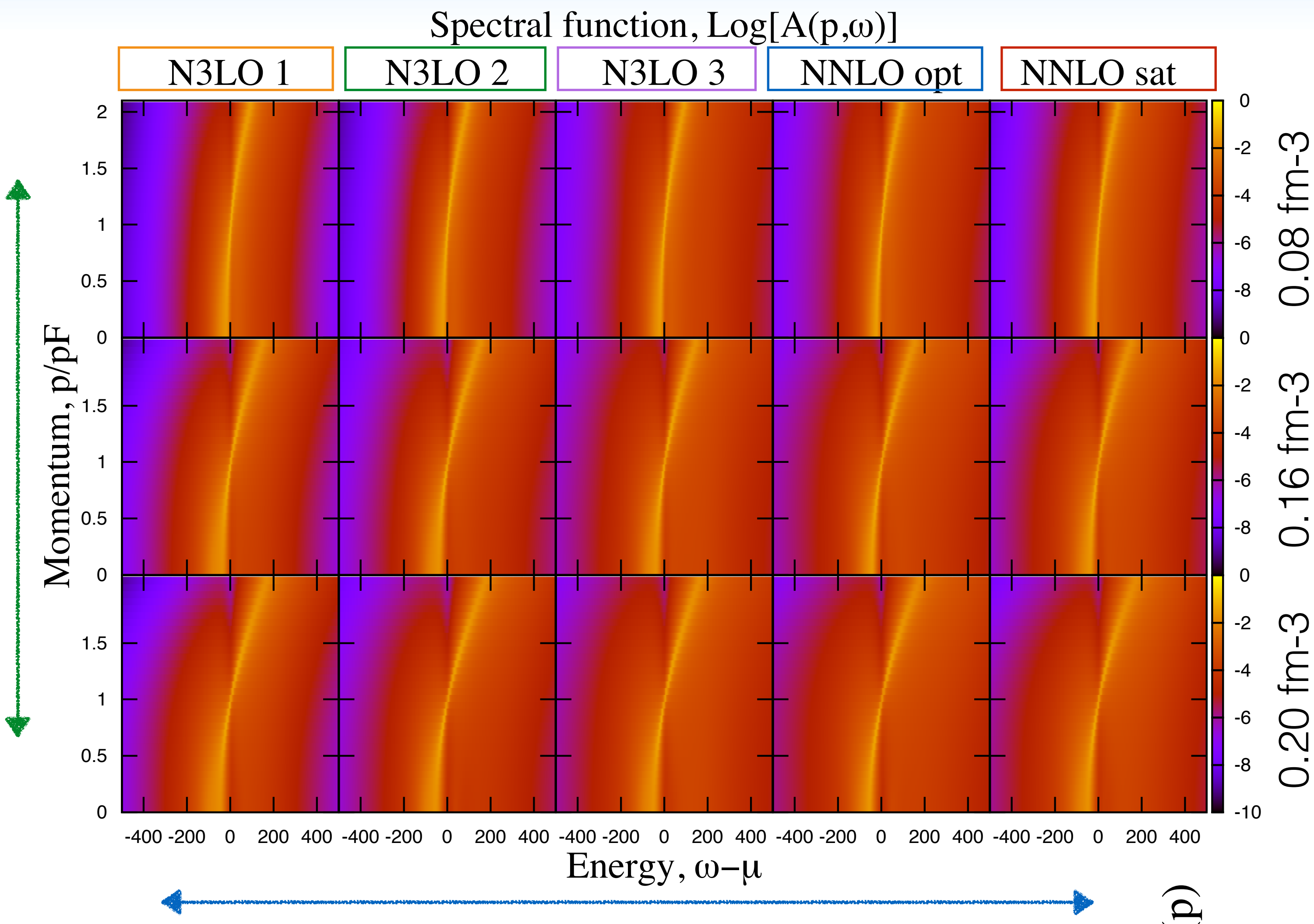

$$n(p) = \int \frac{d\omega}{2\pi} \mathcal{A}(p,\omega) f(\omega)$$

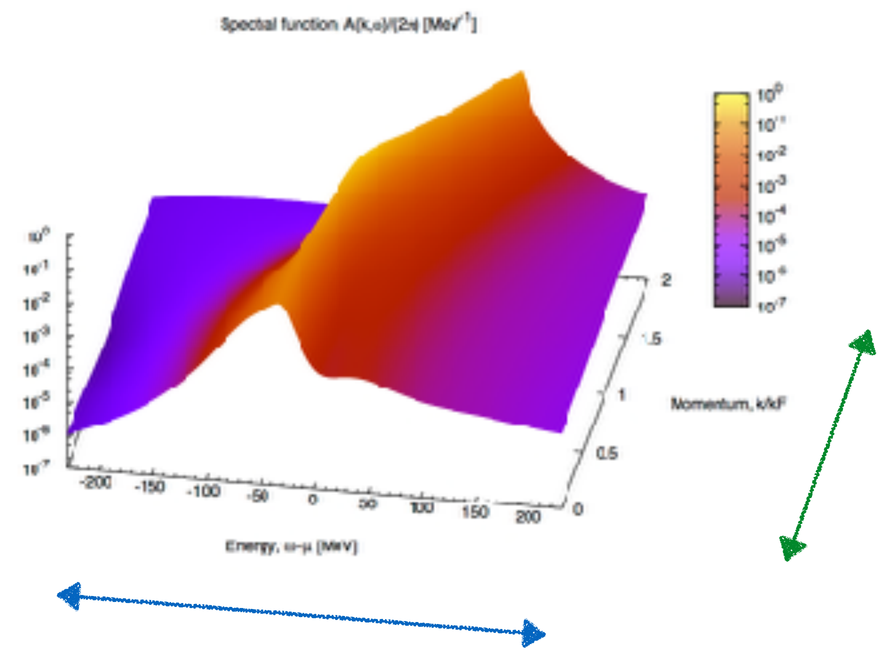

- energy tails affected by the cutoff on the NN force
- high-momentum region also affected by cutoff and density dependence
- effects clearly visible in momentum distribution

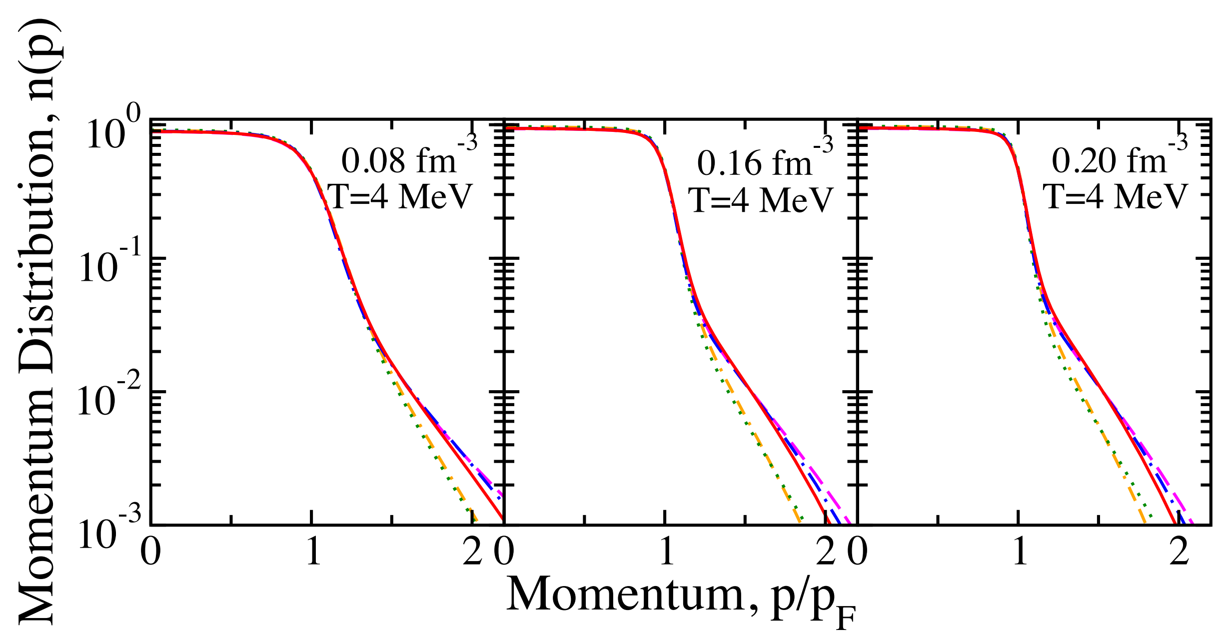

Self-consistent Green's functions

- Green's function: a tool to solve the nuclear many-body problem

particle exits · particle enters · hole exits · hole enters

$$G_{\alpha\beta}(\omega) = \sum_m \frac{\langle \Psi_0^N | a_\alpha | \Psi_m^{N+1} \rangle \langle \Psi_m^{N+1} | a_\beta^\dagger | \Psi_0^N \rangle}{\omega - (E_m^{N+1} - E_0^N) + i\eta} + \sum_n \frac{\langle \Psi_0^N | a_\beta^\dagger | \Psi_n^{N-1} \rangle \langle \Psi_n^{N-1} | a_\alpha | \Psi_0^N \rangle}{\omega - (E_0 - E_n^{N-1}) + i\eta}$$

energy with an added particle *energy with a removed particle*

quasi-particle peak

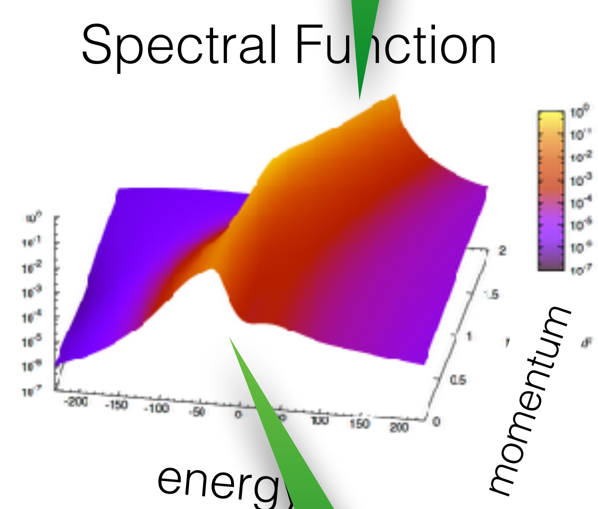

beyond mean-field

- Self-consistent nonperturbative method:

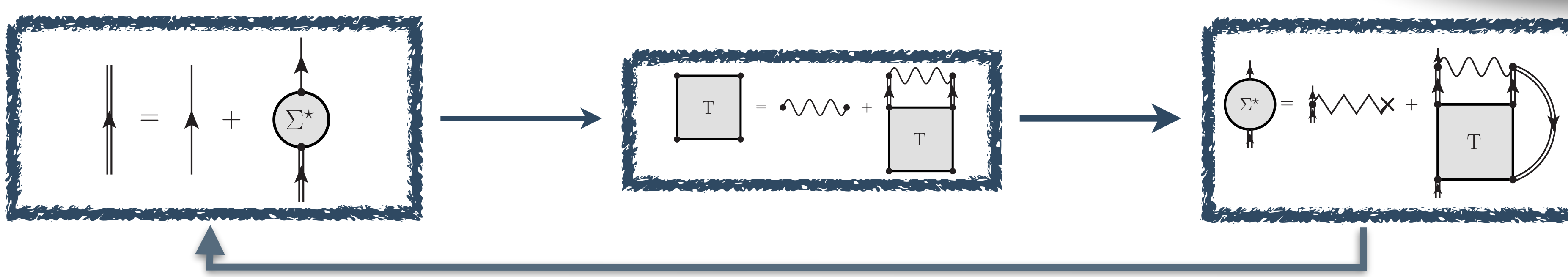

Dyson equation

- Breakthrough: full formal extension to consistently include 3BFs

Carbone, Cipollone, Barbieri, Rios, Polls, PRC **88**, 054326 (2013)

From microscopic… to macroscopic

Symmetric nuclear matter

The microscopic picture: momentum distribution

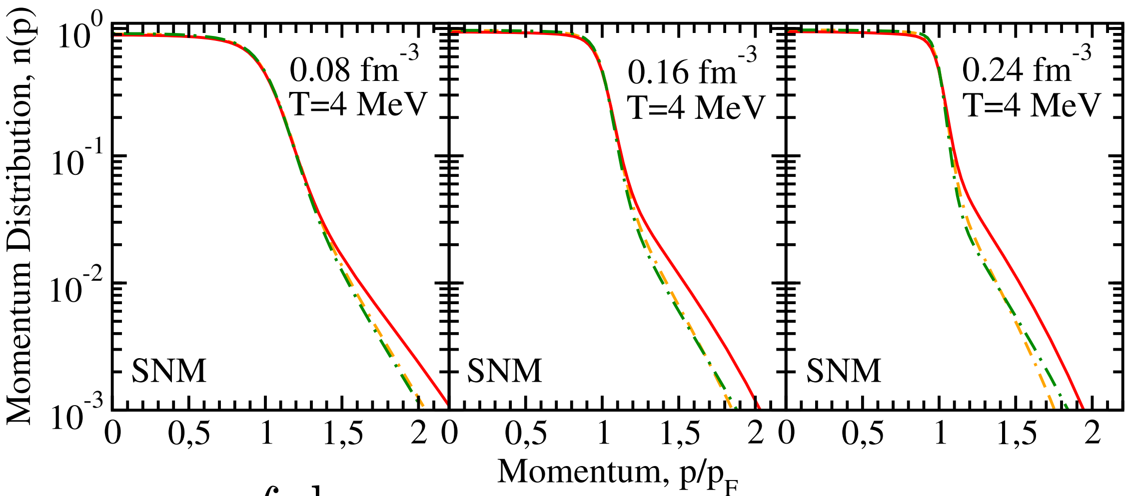

$$n(p) = \int \frac{\mathrm{d}\omega}{2\pi} \mathcal{A}(p,\omega) f(\omega)$$

- N2LOsat high-momentum states

From microscopic… to macroscopic

Symmetric nuclear matter

The microscopic picture: momentum distribution

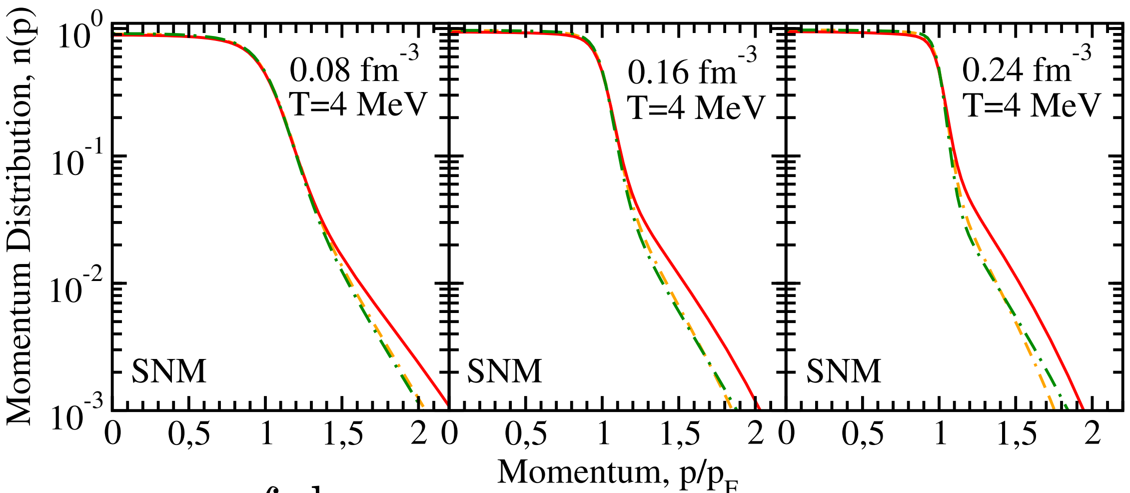

$$n(p) = \int \frac{\mathrm{d}\omega}{2\pi} \mathcal{A}(p,\omega) f(\omega)$$

- N2LOsat high-momentum states

…start seeing the big picture: the self-energy

$$\varepsilon_{qp}(p) = \frac{p^2}{2m} + \mathrm{Re}\Sigma^\star(p, \varepsilon_{qp}(p))$$

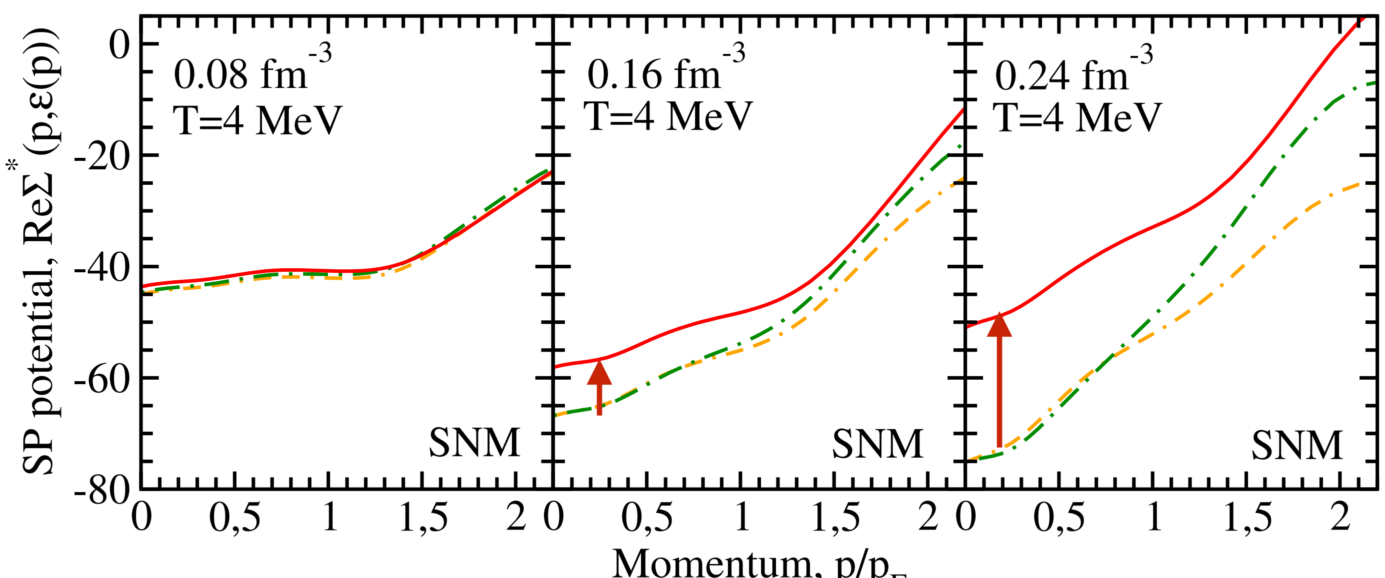

- 3NF effects as density increases
- N2LOsat more repulsive

From microscopic... to macroscopic

Symmetric nuclear matter

The microscopic picture: momentum distribution

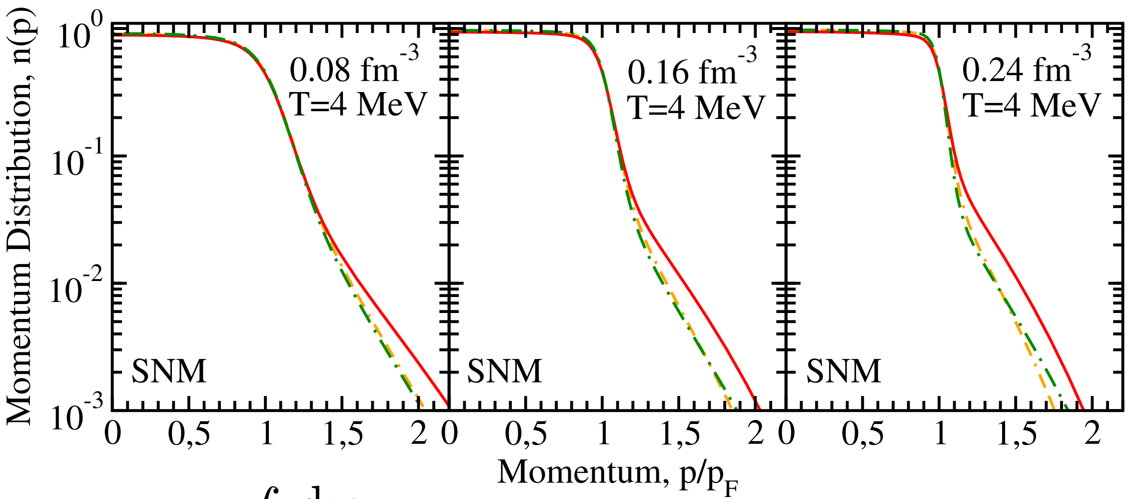

$$n(p) = \int \frac{d\omega}{2\pi} \mathcal{A}(p,\omega) f(\omega)$$

- N2LOsat high-momentum states

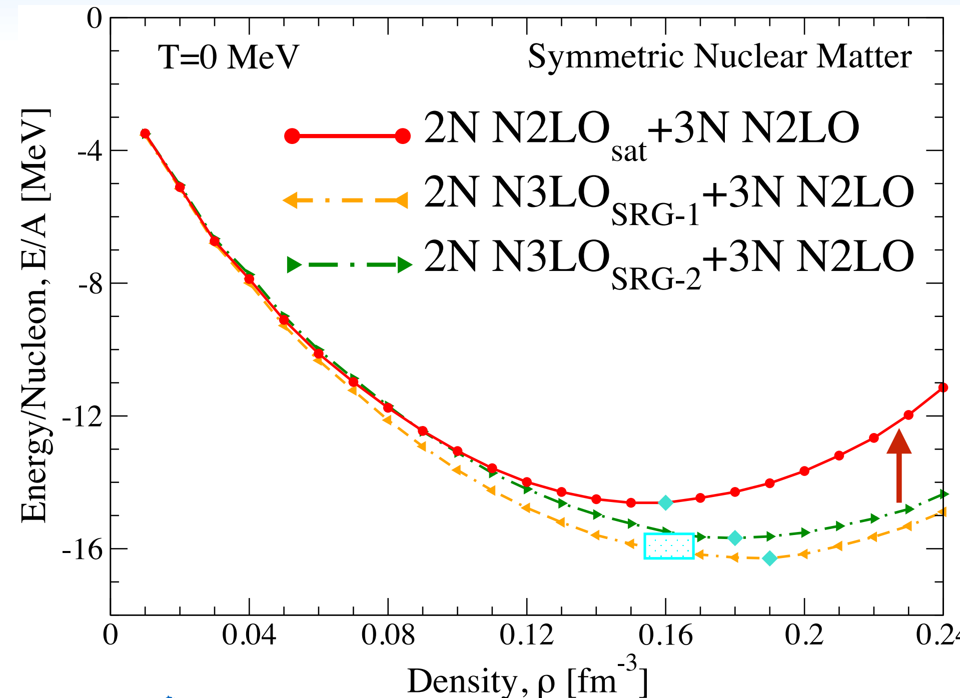

..the macroscopic picture: total energy more repulsive

...start seeing the big picture: the self-energy

$$\varepsilon_{qp}(p) = \frac{p^2}{2m} + \mathrm{Re}\Sigma^\star(p, \varepsilon_{qp}(p))$$

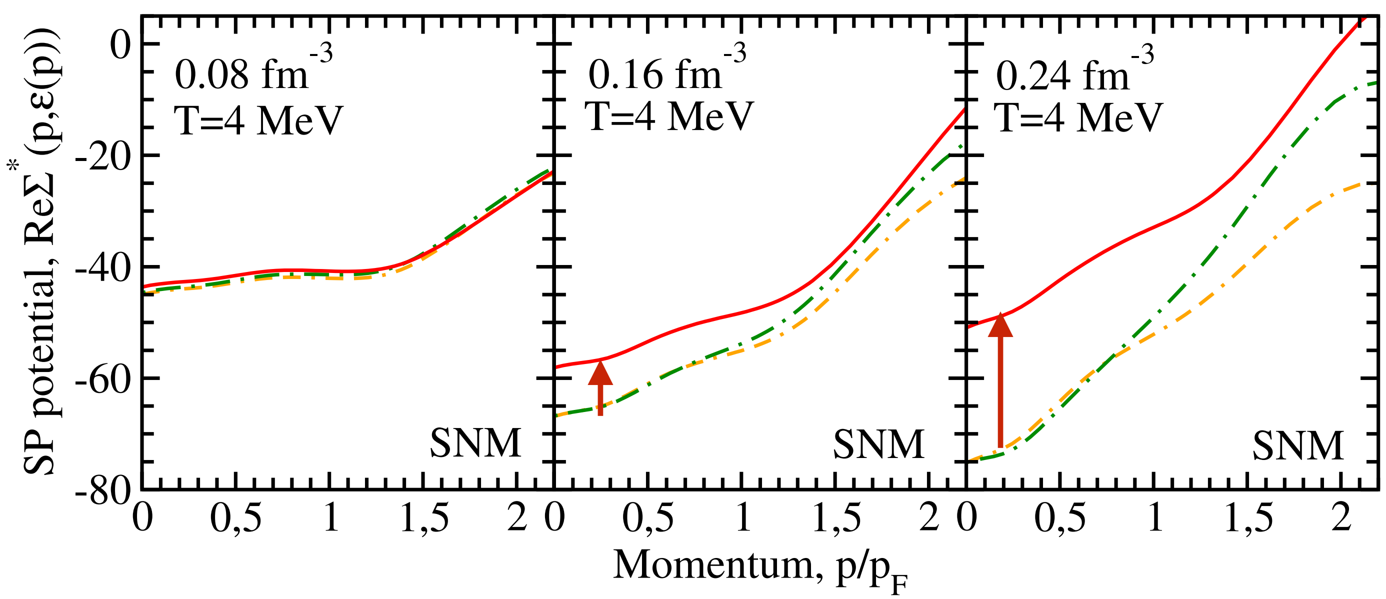

- 3NF effects as density increases
- N2LOsat more repulsive

From microscopic… to macroscopic

Pure neutron matter

The microscopic picture: momentum distribution

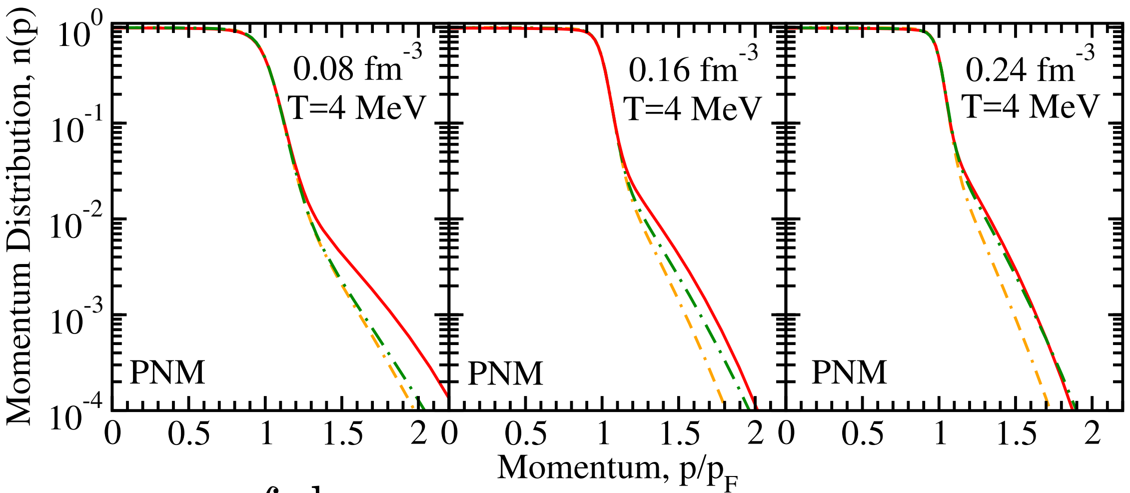

$$n(p) = \int \frac{\mathrm{d}\omega}{2\pi} \mathcal{A}(p,\omega) f(\omega)$$

- N2LOsat high-momentum states

From microscopic... to macroscopic

Pure neutron matter

The microscopic picture: momentum distribution

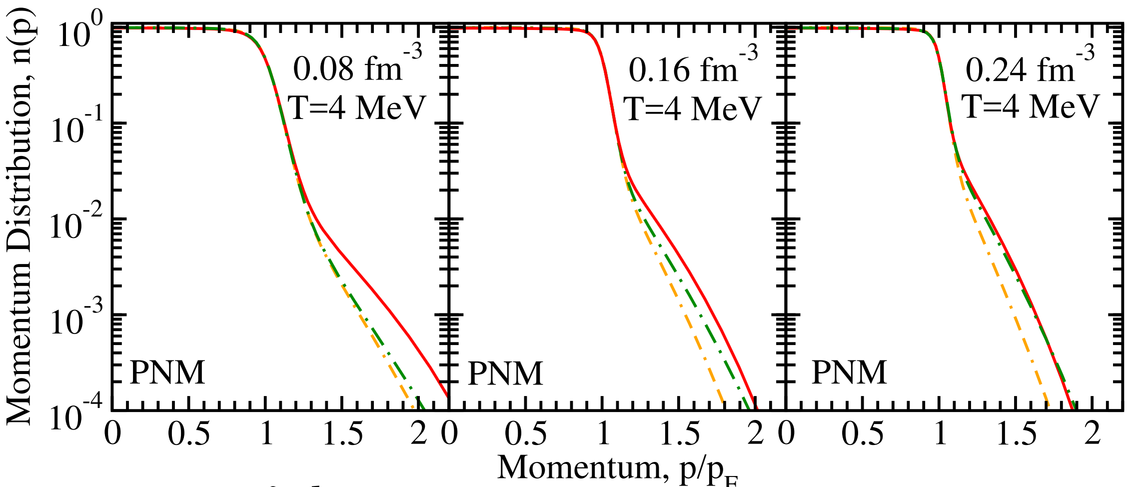

$$n(p) = \int \frac{d\omega}{2\pi} \mathcal{A}(p,\omega) f(\omega)$$

- N2LOsat high-momentum states

...start seeing the big picture: the self-energy

$$\varepsilon_{qp}(p) = \frac{p^2}{2m} + \mathrm{Re}\Sigma^\star(p, \varepsilon_{qp}(p))$$

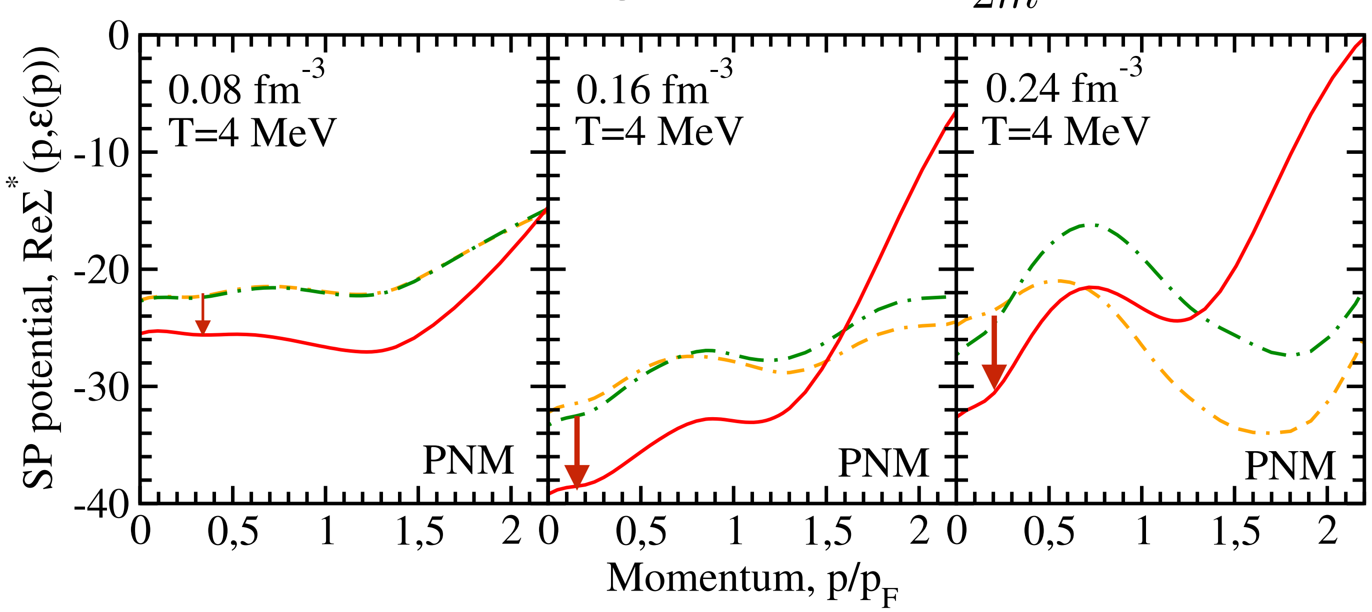

- 3NF effects are reversed
- N2LOsat more attractive

From microscopic… to macroscopic

Pure neutron matter

The microscopic picture: momentum distribution

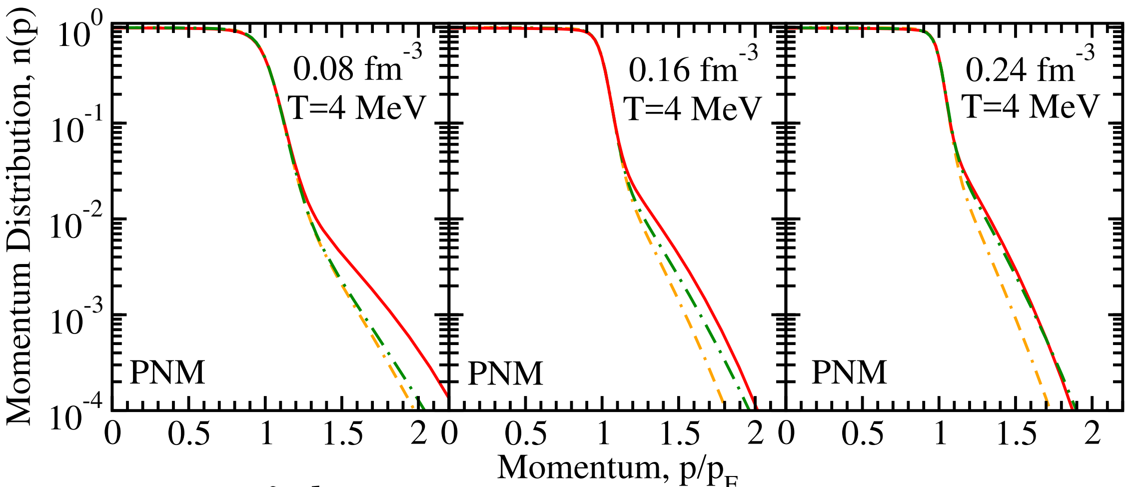

$$n(p) = \int \frac{d\omega}{2\pi} \mathcal{A}(p,\omega) f(\omega)$$

- N2LOsat high-momentum states

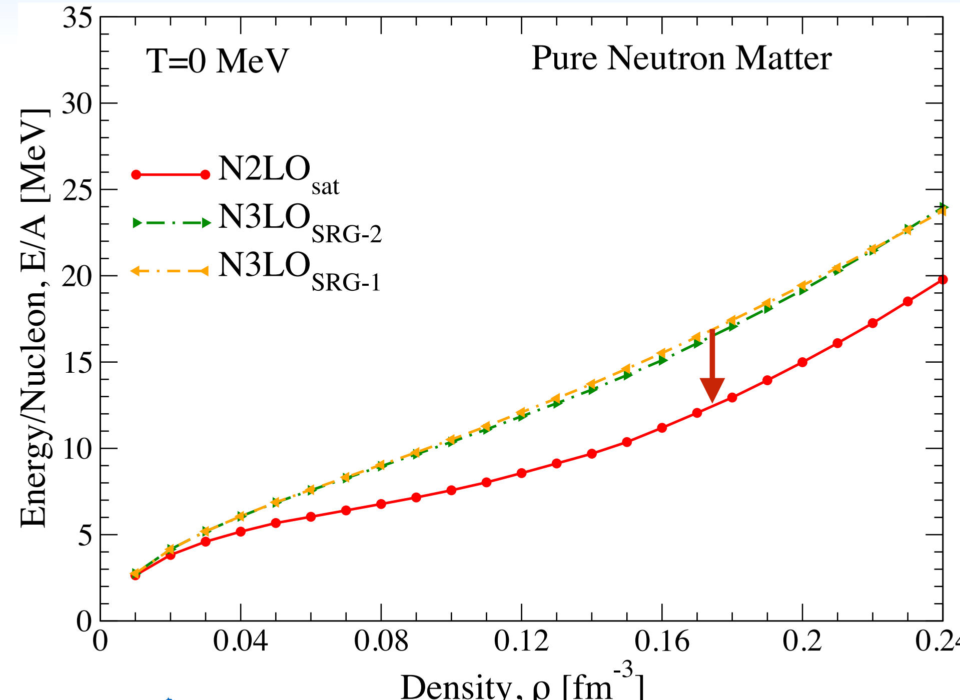

..the macroscopic picture: total energy more attractive

…start seeing the big picture: the self-energy

$$\varepsilon_{qp}(p) = \frac{p^2}{2m} + \mathrm{Re}\Sigma^\star(p, \varepsilon_{qp}(p))$$

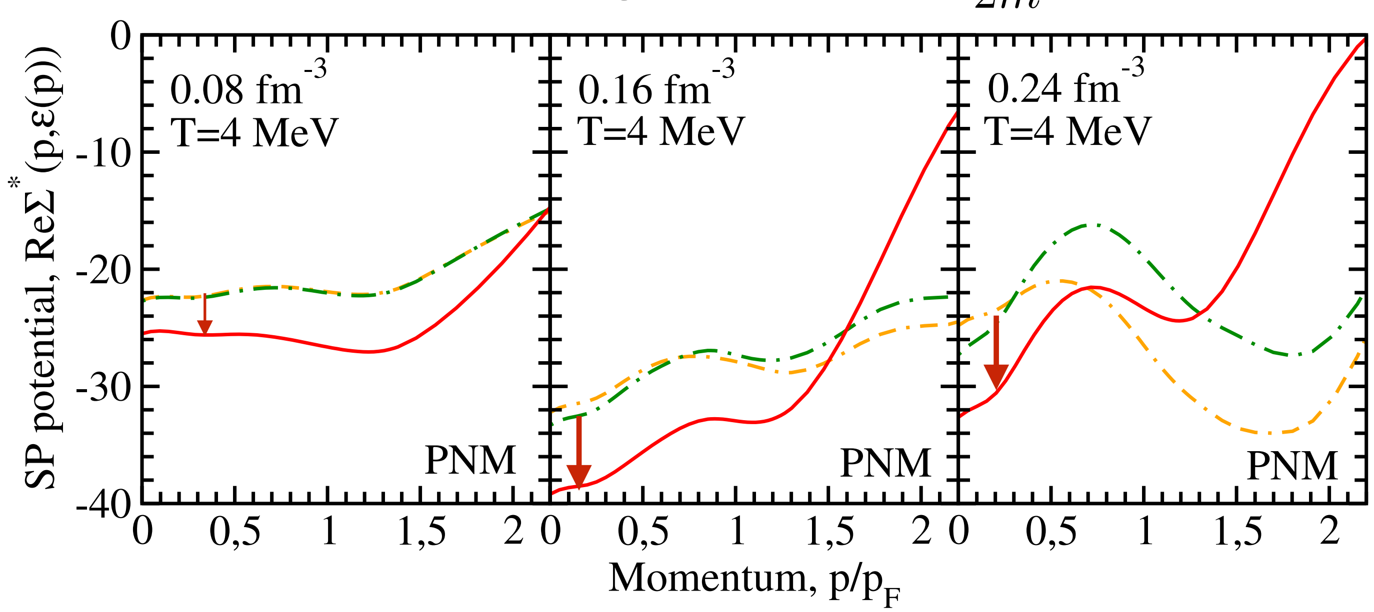

- 3NF effects are reversed
- N2LOsat more attractive

Energy contributions: SNM vs PNM

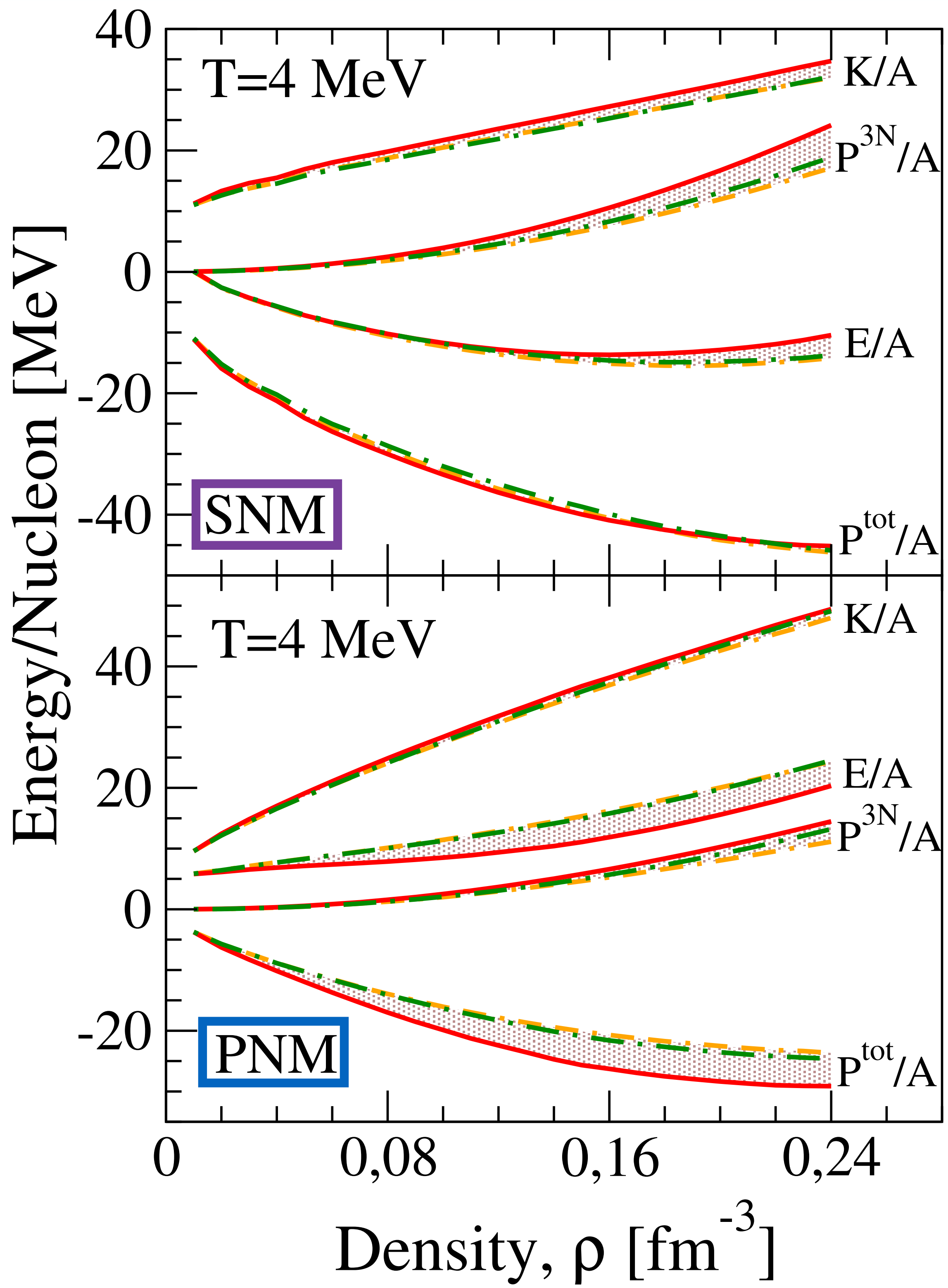

SNM Kinetic Energy

SNM 3N Potential Energy

SNM Total Energy

SNM NN+3N Pot. Ener.

PNM Kinetic Energy

PNM Total Energy

PNM 3N Potential Energy

PNM NN+3N Pot. Ener.

Carbone *(in preparation)*

Energy contributions: SNM vs PNM

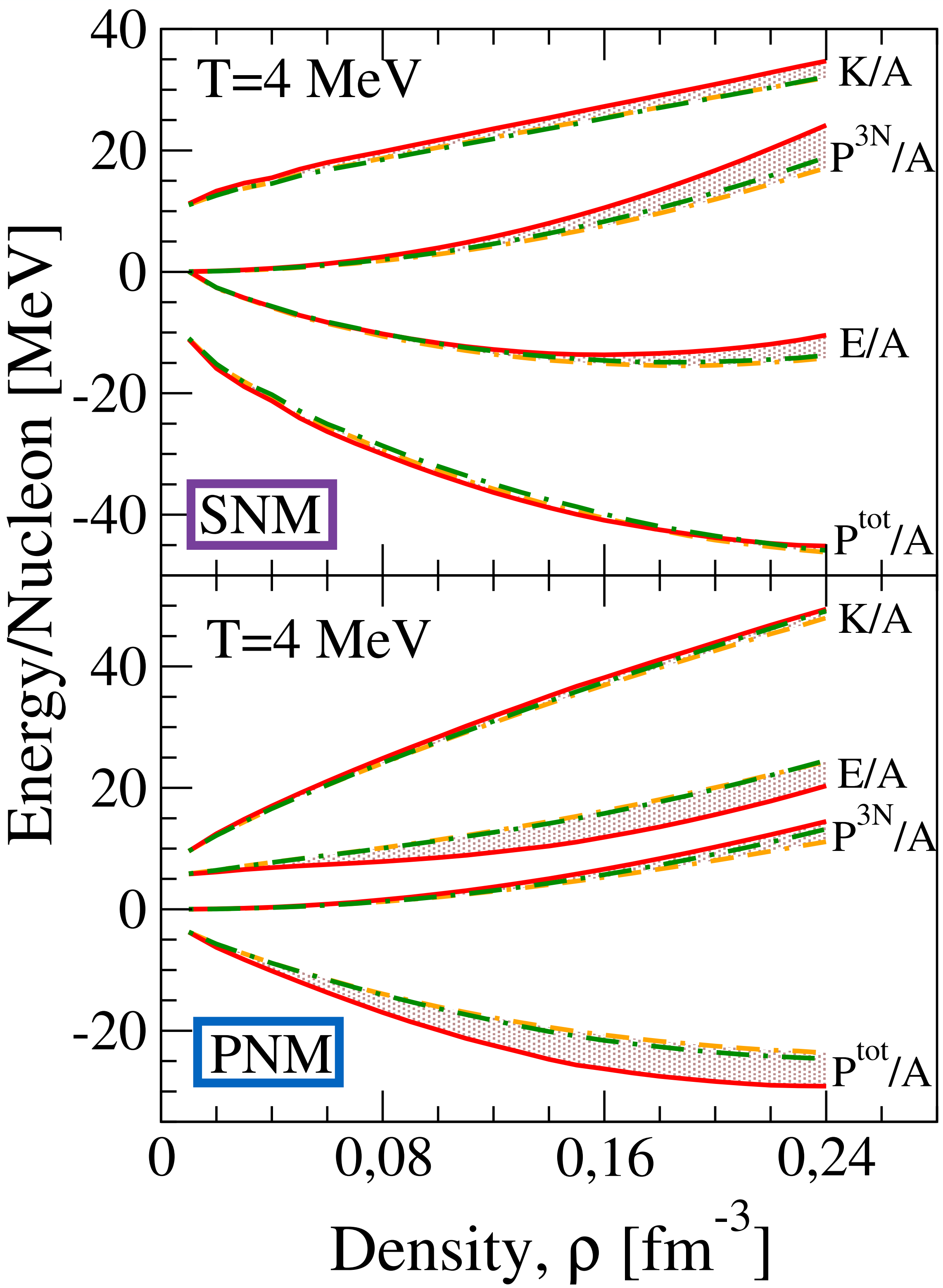

SNM Kinetic Energy

SNM 3N Potential Energy

SNM Total Energy

SNM NN+3N Pot. Ener.

PNM Kinetic Energy

PNM Total Energy

PNM 3N Potential Energy

PNM NN+3N Pot. Ener.

N2LOsat vs N3LO (SRG)

Carbone *(in preparation)*

Energy contributions: SNM vs PNM

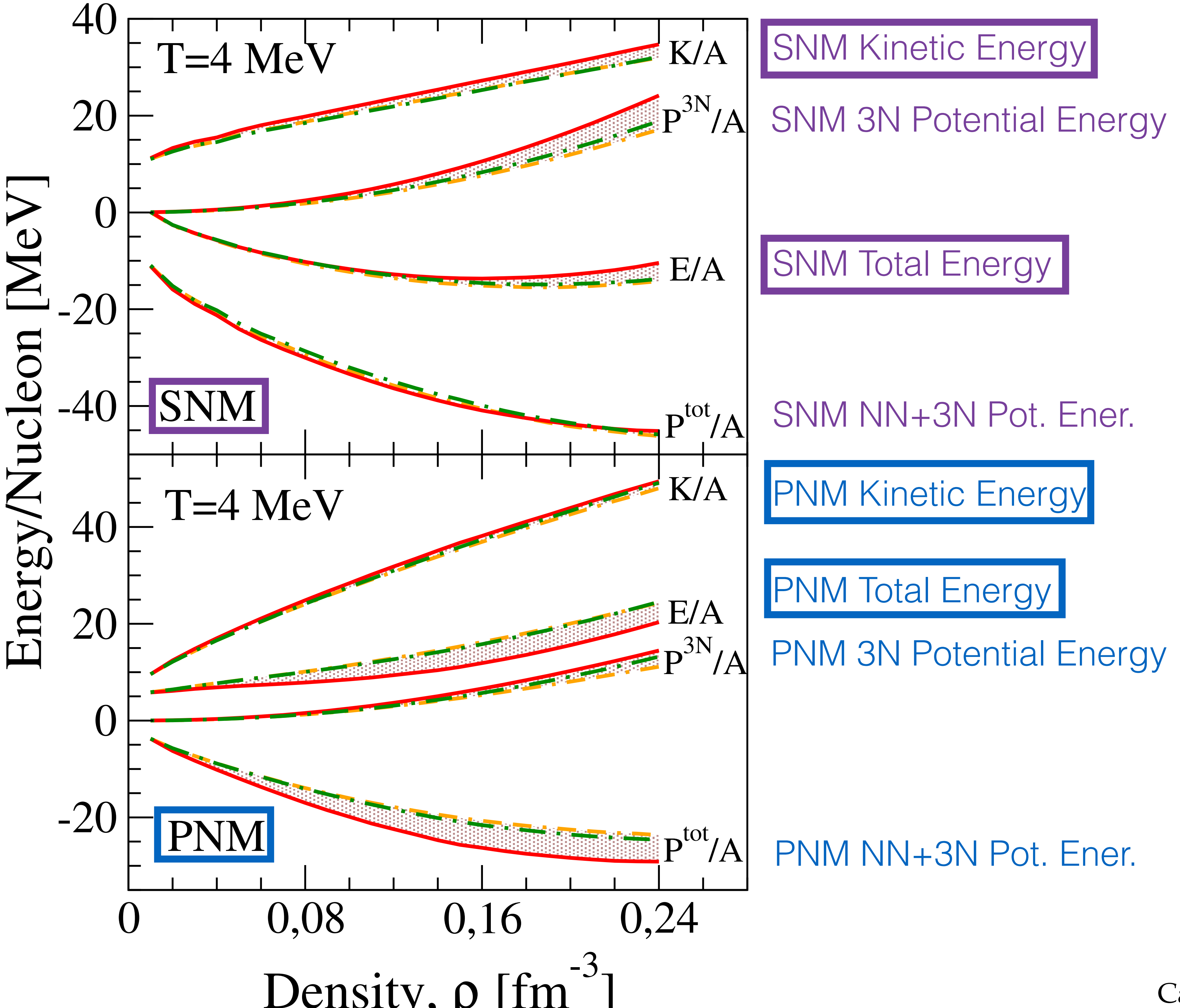

N2LOsat vs N3LO (SRG)

- higher Kinetic Energy

Carbone *(in preparation)*

Energy contributions: SNM vs PNM

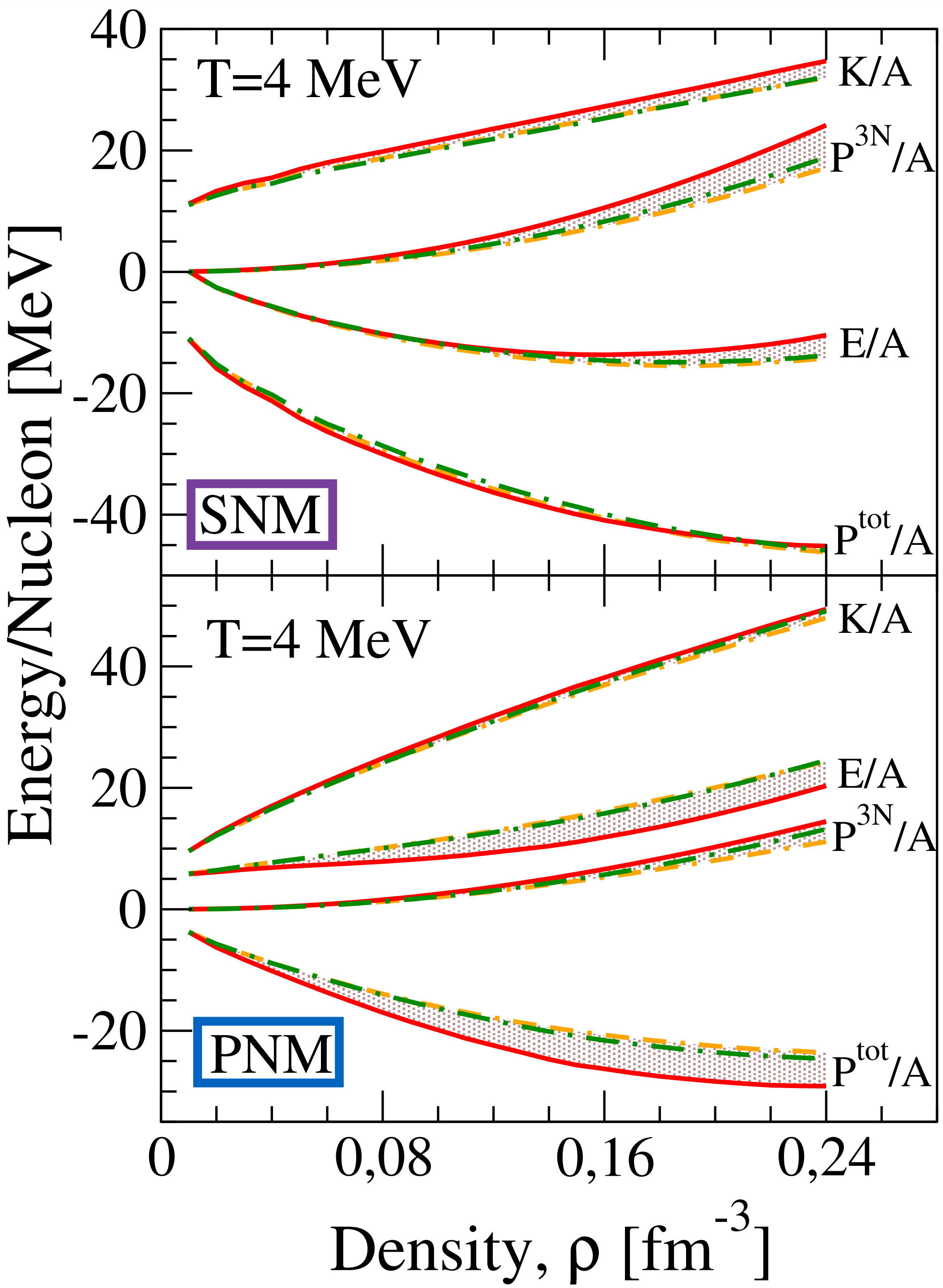

SNM Kinetic Energy

SNM 3N Potential Energy

SNM Total Energy

SNM NN+3N Pot. Ener.

PNM Kinetic Energy

PNM Total Energy

PNM 3N Potential Energy

PNM NN+3N Pot. Ener.

N2LOsat vs N3LO (SRG)

- higher Kinetic Energy
- higher 3N Potential Energy

Carbone *(in preparation)*

Energy contributions: SNM vs PNM

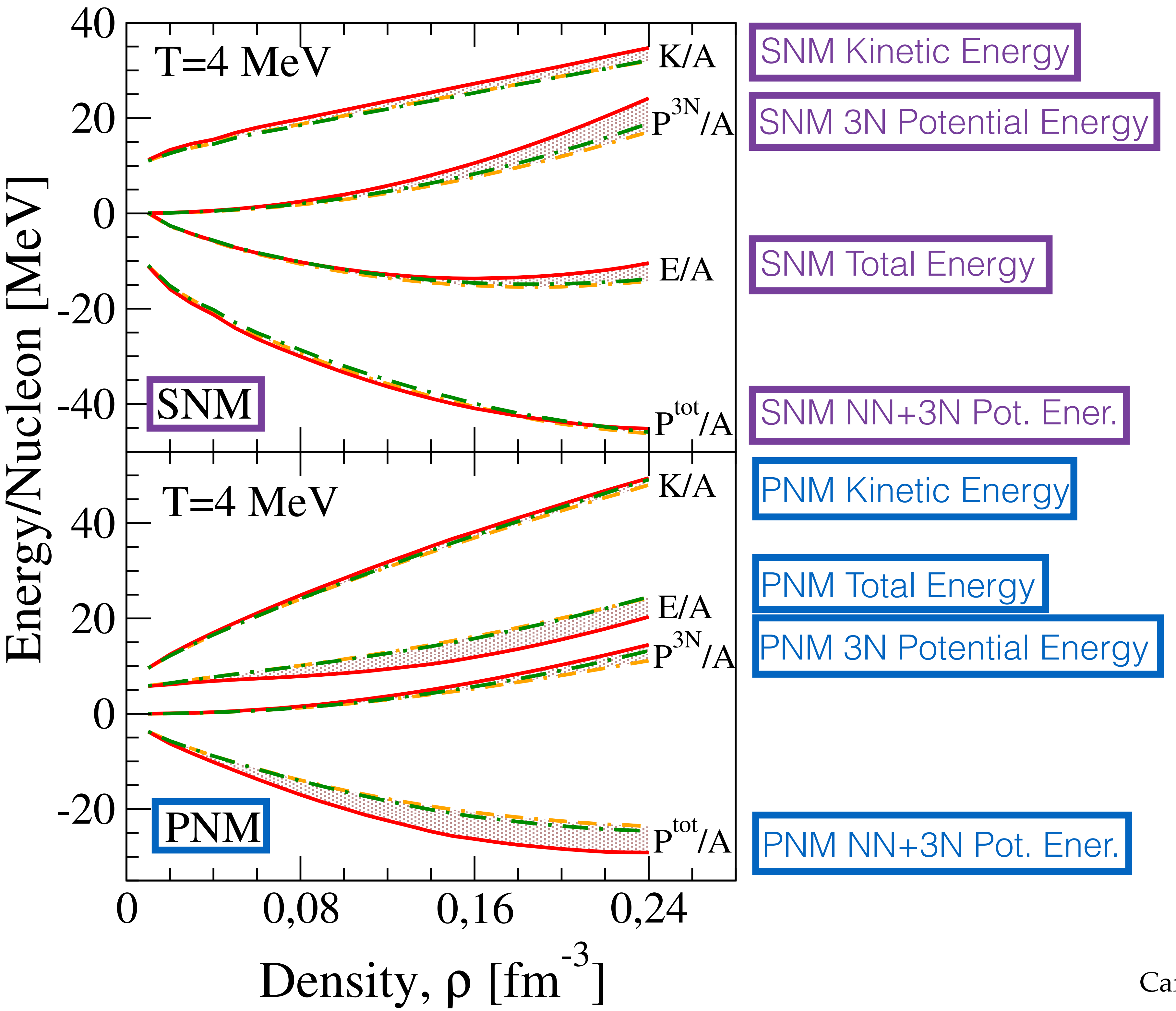

N2LOsat vs N3LO (SRG)

- higher Kinetic Energy
- higher 3N Potential Energy
- PNM NN+3N Potential Energy smaller

Carbone *(in preparation)*

Energy contributions: SNM vs PNM

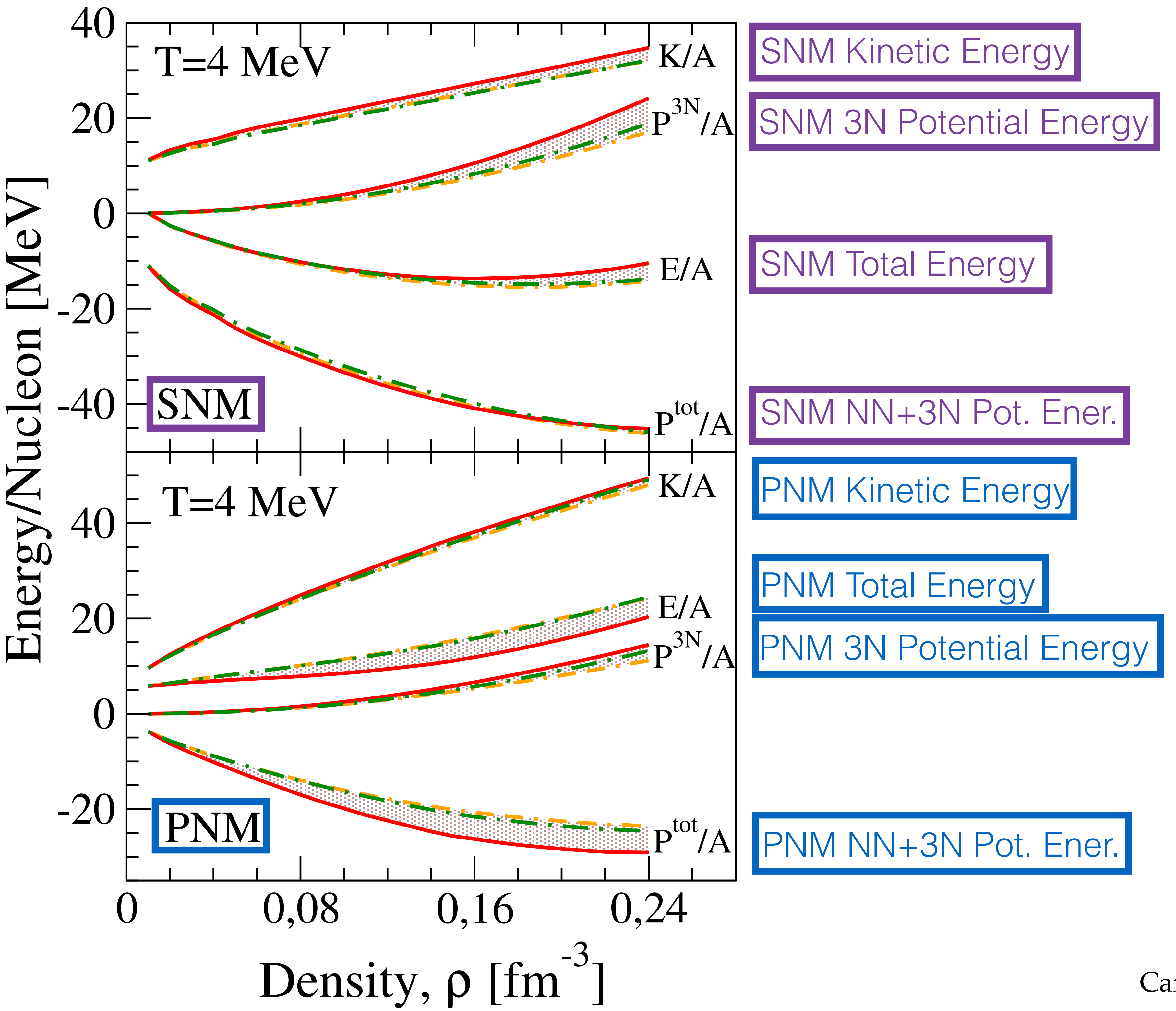

N2LOsat vs N3LO (SRG)

- higher Kinetic Energy
- higher 3N Potential Energy
- PNM NN+3N Potential Energy smaller
- PNM Total Energy more attractive

Carbone *(in preparation)*

Uncertainties due to fitting procedures

- Triton beta-decay is experimentally precisely known
- Constraints on the cD coupling

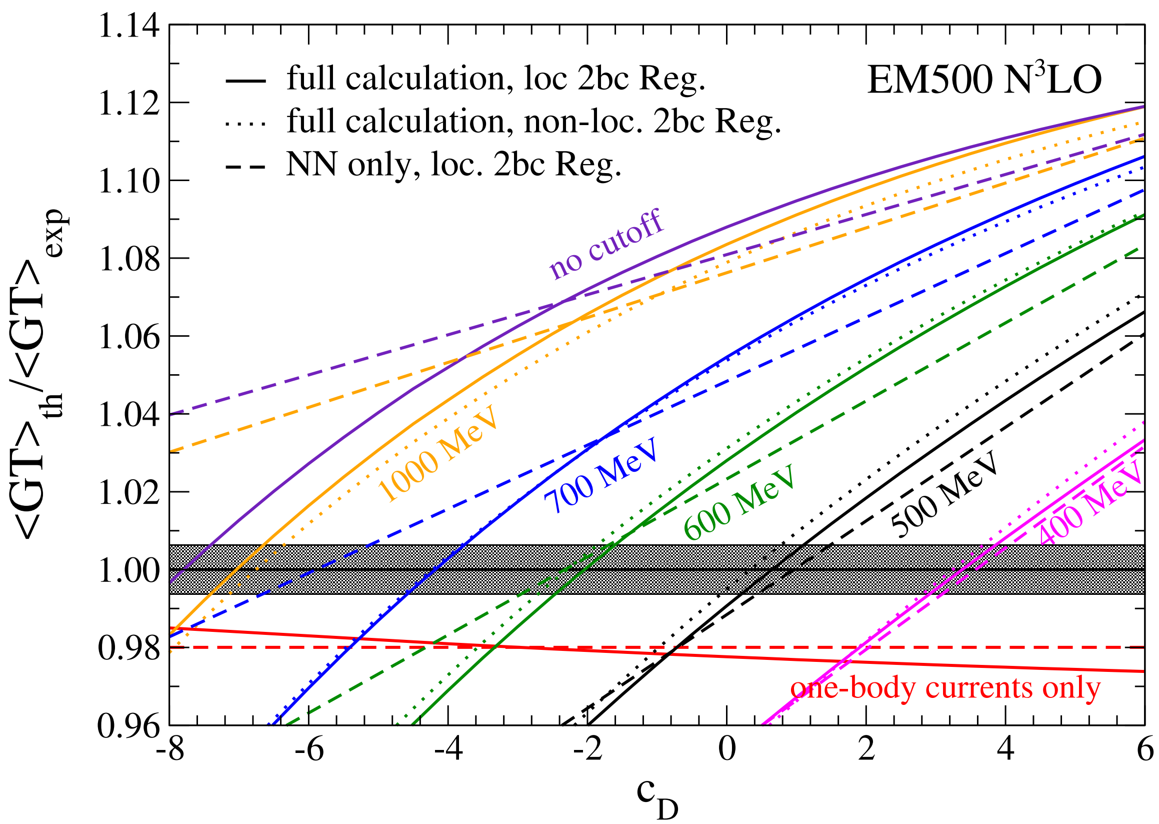

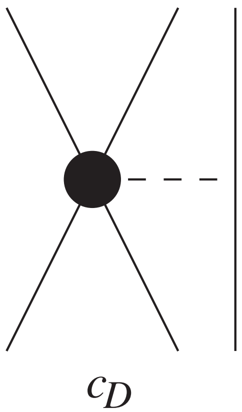

OPE 3N interaction

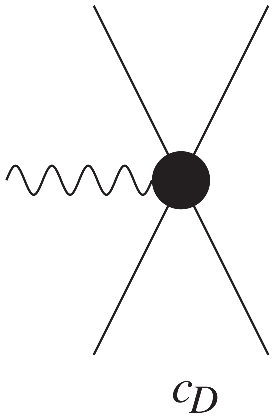

axial vector current

Klos, Carbone, Hebeler, Menéndez, Schwenk, EPJA 53, 168 (2017)

Uncertainties due to fitting procedures

- Triton beta-decay is experimentally precisely known
- Constraints on the cD coupling

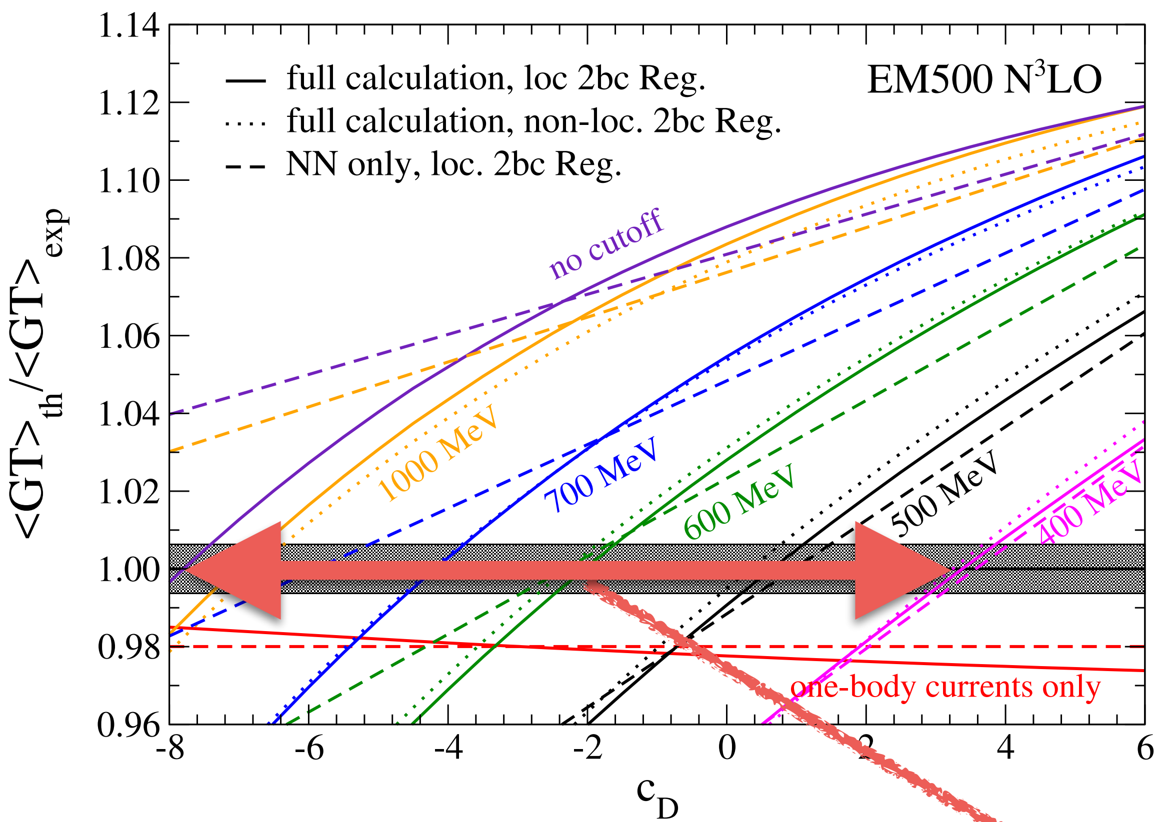

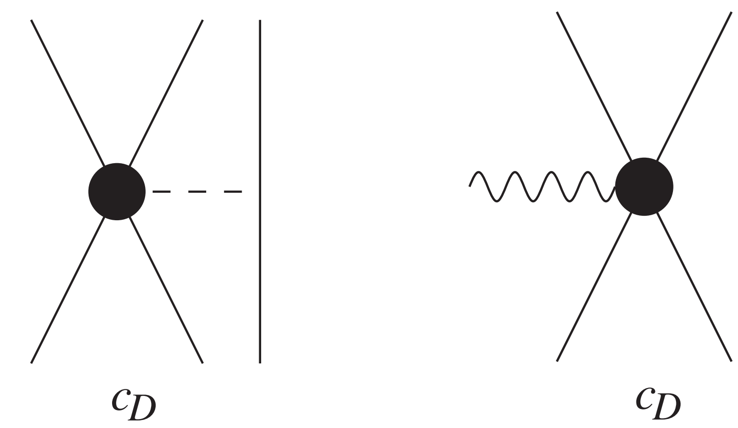

Cutoff dependence on the current

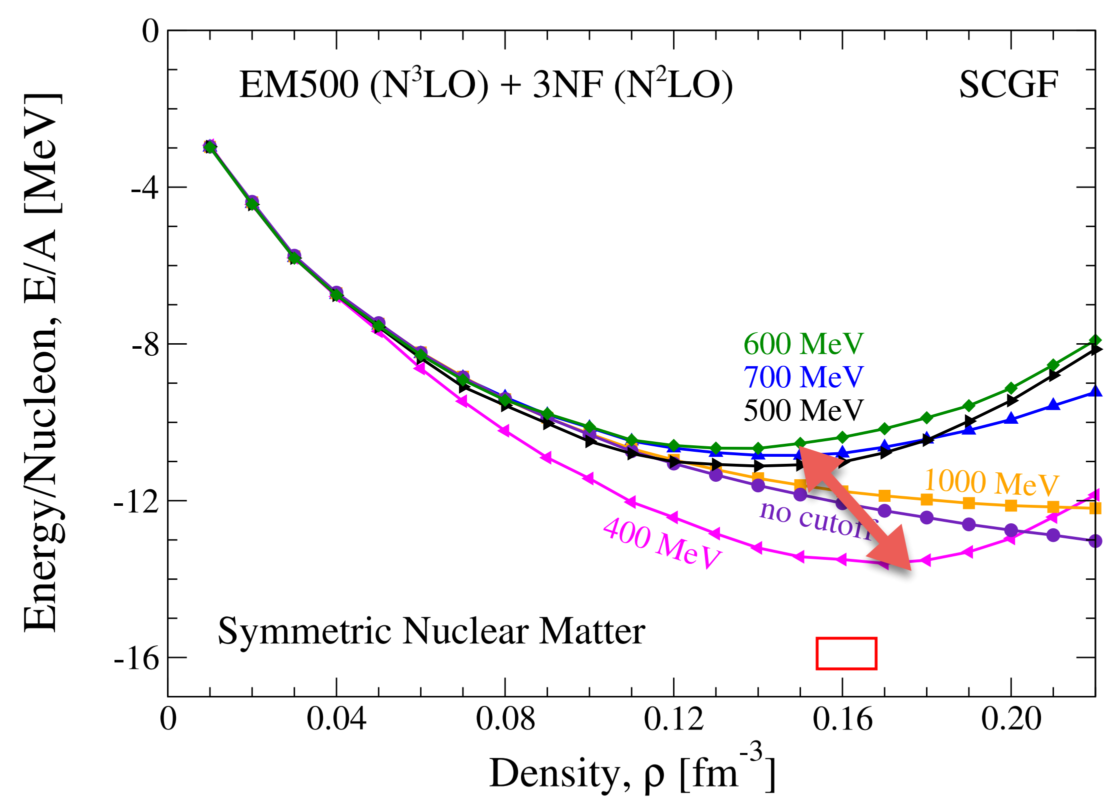

Klos, Carbone, Hebeler, Menéndez, Schwenk, EPJA 53, 168 (2017)

- **Visible effect on the prediction of the saturation point**
- Energy and density range: E=~[-11;-14]MeV; r=~[0.13-0.16]fm^{-3}

Uncertainties due to fitting procedures

- Triton beta-decay is experimentally precisely known
- Constraints on the cD coupling

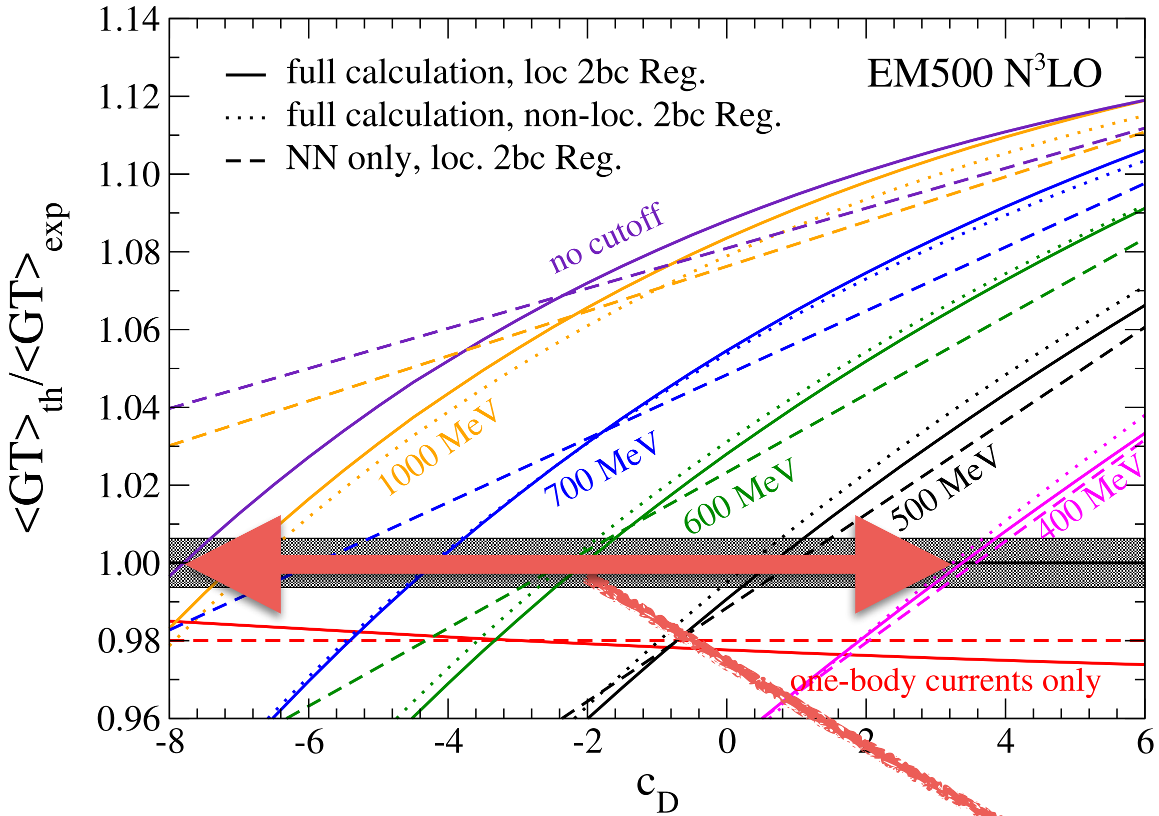

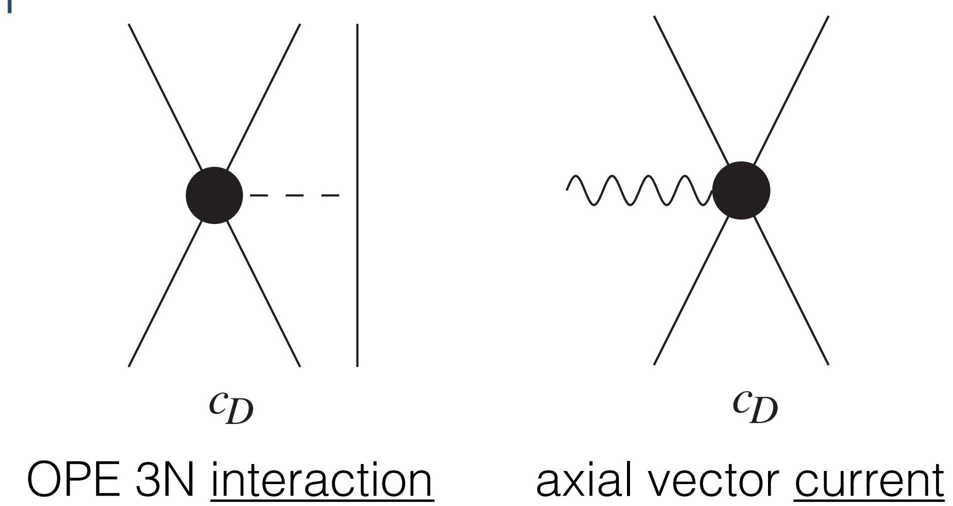

Cutoff dependence on the current

- **Visible effect on the prediction of the saturation point**
- Energy and density range: E=~[-11;-14]MeV; r=~[0.13-0.16]fm^{-3}

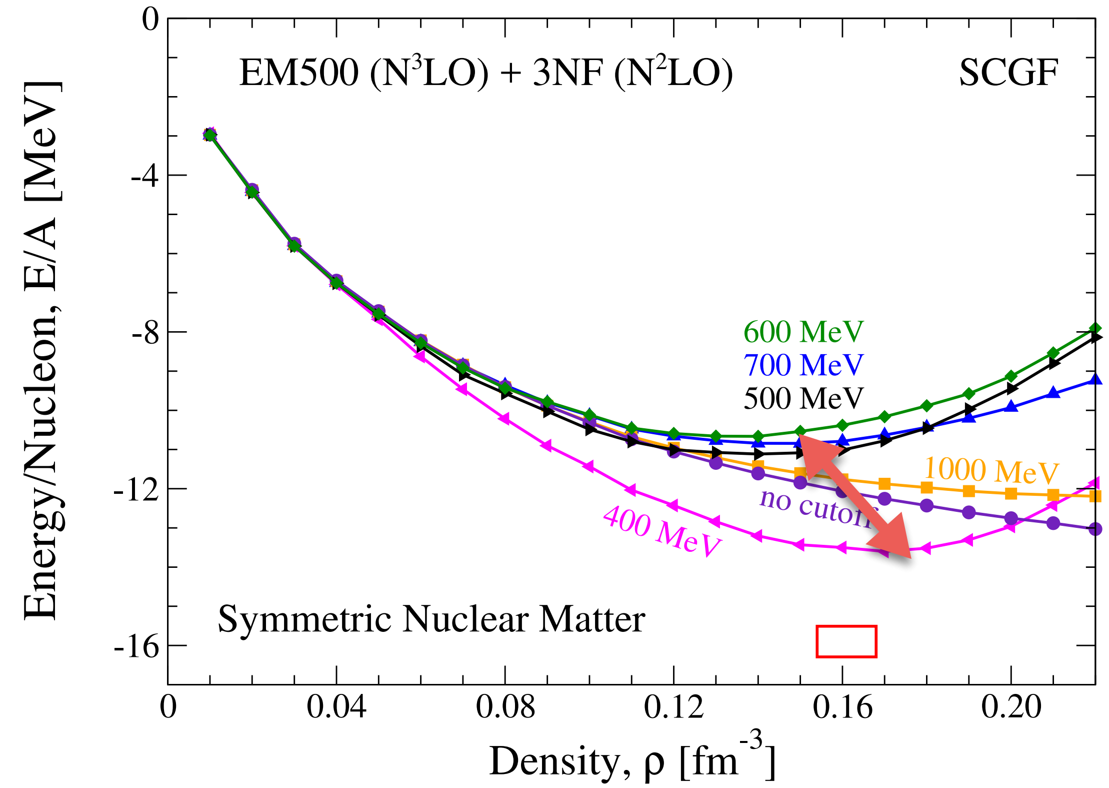

Understand new ways to fit the LECs

Klos, Carbone, Hebeler, Menéndez, Schwenk, EPJA 53, 168 (2017)

Pure neutron matter with 2N + 3N at N3LO

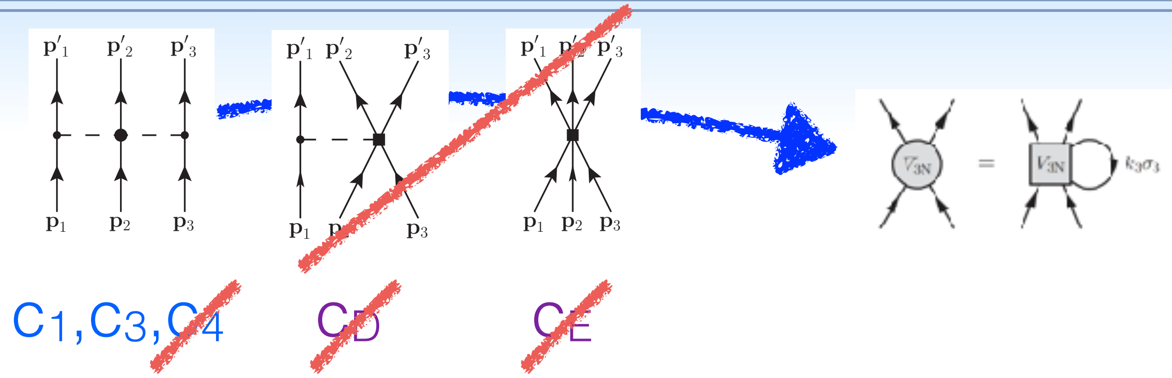

Improved 3NF matrix elements Hebeler et al. 2015
Partial-wave based 3NF average Drischler 2014-2015

EM N3LO500

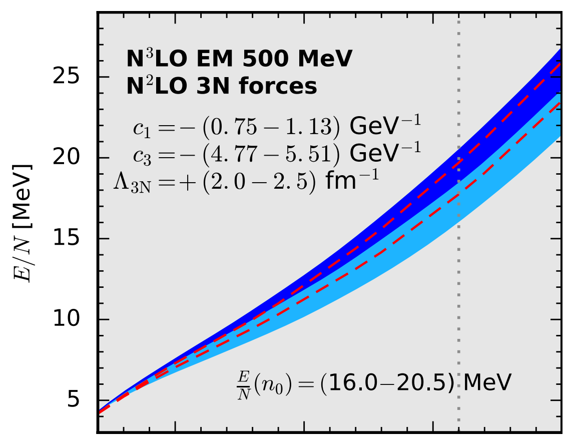

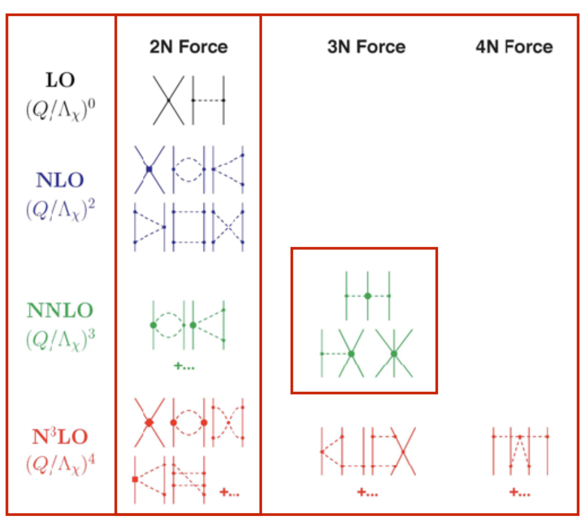

Drischler, Carbone, Hebeler, Schwenk PRC94, 054307 (2016)

Pure neutron matter with 2N + 3N at N3LO

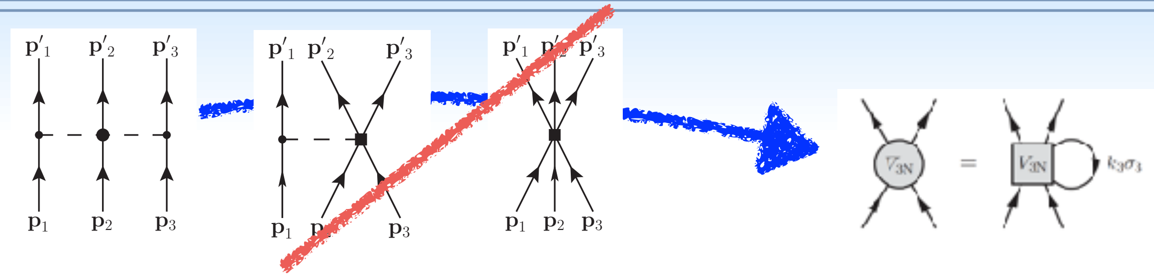

Improved 3NF matrix elements Hebeler et al. 2015
Partial-wave based 3NF average Drischler 2014-2015

c_1, c_3, ~~c_4~~ ~~c_D~~ ~~c_E~~

1. many-body approximation uncertainty : **MBPT** vs **SCGF**

EM N3LO500

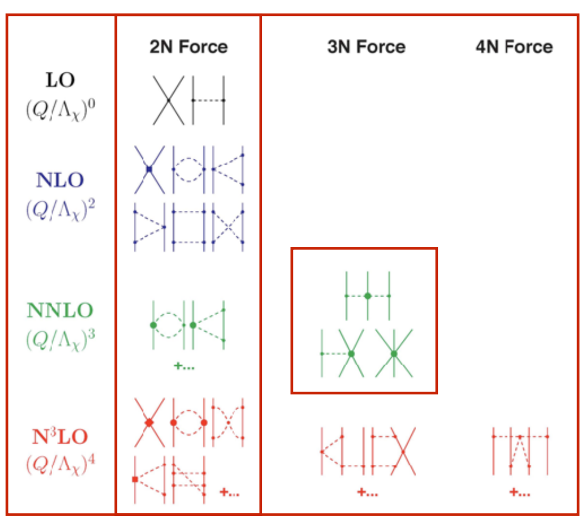

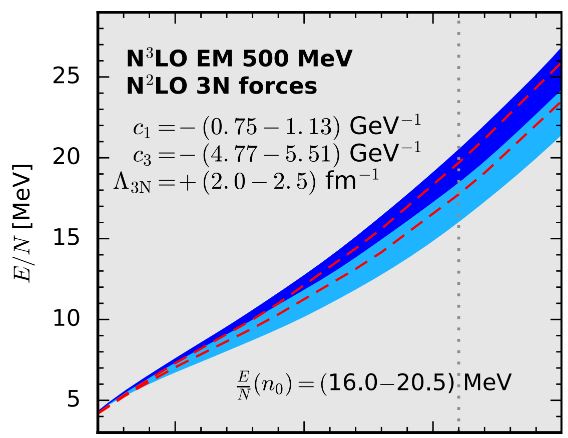

Drischler, Carbone, Hebeler, Schwenk PRC94, 054307 (2016)

Pure neutron matter with 2N + 3N at N3LO

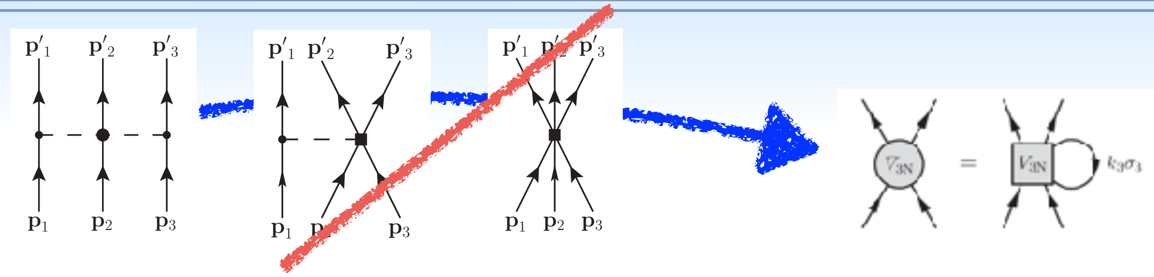

C1,C3,C4   CD   CE

Improved 3NF matrix elements Hebeler et al. 2015
Partial-wave based 3NF average Drischler 2014-2015

1. many-body approximation uncertainty : **MBPT** vs **SCGF**

How perturbative is the potential:
MBPT vs **SCGF**
band shrinks

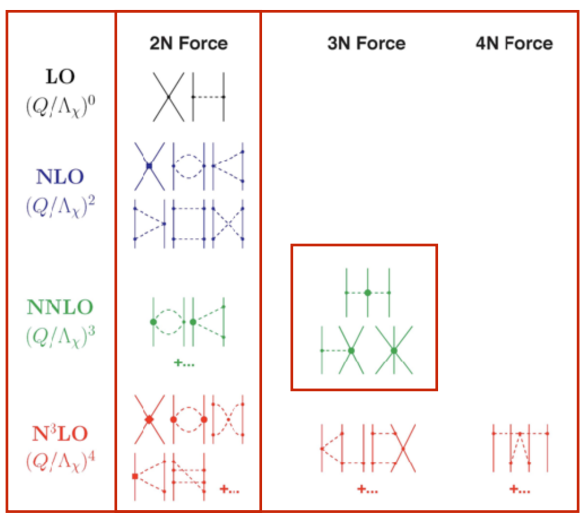

EM N3LO500   EGM 450/500   EGM 450/700

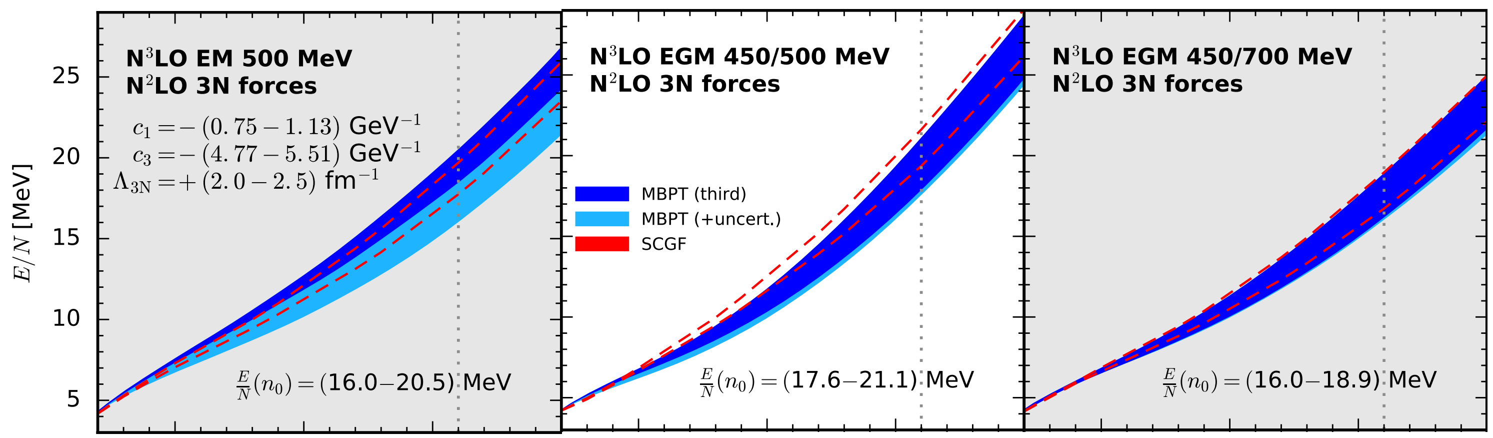

Drischler, Carbone, Hebeler, Schwenk PRC94, 054307 (2016)

Pure neutron matter with 2N + 3N at N3LO

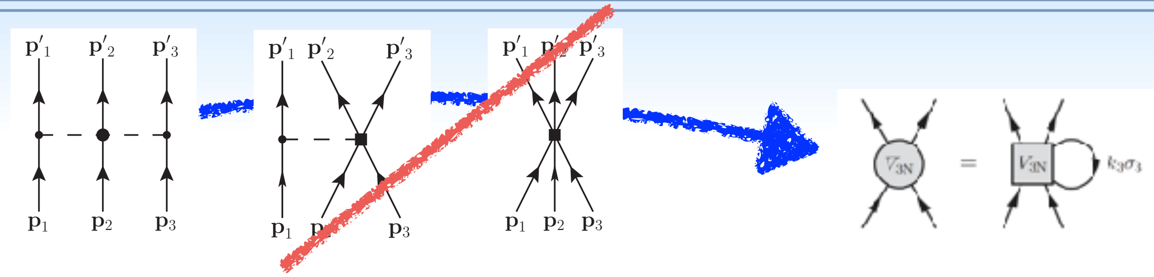

Improved 3NF matrix elements Hebeler et al. 2015
Partial-wave based 3NF average Drischler 2014-2015

C1,C3,~~C4~~ ~~CD~~ ~~CE~~

1. many-body approximation uncertainty : **MBPT** vs **SCGF**

How perturbative is the potential: **MBPT** vs **SCGF** band shrinks

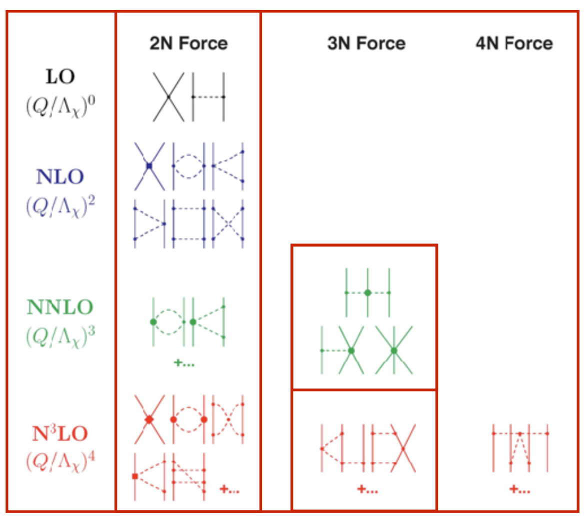

EM N3LO500 EGM 450/500 EGM 450/700

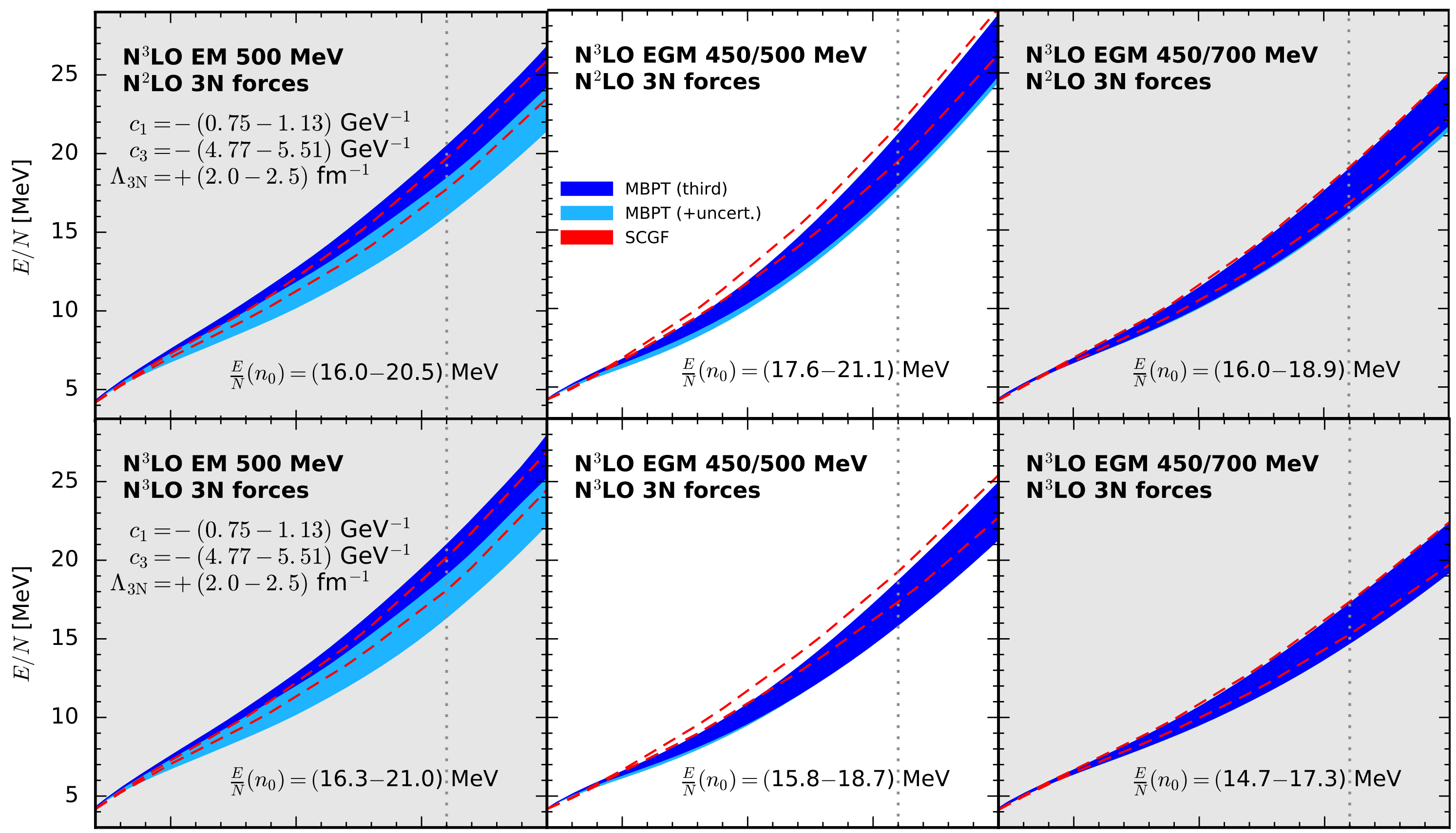

2. chiral 3NFs uncertainty: N2LO vs N3LO

N3LO 3NF shift in energy bands

3N N2LO

3N N3LO

Drischler, Carbone, Hebeler, Schwenk PRC94, 054307 (2016)

Many-body convergence at full 2N+3N N3LO in PNM

Improved 3NF matrix elements Hebeler et al. 2015
Partial-wave based 3NF average Drischler 2014-2015

Energy/Nucleon at saturation density: 0.16 fm^{-3}

EM N3LO500 EGM 450/500 EGM 450/700

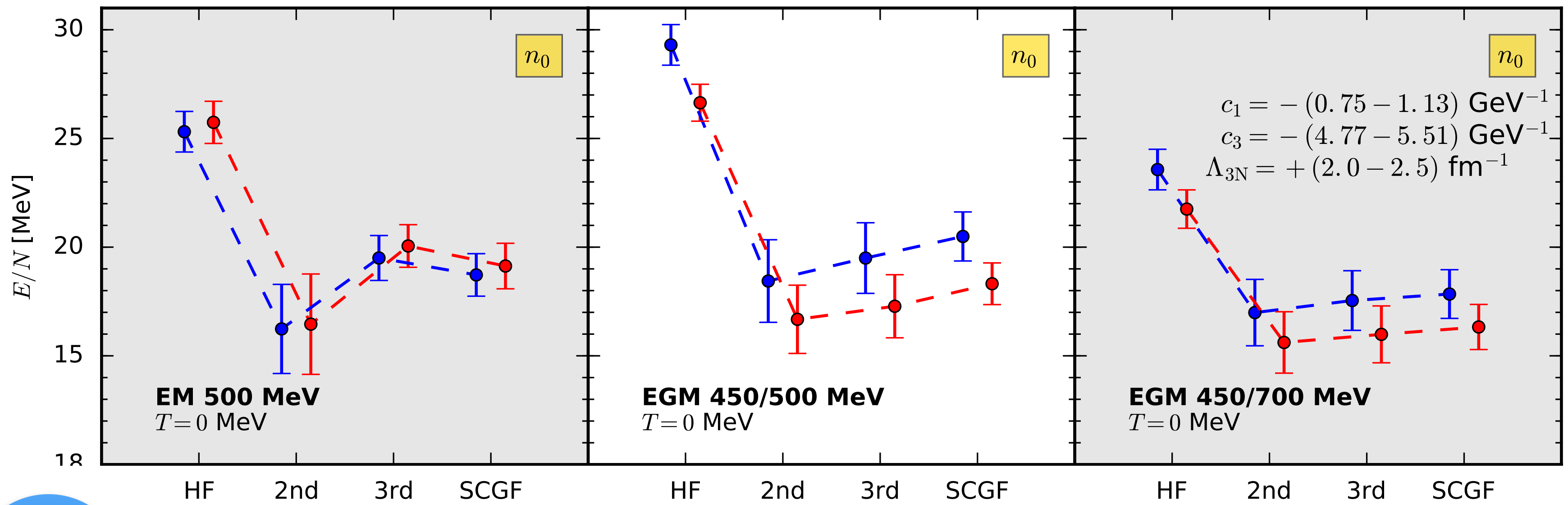

1. many-body truncation
attractive 2nd order
repulsive 3rd order

Drischler, Carbone, Hebeler, Schwenk PRC94, 054307 (2016)

Many-body convergence at full 2N+3N N3LO in PNM

Improved 3NF matrix elements Hebeler et al. 2015
Partial-wave based 3NF average Drischler 2014-2015

Energy/Nucleon at saturation density: 0.16 fm^{-3}

EM N3LO500 EGM 450/500 EGM 450/700

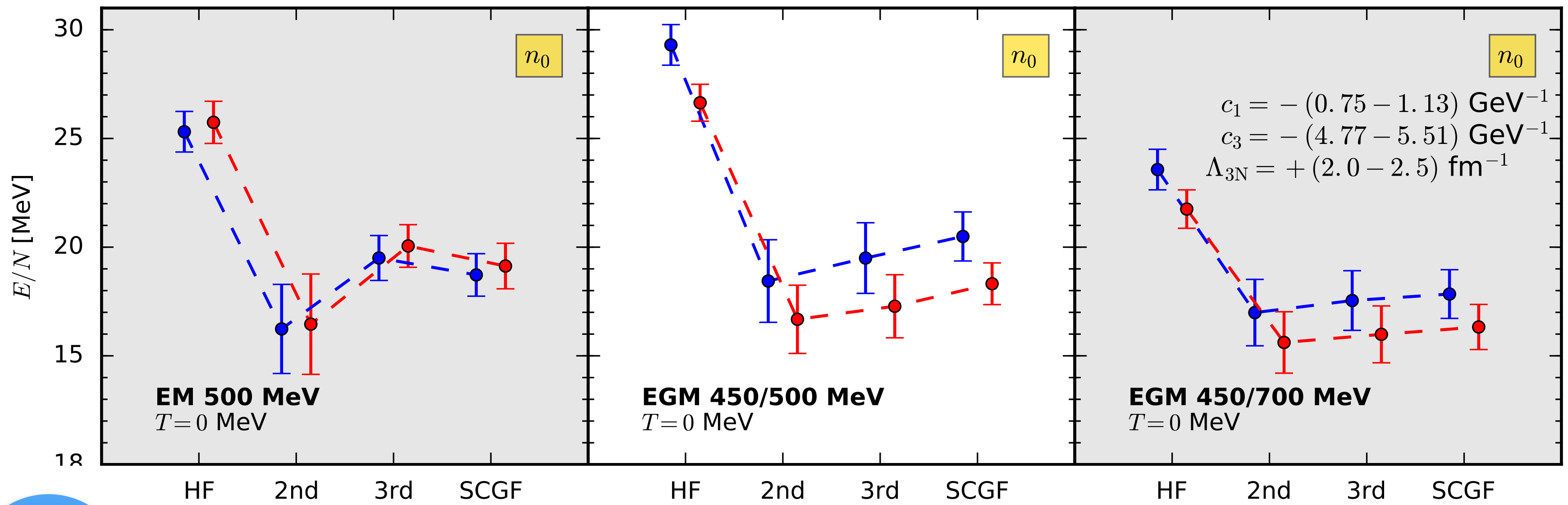

1. many-body truncation
attractive 2nd order
repulsive 3rd order

2. EM N3LO500 EGM 450/500 EGM 450/700

How perturbative is the potential: smaller beyond of 3rd order

Drischler, Carbone, Hebeler, Schwenk PRC94, 054307 (2016)

Many-body convergence at full 2N+3N N3LO in PNM

Improved 3NF matrix elements Hebeler et al. 2015
Partial-wave based 3NF average Drischler 2014-2015

Energy/Nucleon at saturation density: 0.16 fm^{-3}

EM N3LO500 | EGM 450/500 | EGM 450/700

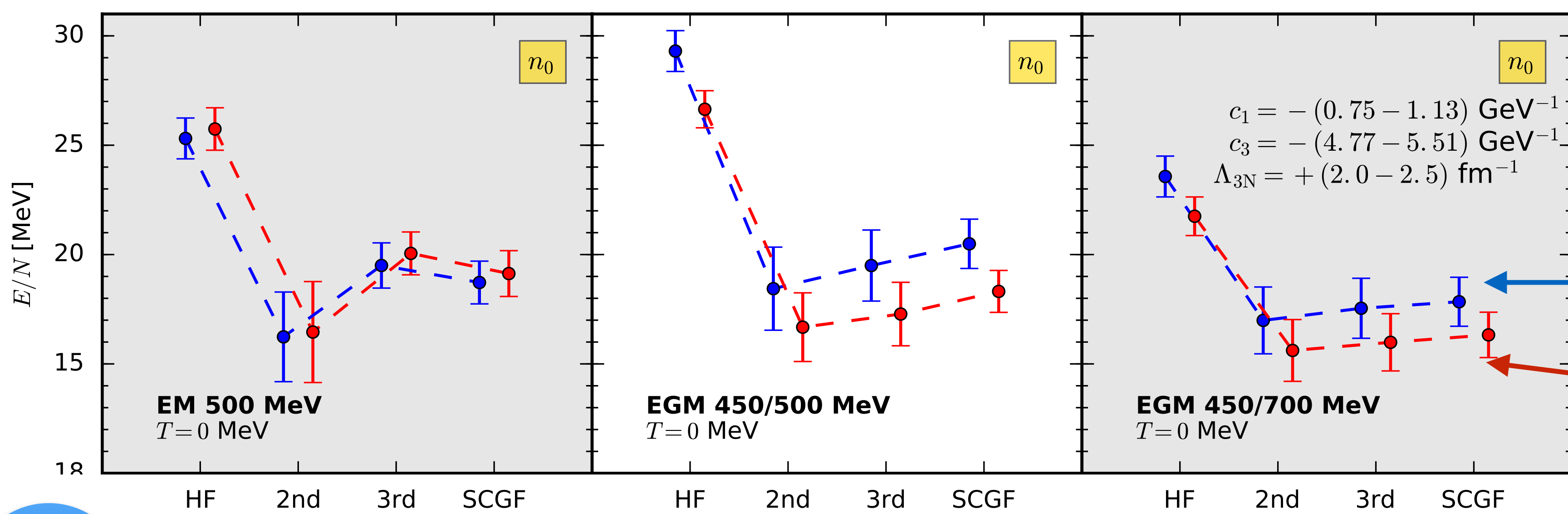

3.

3N N2LO

3N N3LO

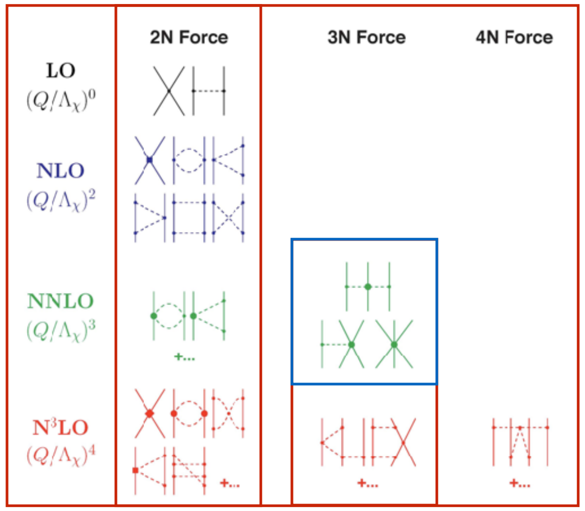

1.

many-body truncation
attractive 2nd order
repulsive 3rd order

2.

EM N3LO500 | EGM 450/500 | EGM 450/700

How perturbative is the potential: smaller beyond of 3rd order

Drischler, Carbone, Hebeler, Schwenk PRC94, 054307 (2016)

The pairing gap in neutron matter

$$\Delta_L^{JST}(k) = -\sum_{L'} \int_0^\infty \frac{\mathrm{d}k\, k'^2}{\pi} \frac{\langle k|V_{LL'}^{JST}|k'\rangle}{\xi(k')} \Delta_{L'}^{JST}(k')$$

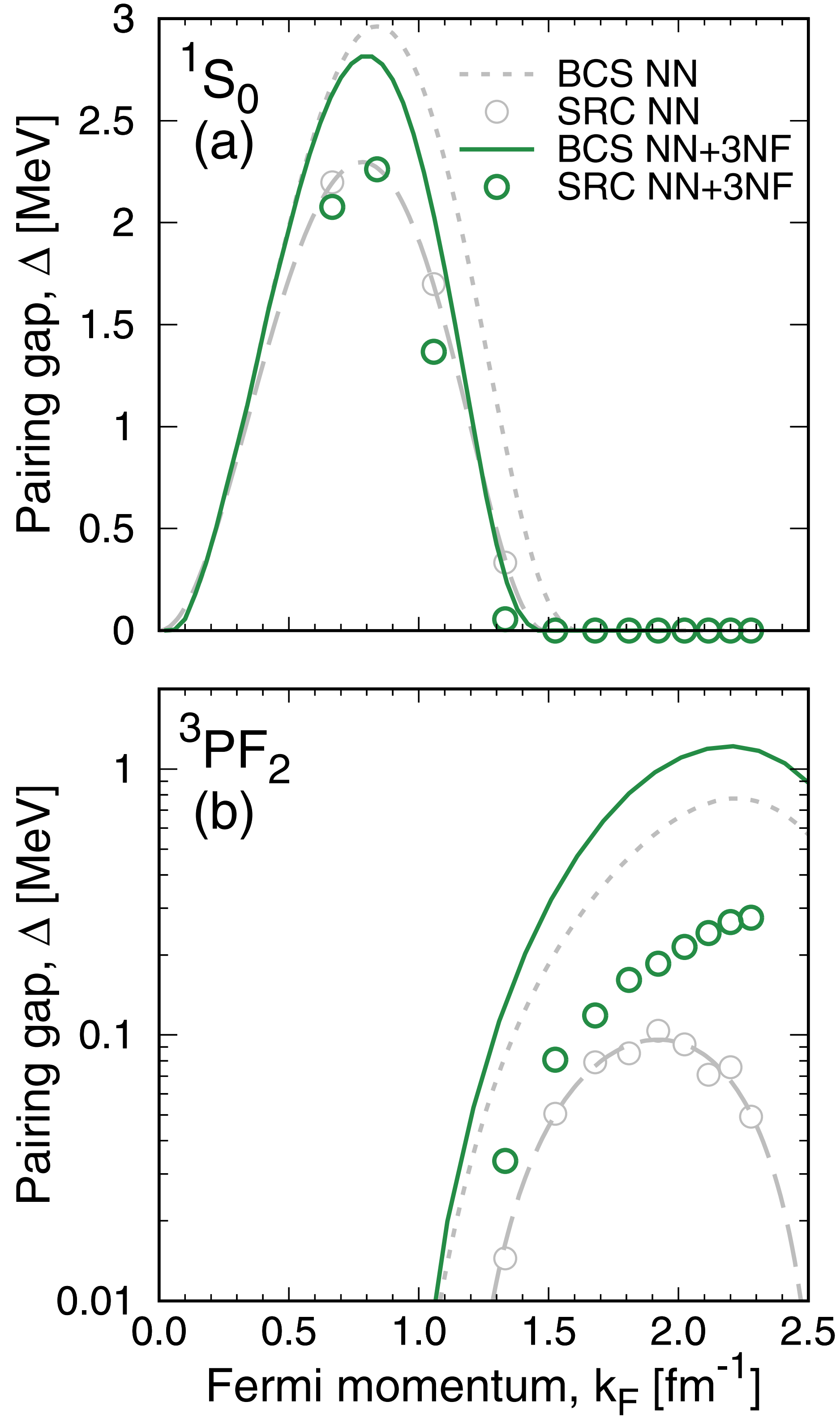

Ding et al., PRC94, 025802 (2016)

The pairing gap in neutron matter

$$\Delta_L^{JST}(k) = -\sum_{L'} \int_0^\infty \frac{\mathrm{d}k\, k'^2}{\pi} \frac{\langle k | V_{LL'}^{JST} | k' \rangle}{\xi(k')} \Delta_{L'}^{JST}(k')$$

Beyond BCS: correlations strongly reduce gap

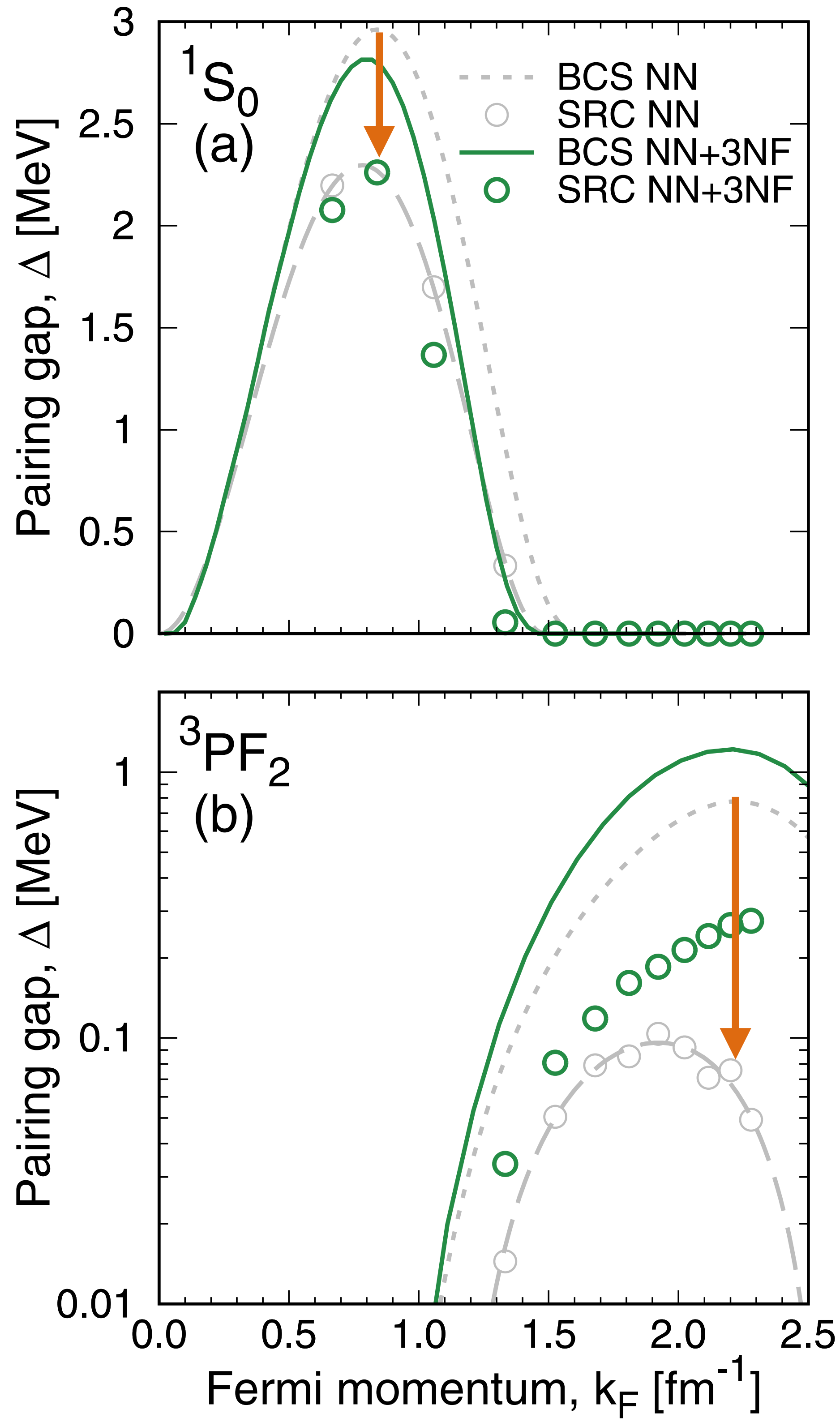

Ding et al., PRC94, 025802 (2016)

The pairing gap in neutron matter

$$\Delta_L^{JST}(k) = -\sum_{L'} \int_0^\infty \frac{\mathrm{d}k\, k'^2}{\pi} \frac{\langle k|V_{LL'}^{JST}|k'\rangle}{\xi(k')} \Delta_{L'}^{JST}(k')$$

Beyond BCS: correlations strongly reduce gap

- effect of 3NFs:
  - 1S0: weaker, repulsive, lower densities
  - 3PF2: stronger, attractive, higher densities

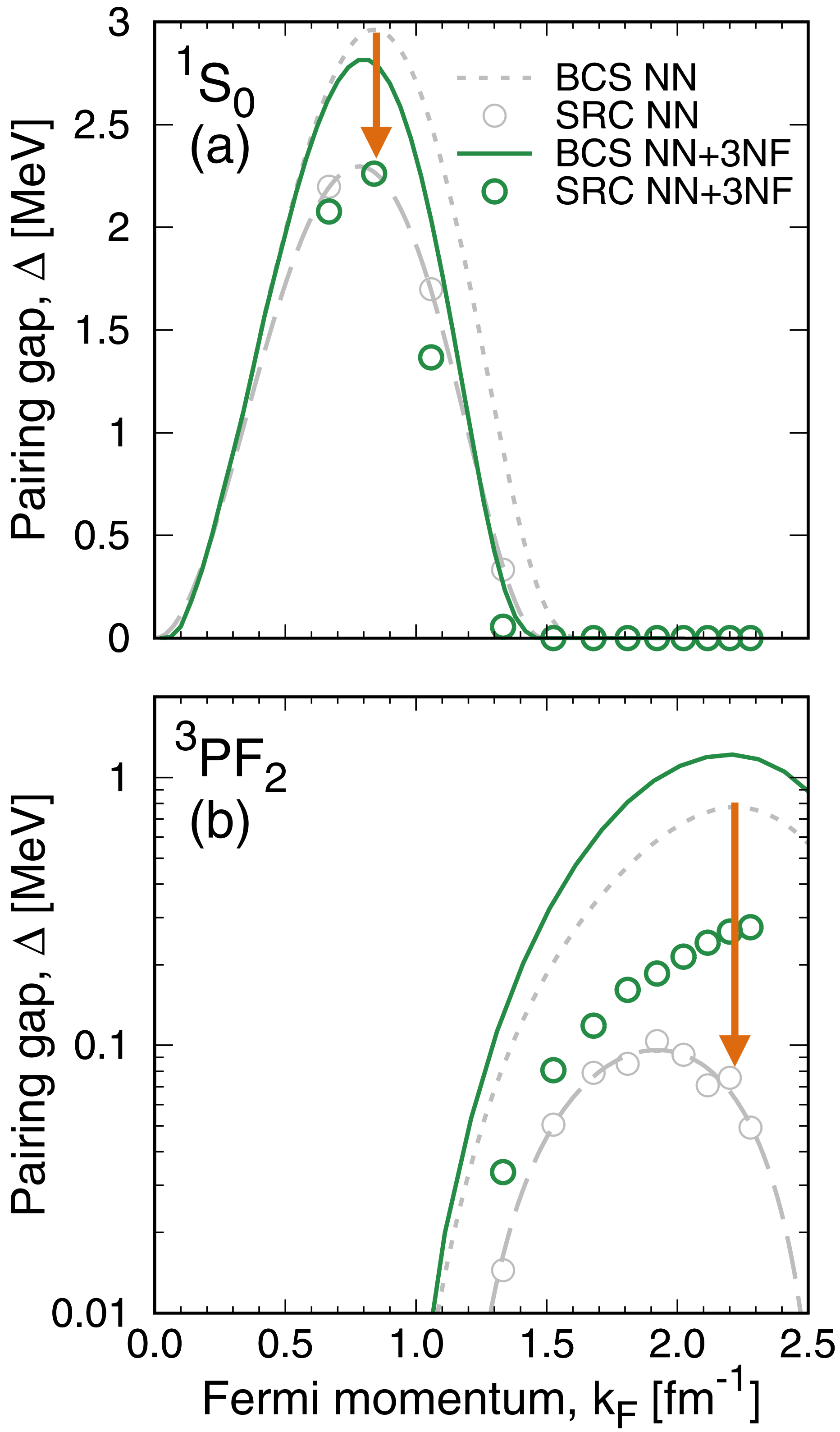

Ding et al., PRC94, 025802 (2016)

The pairing gap in neutron matter

$$\Delta_L^{JST}(k) = -\sum_{L'} \int_0^\infty \frac{dk\, k'^2}{\pi} \frac{\langle k|V_{LL'}^{JST}|k'\rangle}{\xi(k')} \Delta_{L'}^{JST}(k')$$

Beyond BCS: correlations strongly reduce gap

- effect of 3NFs:
  - 1S0: weaker, repulsive, lower densities
  - 3PF2: stronger, attractive, higher densities

Ding et al., PRC94, 025802 (2016)

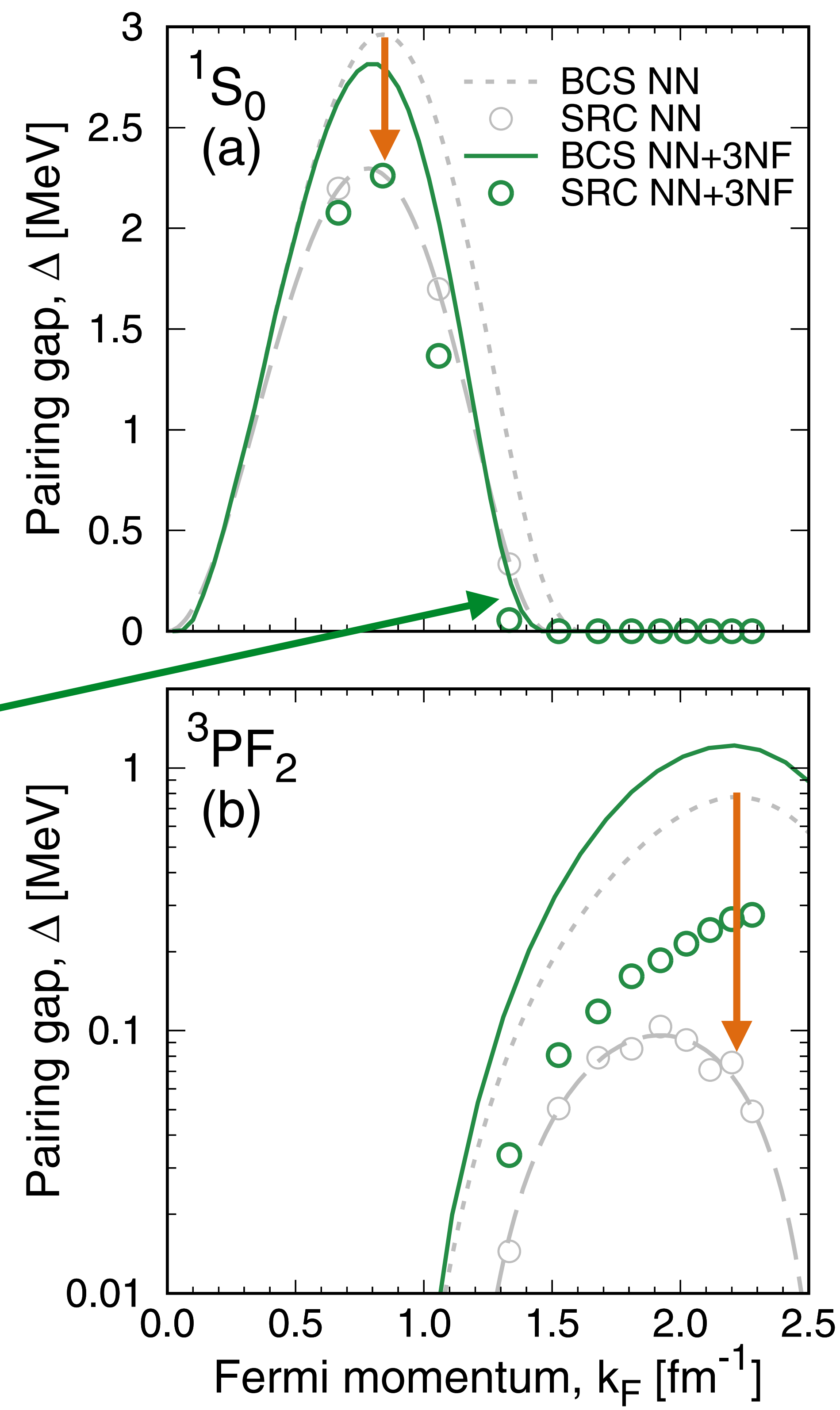

- 1S0 max 2.3 MeV, closes at ~1.5 fm-1
- 3NFs repulsive, pairing smaller

The pairing gap in neutron matter

$$\Delta_L^{JST}(k) = -\sum_{L'} \int_0^\infty \frac{dk\, k'^2}{\pi} \frac{\langle k|V_{LL'}^{JST}|k'\rangle}{\xi(k')} \Delta_{L'}^{JST}(k')$$

Beyond BCS: correlations strongly reduce gap

- effect of 3NFs:
  - 1S0: weaker, repulsive, lower densities
  - 3PF2: stronger, attractive, higher densities

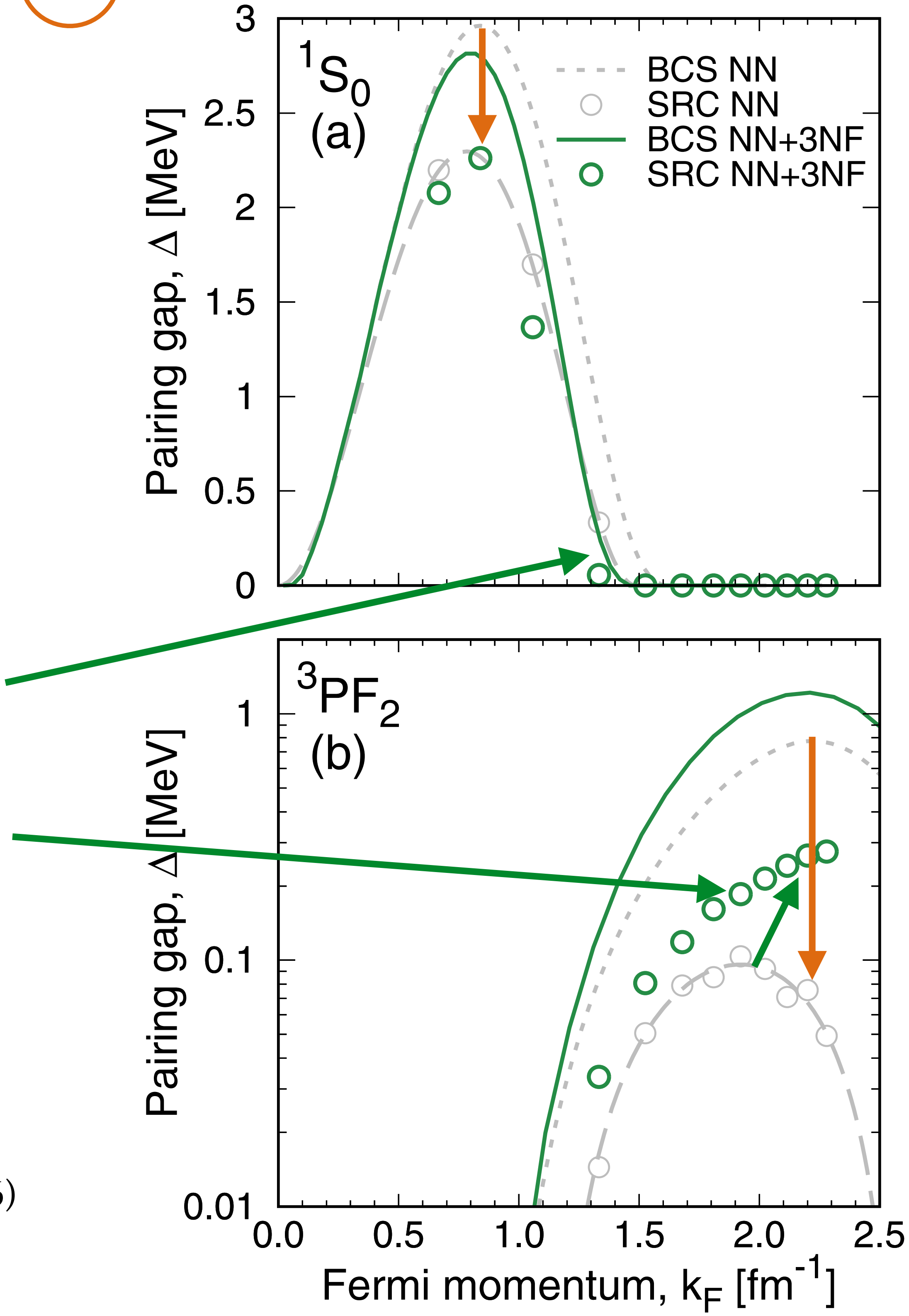

- 1S0 max 2.3 MeV, closes at ~1.5 fm-1
- 3NFs repulsive, pairing smaller

- No closure for 3PF2 gap with 3N
- limits of applicability of chiral forces

Ding et al., PRC94, 025802 (2016)